Title
Requirement for the plasminogen system in adipocyte differentiation and tissue remodeling during involution

Author
Selvarajan, Sushma,

Publication Date
2000

Peer reviewed|Thesis/dissertation

Requirement for the Plasminogen System in Adipocyte Differentiation and Tissue Remodeling during Involution

by

Sushma Selvarajan

DISSERTATION

Submitted in partial satisfaction of the requirements for the degree of

DOCTOR OF PHILOSOPHY

in

Pharmaceutical Chemistry

in the

GRADUATE DIVISION

of the

UNIVERSITY OF CALIFORNIA SAN FRANCISCO

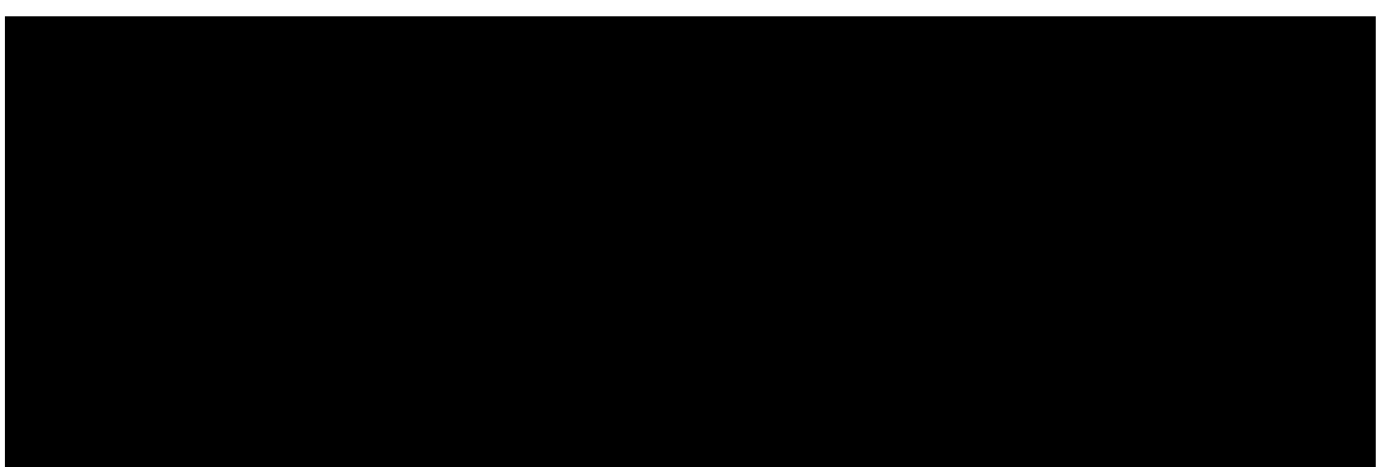

Date University Librarian

Degree Conferred: .....

Acknowledgments

I would like to thank the people who have played a pivotal role in my graduate career:

Prof. Charles Craik and Prof. Zena Werb, my two thesis advisors, were largely responsible for making my graduate experience both memorable and successful. I am thankful to Charly for his willingness to initiate a collaborative project with Zena and for agreeing to be a co-advisor. He was always available to discuss my research and other concerns, but also gave me the freedom to take my project in the direction most suited to my interests and abilities. Zena has been an inspiration both as a scientist and as a person. She was an incredible resource for my project, and created an environment in her lab where people thrived both professionally and personally. I have been fortunate in having two advisors who are both outstanding scientists and mentors.

My qualifying exam committee – Prof. Les Benet, Prof. Susan Fisher, Prof. Caroline Damsky and Prof. James McKerrow had several helpful suggestions. Dr. Marc Shuman, who is the third member of my thesis committee, provided useful advice and brought a clinical perspective to my project.

I learned a great deal from Zena's talented post-doctoral and M.D. fellows and technicians – Ole Behrendtsen, Farrah Kheradmand, Babette Heyer, Jean-Phillipe Rougier, Yibing Yan, Mark Sternlicht, and especially Thiennu Vu who was a major source of support both in and out of the lab. Helen Capilli assisted in the preparation of

tissue sections. Two former Werb lab members - Leif Lund and Caroline Alexander - were my collaborators on the adipogenesis projects. Leif, who now works in Copenhagen, patiently bred the gene-deficient mice described in Chapter Five and made several trips to San Francisco to bring us tissue samples. Caroline Alexander initiated the research on the stromelysin-1-deficient mice described in Chapter Six. In addition to great science, the Werb lab had several gourmet cooks (including Zena) who provided a lot of culinary thrills (and much weight gain) in the lab.

Several people in the Craik lab helped with my project - Chris Eggers provided ecotin, Jennifer Harris helped with the substrate libraries, and Ibrahim Adiguzel helped with ecotin purification. I would like to especially acknowledge Toshihiko Takeuchi, who helped with the ecotin studies, and was always willing to discuss ideas. Helena Rodriguez, a student from Brazil whose work is included in Chapter Two, developed ecotin as an affinity chromatography reagent. Sami Mahrus, who shared a room with me in the Craik lab, not only helped with reagents and techniques, but was also a good listener. Steven Todd and Martha Laboissiere were supportive throughout graduate school.

At UCSF, Prof. Nigel Killeen, and Annemieke VanZante and Prof. Steven Rosen were of great help with the FACS analyses discussed in Chapter Four.

My parents Ananth and Indira Selvarajan, and my sister, Sukrutha Selvarajan, have always given me their love and support. They constantly encouraged me in all my endeavors. None of this would have been possible but for them.

Preface

The focus of this thesis is to understand the role played by the plasminogen (Plg) system of serine proteases in the tissue remodeling that occurs during involution, and to investigate novel enzymes involved in the Plg cascade. Chapter One contains an introduction to the Plg system and extracellular proteolysis. Ecotin is a unique macromolecular inhibitor and a versatile tool that can be used to probe serine protease function as described in Chapter Two which is a paper (manuscript in preparation) by Helena C. Castro, Toshihiko Takeuchi, Sushma Selvarajan, Russolina B. Zingali and Charles S.Craik entitled "Ecotin: A tool for identifying serine proteases with a chymotrypsin fold in different biological systems". The role played by the Plg system in involution is described in Chapter Three. One of the events that occurs during involution is lymphocyte egress and remodeling of the mammary lymph node, which is discussed in Chapter Four. Chapter Five is a paper (accepted for publication in *Nature Cell Biology*) by Sushma Selvarajan, Leif R. Lund, Toshihiko Takeuchi, Charles S. Craik and Zena Werb entitled "A plasminogen cascade dependent on plasma kallikrein is required for adipocyte differentiation". It contains a description of the role of the Plg system during adipogenesis in culture and during involution. Chapter Six is a paper (submitted) by Caroline M. Alexander, Sushma Selvarajan, John Mudgett and Zena Werb entitled "Stromelysin-1 Regulates Adipogenesis during Mammary Gland Involution" and describes the role of matrix metalloproteases in adipocyte differentiation and involution. The addendum sections to Chapters Two, Five and Six contain data not included in the

papers that constitute those chapters. The major conclusions of this research and future experiments are described in Chapter Seven.

Abstract

Requirement for the Plasminogen System in Adipocyte Differentiation and Tissue Remodeling during Involution

Sushma Selvarajan

Involution of the mouse mammary gland is a model system to study the role of proteolytic enzymes in epithelial remodeling, adipogenesis and lymph node regression. This research demonstrates that the plasminogen (Plg) system consisting of urokinase-type plasminogen activator (uPA), tissue-type plasminogen activator (tPA) and plasmin(ogen) is required for epithelial and stromal remodeling during involution. Ecotin, an inhibitor of chymotrypsin-fold serine proteases, was used to inhibit and isolate target proteases during involution. The variant ecotin Met84Arg/Met85Arg, which is a potent inhibitor of uPA, delayed epithelial remodeling. The Plg system was shown to be required for the degradation of extracellular matrix molecules including entactin and fibronectin, and regulated the activation of gelatinase A and B, and the bioavailability of transforming growth factor-β. Treatment of involuting mice with ecotin resulted in enlarged lymph nodes and changes in the lymphocyte subpopulations present in the mammary lymph node. Mammary lymph node lymphocytes were found to be distinct from gut-associated lymphocytes, and the lymphocyte subpopulations varied depending on the functional state of the mammary gland. Adipogenesis during involution and in culture required a plasma kallikrein (PKal)-mediated (Plg) cascade. Ecotin inhibited cell

shape change, adipocyte-specific gene expression, and lipid accumulation during adipogenesis in culture. Deficiency of Plg, but not uPA and tPA, suppressed adipogenesis during 3T3-L1 differentiation and mammary gland involution. PKal, which is inhibited by ecotin, was required for adipose conversion, and for Plg activation and 3T3-L1 differentiation under serum-free conditions. Human plasma deficient in PKal did not support 3T3-L1 differentiation. The matrix metalloproteinase (MMP), MMP-3/stromelysin-1 (Str1), is highly expressed during mammary gland involution. Mice carrying a targeted mutation in *Str1* showed accelerated differentiation and hypertrophy of adipocytes. The addition of MMP inhibitors (GM 6001 and tissue inhibitor of metalloproteases-1) accelerated adipocyte differentiation. In contrast to the Plg system, MMPs appear to exert an anti-adipogenic effect. The major findings of this research are that the Plg system regulates epithelial remodeling and lymph node regression during involution of the mammary gland, and that Plg and PKal mediate adipocyte differentiation *in vivo* and in culture.

Signature of chairperson: 

(Charles S. Craik)

Table of Contents

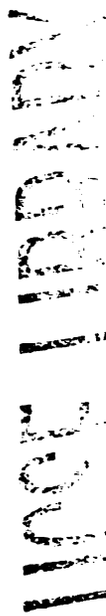

List of Tables

List of Figures/Illustrations

Chapter One

Introduction to the Plasminogen System and Extracellular Proteolysis

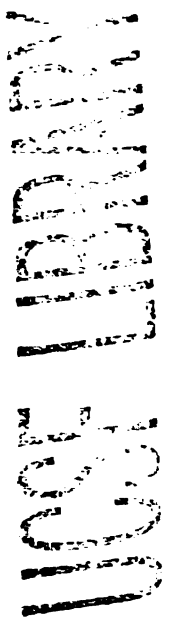

Plasminogen cascade of serine proteases

Focalized proteolysis of the extracellular matrix (ECM) is an important regulator of various physiological and pathological processes. Several classes of proteases including the matrix metalloproteases (MMPs), cysteine proteases and serine proteases play an important role in these events.

Serine proteases that have been implicated in the degradation of ECM molecules include neutrophil elastase, cathepsin G, granzymes, trypsin, chymotrypsin, and members of the fibrinolytic (plasminogen) system that consists of urokinase-type plasminogen activator (uPA), tissue-type plasminogen activator (tPA) and plasmin.

Native or glu-type plasminogen (Plg) is a single-chain zymogen that is synthesized in the liver and is found in the plasma at a concentration of about 2 μM. The zymogen Plg can be activated to the proteolytic enzyme plasmin by specific hydrolysis of its Arg-560-Val-561 peptide bond by the action of two physiological Plg activators, uPA and tPA. Other enzymes that have been implicated in Plg activation include plasma kallikrein (Colman, 1969) and factor XIIa (Schousboe et al., 1999). The two-chain active enzyme plasmin is a chymotrypsin-fold serine protease with P1-Lys specificity (Harris et al., 2000). The A chain of plasmin contains the kringle domains that facilitate binding to various substrates. The B-chain consists of the protease domain with the classic serine protease catalytic triad His-602/Asp-645/Ser-740. The two chains are linked by two disulfide bonds. Plasmin is inhibited by various endogenous inhibitors including the serpins α2-antiplasmin (Lijnen and Collen, 1990) and α1-protease inhibitor (Kwaan, 1992). Substrates for plasmin include the clot protein fibrin (Collen and Lijnen, 1994) and the ECM proteins fibronectin, laminin and vitronectin (Liotta et al., 1981). Plasmin

may also play a role in the activation of various pro-MMPs including pro-collagenase 1 (MMP-1), pro-collagenase 3 (MMP-13), gelatinase B (MMP-9) and stromelysin-1 (MMP-3) (Werb et al., 1977).

Plasmin has been implicated in various remodeling events including wound healing (Romer et al., 1996), fibrin clot dissolution (Bugge et al., 1995), and excitotoxin-induced neuronal death (Chen and Strickland, 1997). Mice deficient in the gene for plasminogen (Plg-/-) are viable, but are predisposed to severe thrombosis which leads to organ damage in the liver, kidney, stomach and other tissues and subsequently results in high mortality (Bugge et al., 1995). The effects of Plg deficiency are alleviated by deletion of the fibrinogen gene in mice, suggesting that the essential physiological substrate of plasmin is fibrin(ogen) (Bugge et al., 1996).

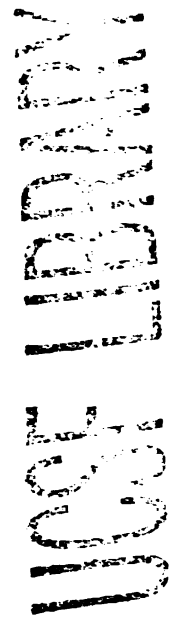

uPA is a chymotrypsin-fold serine protease with P1-Arg specificity (Harris et al., 2000) and a high affinity for Plg. It is expressed by various epithelial cells and stromal fibroblasts as a single-chain zymogen, pro-uPA, and is present at a concentration of 3-5 ng/ml in the plasma. Potential activators of pro-uPA include plasmin (Dano et al., 1985) and plasma kallikrein (Loza et al., 1994), which cleave the Lys-158-Ile-159 peptide bond in pro-uPA to generate active two-chain uPA. The B chain of uPA contains the protease domain with the catalytic triad His-204/Asp-255/Ser-356. It has been suggested that a positive feedback activation cascade involving plasmin is the primary physiological mechanism for activation of pro-uPA (Dano et al., 1985). However, normal levels of active uPA are detected in the urine of Plg-/- mice, indicating that other proteases function as pro-uPA activators *in vivo* (Bugge et al., 1995). uPA is inhibited by the serpins plasminogen activator inhibitor-1and -2 [PAI-1 and –2; (Rijken, 1995)].

uPA binds specifically to the cell-surface uPA receptor, uPAR [CD87; (Dano et al., 1985)], and is thought to be the primary activator of Plg in cell-associated processes. It also activates hepatocyte growth factor [HGF or scatter factor; (Dano et al., 1985)]. uPA has been implicated in various biological processes including macrophage invasion (Unkeless et al., 1974), ovulation (Huarte et al., 1985), angiogenesis (Moscatelli and Rifkin, 1988), wound healing (Morioka et al., 1987) and cancer progression (Dano et al., 1985). Mice deficient in the gene for uPA (uPA-/-) are viable, have a normal life span and occasionally develop fibrin deposits in normal and inflamed tissues (Carmeliet et al., 1994).

tPA is primarily synthesized by vascular endothelial cells and is present in the plasma at a concentration of 5-10 ng/ml. It is secreted as a single-chain molecule and can be cleaved by plasmin at the Arg-275-Ile-276 peptide bond to generate two-chain tPA. Both forms of tPA (Dano et al., 1985) are active. tPA is a chymotrypsin-fold serine protease with P1-Arg specificity (Harris et al., 2000). It is inhibited by the serpins PAI-1, PAI-2 and maspin (Dano et al., 1985; Sheng et al., 1998).

tPA is thought to be primarily involved in Plg activation during clot dissolution in the vasculature. It has a high affinity for both fibrin and Plg and thereby promotes formation of a tPA/Plg/fibrin complex during clot lysis (Collen and Lijnen, 1991). Mice deficient in the gene for tPA (tPA-/-) are viable, fertile and have a normal life span (Carmeliet et al., 1994). They exhibit impaired clot lysis and are susceptible to thrombosis when challenged with endotoxin. tPA has been implicated in neuronal cell death and may play an important role in seizures (Tsirka et al., 1997). Mice with combined uPA and tPA deficiency (uPA-/-tPA-/-) have a more severe phenotype than the

single-deficient mice and exhibit extensive fibrin deposits, reduced fertility, growth retardation and shortened life span (Carmeliet et al., 1994).

Various lines of evidence suggest a role for Plg activators other than uPA and tPA *in vivo*. First, uPA is primarily involved in cell-associated Plg activation, while tPA is mainly involved in fibrin-dependent Plg activation in the vasculature. The lack of phenotype in both uPA-/- and tPA-/- mice indicates the presence of alternate Plg activators in both the cellular and the vascular context. Second, uPA-/-tPA-/- mice show impaired but not completely abolished thrombolysis, again suggesting that other enzymes play a compensatory role. Third, Plg-/- mice exhibit ECM remodeling defects, including impaired mammary gland involution (Lund et al., 2000), that are not observed in uPA-/-tPA-/- mice. The primary phenotype observed in Plg-/- mice is extensive fibrin deposits, which are also observed in uPA-/-tPA-/- mice (Bugge et al., 1995; Carmeliet et al., 1994). This phenotype is abolished in mice that lack the genes for both fibrinogen and Plg (Bugge et al., 1996). However, the requirement for plasmin in fibrin-independent processes such as mammary gland involution and cancer progression indicates that proteases other than uPA and tPA may play an important role.

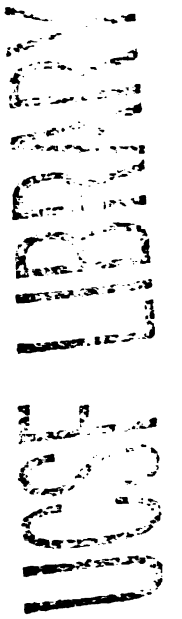

Plasma kallikrein (PKal) is a chymotrypsin-fold serine protease that can activate both Plg and pro-uPA (Lin et al., 1997; Loza et al., 1994). It is synthesized as the zymogen plasma prekallikrein and is present in the plasma at a concentration of 30-50 μg/ml. Plasma prekallikrein is activated by factor XII, and the active enzyme then cleaves high molecular weight (HMW) kininogen to generate the peptide bradykinin that plays an important role in vasodilation (Wachtfogel et al., 1993). The proteins PKal, HMW kininogen and factor XII together constitute the contact system. In the contact

system-dependent intrinsic fibrinolysis pathway (Figure 1-1), factor XII activates plasma prekallikrein bound to HMW kininogen on the surface of platelets (Loza et al., 1994) and endothelial cells (Lin et al., 1997). PKal then activates pro-uPA, which subsequently leads to Plg activation and fibrinolysis. PKal can activate pro-uPA at physiologically relevant concentrations (Lin et al., 1997; Loza et al., 1994). It can also activate Plg directly, albeit at a much lower rate than uPA or tPA (Colman, 1969).

The Plg system has been implicated in various remodeling events that occur during early development, including fertilization and implantation. Tissue remodeling also occurs during adult development, most notably during involution of the prostate, uterus and mammary gland. What role does the Plg system play in the remodeling events that occur in the mammary gland?

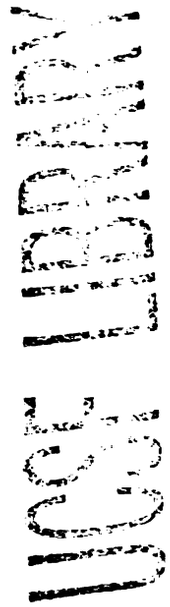

ECM remodeling and mammary gland involution

The mouse mammary gland is a model system to study the role of proteolytic enzymes in ECM remodeling. The anatomy of the gland is well characterized, and it relatively easy to access. It consists of major two tissue components – the mammary parenchyma or epithelial component which forms the ducts and secretory acini, and the stroma or "fat pad" which is comprised of adipocytes and mammary fibroblasts and provides a structural framework for the development of the mammary epithelium (Figure 1-2). The mammary gland undergoes defined changes in morphology depending on its functional state. Following lactation and weaning in the mouse, a remodeling program termed involution is initiated (Lascelles and Lee, 1978). During involution, the expression of milk-associated genes ceases and the secretory epithelial tissue involved in lactation is

replaced by adipose tissue through a combination of apoptosis, proteolysis and *de novo* regeneration of adipocytes (Lascelles and Lee, 1978; Lund et al., 1996).

Expression of the MMPs stromelysin-1, stromelysin-3 and gelatinase B (Lund et al., 1996; Talhouk et al., 1992) increases during involution. uPA expression and protein levels (Lund et al., 1996) also increase during involution, which suggests a role for the Plg system. Indeed Plg-deficient mice show impaired remodeling during involution (Lund et al., 2000). The role of uPA and related enzymes in this remodeling is yet to be defined.

A major morphological change that occurs during involution is repopulation of the mammary gland with adipocytes. While the process of adipocyte differentiation has been well characterized *in vitro*, the mechanisms by which adipogenesis occurs during involution have not been studied.

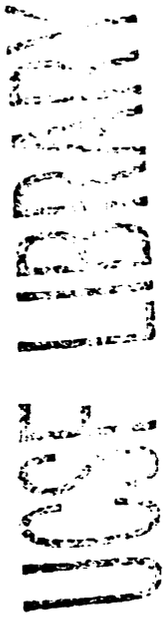

Role of the ECM in adipocyte differentiation

The role of transcription factors such as CCAAT/enhancer binding protein β (C/EBPβ; (Cao et al., 1991)) and peroxisome proliferator-activated receptor γ (PPARγ; (Lowell, 1999), as well as hormones such as leptin (Hwang et al., 1997) and cytokines such as insulin-like growth factor-1 (Smith et al., 1988) and transforming growth factor β (Bortell et al., 1994) in adipocyte differentiation has been extensively studied. However, it is not generally appreciated that the ECM and ECM proteolysis are likely to be key regulators of adipogenesis. Adipocyte differentiation *in vivo* occurs in close association with the surrounding epithelial, stromal and vascular cells, and ECM molecules may modulate interactions between these various cell types. The ECM is physically connected to the

nucleus via the cytoskeleton (Jones et al., 1993), and alterations in ECM molecules may lead to cytoskeletal rearrangements and thereby influence gene expression during differentiation. The ECM also modulates cell adhesion, and regulates the exposure of cells to hormones and cytokines (Murphy-Ullrich et al., 1992; Yamaguchi et al., 1990).

3T3-L1 preadipocytes are used to study adipocyte differentiation in culture. These cells are committed to the adipocyte lineage and have many of the characteristics of adipocytes differentiated *in vivo*. Upon the induction of differentiation, 3T3-L1 cells undergo a cell shape change from a flat-fibroblast like conformation to a rounded conformation characteristic of adipocytes. This rounding-up is accompanied by changes in gene expression including the expression of adipocyte-specific genes such as leptin and lipoprotein lipase as well as increased C/EBPβ and PPARγ expression (Smas and Sul, 1995). During 3T3-L1 differentiation, the stromal matrix of preadipocytes is replaced with the basement membrane associated with adipocytes. The expression of ECM components is highly regulated during adipocyte differentiation. Type I and III collagen, fibronectin and β-integrins are downregulated, while type IV collagen and entactin are upregulated (Gregoire et al., 1998). Growth of preadipocytes on a fibronectin matrix inhibits adipocyte differentiation, and this effect is overcome by the addition of cytochalasin D, which disrupts actin filaments and promotes rounding-up of cells (Spiegelman and Ginty, 1983). This indicates that cell shape change is crucial to differentiation, and that this change in shape is modulated by ECM components. The requirement for cell shape change during adipocyte differentiation suggests a role for ECM-degrading proteases. The Plg system is of particular interest since fibronectin is a substrate of plasmin (Liotta et al., 1981).

Several approaches exist to study the function of proteases in biological processes both *in vitro* and *in vivo*.

Approaches to studying protease function

The two most commonly used approaches to analyzing protease function include:

1) Gain-of-function experiments by overexpressing the protease gene in target cells, or by the addition of exogenous proteases
2) Loss-of-function experiments using specific protease inhibitors, depletion of the protease, or gene deletion

In addition, the function of a specific protease can be studied by determining the pattern of expression, localization, and regulation by other biological factors including endogenous activators, inhibitors, and modulators of gene expression such as hormones and cytokines.

This research primarily used a loss-of-function approach to study the role of the Plg system in involution and adipogenesis. Gene-deficient mice including Plg-/-, uPA-/-, and uPA-/-tPA-/- mice were analyzed to determine the function of these proteases. In addition, a unique macromolecular serine protease inhibitor, ecotin (Chung et al., 1983), was utilized to block the activity of proteases in the Plg cascade. Ecotin is a versatile tool and can be modified for use in a variety of applications that are described in Chapter Two.

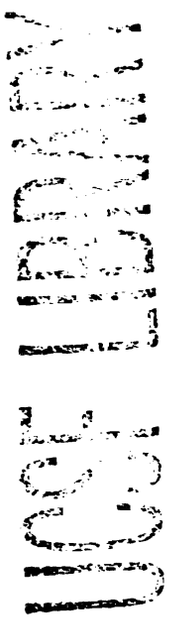

References

Bortell, R., Owen, T. A., Ignotz, R., Stein, G. S., and Stein, J. L. (1994). TGF beta 1 prevents the down-regulation of type I procollagen, fibronectin, and TGF beta 1 gene expression associated with 3T3-L1 pre- adipocyte differentiation. J Cell Biochem *54*, 256-63.

Bugge, T. H., Flick, M. J., Daugherty, C. C., and Degen, J. L. (1995). Plasminogen deficiency causes severe thrombosis but is compatible with development and reproduction. Genes Dev *9*, 794-807.

Bugge, T. H., Kombrinck, K. W., Flick, M. J., Daugherty, C. C., Danton, M. J., and Degen, J. L. (1996). Loss of fibrinogen rescues mice from the pleiotropic effects of plasminogen deficiency. Cell *87*, 709-19.

Cao, Z., Umek, R. M., and McKnight, S. L. (1991). Regulated expression of three C/EBP isoforms during adipose conversion of 3T3-L1 cells. Genes Dev *5*, 1538-52.

Carmeliet, P., Schoonjans, L., Kieckens, L., Ream, B., Degen, J., Bronson, R., De Vos, R., van den Oord, J. J., Collen, D., and Mulligan, R. C. (1994). Physiological consequences of loss of plasminogen activator gene function in mice. Nature *368*, 419-24.

Chen, Z. L., and Strickland, S. (1997). Neuronal death in the hippocampus is promoted by plasmin-catalyzed degradation of laminin. Cell *91*, 917-25.

Chung, C. H., Ives, H. E., Almeda, S., and Goldberg, A. L. (1983). Purification from Escherichia coli of a periplasmic protein that is a potent inhibitor of pancreatic proteases. J Biol Chem *258*, 11032-8.

Collen, D., and Lijnen, H. R. (1991). Basic and clinical aspects of fibrinolysis and thrombolysis. Blood *78*, 3114-24.

Collen, D., and Lijnen, H. R. (1994). Fibrinolysis and the control of hemostasis. In The molecular basis of blood diseases, G. S. Stamatoyannopoulos, A. W. Nienhius, P. W. Majerus and H. Varmus, eds. (Philadelphia, PA: W. B. Saunders Co.), pp. 725-752.

Colman, R. W. (1969). Activation of plasminogen by human plasma kallikrein. Biochem Biophys Res Commun *35*, 273-9.

Dano, K., Andreasen, P. A., Grondahl-Hansen, J., Kristensen, P., Nielsen, L. S., and Skriver, L. (1985). Plasminogen activators, tissue degradation, and cancer. Adv Cancer Res *44*, 139-266.

Gregoire, F. M., Smas, C. M., and Sul, H. S. (1998). Understanding adipocyte differentiation. Physiol Rev *78*, 783-809.

Harris, J. L., Backes, B. J., Leonetti, F., Mahrus, S., Ellman, J. A., and Craik, C. S. (2000). Rapid and general profiling of protease specificity by using combinatorial fluorogenic substrate libraries. Proc Natl Acad Sci U S A *97*, 7754-9.

Huarte, J., Belin, D., and Vassalli, J. D. (1985). Plasminogen activator in mouse and rat oocytes: induction during meiotic maturation. Cell *43*, 551-8.

Hwang, C. S., Loftus, T. M., Mandrup, S., and Lane, M. D. (1997). Adipocyte differentiation and leptin expression. Annu Rev Cell Dev Biol *13*, 231-59.

Jones, P. L., Schmidhauser, C., and Bissell, M. J. (1993). Regulation of gene expression and cell function by extracellular matrix. Crit Rev Eukaryot Gene Expr *3*, 137-54.

Kwaan, H. C. (1992). The plasminogen-plasmin system in malignancy. Cancer Metastasis Rev *11*, 291-311.

Lascelles, A. K., and Lee, C. S. (1978). Involution of the Mammary Gland. In Lactation: A Comprehensive Treatise, B. L. Larson, ed. (New York: Academic Press), pp. 115-176.

Lijnen, H. R., and Collen, D. (1990). Serine proteases and their serpin inhibitors in the nervous system, B. W. Festoff, ed. (New York: Plenum Press).

Lin, Y., Harris, R. B., Yan, W., McCrae, K. R., Zhang, H., and Colman, R. W. (1997). High molecular weight kininogen peptides inhibit the formation of kallikrein on endothelial cell surfaces and subsequent urokinase- dependent plasmin formation. Blood *90*, 690-7.

Liotta, L. A., Goldfarb, R. H., Brundage, R., Siegal, G. P., Terranova, V., and Garbisa, S. (1981). Effect of plasminogen activator (urokinase), plasmin, and thrombin on glycoprotein and collagenous components of basement membrane. Cancer Res *41*, 4629-36.

Lowell, B. B. (1999). PPARg: An essential regulator of adipogenesis and modulator of fat cell function. Cell *99*, 239-42.

Loza, J. P., Gurewich, V., Johnstone, M., and Pannell, R. (1994). Platelet-bound prekallikrein promotes pro-urokinase-induced clot lysis: a mechanism for targeting the factor XII dependent intrinsic pathway of fibrinolysis. Thromb Haemost *71*, 347-52.

Lund, L. R., Bjorn, S. F., Sternlicht, M. D., Nielsen, B. S., Solberg, H., Usher, P. A., Osterby, R., Christensen, I. J., Stephens, R. W., Bugge, T. H., Dano, K., and Werb, Z. (2000). Lactational competence and involution of the mouse mammary gland require plasminogen. Development *127*, 4481-4492.

Lund, L. R., Romer, J., Thomasset, N., Solberg, H., Pyke, C., Bissell, M. J., Dano, K., and Werb, Z. (1996). Two distinct phases of apoptosis in mammary gland involution: proteinase-independent and -dependent pathways. Development *122*, 181-93.

Morioka, S., Lazarus, G. S., Baird, J. L., and Jensen, P. J. (1987). Migrating keratinocytes express urokinase-type plasminogen activator. J Invest Dermatol *88*, 418-23.

Moscatelli, D., and Rifkin, D. B. (1988). Membrane and matrix localization of proteinases: a common theme in tumor cell invasion and angiogenesis. Biochim Biophys Acta *948*, 67-85.

Murphy-Ullrich, J. E., Schultz-Cherry, S., and Hook, M. (1992). Transforming growth factor-beta complexes with thrombospondin. Mol Biol Cell *3*, 181-8.

Rijken, D. C. (1995). Plasminogen activators and plasminogen activator inhibitors: biochemical aspects. Baillieres Clin Haematol *8*, 291-312.

Romer, J., Bugge, T. H., Pyke, C., Lund, L. R., Flick, M. J., Degen, J. L., and Dano, K. (1996). Impaired wound healing in mice with a disrupted plasminogen gene [see comments]. Nat Med *2*, 287-92.

Schousboe, I., Feddersen, K., and Rojkjaer, R. (1999). Factor XIIa is a kinetically favorable plasminogen activator. Thromb Haemost *82*, 1041-6.

Sheng, S., Truong, B., Fredrickson, D., Wu, R., Pardee, A. B., and Sager, R. (1998). Tissue-type plasminogen activator is a target of the tumor suppressor gene maspin. Proc Natl Acad Sci U S A *95*, 499-504.

Smas, C. M., and Sul, H. S. (1995). Control of adipocyte differentiation. Biochem J *309*, 697-710.

Smith, P. J., Wise, L. S., Berkowitz, R., Wan, C., and Rubin, C. S. (1988). Insulin-like growth factor-I is an essential regulator of the differentiation of 3T3-L1 adipocytes. J Biol Chem *263*, 9402-8.

Spiegelman, B. M., and Ginty, C. A. (1983). Fibronectin modulation of cell shape and lipogenic gene expression in 3T3-adipocytes. Cell *35*, 657-66.

Talhouk, R. S., Bissell, M. J., and Werb, Z. (1992). Coordinated expression of extracellular matrix-degrading proteinases and their inhibitors regulates mammary epithelial function during involution. J Cell Biol *118*, 1271-82.

Tsirka, S. E., Rogove, A. D., Bugge, T. H., Degen, J. L., and Strickland, S. (1997). An extracellular proteolytic cascade promotes neuronal degeneration in the mouse hippocampus. J Neurosci *17*, 543-52.

Unkeless, J. C., Gordon, S., and Reich, E. (1974). Secretion of plasminogen activator by stimulated macrophages. J Exp Med *139*, 834-50.

Wachtfogel, Y. T., DeLa Cadena, R. A., and Colman, R. W. (1993). Structural biology, cellular interactions and pathophysiology of the contact system. Thromb Res *72*, 1-21.

Werb, Z., Mainardi, C. L., Vater, C. A., and Harris, E. D., Jr. (1977). Endogenous activiation of latent collagenase by rheumatoid synovial cells. Evidence for a role of plasminogen activator. N Engl J Med *296*, 1017-23.

Yamaguchi, Y., Mann, D. M., and Ruoslahti, E. (1990). Negative regulation of transforming growth factor-beta by the proteoglycan decorin. Nature *346*, 281-4.

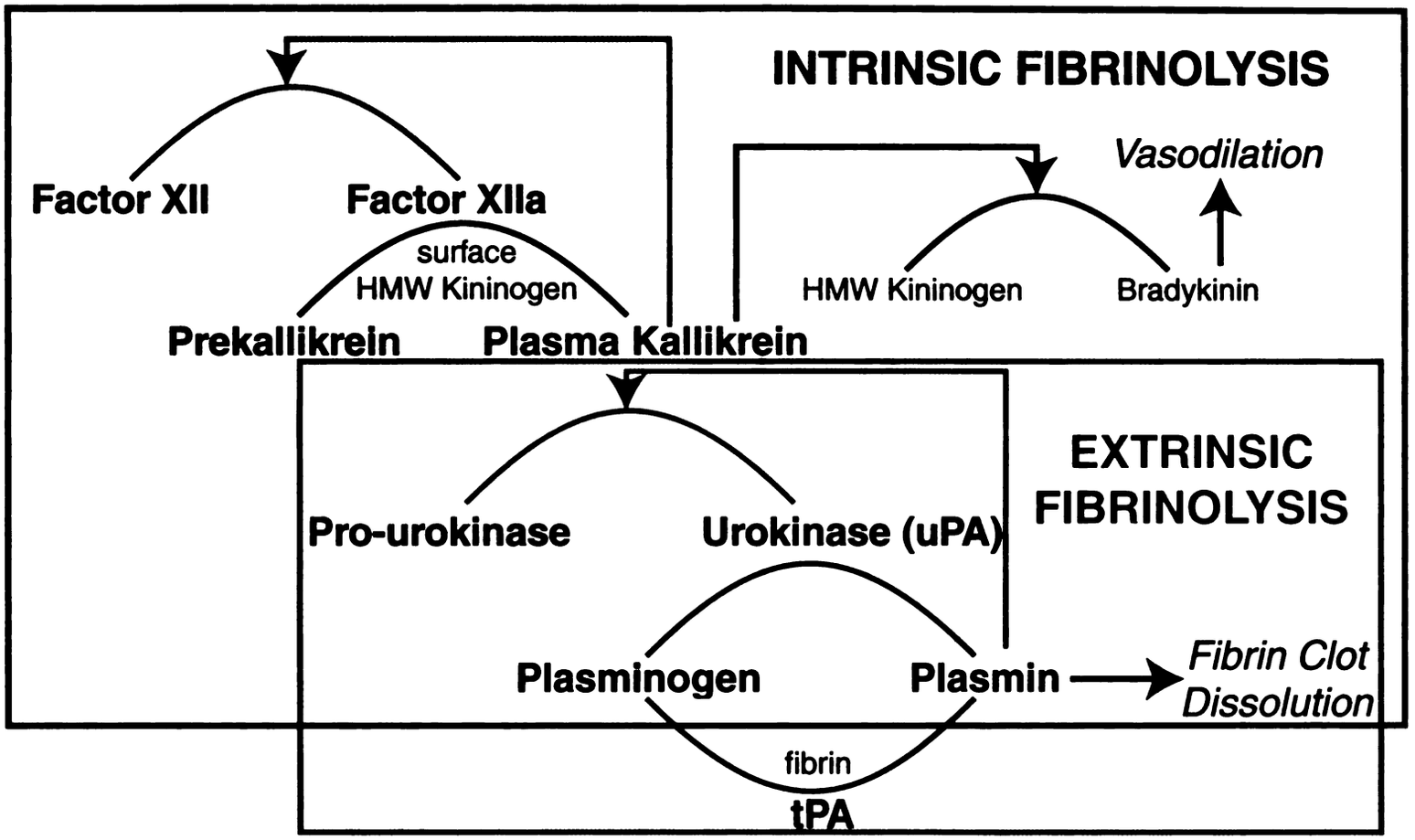

Figure 1-1. The contact system-dependent intrinsic fibrinolysis pathway (black rectangle). The reciprocal activation of Factor XII by plasma kallikrein requires high molecular weight (HMW) kininogen. Plasma kallikrein cleaves HMW kininogen to release bradykinin, and activates pro-urokinase. Plasminogen in turn activates urokinase in a feedback loop. In the extrinsic fibrinolyis pathway (brown rectangle), uPA and tPA activate plasminogen.

Figure 1-2. Histology of the mouse mammary gland. The fat pad provides structural support for the growth of ducts and alveoli. Cross-section of the gland reveals various cell types. The epithelial cells are separated from the stroma (fibroblasts and adipocytes) by the basement membrane (BM).

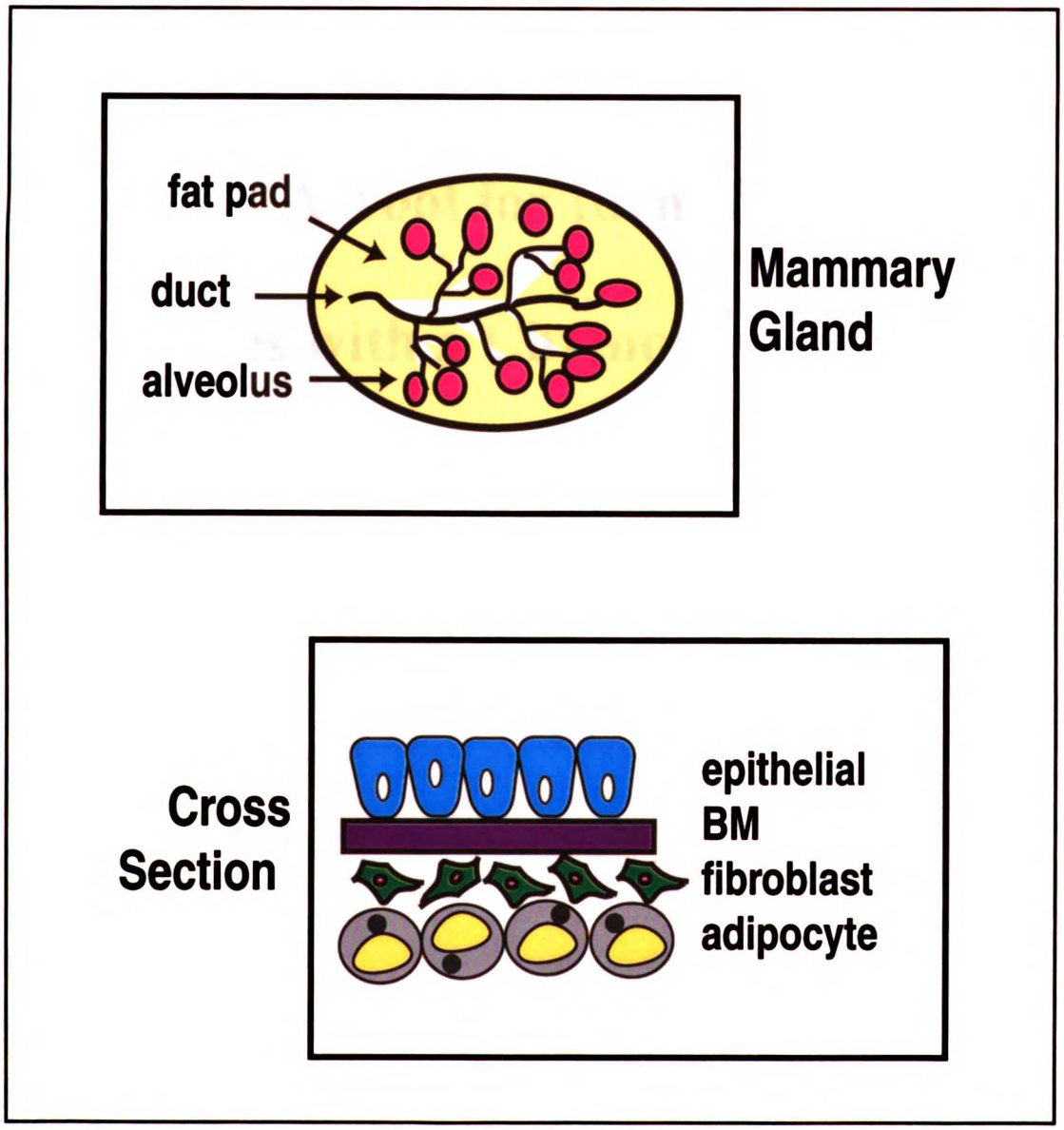

Chapter Two

Ecotin: A Tool for Identifying Serine Proteases with a Chymotrypsin Fold in Different Biological Systems

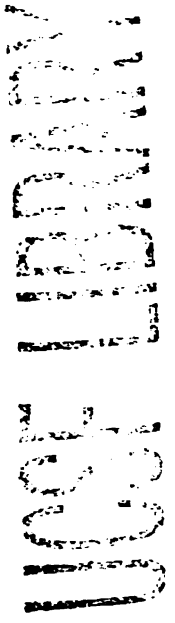

Abstract

Ecotin is a bidentate inhibitor of serine proteases that have a chymotrypsin fold, and can be altered by site-directed mutagenesis to increase its affinity and specificity. Ecotin and ecotin variants can inhibit the evolution of different biological processes where serine proteases are involved, such as tumor progression and mammary gland involution. These observations led us to develop an approach for protease identification and analysis. In this work we report that ecotin variants can be utilized as an affinity purification reagent for the purification of target enzymes. Urokinase-type plasminogen activator (u-PA) was retained on an ecotin affinity column constructed using ecotin-RR (M84R, M85R), and remained fully active after elution from the column. We subsequently showed that u-PA could be be isolated from more complex mixtures such as the conditioned media of the PC-3 prostate cancer cell line and whole tissue lysates derived from involuting mouse mammary glands. In addition to secreted proteases, a type-II transmembrane protease known as membrane-type serine protease 1 (MT-SP1) was isolated from the Triton X-100 solubilized cell lysates from the PC-3 cell line. This affinity purification technique also proved to be useful for the isolation of a thrombin-like enzyme from snake venom using an affinity matrix directed against thrombin (ecotin TSRR/R). Ecotin is a fold-specific serine protease inhibitor that recognizes the chymotrypsin fold. Interestingly, in mammary gland lysates, haptoglobin, which contains a chain that is a serine protease homologue without catalytic activity, also bound to the ecotin-RR affinity column. Binding to haptoglobin does not prevent proteolytic inhibition of u-PA, suggesting that haptoglobin can serve as a carrier for ecotin within serum. Herein we show that ecotin and ecotin variants provide robust tools for the isolation and characterization of proteins

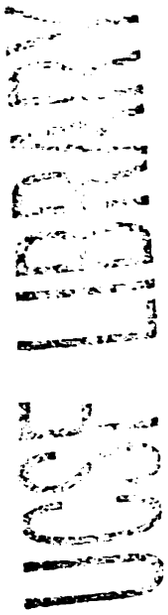

with chymotrypsin fold and can assist in the understanding of the role of these molecules in different biological processes. (Helena C. Castro, Toshihiko Takeuchi, Sushma Selvarajan, Russolina B. Zingali and Charles S.Craik; manuscript in preparation).

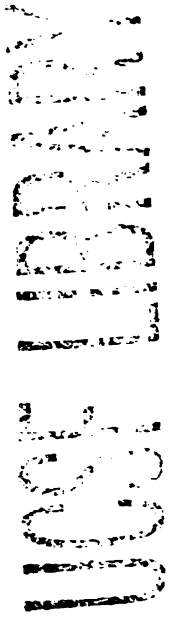

Introduction

Serine proteases with a chymotrypsin fold are involved in many different biological processes, including blood coagulation (1), metastasis of cancer cells (2), fibrinolysis (3) and mammary gland involution (4). One powerful tool for the investigation and characterization of serine proteases is a "fold-specific" inhibitor ecotin (5, 6), which is a periplasmic *Escherichia coli*-derived protein that has an unusually broad specificity and strongly inhibits proteases like trypsin, chymotrypsin, elastase, factor Xa, kallikrein and factor XIIa (7). This inhibitor uses two distinct binding sites to recognize its target, and these binding sites can be engineered to potently and specifically inhibit proteases such as urokinase-type plasminogen activator (uPA) (6, 8). Since wild type ecotin is able to purify recombinant trypsinogen expressed in *E. coli* (9), ecotin mutants should be able to interact with a vast array of serine proteases and may be developed to isolate and characterize proteases from a variety of biological samples.

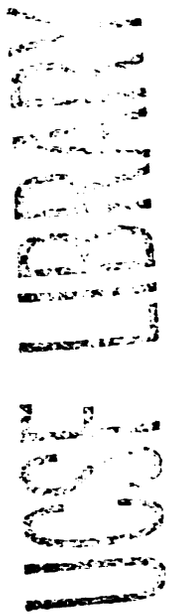

Tissue culture cell lines can serve as valuable models for cancer and cancer progression. We have been utilizing the human PC-3 prostate carcinoma cell line (10) as a model of prostate cancer. This cell line expresses the serine protease u-PA (11), and we have recently reported the expression of membrane-type serine protease 1 (MT-SP1) (12). Isolation of proteases such as u-PA from the conditioned media and/or MT-SP1 from cell lysates would be valuable for the characterization of these proteases and may serve as a means of discovering novel serine proteases derived from cell lines. Of greater complexity would be the isolation of proteases directly from tissue lysates. Serine proteases have been implicated in mammary gland involution (13), and ecotin may allow isolation and identification of proteases directly from involuting murine mammary

glands. Snake venom also has been reported to contain serine proteases of the trypsin family (14,15). Isolation of proteases from snake venom may allow *in vitro* characterization of components within the envenomation process. In the present work, proteins from these diverse biological sources were purified using affinity columns that contained mutant ecotins tethered to an agarose matrix, allowing simple and rapid purification of chymotrypsin-fold proteins.

Materials and Methods

Materials

Snake venom was obtained from *Lachesis muta,* cyanogen bromide-activated agarose and haptoglobin were purchased from Sigma (St Louis, MO). PC-3 (CRL-1435) cells were obtained from American Type Culture Collection (Rockville, MD) and grown according to the supplier's instructions. Human u-PA, SPECTROZYME®UK substrate and anti-u-PA polyclonal antibody were obtained from American Diagnostica (Greenwich, CT). All other reagents were obtained from Sigma or Fisher Scientific unless otherwise noted.

Preparation of ecotin affinity column

Ecotin mutants used in this study were ecotin-RR (M84R and M85R) constructed against u-PA, and ecotin-TSRR/R (V81T, T83S, M84R, M85R and D70R), against thrombin and u-PA. They were purified from *E. coli* as described (5).

Affinity columns were prepared by incubating the engineered ecotin (45 mg) with cyanogen bromide-activated agarose (15 mL) overnight in 100 mM Na bicarbonate (pH 8) at 4°C. The ecotin column was washed extensively with phosphate-buffered saline

(PBS) pH 7.5 and any unbound ecotin was washed out using 50 mM glycine, 100 mM NaCl, pH 3.0. The final product was equilibrated with PBS and stored at 4°C.

Sample preparation

-Standard serine protease

Human urokinase-type plasminogen activator (3000 IU) was diluted on 3 ml of PBS and applied directly to the ecotin-RR column.

-Conditioned media of prostate cancer cells (PC-3)

The PC-3 (CRL-1435) cell line was grown at 37°C in serum-free medium in a 100-mm dish and the supernatant was collected when cells had reached 90% confluency. This material (40 mL) was dialyzed against PBS, concentrated four fold and stored at 4°C until applied directly to the ecotin-RR column.

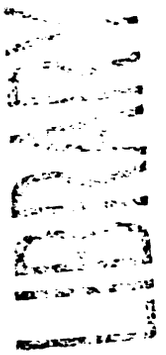

–PC-3 Cell Lysates

The PC-3 cell line was grown to 90% confluency as listed above. The cells on the plate were washed twice with PBS. After washing, the cells were lysed with 1% Triton X-100, 5 mM EDTA in PBS. The cell lysate was collected and centrifuged, and the supernatant (10 mL) was collected and applied to an ecotin-RR column.

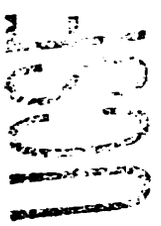

-Mammary gland cells

Female CF1 mice were crossed with CD1 males (Charles River Biologicals, Wilmington, MA) and allowed to undergo a normal pregnancy. The pups were weaned following 7-10 days of lactation (day 0 of involution) and the dams were sacrificed on day 5 of involution. Freshly isolated mammary tissue was snap frozen in liquid nitrogen and then homogenized in RIPA buffer (50mM Tris-Cl, pH 8.0, 150 mM NaCl, 1% NP40, 0.5%

DOC, 0.1%SDS) and the supernatant was collected as described (13). The supernatant (10 mL) was dialyzed against PBS and stored at –80°C until application on the ecotin-RR column.

-Snake venom

Lachesis muta venom (50 mg) was partially purified using a Mono-Q column (H10/10) on a Pharmacia FPLC^R system. Proteins were eluted with a linear gradient of 0-1 M NaCl in 20 mM Tris pH 7.5 at a flow rate of 2 ml/min. Fractions with the major proteolytic activity were pooled (10 mL), exhaustively dialyzed against PBS and applied to the ecotin-TSRR/R column.

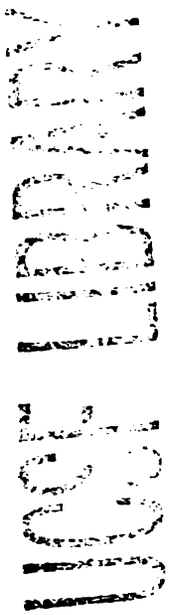

Affinity chromatography with ecotin-column

The column (3 ml) with one of the ecotin mutants bound to the agarose was initially equilibrated using 30 mL of PBS. Then it was incubated with one of the protein samples for 1 h at room temperature in a closed flow system using a Pharmacia pump (0.5 mL/min) followed by washing with PBS (30 mL). Retained fractions were eluted with buffer containing 50 mM glycine and 100 mM NaCl pH 3.0, at 1 mL/min. Fractions were neutralized with 1 M Tris (10 µl/ml). Protein elution was monitored at 280 nm using an UVIKON 860 spectrophotometer. Protein-containing fractions were pooled and concentrated 10 fold using a Centricon 10 concentrator (Amicon). The eluted material was resolved by SDS-PAGE and sequenced or analyzed by Western blotting.

PAGE and Western-blot analysis

Protein samples were electrophoresed on 10% polyacrylamide–sodium dodecyl sulfate (SDS) gels according to Laemmli (16). For immunoblot analysis, bands were transferred onto a nitrocellulose membrane and treated with Tris-buffered saline with 0.1% [v/v] Triton X-100 (TBST) containing 5% (w/v) nonfat dry milk. The membrane was probed with a 1:5000 dilution of the specific antibody in the same buffer for 1 h and washed 3 times with TBST. A 1:5000 dilution of goat anti-rabbit horseradish peroxidase conjugated serum (Pierce) was applied in TBST-1% milk and incubated for 1 h with the membrane. The membrane was washed and antibody-bound protein bands were detected by enhanced chemiluminescence (12).

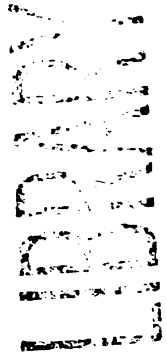

Substrate gels (zymography)

Samples were run on SDS-polyacrylamide gels containing 3 mg/mL (dry wt) gelatin as a substrate. Gels were washed with 2.5% Triton X-100 for 30 min, then incubated with 20 mM Tris-HCl buffer, pH 8.0, containing 5 mM $CaCl_2$ and 0.02% NaN_3, for 12 h at 37°C. Cleavage of the gelatin by proteases results in clear bands upon staining with Coomassie Blue R250 (12). Plasminogen gels were prepared by adding plasminogen (50 μg/mL) to the gelatin. For preparation of casein-plasminogen gels, gelatin was replaced with 1 mg/mL casein and 10 μg/ml plasminogen.

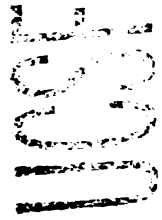

N-terminal sequencing

Proteins were resolved on SDS-PAGE, electrotransferred to a PVDF membrane and sequenced on a Perkin-Elmer Procise 491 by the Biomolecular Resource Center of the University of California, San Francisco.

Amidolytic activity

For urokinase assays, hydrolysis of the chromogenic substrate SPECTROZYME®UK (Cbo-L-(γ)Glu(α-t-BuO)-Gly-Arg-pNA.2AcOH) was measured using a Thermomax Microplate ELISA Reader (Molecular Devices, Menlo Park, CA). Ecotin-RR (2 nM) was incubated with haptoglobin (2 μM) in 50 mM Tris-HCl containing 50 mM NaCl and 10 mM $CaCl_2$ (pH 8.0). Following a 30-min equilibration at room temperature, two aliquots were taken for analysis. One was subjected to electrophoresis on a non-denaturing gel to observe the ecotin-haptoglobin complex formation as described (17). u-PA (1 IU) was added to the other aliquot and the reaction was initiated after 2 min at 37°C by addition of SPECTROZYME®UK (0.2 mM, final concentration). Absorbance was followed at 450nm.

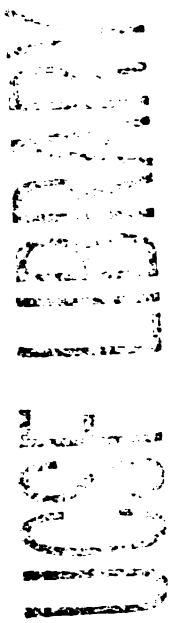

Fibrinogen clotting

Fibrinogen clotting was measured in the Thermomax Microplate ELISA Reader. Ecotin (1-50 μM) was incubated with *Lachesis muta* thrombin–like enzyme (LM-TL) (2 nM) in 10 mM Tris-HCl, 10 mM Hepes, 100 mM NaCl, 0.1 % PEG 8000 (pH 7.5). Following a 5-min equilibration at room temperature, reaction was initiated by addition of fibrinogen 4 mg/mL (dry wt) and monitored at 405 nm as described (18).

Results and Discussion

In this work, we have evaluated the utility of the serine protease inhibitor ecotin and ecotin variants as affinity chromatography reagents for the purification of proteases from diverse biological sources. Ecotin can interact with target proteases using two distinct binding sites, and these binding sites can be fine tuned to potently and specifically inhibit a target of interest (6, 8). Thus these ecotin affinity columns may be tailored to capture proteases of interest. Ecotin and variant ecotins can inhibit proteases in the low nanomolar to subnanomolar range, suggesting the formation of stable complex. The inhibitory effects of ecotin also have been observed *in vivo*, suggesting that complex formation can be achieved within complex biological mixtures (19). The chromatographic efficiency of ecotin variants as affinity reagents was analyzed for different biological samples ranging from partially purified snake venom to tissue lysates.

For the first control experiment, commercial human urokinase-type plasminogen activator (3000 IU) was suspended in PBS (3 mL) and applied to an ecotin-RR affinity column according to Materials and Methods. The enzyme appeared as a diffuse band on SDS-PAGE prior to application on the column and following elution at pH 3.0 was recovered as a distinct band at 52 kDa (Fig. 1A). This band was recognized by u-PA antibodies (Fig.1B) and was also fully active upon plasminogen gels after elution (Fig. 1C). About 95% of the original activity was recovered suggesting that the diffuse material in Fig. 1A (Lane 1) is a contaminant. These results show that binding of u-PA to the ecotin-RR column is reversible and suggest that the column will be useful for purification of other serine proteases with a chymotrypsin fold.

u-PA is expressed by the PC-3 cell line, as assayed by ELISA (11). It would be of interest to develop techniques to isolate u-PA and other proteases derived from tissue culture cell lines for further characterizing the role of these chymotrypsin-fold proteases in cancer progression. Thus we have applied the ecotin-RR affinity column to test whether u-PA can be captured from the conditioned media of the PC-3 cell line. The supernatant from PC-3 cells grown to confluency was concentrated four fold and loaded onto an ecotin-RR column as described in Materials and Methods (Fig. 2A). The eluted material appeared as one band of about 52 kDa on SDS-PAGE and could also be observed on a gelatin-plasminogen gel and following Western blotting using u-PA antibodies (Fig. 2A inset). The N-terminal sequence of this band confirmed the identity as u-PA (Table 1). This result shows that the affinity column is effective in separating this enzyme from all of other proteins secreted into the culture medium by these cancer cells.

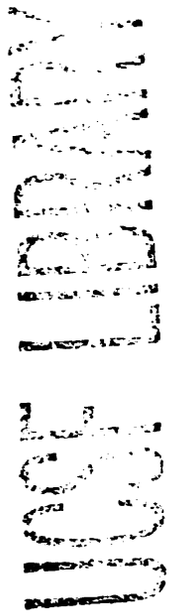

The PC-3 cell line also expresses membrane-type serine protease 1 (MT-SP1) (12). Unlike u-PA, MT-SP1 is not secreted and remains localized to the extracellular surface. Capture of MT-SP1 and other membrane localized proteases may be possible from solubilized cell lysates. Since ecotin-RR is a subnanomolar inhibitor of MT-SP1 (12), this affinity matrix should allow capture of MT-SP1. Indeed, direct application of PC-3 Triton X-100 extracts (Figure 2B, lane 1) allowed the capture of three high molecular weight bands (Figure 2B, lane 2). Immunoblotting with anti-MT-SP1 antibodies confirmed the identity of the 87 kDa band as the full-length MT-SP1 protein (Figure 2B, lane 3). Thus, ecotin-RR affinity columns are capable of capturing uPA from the conditioned media and MT-SP1 from the solubilized cell lysates.

Urokinase plasminogen activator has also been implicated in processes such as cell migration and tissue remodeling, which require extracellular proteolytic activity (20). Since ecotin-RR affinity chromatography was capable of capturing u-PA in other conditions, we tested whether u-PA could be captured from lysates of involuting mouse mammary glands. Whole-cell lysate (10 mL) was loaded onto an ecotin-RR column and incubated for 1 h as described in Materials and Methods (Figure 3A). SDS-PAGE showed proteins of about 48 kDa and 80 kDa in the material eluted at pH 3.0 that also exhibited proteolytic activity on substrate gels containing casein and plasminogen (Figure 3A, inset). Western blot with u-PA antibodies recognized the 48-kDa band indicating that u-PA was retained on the column and eluted at pH 3.0 (Figure 3A inset). We have identified the 80 kD proteolytic activity as plasma kallikrein (Selvarajan, S., Lund, L. R., Takeuchi, T., Craik, C. S., and Werb, Z., unpublished results). On the other hand, N-terminal amino acid sequencing identified the 80 kDa band seen by SDS-PAGE analysis as haptoglobin (Table I). Plasma kallikrein was likely masked by this haptoglobin band. Haptoglobin (Hp) is a α_2-acidic glycoprotein with hemoglobin-binding capacity, present in most body fluids of humans and other mammals (21). It is a tetramer composed of two light chains (α) and two heavy chains (β) linked by disulfide bridges. The β-chain is homologous to members of the mammalian serine protease family (22). Ecotin-RR affinity chromatography and immunoassays using trypsin antibodies (3A inset) reinforce the prediction that Hp conserves a chymotrypsin-like structure (23). However, the Ser195 and His57, which are required for enzymatic activity, are missing in haptoglobin, resulting in an inactive protein of the chymotrypsin fold (22, 23). On that account and since haptoglobin (2 μM) does not interfere with ecotin-RR binding (2 nM) to u-PA

(Figure 3B), it is feasible that Hp interacts with ecotin through its secondary binding site, allowing access of the primary binding site of ecotin for inhibition of proteases such as u-PA.

In vivo experiments have shown that ecotin-RR has a half-life of about 12 h (Wang, C-I, unpublished), unusually long for peptides and small proteins. Since haptoglobin does not affect ecotin's ability to inhibit proteases, our data suggest that haptoglobin may serve as a reservoir or carrier for ecotin in plasma. Experiments incubating bovine serum with ecotin-RR column confirmed haptoglobin as the major ecotin binding protein in the plasma (data not shown). Although we cannot discard the possibility of contamination from plasma during collection of mammary gland cells, the large amounts of haptoglobin that were recovered by the affinity column suggest that haptoglobin is expressed in the mammary gland, most likely by mammary adipocytes. Biosynthesis of haptoglobin normally occurs in the liver, but it has also been reported to be synthesized in adipose tissue and in the lung, where it is thought to have antioxidant and antimicrobial activities (24, 25).

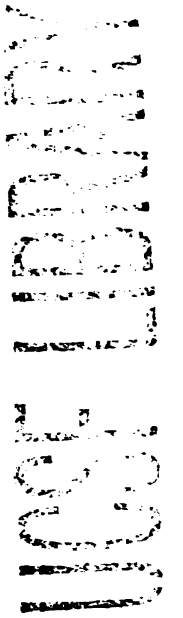

Finally another source of chymotrypsin-fold serine proteases that may be amenable to affinity purification is snake venom. Brazilian snake venoms alter blood coagulation and several procoagulant proteins from these venoms are serine proteases of the trypsin family (26, 27, 28). Therefore we have been interested in characterizing a protease of the chymotrypsin fold similar to thrombin from *Lachesis muta* venom. For this purpose, we have utilized a variant of ecotin called ecotin-TSRR/R that can target α-thrombin.

Lachesis muta venom (50 mg) was first partially purified on a Mono-Q (H10/10) column (Pharmacia) and non-retained material showing protease activity on gelatin gels was applied to the ecotin-TSRR/R affinity column (Fig. 4). The material eluted at pH 3.0 exhibited a 16-kDa band on SDS-PAGE (Fig. 4, inset) and a 40-kDa band with catalytic activity on substrate gels (Fig. 4B). The N-terminal sequence of the 16-kDa band (Table 1) revealed 90% identity with the N-terminal sequence of LM-TL, a thrombin-like protein (228 aa) purified from this venom (29). Since the literature describes proteases in brazilian snake venom that generate peptides or small proteins (30, 31), the inactive 16-kDa band may be a degradation product of the 40-kDa band. In order to verify the identity of the 40-kDa band, we purified LM-TL from *L. muta* venom using the original method (29) and tested for inhibition of its proteolytic activity by the ecotin mutant, using a fibrinoclotting assay. Ecotin TSRR/R inhibited LM-TL fibrinoclotting activity with an IC_{50} of 10 μM (Fig. 4C). Since ecotin can form a stable complex with LM-TL, structural characterization of this enzyme and its mechanism of binding to ecotin may be facilitated, since ecotin previously has enhanced the crystallization of proteases (32).

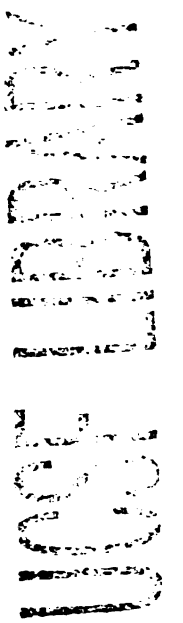

In summary this work showed that mutant ecotins are able to interact with a vast array of serine proteases and may be developed to isolate and characterize proteases from diverse biological samples. This technique should not only assist in the isolation of proteases but may also be useful in structural, pharmacological, and biological studies.

Acknowledgments

We thank Dr Martha Sorenson for careful revision of the manuscript. This study was supported by National Institutes of Health Grant CA72006 and by CAPES (Brazil).

References

1. Davie, E.W., Fujikawa, K., & Kisiel, W. (1991) The coagulation cascade: Initiation, maintenance and regulation. *Biochemistry* **30**, 10363-10370.

2. Andreasen, P.A., Kjoller, L., Christensen, L., & Duffy, M.J. (1997). The urokinase-type plasminogen activator system in cancer metastasis: A review. *Int. J. Cancer* **72**, 1-22.

3. Chandler, W.L. (1996) The human fibrinolytic system. *Crit. Rev. Oncol. Hematol.* **24**, 27-45.

4. O'Grady, R.L., Upfold, L.I. & Stephens, R.W. (1981) Rat mammary carcinoma cells secrete active collagenase and activate latent enzymes in the stroma via plasminogen activator. *Int. J. Cancer* **28**, 509-515.

5. Wang, C.I., Yang, Q. & Craik, C.S. (1995) Isolation of a high affinity inhibitor of urokinase-type plasminogen activator by phage display of ecotin. *J. Biol. Chem.* **270**, 12250-12256.

6. Yang, S.Q. & Craik, C.S. (1998) Engineering bidentate macromolecular inhibitors for trypsin and urokinase-type plasminogen activator. *J. Mol. Biol.* **279**, 1001-1011.

7. McGrath, M.E., Gillmor, S.A. & Fletterick, R.J. (1995) Ecotin: Lessons on survival in a protease-filled world. *Prot. Sci.* **4**, 141-148.

8. Yang, S.Q., Cheng-I W., Gillmor, S.A., Fletterick, R.J. & Craik, C.S. (1998) Ecotin: a serine protease inhibitor with two distinct and interacting binding Sites *J. Mol. Biol.* **279**, 945-957.

9. Lengyel, Z., Pal, G. & Sahin-Toth, M. (1998) Affinity purification of recombinant trypsinogen using immobilized ecotin. *Protein Expr Purif.* **12**, 291-294.

10. Kaighn, M.E., Narayan, K.S., Ohnuki, Y., Lechner, J.F., & Jones, L.W. (1979) Establishment and characterization of a human prostatic carcinoma cell line (PC-3). *Invest. Urology* **17**, 16-23.

11. Yoshida, E., Verrusio, E.N., Mihara, H., Oh, D., & Kwaan, H.C. (1994) *Cancer* Enhancement of the expression of urokinase-type plasminogen activator from PC-3 human prostate cancer cells by thrombin. *Cancer Res.* **54**, 3300-3304.

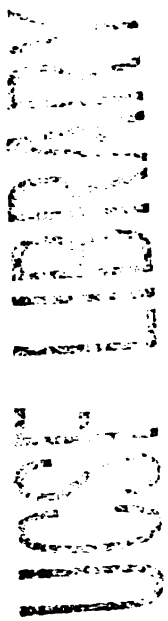

12. Takeuchi, T., Shuman, M.A. & Craik, C.S. (1999) Reverse biochemistry: Use of macromolecular protease inhibitors to dissect complex biological processes and identify a membrane-type serine protease in epithelial cancer and normal tissue. *Proc. Natl. Acad. Sci. U. S. A.* **96**, 11054-11061.

13. Talhouk, R.S., Bissel, M.J. & Werb, Z. (1992) Coordinated expression of extracellular matrix-degrading proteinases and their inhibitors regulates mammary epithelial function during involution. *J. Cell Biol.* **118**, 1271-1282.

14. Markland, F.S. (1998) Snake venoms and the hemostatic system. *Toxicon* **12**, 1749-1780.

15. Pirkle, H. (1998) Thrombin-like enzymes from snake venoms: An update inventory. *Thromb. Haemost.* **79**, 675-683.

16. Laemmli, U.K. (1970) Cleavage of structural proteins during the assembly of the head of bacteriophage T4. *Nature* **227**, 680-685.

17. Zingali, R.B., Jandrot-Perrus, M., Guillin, M.C. & Bon. C. (1993) Bothrojaracin: A new thrombin inhibitor isolated from *Bothrops jararaca* venom. Characterization and mechanism of thrombin inhibition. *Biochemistry* **32**, 10794-10802.

18. Ribeiro, J.M.C., Scheneider,M. & Guimarães, J.A. (1995) Purification and caracterization of prolixin S (nitrophorin 2), the salivary anticoagulant of the blood sucking bug *Rhodnius prolixus*. *Biochem. J.* **308**, 243-249.

19. Elfman, F., Takeuchi, T., Craik, C., Shuman, M. & Cunha, G. (1999) Retarded development and apoptosis of the rat ventral prostate by selective inhibition of serine proteases. (Submitted in *J. Biol. Chem.*).

20. Warburton, M.J., Dundas, S.R., Gusterson, B.A & O'Hare M.J. (1996). Regulation of urokinase-type plasminogen activator production by rat mammary myoepithelial cells. *Exp. Cell. Res.* **228**, 76-83.

21. Dobryszycka, W. (1997) Biological functions of haptoglobin-New pieces to an old puzzle. *Eur. J. Clin. Biochem.* **35**, 647-654.

22. Kurosky, A., Barnett, D.R., Rasco, M.A., Lee, T.H. & Bowman, B.H (1974) Evidence of homology between the beta-chain of human haptoglobin and the chymotrypsin family of serine proteases. *Biochem. Genet.* **11**, 279-293.

23. Greer, J. (1980) Model for haptoglobin heavy chain based upon structural homology. *Proc. Natl. Acad. Sci. U.S.A.* **77**, 3393-3397.

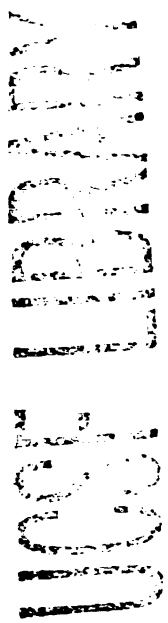

24. Friedricks, W.E., Navarijo-Ashbaugh, A.L., Bowman, B.H. & Yang, F. (1995) Expression and inflamatory regulation of haptoglobin gene in adipocytes. *Biochem. Biophys. Res.* **209**, 250-256.

25. Yanf, F., Friedricks, W.E., Navarijo-Ashbaugh, A.L., Degraffenried, L.A., Bowman, B. H. & Coalson, J.J. (1995) Cell type-specific and inflamatory induced expression of haptoglobin gene in lung. *Lab. Invest.* **73**, 433-439.

26. Maruyama, M., Suguki, M., Yoshida, E., Mihara, H. & Nakajima, N. (1992) Purification and characterization of two fibrinolytic enzymes from *Bothrops jararaca* (jararaca) venom. *Toxicon* **30**, 853-864.

27. Zhang, Y., Wisner, A., Maroun, R.C., Choumet, V., Xiong, Y. & Bon, C. (1997) *Trimerusurus stejneri* snake venom plasminogen activator. *J. Biol. Chem.* **272**, 20531-20537.

28. Aguiar, A.S., Alves, C.R., Melgarejo, A. & De-Simone, G. (1996) Purification and partial characterization of a thrombin-like/gyroxin enzyme from Bushmaster (*Lachesis muta rhombeata*) venom. *Toxicon* **34**, 555-565.

29. Silveira, A.M.V., Magalhães, A., & Diniz, C.R. (1987) Purification and properties of the thrombin-like enzyme from the venom of *Lachesis muta muta. Int. J. Biochem.* **103**, 596-605.

30. Paine, M.J.I., Desmond, H.P., Theakston, R.D.G. & Crampton, J.M. (1992) Purification, cloning and molecular characterization of a high molecular weight hemorrhagic metalloprotease, jararrhagin, from *Bothrops jararaca* venom. *J. Biol. Chem.* **32**, 22869-22876.

31. Usami, Y., Fujimura, Y., Miura, S., Shima, H., Yoshida, A., Hirano, K., Suzuki, M. & Titani, K. (1994) A 28-kDa protein with disintegrin-like structure (jarahagin-C) purified from *Bothrops jararaca* venom inhibits collagen- and ADP-induced platelet aggregation. *Biochem. Biophys. Res. Commun.* **201**, 331-339.

32. Perona, J.J., Tsu, C.A., Craik, C.S. & Fletterick, R.J. (1997) Crystal structure of an ecotin-collagenase complex suggests a model for recognition and cleavage of the collagen triple helix. *Biochemistry*. **36**, 5381-5392.

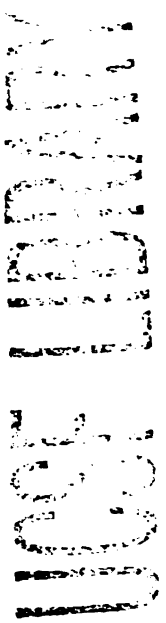

Figure 2-1.

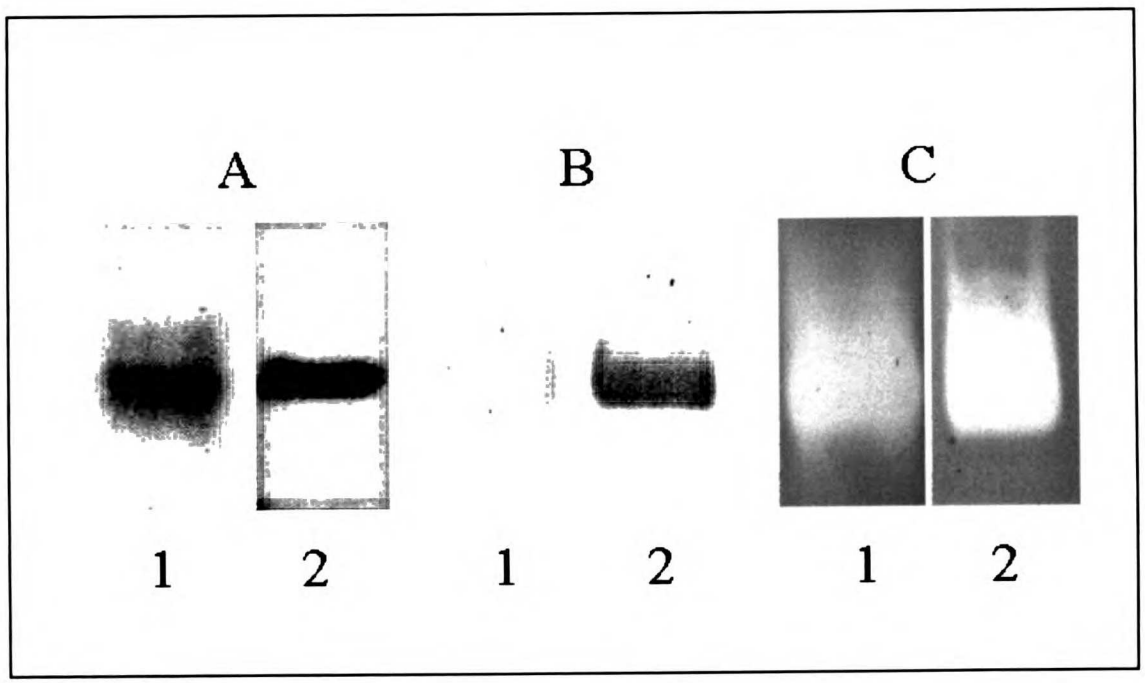

Figure 2-1. Analysis of commercial u-PA using ecotin-RR affinity column. SDS-PAGE (A), Western blot analysis (B) and plasminogen-gelatin gels (C) of commercial u-PA before application on the ecotin-RR column (Lane 1) and after elution at pH 3.0 (Lane 2). Each lane contains 5 μg of enzyme.

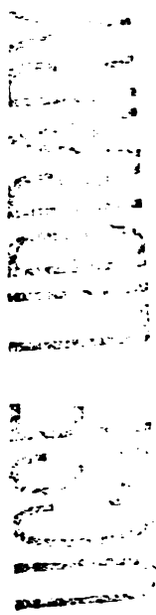

Figure 2-2.

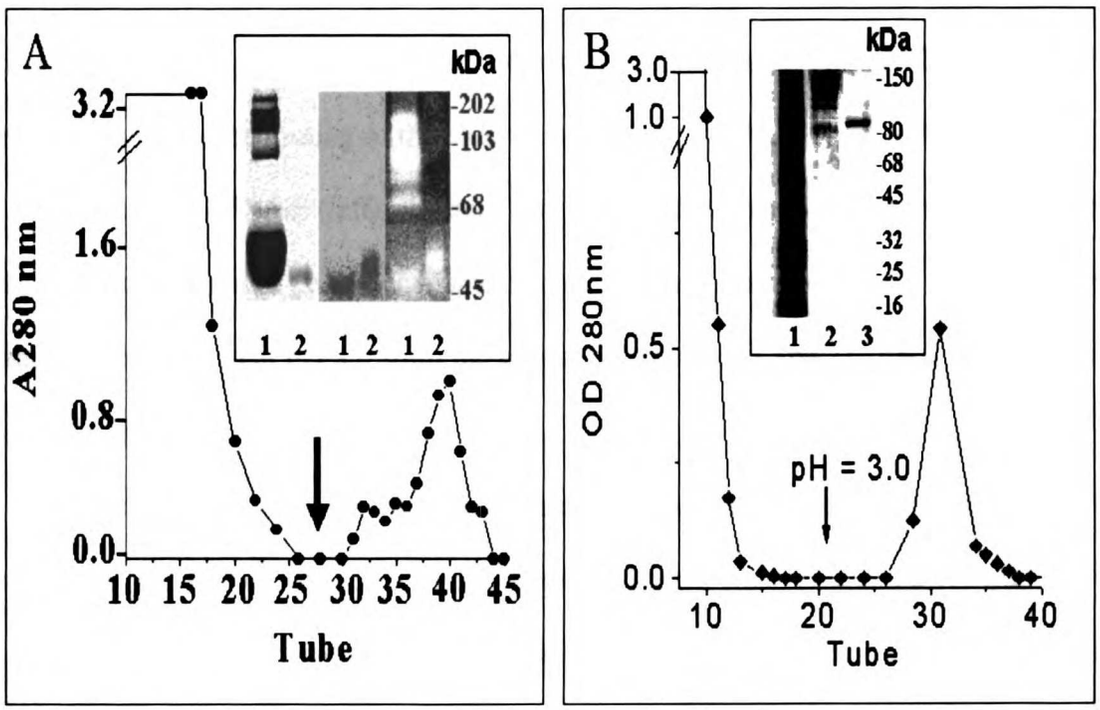

Figure 2-2. Analysis of prostate cancer cells using the ecotin-RR affinity column.

A) Elution pattern of conditioned medium from prostate cancer cells. The graph shows the elution profile (1 mL/fraction) following application of 10 mL of concentrated conditioned medium of untreated cancer cells to a column equilibrated with PBS pH 7.5. Arrow indicates the beginning of the elution step using 50 mM glycine in 100 mM NaCl, pH 3.0. Inset: SDS-PAGE (left), Western blot using u-PA polyclonal antibodies (center) and plasminogen-gelatin gels (right) of untreated medium from cancer cell cultures (Lane 1) and material eluted at pH 3.0 from the ecotin-RR column (Lane 2). Each lane contains 8 μg of sample protein.

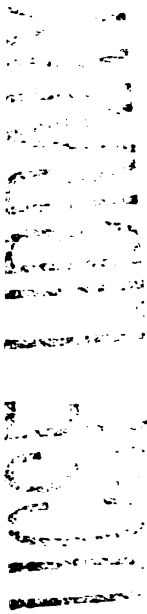

B) Analysis of eluted material from Tween-extracted cell membrane from prostate cancer cells (PC_3) on ecotin-RR column. Arrow indicates when elution buffer was loaded. Inset: SDS-polyacrylamide gel (10%) electrophoresis of extracted cell membrane material

(Lane 1), affinity eluate (Lane 2), imunoreactivity probed with MTSP1 antibodies (Lane 3).

Figure 2-3.

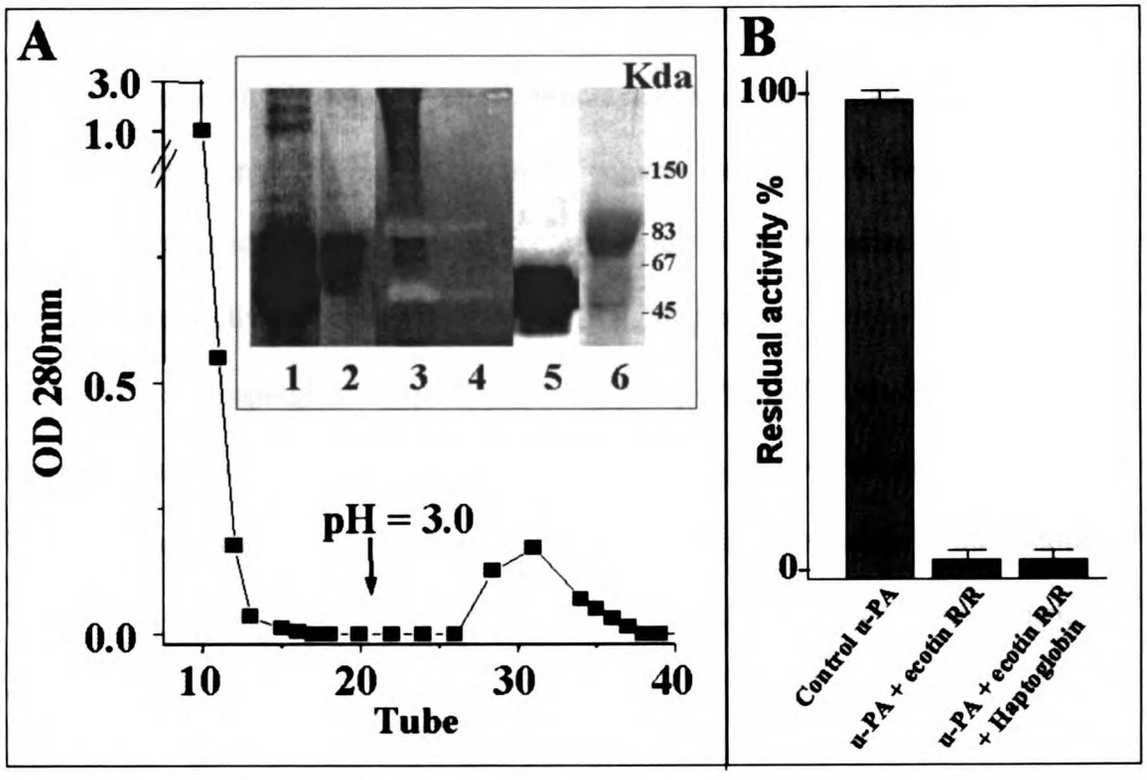

Figure 2-3. Analysis of mammary gland lysate using the ecotin-RR affinity column.

A) Elution profile following application of 10 mL of sample to the column. Fractions 2 mL/min. Arrow indicates the beginning of the elution at pH 3.0. Inset: SDS-PAGE (left) and substrate gels (right). Lane 1 and 3, Whole mammary gland; Lane 2 and 4, Lysate material eluted at pH 3.0 from the ecotin-RR column; Lane 5 and 6, Western blot analysis of retained material on affinity column using u-PA antibodies and trypsin antibodies respectively. Each lane contains 10 μg of protein.

B) Influence of haptoglobin (2 μM) on the inhibitory effect of ecotin-RR (2 nM) on hydrolysis of chromogenic substrate by u-PA. Experimental conditions are described in Materials and Methods. Residual activity is expressed as a percentage of the control ΔA405/min observed in control u-PA. Values are mean ± SD of three independent experiments.

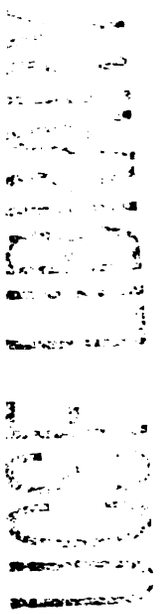

Figure 2-4.

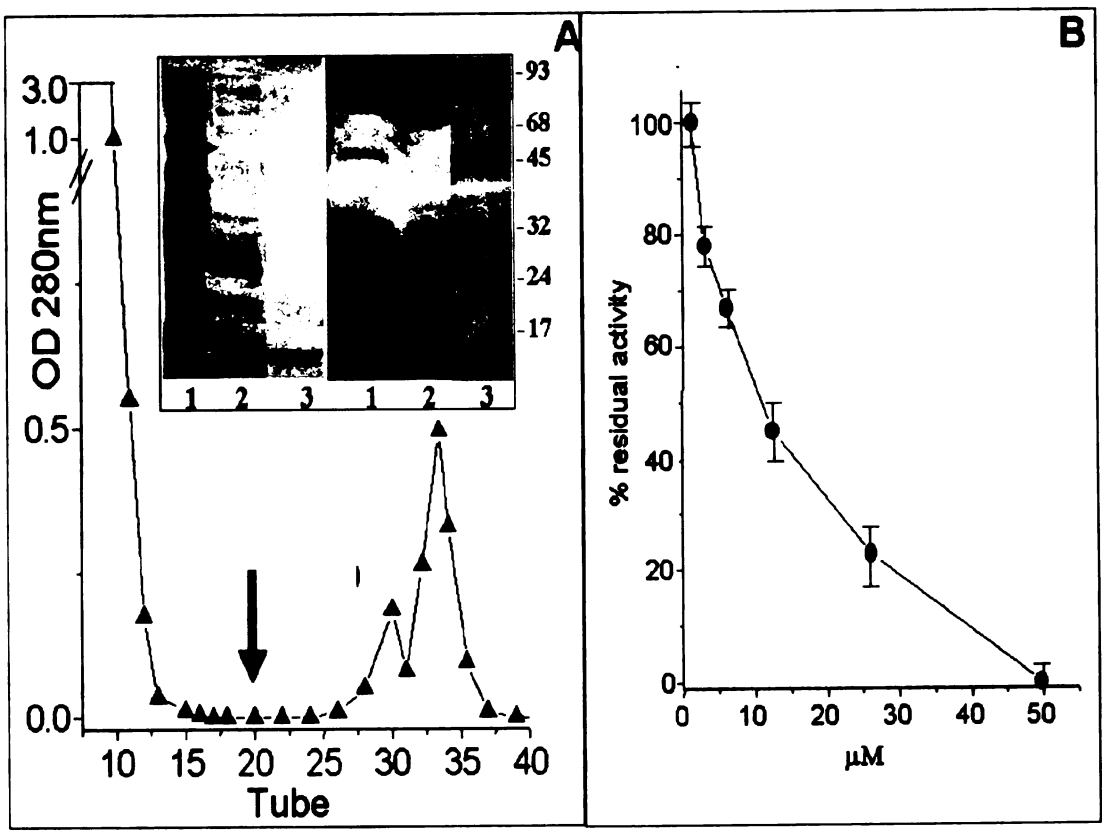
A
B
3.0
1.0
0.5
0.0
OD 280nm
10 15 20 25 30 35 40
Tube
93
68
45
32
24
17
1 2 3 1 2 3
100
80
60
40
20
0
% residual activity
0 10 20 30 40 50
μM

Figure 2-4. Analysis of snake venom using an ecotin-TSRR/R affinity column.

A) Elution profile of a partially purified snake venom. *L. muta* venom was partially purified on a Mono-Q column (FPLC) and non-retained material was applied to an ecotin-TSRR/R affinity column as described in Materials and Methods. Arrow indicates the beginning of the elution step. Inset: SDS-PAGE (left) and Substrate gel (right). Lanes 1, crude venom; Lanes 2, non-retained material from Mono-Q column; Lanes 3, material eluted at pH 3.0 from ecotin-TSRR/R column. Each lane contains 10 μg of protein.

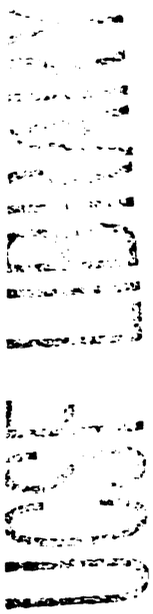

B) Inhibitory effect of ecotin-TSRR/R upon fibrinoclotting activity of purified LM-TL. The enzyme (60 nM) was preincubated for 5 min at room temperature with different concentrations of ecotin-TSRR/R (1- 50 μM). Fibrinogen (4 mg/mL) was then added to the assay and the absorbance at 405 nm was recorded continuously. Residual activity is expressed as a percentage of the control ΔA405/min observed in the absence of the ecotin. Values are mean ± SD of three independent experiments.

Table 2. N-Terminal sequence of proteins from retained material of supernatant of cancer cells, mammary gland cell lysate, and snake venom. Protein identification was determined using the Swiss Protein Data Base.

Source	kDa	Sequence	Identity
Prostate cancer cells	52	IIGGEFTTIENQPWFFAAI Y	uPA
Mammary gland lysate	~80	IELGNDDAKGEFDWQAK MIS	Haptoglobin α–chain
		VIGGSMAMDFSDPSXPK PPE	Haptoglobin β-chain
Snake venom	16	VVGGDEXNINEHRXLVL VYX	LM-TL

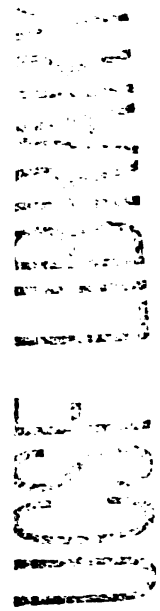

Addendum

Methods

Ecotin treatment and mammary lysates

For ecotin treatment, female CF1 mice crossed with CD1 males were allowed to undergo a normal pregnancy. The number of pups was normalized to 8 for each experiment and they were weaned following 7-10 days of lactation (day 0 of involution). The mice were injected intraperitoneally with 100 μg of ecotin WT, ecotin RR or the carrier PBS twice a day on days 1-4 of involution and the animals were killed on day 5 of involution (12 hours after the last ecotin injection). Freshly isolated mammary glands were snap frozen in liquid nitrogen and stored at –80^{O}C. Frozen mammary tissue was homogenized in RIPA buffer (50 mM Tris-Cl, pH 8.0, 150 mM NaCl, 1% NP40, 0.5% DOC, 0.1%SDS) and the supernatant (mammary lysate) was collected for western blot analysis of ecotin levels using a rabbit polyclonal anti-ecotin antibody.

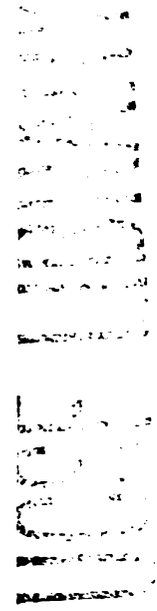

"Farwestern" blot

HMW and LMW human uPA (American Diagnostica Inc.), bovine trypsin (Sigma), active MMP-2 and MMP-9 (Calbiochem), and mammary lysate with or without the addition of exogenous human HMW uPA were electrophoresed on an SDS-PAGE gel. Standard protocols were used to perform western blot analyses, except that for the modified "farwestern protocol" (Blanar and Rutter, 1992), 500 nM ecotin RR was used as the primary "antibody", rabbit polyclonal anti-ecotin IgG (McGrath et al., 1991) as the secondary antibody, and horseradish peroxidase-conjugated donkey anti-rabbit IgG (Amersham) as the tertiary antibody.

Results

Ecotin is detected in mammary lysates. To evaluate the utility of ecotin as an inhibitor for *in vivo* studies, mammary lysates were assayed to determine if ecotin could be detected in the mammary gland. Twelve hours after the final ecotin injection, significant amounts of ecotin were detected in animals treated with either ecotin WT or ecotin RR (Figure 2-5). This suggests that ecotin has a long half-life, and may be used to inhibit serine proteases *in vivo*. Since ecotin was detected in mammary lysates, it would appear that it circulates freely and can be used to target proteases in tissues of interest.

Ecotin can be modified for use as an "antibody". The use of ecotin RR as an "antibody" was tested using the farwestern protocol (Blanar and Rutter, 1992). Ecotin RR bound to both high and low molecular weight (H and LMW) uPA in a concentration-dependent fashion, and increasing the amount of uPA resulted in bands with increased intensity on a farwestern blot (Figure 2-6A). Ecotin can therefore be used to measure increases in the levels of target proteases. Ecotin RR did not bind to either gelatinase A or B (MMP-2 and 9), which belong to the matrix metalloprotease family, but did bind to trypsin. This indicates that it specifically binds to chymotrypsin-fold serine proteases during farwestern blotting. Using ecotin as the primary antibody, several bands including uPA were detected in involuting mammary lysate (Figure 2-6B). These data suggest that ecotin may be used as a tool to detect chymotrypsin-fold serine proteases in biological fluids.

Discussion

In addition to being used as an affinity chromatography reagent to isolate and purify chymotrypsin-fold serine proteases from complex biological mixtures, ecotin may be used as an "antibody" in the farwestern immunoblotting protocol. A combination of affinity chromatography and farwestern blotting may be an effective method to isolate and identify novel chymotrypsin-fold serine proteases. The sensitivity and specificity of the farwestern blot may be improved by modification of ecotin using a biotin-tag and subsequent use of the biotin-streptavidin system for detection.

The finding that ecotin has a long half-life *in vivo* (about 12 hours, Cheng-I Wang, unpublished data) and the fact that ecotin is detected in mammary lysates 12 hours after injection, indicates that ecotin may be an effective inhibitor *in vivo*. This novel macromolecular inhibitor was therefore used to study the function of serine proteases during mammary gland involution, as described in Chapter Three.

References

Blanar, M. A., and Rutter, W. J. (1992). Interaction cloning: identification of a helix-loop-helix zipper protein that interacts with c-Fos. Science *256*, 1014-8.

McGrath, M. E., Hines, W. M., Sakanari, J. A., Fletterick, R. J., and Craik, C. S. (1991). The sequence and reactive site of ecotin. A general inhibitor of pancreatic serine proteases from Escherichia coli. J Biol Chem *266*, 6620-5.

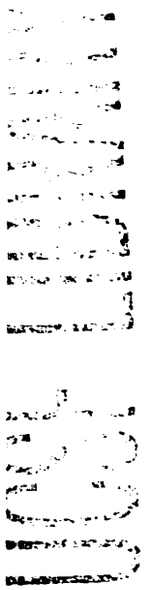

Figure 2-5.

Figure 2-6.

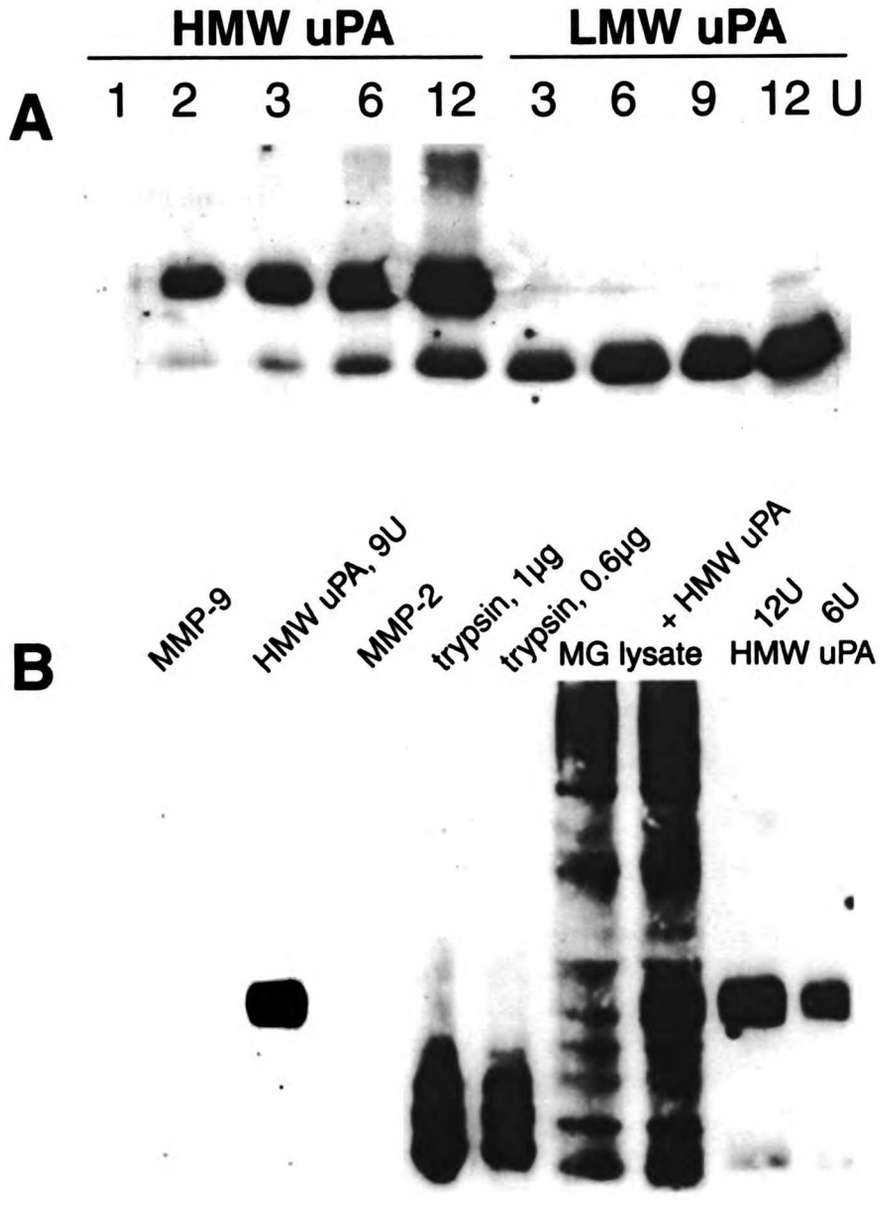

Figure 2-5. Detection of ecotin in mammary gland lysates. Western blot analysis of involuting samples from animals treated with PBS (control), ecotin WT (EcoWT), or ecotin RR (EcoRR). Ecotin RR was used as a control.

Figure 2-6. Farwestern blot using ecotin.

A) Ecotin used as a primary antibody to detect increasing amounts (1-12 international units (U) as indicated) of high molecular weight (HMW) and low molecular weight (LMW) urokinase-type plasminogen activator (uPA).

B) Use of ecotin to detect chymotrypsin like serine proteases in mammary gland lysate (MG lysate) without and with the addition of HMW uPA. HMW uPA, trypsin, gelatinase B (MMP-9) and gelatinase A (MMP-2) were used as controls.

Chapter Three

Plasminogen System Regulates Epithelial and Stromal Remodeling During Involution

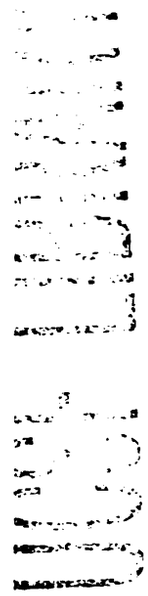

Abstract

Involution of the mammary gland is a complex remodeling process that requires extracellular proteolysis. The serine protease urokinase-type plasminogen activator (uPA) is upregulated during involution. To determine the function of uPA and related proteases during involution, a novel macromolecular inhibitor, ecotin, was used to inhibit chymotrypsin-fold serine proteases *in vivo*. Wild-type ecotin (ecotin WT) does not inhibit uPA. The variant ecotin Met84Arg/Met85Arg (ecotin RR), which is a potent inhibitor of uPA, delayed epithelial remodeling during involution. Both ecotin WT and ecotin RR inhibited the repopulation of the mammary gland with adipocytes, suggesting a role for a protease other than uPA. A yet-to-be-identified 80 kD serine protease, which was inhibited by both ecotins, may be required for stromal remodeling and adipogenesis during involution. Cleavage of the extracellular matrix (ECM) proteins entactin and fibronectin was affected by ecotin treatment. Ecotin treatment also resulted in decreased levels of the matrix metalloproteases (MMPs) gelatinase A and B, and increased levels of the cytokine transforming growth factor-β. Chymotrypsin-fold serine proteases may regulate remodeling during involution by mediating the degradation of the ECM, both by direct cleavage, and by the activation of MMPs. In addition, they may also regulate the bioavailability of cytokines such as TGF-β that regulate mammary gland function.

Introduction

Following lactation and weaning in the mouse, the mammary gland undergoes a program of morphological and biochemical changes termed involution. During involution, the secretory epithelial tissue involved in lactation is replaced with adipose tissue through apoptosis and proteolysis (Lund et al., 1996). This remodeling process involves cessation of lactation-associated gene expression, collapse of alveoli, degradation of the basement membrane and extracellular matrix (ECM) by proteolysis, apoptosis of epithelial cells, phagocytosis by macrophages, and repopulation of the gland with adipocytes (Figure 3-1). The morphology of the gland changes dramatically during involution. The secretory alveoli and epithelial cells that are the major component of the lactating gland disappear as involution proceeds (Figure 3-2).

Involution of the mammary gland involves extensive remodeling of both the epithelial and stromal components of the gland. A number of extracellular proteases including the matrix metalloproteases stromelysin-1, stromelysin-3 and gelatinase A (Dickson and Warburton, 1992; Lefebvre et al., 1992; Talhouk et al., 1992), as well as the serine proteases urokinase plasminogen activator (uPA) and tissue-type plasminogen activator (tPA) are expressed by the involuting mammary gland (Busso et al., 1989; Ossowski et al., 1979). The levels of both uPA mRNA and protein are upregulated (Lund et al., 1996), suggesting a role for this protease in tissue remodeling during involution.

The plasminogen (Plg) system of serine proteases plays an important role in various remodeling events. The zymogen Plg can be activated to plasmin by uPA and tPA (Dano et al., 1985). Plasmin can directly cleave various ECM molecules including fibronectin (Liotta et al., 1981) and laminin (Chen and Strickland, 1997), as well as

modulate the function of cytokines such as transforming growth factor–β [TGF-β; (Grainger et al., 1995; Khalil et al., 1996) and insulin-like growth factor-1 [IGF-1; (Booth et al., 1996; Campbell and Andress, 1997)]. Plasmin can also lead to ECM degradation by activating various pro-matrix metalloproteases (MMPs) including collagenase-1, stromelysin-1, and gelatinase B (Murphy et al., 1999; Werb et al., 1977). Mice that are deficient in the gene for Plg (Plg-/-) exhibit various remodeling defects including impaired wound healing and extensive fibrin deposits (Bugge et al., 1995). Mammary gland development and lactational competence is diminished in Plg-/- mice (Lund et al., 2000). Involution is retarded in these mice, and the collapse of alveolar structures and remodeling of the stroma is markedly reduced.

Since uPA is considered to be the primary activator of Plg in cell-associated processes (Dano et al., 1985), does the requirement for Plg during involution also indicate that uPA is required? Are uPA and related serine proteases required for both epithelial and stromal remodeling during involution? To answer these questions, a novel inhibitor-based "reverse biochemistry" approach (Takeuchi et al., 1999) was used to investigate the role of uPA and related serine proteases in involution. uPA, tPA and plasmin all possess a chymotrypsin fold. Ecotin is an unique macromolecular inhibitor that inhibits serine proteases with the chymotrypsin fold (Chung et al., 1983). Wild-type ecotin (ecotin WT) is a poor inhibitor of uPA, but the variant ecotin Met84Arg/Met85 Arg (ecotin RR) is a potent inhibitor of uPA (Wang et al., 1995). These inhibitors were used to determine whether uPA is required for normal involution and to analyze the function of chymotrypsin-fold serine proteases in this remodeling process. This inhibitor-based

biochemical approach reveals a requirement for chymotrypsin-fold serine proteases in epithelial and stromal remodeling during involution.

Methods

Preparation of ecotin

Ecotins were prepared and purified as previously described (Wang et al., 1995). The purified samples were tested and found to be free of endotoxin. Samples used for animal injections were diluted in phosphate buffered saline (PBS), pH 7.4.

Animal studies

Female CF1 mice were crossed with male CD1 mice and allowed to undergo a normal pregnancy. The mice lactated for 7-10 days, with the pups normalized to 8 for each experiment. Pups were removed from the mothers (day 0 of involution) and the mice were allowed to undergo 4 days of involution. Animals were injected on days 1-4 of involution with 100 μg of ecotin WT, ecotin RR or the carrier PBS. Each cohort contained 4 animals, and the experiments were repeated 4 times. The animals were sacrificed on day 5 of involution, perfused with PBS and mammary glands were collected.

Whole mounts

Whole mammary glands were placed in Carnoy's solution (3:1 ethanol:acetic acid) for 12 hours and washed with 70% ethanol followed by tap water. Washed glands were immersed in 0.2% Carmine (Sigma) stain for 24 hours, washed with 70%, 90% and 100%

ethanol and then placed in xylene for 30 minutes. Glands were stored in methylsalicylate thereafter.

Frozen sections and Oil red O staining

Glands were embedded in OCT and frozen in a dry ice/alcohol bath. 10 μM frozen sections were prepared and rinsed in distilled water and fixed in 50% ethanol. The sections were immersed in 0.2% Oil red O (Sigma) stain for 30 minutes and washed with 50% ethanol followed by distilled water. The sections were counterstained with hematoxylin.

To quantitate the area occupied by adipocytes in the mammary gland, Oil red O stained sections were photographed at 20X magnification. Adobe Photoshop software was used to calculate the area (in pixels) stained with Oil red O dye. Data were collected from 4 sections of 2 glands from each treatment group. The mean and standard deviation (S.D.) were calculated using Microsoft Excel software. For graphical representation, the data were normalized, with the mean of the ecotin RR treatment group normalized to 1.

Preparation of mammary lysates, substrate zymography and western blotting

Freshly isolated glands were snap frozen in liquid nitrogen for preparation of mammary lysates. Frozen mammary tissue was homogenized in RIPA buffer (50 mM Tris-Cl, pH 8.0, 150 mM NaCl, 1% NP40, 0.5% DOC, 0.1%SDS) and the supernatant (mammary lysate) was collected. The pellet (insoluble fraction) was resuspended in SDS-loading buffer.

For substrate zymography, the samples were loaded into non-reducing SDS-PAGE gels containing 1 mg/ml casein and 10 μg/ml Plg (Talhouk et al., 1991). The gels were incubated overnight at 37°C in substrate buffer (50 mM Tris-Cl, pH 8.0, 5 mM $NaCl_2$, 0.02% NaN_3) in the presence and absence of 500 nM ecotin WT or ecotin RR. Human uPA and tPA (American Diagnostica Inc.) were used as controls.

uPA was detected by western blotting of mammary lysates using a goat polyclonal anti-human uPA antibody (American Diagnostica Inc.) and tPA was detected using a goat polyclonal anti-human tPA antibody (American Diagnostica Inc.).

Type I collagen was detected by western blotting of the reduced insoluble fraction with a rabbit polyclonal anti-mouse collagen type I antibody (Calbiochem). Entactin was detected by western blotting of the reduced insoluble fraction using a rat monoclonal anti-mouse entactin antibody (Upstate Biotechnology Inc.). Laminin was detected by western blotting of the reduced insoluble fraction using a rabbit polyclonal anti-mouse laminin antibody (Collaborative Research Inc.)

TGF-β was detected by western blotting of reduced mammary lysates using a chicken polyclonal anti-human TGF-β1 antibody (R&D Systems) . Porcine TGF-β (R&D Systems) was used as a control.

To detect gelatinolytic activity, mammary lysates were analyzed on a SDS-PAGE gel containing 3 mg/ml gelatin. The gel was incubated overnight at 37°C in substrate buffer (50 mM Tris-Cl, pH 8.0, 5 mM $NaCl_2$, 0.02% NaN_3). The active forms of human gelatinase A and B (Calbiochem) were used as controls.

Activation of Plg and fibronectin cleavage

Human glu-type Plg (American Diagnostica Inc.) was incubated at a concentration of 1 μM with mammary lysate in activity buffer (50mM Tris-Cl, pH 7.5, 10 mM $CaCl_2$, 0.01% Tween-20) for 30 minutes at 37°C. The reaction mixture was analyzed on a SDS-PAGE gel containing 3 mg/ml gelatin. The gel was incubated overnight at 37°C in substrate buffer (50 mM Tris-Cl, pH 8.0, 5 mM $NaCl_2$, 0.02% NaN_3) to detect the gelatinolytic activity of plasmin. To test for inhibition of Plg activation, 500 nM ecotin RR was added to the reaction mixture along with the mammary lysate.

To assay for fibronectin cleavage, 500 nM human plasma fibronectin (Roche Molecular Biochemicals) was incubated with 10 nM bovine trypsin (Sigma), human tPA, high molecular weight uPA, or plasmin (American Diagnostica Inc.) in activity buffer for 30 minutes at 37°C. The cleavage products were reduced and electrophoresed onto a 10% SDS-PAGE gel. Fibronectin was detected by western blotting with a mouse monoclonal anti-human fibronectin antibody (Calbiochem). To test for inhibition of fibronectin cleavage, 500 nM ecotin RR was added to each reaction mixture along with the enzymes or mammary lysate. Reduced and non-reduced human fibronectin were used as controls.

Immunohistochemistry

5 μM paraffin sections were stained with hematoxylin and eosin. 10 μM frozen sections were stained for endothelial cells using a rat monoclonal anti-mouse CD-31 (PECAM-1) antibody (Pharmingen).

Results

Inhibition of uPA leads to delayed involution

The secretory epithelial tissue involved in lactation is normally remodeled during involution, as evidenced by the disappearance of alveolar structures by day 5 of involution. In order to determine the role played by chymotrypsin-fold serine proteases, ecotin was used to block the activity of uPA and related enzymes during involution. Wild-type ecotin (WT) inhibits a broad range of chymotrypsin-like serine proteases including trypsin, chymotrypsin and elastase, but it is a poor inhibitor of uPA [Ki = 2.8 μM; (Wang et al., 1995)]. The variant Met84Arg/Met85Arg ecotin (RR) is a potent inhibitor of uPA [Ki = 1 nM; (Wang et al., 1995)]. Animals treated with ecotin WT showed normal epithelial remodeling, and no major alveolar structures were detected on day 5 of involution by Carmine staining (Figure 3-3). However, the remodeling process was delayed in animals treated with ecotin RR. Dense and darkly stained alveoli were detected in these animals and the morphology of the gland resembled day 2 of involution rather than day 5. These data suggest that an uPA-dependent pathway is important in epithelial remodeling during involution.

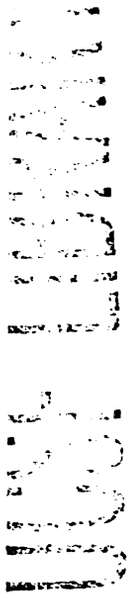

Adipogenesis during involution requires serine protease activity

Since uPA was required for epithelial remodeling, was it also important in stromal remodeling and adipogenesis during involution? Adipocytes were not detected by Oil red O staining for lipids in the lactating mammary gland (Figure 3-4). Adipocyte infiltration is normally observed by day 2 of involution (Lascelles and Lee, 1978). By day 5 of involution, the gland is completely repopulated with adipocytes. However, regeneration

of adipose tissue was impaired in animals treated with either ecotin WT or ecotin RR (Figure 3-4). In contrast to carrier-treated animals, the average area occupied by adipocytes was about 7-fold less in ecotin WT-treated animals and about 14-fold less in ecotin RR-treated animals (Figure 3-5). Since both ecotins affect adipogenesis, it appears that a protease other than uPA was required for the repopulation of the mammary gland with adipocytes during involution.

uPA, tPA and a 80kD protease are expressed during involution

In order to determine which proteases were responsible for the phenotype observed with ecotin treatment, mammary lysates from involuting female mice were assayed by casein-Plg zymography. uPA, tPA and a novel 80 kD serine protease, sp80, were detected during involution (Figure 3-6). The identity of uPA and tPA was confirmed by western blotting of involuting mammary lysates (Figure 3-7). Animals treated with either ecotin had normal levels of uPA, tPA and sp80 (Figure 3-6). In order to identify potential targets of ecotin during involution, we tested the ability of ecotin WT and ecotin RR to inhibit these proteases. Ecotin WT only inhibited sp80, while ecotin RR inhibited both sp80 and uPA. tPA was not inhibited by either ecotin.

Involuting mammary lysate contained proteases that could activate Plg to plasmin (Figure 3-8). In order to test if Plg activation by mammary lysates was affected by ecotin treatment, ecotin RR was used to inhibit uPA and sp80. Ecotin RR completely inhibited Plg activation by mammary lysate. This indicates inhibition of sp80 and uPA was sufficient to abolish Plg activation.

Degradation of ECM molecules is impaired by ecotin treatment

Western blotting was used to analyze the cleavage of the ECM proteins type I collagen, entactin and laminin to assess whether degradation of the ECM was affected by ecotin inhibition of serine proteases during involution. The levels and cleavage pattern of type I collagen and laminin present in the insoluble fraction of mammary lysates were not significantly affected by ecotin treatment (Figure 3-9). Normal levels of entactin and high molecular weight entactin cleavage products were detected in both carrier-treated and ecotin-treated animals. However, in some animals treated with ecotin RR, the level of a low molecular weight entactin cleavage product was increased (Figure 3-9). It has been reported that low molecular weight entactin degradation products accumulate in Plg-/- mice (Lund et al., 2000). The effect observed with ecotin RR treatment suggests that inhibition of uPA, similar to Plg-deficiency, may affect cleavage of entactin during involution.

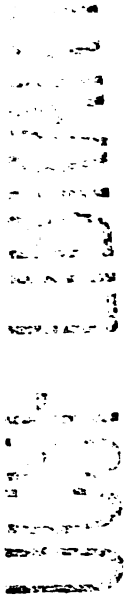

Fibronectin is an component of the stromal ECM and is a substrate of plasmin (Liotta et al., 1981). The ability of trypsin, uPA, tPA and plasmin to cleave fibronectin was tested *in vitro*. Only trypsin and plasmin cleaved fibronectin into various fragments (Figure 3-10). Mammary lysate also cleaved fibronectin into numerous fragments. Incubation with ecotin RR resulted in the loss of some of the cleavage products observed with mammary lysate. uPA does not directly cleave fibronectin, and ecotin RR does not inhibit the degradation of fibronectin by plasmin (Figure 3-10). It would therefore appear that ecotin decreases cleavage of fibronectin by mammary lysate by inhibiting uPA-mediated Plg activation.

Ecotin treatment results in decreased gelatinase activity and increased levels of TGF-β

To further understand the mechanism by which serine proteases promote epithelial and stromal remodeling in the mammary gland, the hypothesis that inhibition of Plg activators leads to a reduction in the activity of downstream enzymes and cytokines was studied. Plasmin has been shown to activate various pro-MMPs including gelatinase B (Murphy and Crabbe, 1995). The levels of active and pro-gelatinases present in lysates of involuting mammary glands was analyzed by substrate zymography. Both gelatinase A and B were expressed during involution (Figure 3-11A). However, in animals treated with ecotin RR, but not ecotin WT, the level of active gelatinase B was reduced. This indicates that inhibition of uPA during involution leads to a decrease in gelatinase B activity, and suggests that the uPA/plasmin system may be important in gelatinase B activation in the mammary gland. Interestingly, the level of active gelatinase A was reduced in animals treated with either ecotin, which suggests that chymotrypsin-fold serine proteases other than uPA may be upstream of gelatinase A activation.

The repopulation of the mammary gland with adipocytes during involution appears to require chymotrypsin-fold serine proteases. Plasmin can activate TGF-β (Grainger et al., 1995; Khalil et al., 1996), and it has been shown that TGF-β has an inhibitory effect on adipocyte differentiation (Bortell et al., 1994). The levels of TGF-β present in the mammary gland during involution was analyzed by western blotting (Figure 3-11B). Both latent and active forms of TGF-β were detected in lysates from involuting mammary glands. However, there was a pronounced increase in both forms of TGF-β in lysates from mice treated with either ecotin. The activity of TGF-β is

modulated by various binding proteins (Raftery and Sutherland, 1999; Saharinen et al., 1999), and forms of TGF-β that may be complexed with binding proteins (TGFBPs) were detected in involuting mammary lysates.

Discussion

Involution of the mammary gland is a model system to study the role of proteases in tissue remodeling. Ecotin is a unique macromolecular inhibitor that can be used to study the role of chymotrypsin-fold serine proteases in involution. The phenotype observed with ecotin inhibition can be combined with the body of knowledge available regarding the structure and function of chymotrypsin-fold serine proteases to elucidate the role of these proteases in complex remodeling processes.

The finding that inhibition of uPA leads to delayed epithelial remodeling indicates a requirement for uPA during involution. Since the activation of Plg in the mammary gland is diminished by inhibition of uPA (Figure 3-8), and Plg-/- mice show impaired remodeling (Lund et al., 2000), it would appear that uPA-mediated Plg activation is an important regulator of epithelial remodeling during involution. Although tPA is present in mammary lysate, it does not appear to play a role in Plg activation, since inhibition of uPA and sp80 by ecotin RR was sufficient to abolish plasmin generation (Figure 3-8). Mice deficient in the gene for uPA have been generated (Carmeliet et al., 1994) and it would be of interest to analyze their phenotype during involution, and to determine if it overlaps with the phenotype observed in ecotin RR treated mice.

The detection of an as-yet-unidentified serine protease, sp80, provides an avenue for further research. Since this protease is inhibited by both ecotin WT and ecotin RR it

may be responsible for the impaired adipogenesis observed in mice treated with either ecotin. This protease was purified from mammary lysates using an ecotin affinity column (Chapter Two), but the protein level was too low to permit identification of this protease by sequencing. However, inhibition by ecotin reveals that sp80 is a chymotrypsin-fold serine protease. This information can be used to design degenerate primers using conserved sequences found in chymotrypsin-fold serine proteases, and to then isolate this sp80 from mammary mRNA using reverse transcription-PCR. This approach has been successfully used to isolate serine proteases expressed by prostate cancer cells (Takeuchi et al., 1999). The identification and function of sp80 is discussed in Chapter Five.

Chymotrypsin-fold serine proteases may modulate the differentiation of preadipocytes into adipocytes during involution. The function of serine proteases during adipocyte differentiation can be analyzed using the 3T3-L1 cell culture model (Gregoire et al., 1998). The results obtained with this approach, and further analysis of the Plg system in adipogenesis *in vivo*, are discussed in Chapter Five.

Adipose tissue is highly vascularized (Figure 3-12), and adipogenesis and angiogenesis are coordinately regulated *in vivo* (Wasserman, 1965). Adipocytes demonstrate differentiation-dependent expression of the angiogenic factor vascular endothelial growth factor (VEGF; data not shown). uPA has been hypothesized to play a role in angiogenesis (Moscatelli and Rifkin, 1988), and it would be of interest to study the role of the Plg system in angiogenesis in the mammary gland.

Why are chymotrypsin-fold serine proteases required during involution? An attractive hypothesis is that extracellular serine proteases cleave ECM molecules and thereby mediate remodeling. Plasmin can cleave various ECM molecules including

laminin and fibronectin (Chen and Strickland, 1997; Liotta et al., 1981). The finding that the cleavage pattern of entactin is altered in Plg-/- and ecotin-treated mice indicates a role for Plg and uPA in entactin degradation during involution. Plasmin also activates various pro-MMPs including gelatinase B [MMP-9; (Murphy and Crabbe, 1995)]. These MMPs in turn mediate the degradation of ECM and basement membrane molecules. Ecotin treatment resulted in reduced activation of gelatinase B, indicating that uPA-mediated Plg activation may be required for gelatinase B activation in the mammary gland. uPA-/- mice provide an experimental system to test this hypothesis. Inhibition by either ecotin also led to reduced activation of gelatinase A. Since gelatinase A is primarily thought to be activated by membrane type MMP-1 [MT-MMP-1; (Werb, 1997)], it is unclear what role chymotrypsin-fold serine proteases play in gelatinase A activation.

Another hypothesis is that serine proteases regulate the bioavailability of cytokines such as TGF-β that regulate mammary gland function. TGF-β levels, both latent and active, were increased in ecotin-treated mice. This increase in TGF-β levels may be responsible for the diminished adipogenesis observed in ecotin-treated mice since TGF-β is a negative regulator of adipocyte differentiation (Bortell et al., 1994). How do serine proteases regulate TGF-β function? The increase in latent TGF-β may be the result of diminished plasmin generation since plasmin can activate TGF-β. However, other chymotrypsin-fold serine proteases may directly cleave and inactivate TGF-β, and inhibition of these proteases would lead to an increase in active TGF-β. Serine proteases may also modulate the function of TGFBPs. These hypotheses remain to be tested.

During lactation, lymphocytes migrate to the mammary gland. These lymphocytes are thought to play a role in passive immunity in the neonate by producing

antibodies that are secreted into milk. The mammary lymph node increases in size during lactation and is remodeled during involution. Chymotrypsin-fold serine proteases appear to be required to remodel the mammary lymph node during involution, as discussed in Chapter Four.

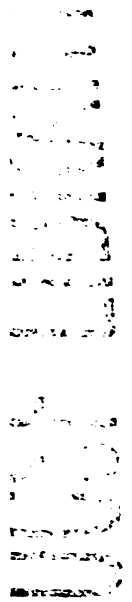

References

Booth, B. A., Boes, M., and Bar, R. S. (1996). IGFBP-3 proteolysis by plasmin, thrombin, serum: heparin binding, IGF binding, and structure of fragments. Am J Physiol *271*, E465-70.

Bortell, R., Owen, T. A., Ignotz, R., Stein, G. S., and Stein, J. L. (1994). TGF beta 1 prevents the down-regulation of type I procollagen, fibronectin, and TGF beta 1 gene expression associated with 3T3-L1 pre- adipocyte differentiation. J Cell Biochem *54*, 256-63.

Bugge, T. H., Flick, M. J., Daugherty, C. C., and Degen, J. L. (1995). Plasminogen deficiency causes severe thrombosis but is compatible with development and reproduction. Genes Dev *9*, 794-807.

Busso, N., Huarte, J., Vassalli, J. D., Sappino, A. P., and Belin, D. (1989). Plasminogen activators in the mouse mammary gland. Decreased expression during lactation. J Biol Chem *264*, 7455-7.

Campbell, P. G., and Andress, D. L. (1997). Plasmin degradation of insulin-like growth factor-binding protein-5 (IGFBP-5): regulation by IGFBP-5-(201-218). Am J Physiol *273*, E996-1004.

Carmeliet, P., Schoonjans, L., Kieckens, L., Ream, B., Degen, J., Bronson, R., De Vos, R., van den Oord, J. J., Collen, D., and Mulligan, R. C. (1994). Physiological consequences of loss of plasminogen activator gene function in mice. Nature *368*, 419-24.

Chen, Z. L., and Strickland, S. (1997). Neuronal death in the hippocampus is promoted by plasmin-catalyzed degradation of laminin. Cell *91*, 917-25.

Chung, C. H., Ives, H. E., Almeda, S., and Goldberg, A. L. (1983). Purification from Escherichia coli of a periplasmic protein that is a potent inhibitor of pancreatic proteases. J Biol Chem *258*, 11032-8.

Dano, K., Andreasen, P. A., Grondahl-Hansen, J., Kristensen, P., Nielsen, L. S., and Skriver, L. (1985). Plasminogen activators, tissue degradation, and cancer. Adv Cancer Res *44*, 139-266.

Dickson, S. R., and Warburton, M. J. (1992). Enhanced synthesis of gelatinase and stromelysin by myoepithelial cells during involution of the rat mammary gland. J Histochem Cytochem *40*, 697-703.

Grainger, D. J., Wakefield, L., Bethell, H. W., Farndale, R. W., and Metcalfe, J. C. (1995). Release and activation of platelet latent TGF-beta in blood clots during dissolution with plasmin. Nat Med *1*, 932-7.

Gregoire, F. M., Smas, C. M., and Sul, H. S. (1998). Understanding adipocyte differentiation. Physiol Rev *78*, 783-809.

Khalil, N., Corne, S., Whitman, C., and Yacyshyn, H. (1996). Plasmin regulates the activation of cell-associated latent TGF-beta 1 secreted by rat alveolar macrophages after in vivo bleomycin injury. Am J Respir Cell Mol Biol *15*, 252-9.

Lascelles, A. K., and Lee, C. S. (1978). Involution of the Mammary Gland. In Lactation: A Comprehensive Treatise, B. L. Larson, ed. (New York: Academic Press), pp. 115-176.

Lefebvre, O., Wolf, C., Limacher, J. M., Hutin, P., Wendling, C., LeMeur, M., Basset, P., and Rio, M. C. (1992). The breast cancer-associated stromelysin-3 gene is expressed during mouse mammary gland apoptosis. J Cell Biol *119*, 997-1002.

Liotta, L. A., Goldfarb, R. H., Brundage, R., Siegal, G. P., Terranova, V., and Garbisa, S. (1981). Effect of plasminogen activator (urokinase), plasmin, and thrombin on glycoprotein and collagenous components of basement membrane. Cancer Res *41*, 4629-36.

Lund, L. R., Bjorn, S. F., Sternlicht, M. D., Nielsen, B. S., Solberg, H., Usher, P. A., Osterby, R., Christensen, I. J., Stephens, R. W., Bugge, T. H., Dano, K., and Werb, Z. (2000). Lactational competence and involution of the mouse mammary gland require plasminogen. Development *127*, 4481-4492.

Lund, L. R., Romer, J., Thomasset, N., Solberg, H., Pyke, C., Bissell, M. J., Dano, K., and Werb, Z. (1996). Two distinct phases of apoptosis in mammary gland involution: proteinase-independent and -dependent pathways. Development *122*, 181-93.

Moscatelli, D., and Rifkin, D. B. (1988). Membrane and matrix localization of proteinases: a common theme in tumor cell invasion and angiogenesis. Biochim Biophys Acta *948*, 67-85.

Murphy, G., and Crabbe, T. (1995). Gelatinases A and B. Methods Enzymol *248*, 470-84.

Murphy, G., Stanton, H., Cowell, S., Butler, G., Knauper, V., Atkinson, S., and Gavrilovic, J. (1999). Mechanisms for pro matrix metalloproteinase activation. Apmis *107*, 38-44.

Ossowski, L., Biegel, D., and Reich, E. (1979). Mammary plasminogen activator: correlation with involution, hormonal modulation and comparison between normal and neoplastic tissue. Cell *16*, 929-40.

Raftery, L. A., and Sutherland, D. J. (1999). TGF-beta family signal transduction in Drosophila development: from Mad to Smads. Dev Biol *210*, 251-68.

Saharinen, J., Hyytiainen, M., Taipale, J., and Keski-Oja, J. (1999). Latent transforming growth factor-beta binding proteins (LTBPs)--structural extracellular matrix proteins for targeting TGF-beta action. Cytokine Growth Factor Rev *10*, 99-117.

Takeuchi, T., Shuman, M. A., and Craik, C. S. (1999). Reverse biochemistry: use of macromolecular protease inhibitors to dissect complex biological processes and identify a membrane-type serine protease in epithelial cancer and normal tissue. Proc Natl Acad Sci U S A *96*, 11054-61.

Talhouk, R. S., Bissell, M. J., and Werb, Z. (1992). Coordinated expression of extracellular matrix-degrading proteinases and their inhibitors regulates mammary epithelial function during involution. J Cell Biol *118*, 1271-82.

Talhouk, R. S., Chin, J. R., Unemori, E. N., Werb, Z., and Bissell, M. J. (1991). Proteinases of the mammary gland: developmental regulation in vivo and vectorial secretion in culture. Development *112*, 439-49.

Wang, C. I., Yang, Q., and Craik, C. S. (1995). Isolation of a high affinity inhibitor of urokinase-type plasminogen activator by phage display of ecotin. J Biol Chem *270*, 12250-6.

Wasserman, F. (1965). The development of adipose tissue. In Handbook of Physiology, A. E. Renold and G. F. Cahill, eds. (Washington D. C.: Am. Physiol. Soc.), pp. 87-100.

Werb, Z. (1997). ECM and cell surface proteolysis: regulating cellular ecology. Cell *91*, 439-42.

Werb, Z., Mainardi, C. L., Vater, C. A., and Harris, E. D., Jr. (1977). Endogenous activiation of latent collagenase by rheumatoid synovial cells. Evidence for a role of plasminogen activator. N Engl J Med *296*, 1017-23.

Figure 3-1. Involution of the mammary gland involves various processes. Expression of milk proteins such as casein is downregulated and the secretory alveoli collapse. Degradation of the extracellular matrix (ECM) and basement membrane (BM) leads to apoptosis of epithelial cells, and phagocytosis by macrophages. The gland is then repopulated with adipocytes.

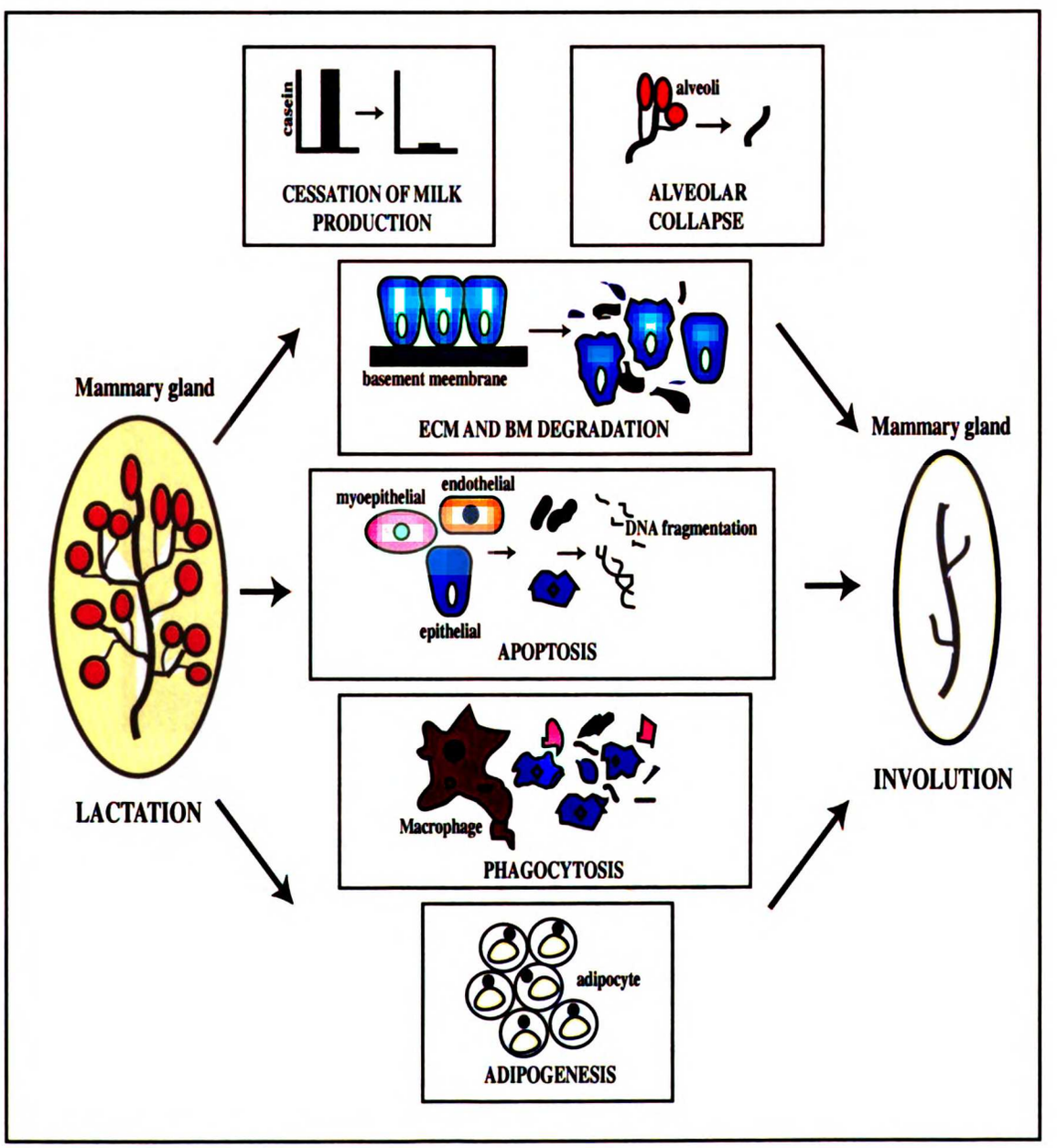

Figure 3-2.

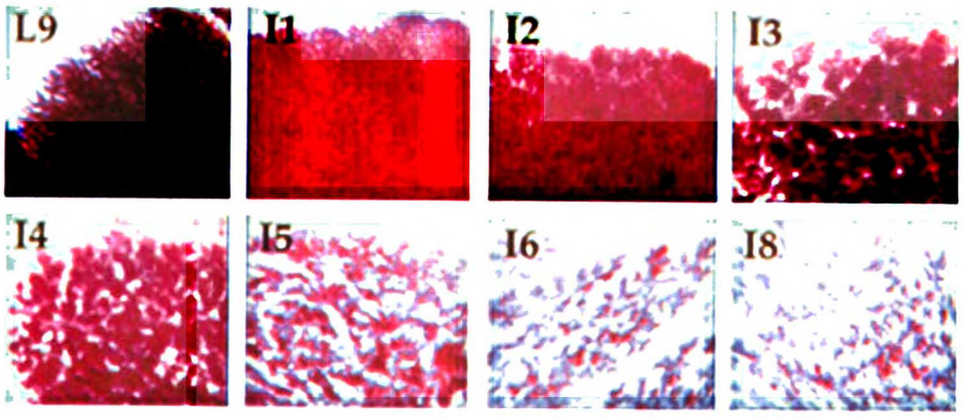

Figure 3-3.

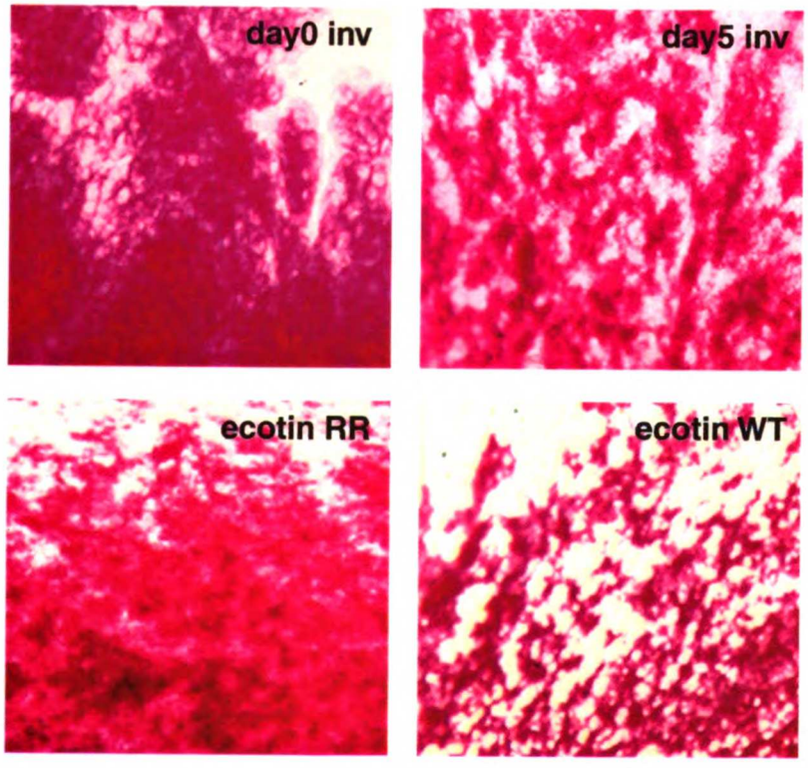

Figure 3-2. The morphology of the mammary gland changes during involution. Whole mammary glands stained with Carmine dye. The darkly-staining alveoli seen on the 9th day of lactation (**L9**) progressively disappear with increasing days of involution (**I1-I8**).

Figure 3-3. Involution is delayed in animals treated with Ecotin RR. Carmine-dye stained whole mammary glands on the first day of weaning/involution (day0 inv), and on day 5 of involution in untreated animals (day5 inv), and animals treated with ecotin RR and ecotin WT.

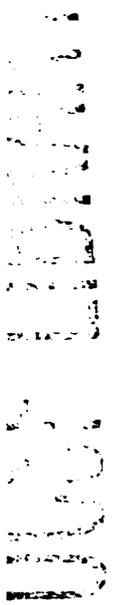

Figure 3-4.

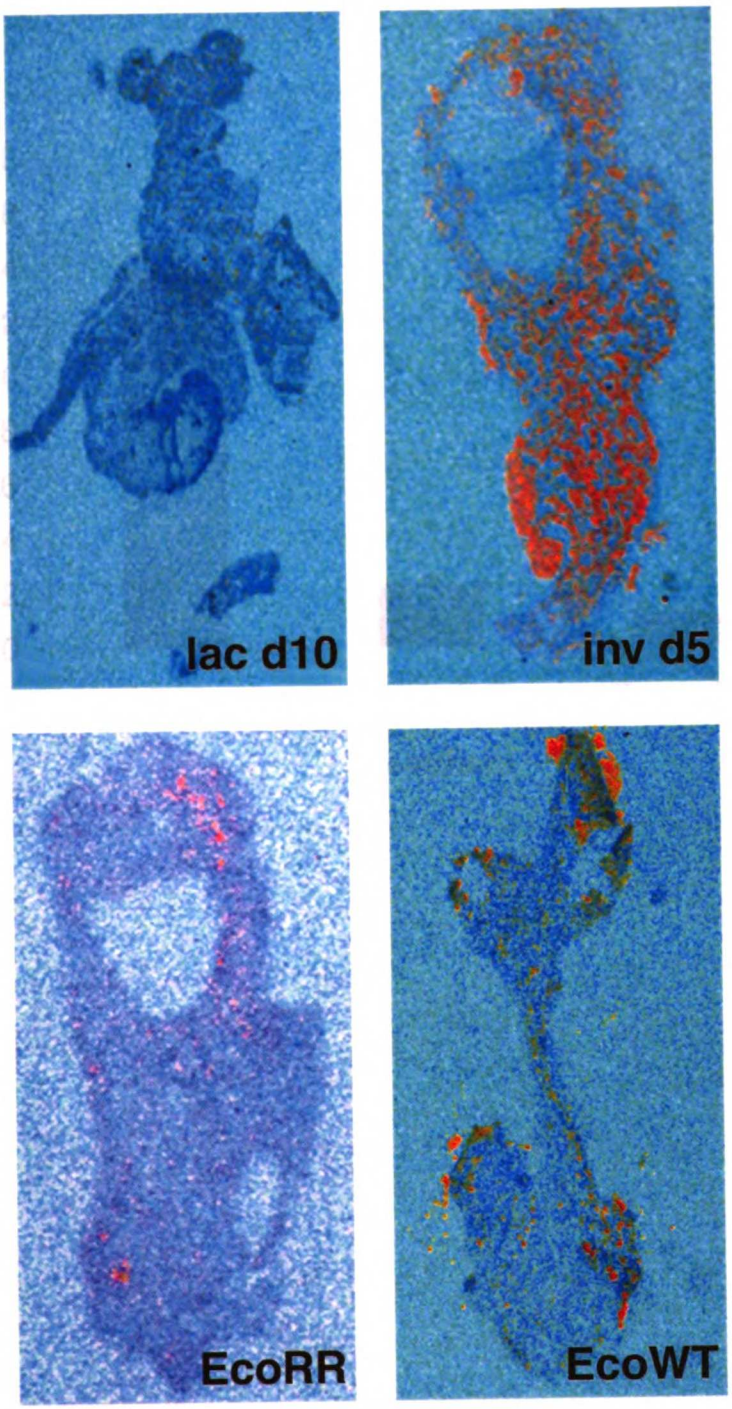

Figure 3-5.

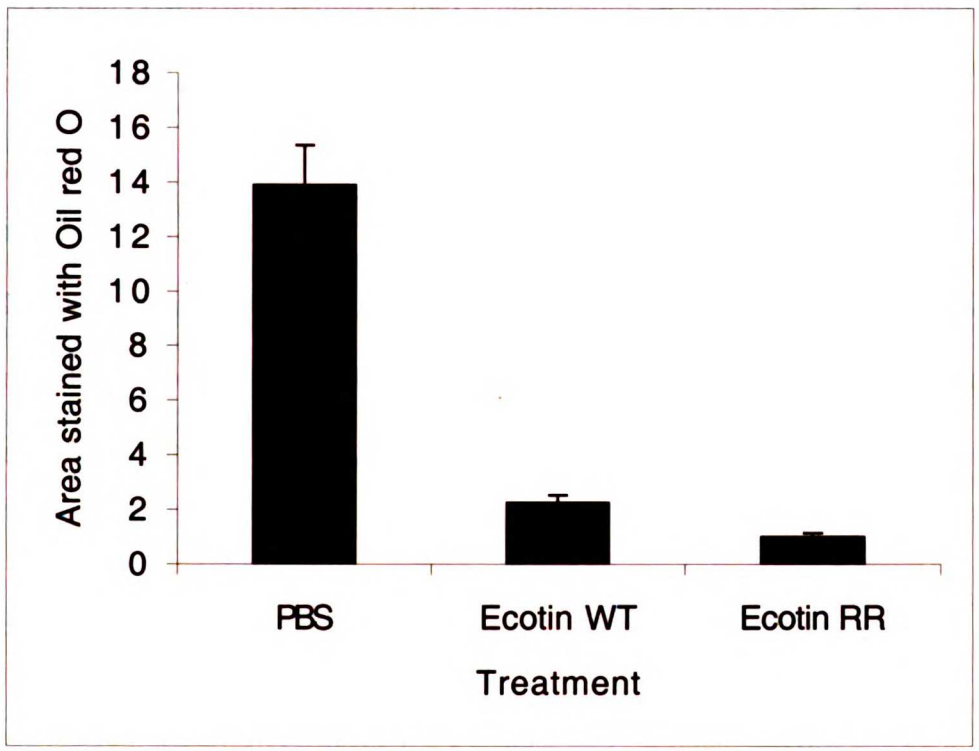

Figure 3-4. Fewer adipocytes are detected in animals treated with ecotin. Mammary glands at 10 days of lactation (lac d10) and five days of involution in untreated animals (inv d5) and animals treated with ecotin RR (EcoRR) or ecotin WT (EcoWT) stained with Oil red O dye (red) to detect lipid accumulation in adipocytes. Sections were counterstained with hematoxylin (blue) to detect nuclei.

Figure 3-5. The area occupied by adipocytes is reduced in involuting animals treated with ecotin. Area stained with the lipid-specific dye Oil red O in mammary glands of animals treated with carrier (PBS), ecotin WT and ecotin RR. Data are represented as the mean $\pm$ S.D., with the ecotin RR mean normalized to 1.

Figure 3-6.

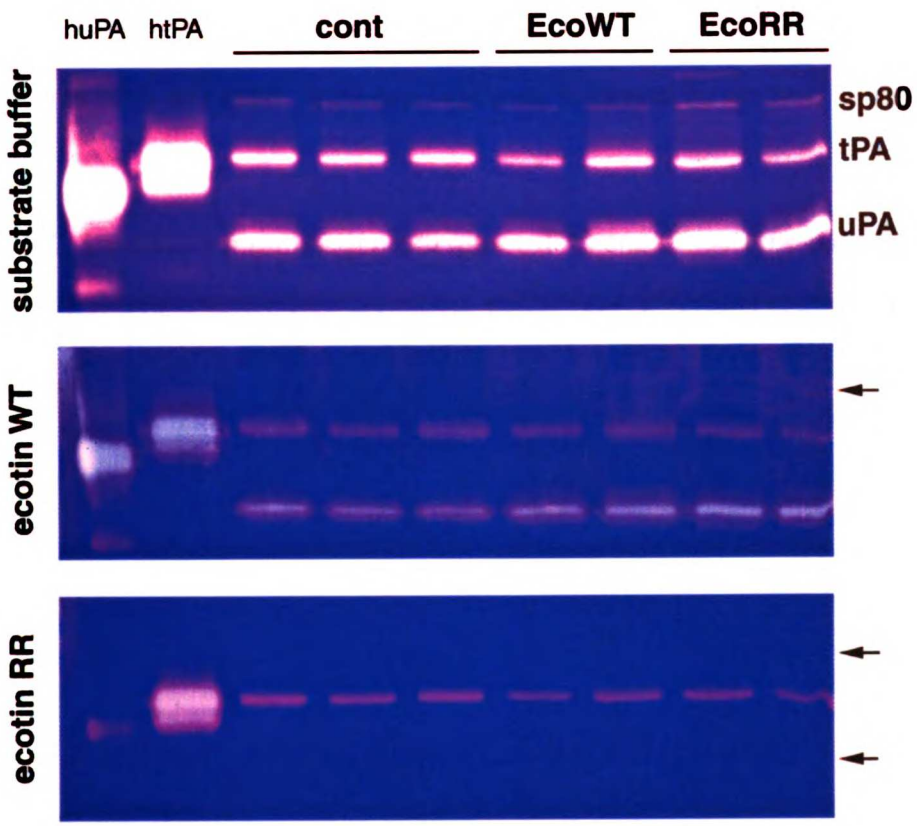

Figure 3-7.

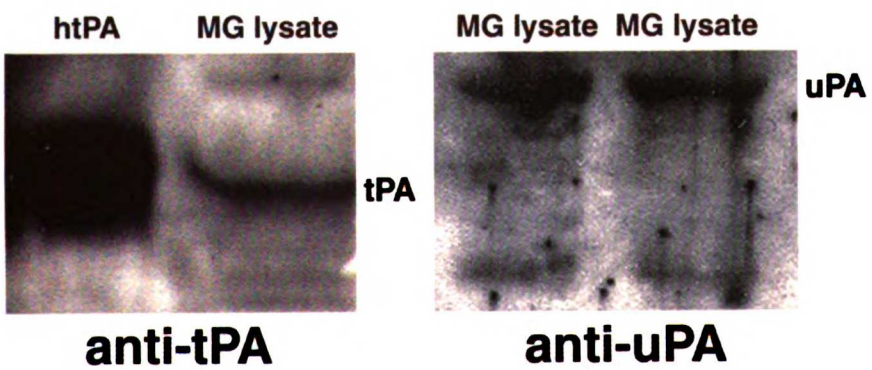

Figure 3-6. Urokinase plasminogen activator (uPA), tissue-type plasminogen activator and a 80 kD serine protease (sp 80) are expressed during involution. Incubation with ecotin WT leads to inhibition of sp80 activity, while incubation with ecotin RR leads to inhibition of uPA and sp80. Inhibited bands are indicated by arrows.

Figure 3-7. Urokinase plasminogen activator (uPA) and tissue-type plasminogen activator (tPA) are detected in involuting mammary lysate (MG lysate). Human tPA was used as a control.

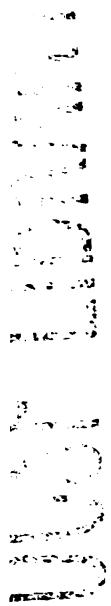

Figure 3-8.

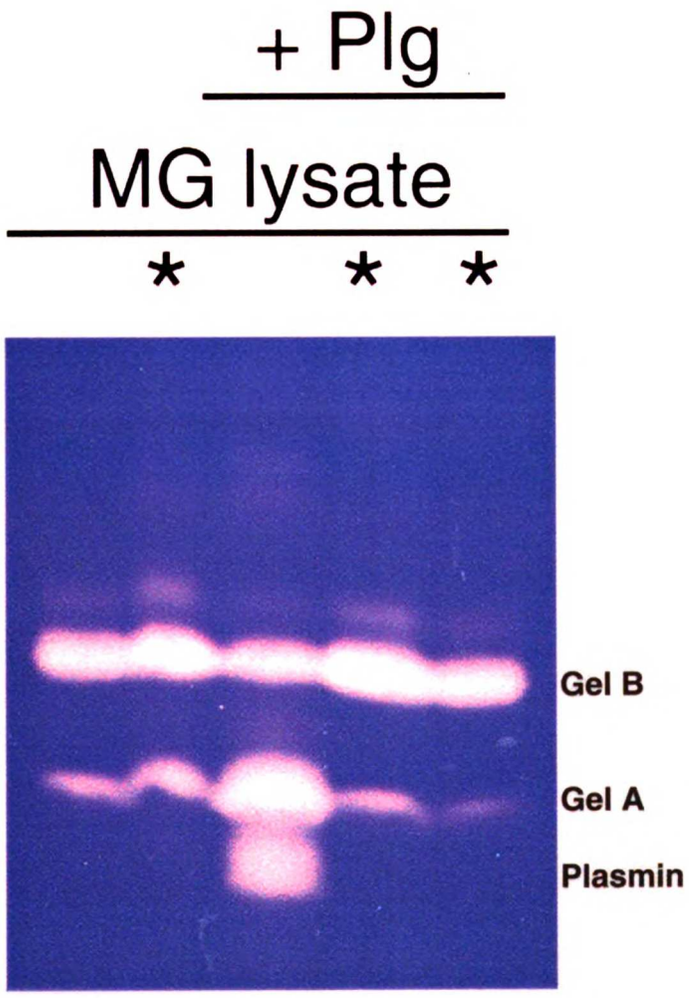

Figure 3-8. Involuting mammary lysate (MG lysate) contains proteases that can activate plasminogen (Plg) to plasmin. The activity of these proteases is inhibited by ecotin RR. MG lysate electrophoresed on gelatin containing SDS-PAGE gels. Samples marked with * were incubated with ecotin RR prior to electrophoresis. Gelatinase A and B (Gel A and Gel B) activity is detected in MG lysates.

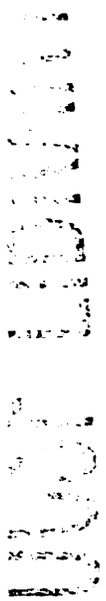

Figure 3-9.

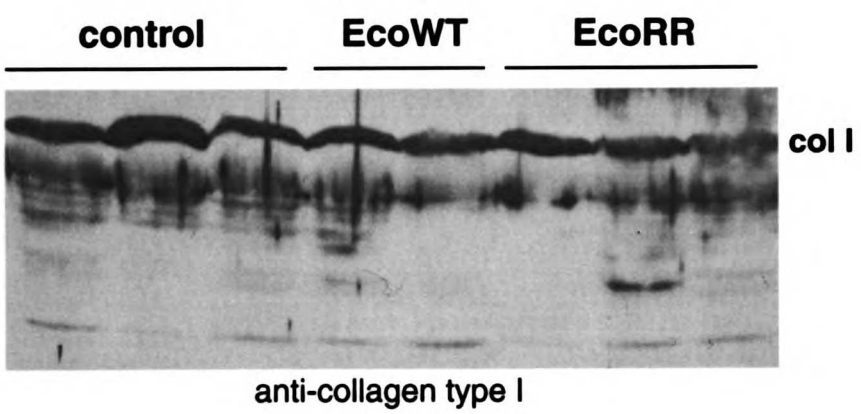

anti-collagen type I

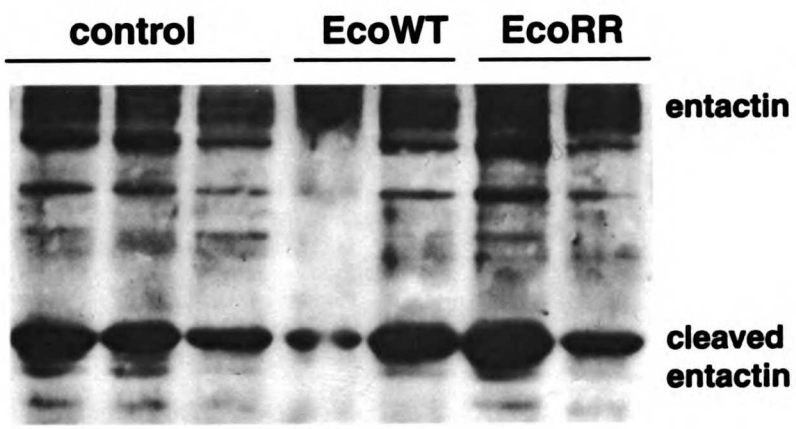

anti-entactin

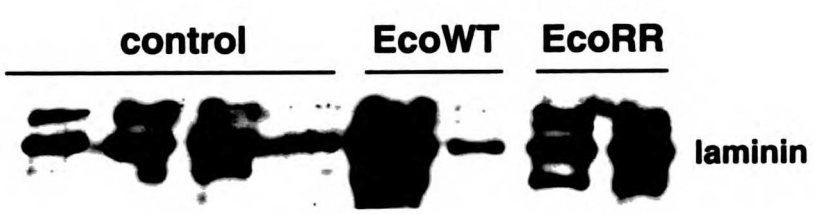

anti-laminin

Figure 3-9. Western blot for type I collagen (col I), entactin and laminin. Insoluble proteins from involuting mammary glands treated with ecotin WT (EcoWT) or ecotin RR (EcoRR) and untreated animals (control).

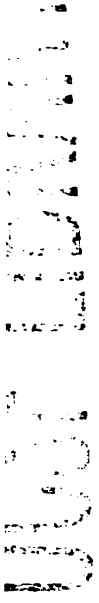

Figure 3-10.

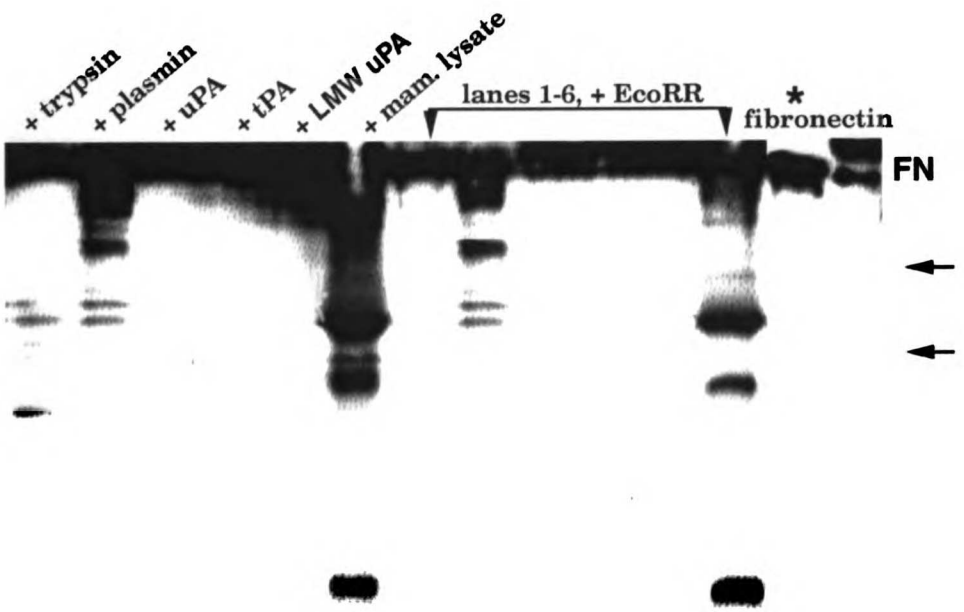
+ trypsin
+ plasmin
+ uPA
+ tPA
+ LMW uPA
+ mam. lysate
lanes 1-6, + EcoRR
*
fibronectin
FN

Figure 3-10. Western blot for fibronectin (FN). Human FN was incubated with trypsin, plasmin, high (uPA) and low molecular weight urokinase plasminogen activator (LMW uPA), tissue-type plasminogen activator (tPA) and mammary lysate (mam. lysate). Cleaved fibronectin bands are seen in samples incubated with trypsin, plasmin and mammary lysate. Ecotin RR (EcoRR) inhibits some of the cleavage observed in samples incubated with mammary lysate. Inhibited cleavage bands are indicated by arrows. Reduced (*) and non-reduced human fibronectin were used as controls.

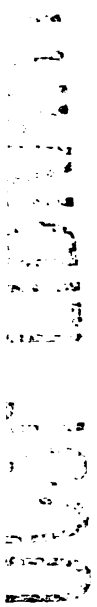

Figure 3-11.

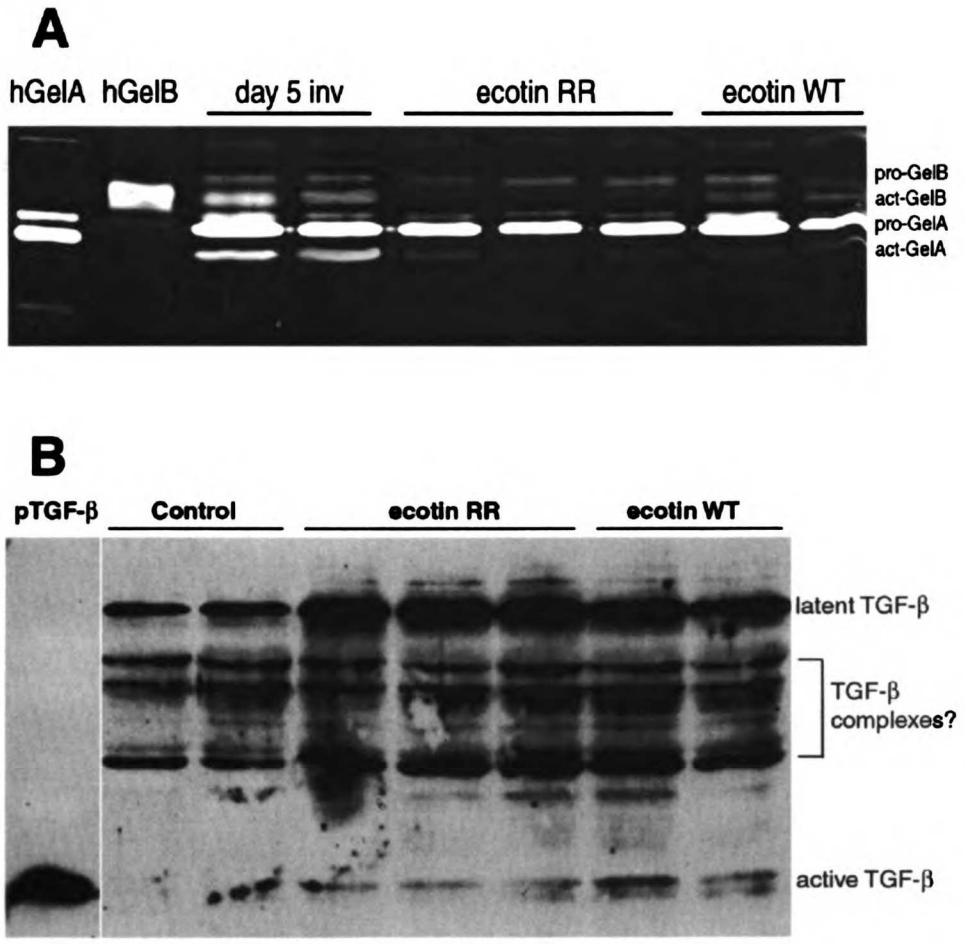

Figure 3-11. Decreased gelatinase activity and increased transforming growth factor-β are detected in animals treated with ecotin. **A**, Gelatin zymogram with mammary lysates from controls (day 5 inv) and animals treated with ecotin RR and ecotin WT. Inactive (pro-) and active (act-) forms of gelatinase A (GelA) and B (GelB) are seen. Human (h) GelA and GelB were used as controls. **B**, Western blot for TGF-β. Involuting mammary lysates from from untreated animals (control) and animals treated with ecotin RR and ecotin WT. Multiple bands corresponding to latent TGF-β, TGF β complexes and active TGF-β are seen. Porcine (p) TGF-β was used as a control.

Figure 3-12.

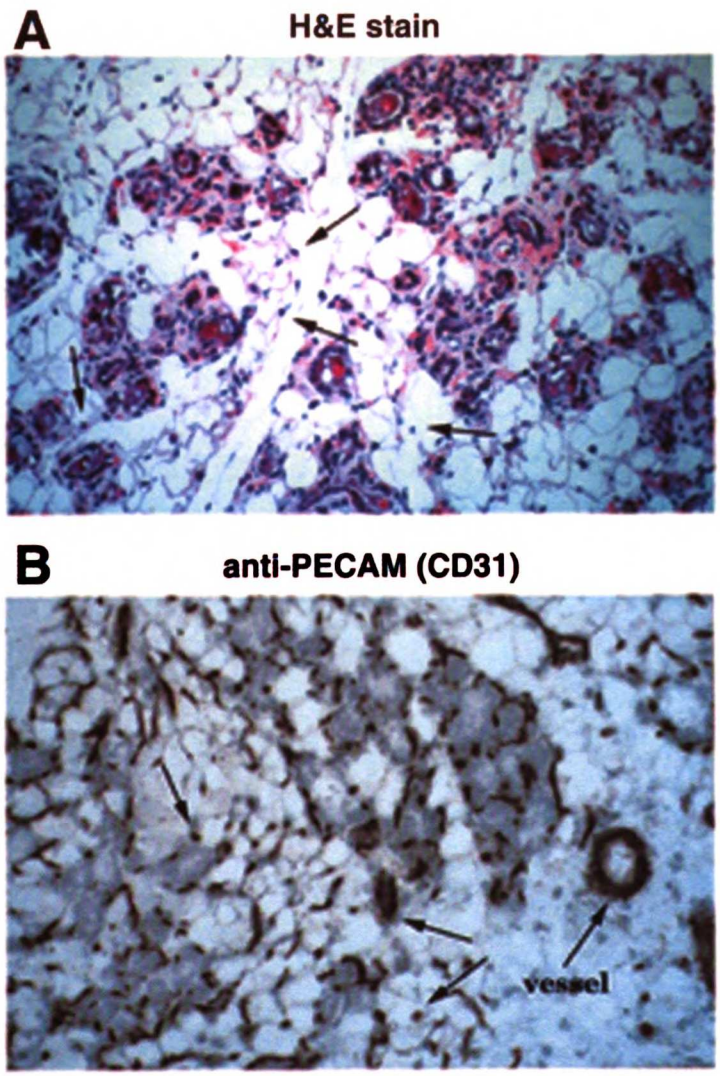

Figure 3-12. Mammary gland adipose tissue is highly vascularized. **A**, Hematoxylin and eosin (H&E) stain showing mammary gland morphology. **B**, Immunohistochemical staining for the endothelial cell marker platelet endothelial cell adhesion molecule (PECAM-1/ CD 31). Endothelial cells are indicated by arrows.

Chapter Four

Involutive Regression of the Mammary Lymph Node Requires the Plasminogen System

Abstract

Lymphocytes associated with the mammary epithelium during lactation are thought to play a role in local host defense mechanisms and in the production of antibodies that are secreted into milk to confer passive immunity to the neonate. The mammary lymph node is enlarged during lactation and regresses during involution of the mammary gland. The nature and function of the lymphocytes present in the mammary lymph node are not clear. Treatment of involuting mice with the macromolecular inhibitor ecotin lead to enlarged lymph nodes, which suggests a role for chymotryspin-fold serine proteases in lymph node regression. Urokinase (uPA), tissue-type plasminogen activator (tPA) and the as-yet-unidentified serine proteases sp80 and sp120, were present in the mammary lymph node during involution, and were also detected in the gut-associated lymphoid tissue (GALT) of virgin mice. Analysis of the lymphocyte population present in the mammary lymph node and GALT in virgin, pregnant, lactating and involuting mice revealed that mammary lymph node lymphocytes are distinct from GALT lymphocytes, and that the lymphocyte subpopulations vary depending on the functional state of the mammary gland. Ecotin treatment during involution resulted in increased numbers of lymphocytes and changes in the lymphocyte subpopulations present in the mammary lymph node. These data indicate that the Plg system is important in lymph node regression and lymphocyte egress during mammary gland involution.

Introduction

Although lymphocytes are primarily detected in the circulation and in lymphoid tissues such as the thymus, spleen and lymph nodes, they also migrate to non-lymphoid tissues such as the respiratory and urogenital tracts, and the lactating mammary gland. Lymphocytes present in the gastrointestinal, urogenital, upper respiratory and mammary tissues collectively constitute the mucosal immune system. Few lymphocytes are present in the resting, non-lactating mammary gland, but during lactation, the mammary gland is infiltrated with lymphocytes (Parmely and Manning, 1983). Mammary lymphocytes are thought to serve two major functions. The first is to provide a local defense mechanism against disease, and the second is the production of antibodies that are secreted into milk.

Mastitis is an inflammation of the mammary gland that occurs fairly frequently in humans, cows and rodents (Riordan and Nichols, 1990). The lymphocyte subpopulation varies during the lactation cycle, and this variation may correlate with susceptibility to mammary infections (Sridama et al., 1982). Mammary lymphocytes possess cytotoxic and antibacterial functions, and may mediate a local response to post-partum mammary infections. Human, bovine and murine milk contain immune cells such as lymphocytes, neutrophils and macrophages (Richie et al., 1982; Taylor et al., 1994; Wei et al., 1986). Mammary gland secretions and milk also contain immunoglobulins. The major function of these secreted immune cells and immunoglobulins is to confer passive immunity to the neonate (Diaz-Jouanen and Williams, 1974).

During lactation, a specific subpopulation of lymphocytes migrates to the mammary gland and becomes associated with the mammary epithelium (Lamm et al., 1978). These lymphocytes are thought to originate from virgin cells that were activated

in the gut-associated lymphoid tissue (GALT), which consists of the tonsils, adenoids, appendix, Peyer's patches, and solitary lymphoid follicles (Janeway and Travers, 1997). Mammary epithelial lymphocytes predominantly produce IgA antibodies specific for antigens encountered by the GALT (Lamm et al., 1978).

While the lymphocyte populations present in the bovine and human mammary gland during pregnancy and lactation have been described in some detail, it is not known whether the population of lymphocytes present in the murine mammary gland changes during different stages of development. The abdominal mammary gland in mice (Figure 4-1) has a major lymph node (mammary lymph node). The lymphocytes present in this lymph node have not been previously described, and it is not known if these lymphocytes represent a distinct population, when compared to GALT lymphocytes and lymphocytes associated with the mammary epithelium. In this study, the lymphocyte population present in the mammary lymph node of virgin, pregnant, lactating and involuting mice was analyzed. This analysis indicates that the lymphocyte population present in the mammary lymph node varies depending on the functional state of the gland, and that it is distinct from the population present in the GALT at the same stage.

The mammary lymph node is significantly enlarged during lactation. This enlargement is normally reversed during involution of the mammary gland. The mechanisms underlying this change in lymph node size are not clear. During involution in plasminogen-deficient [Plg-/-; (Bugge et al., 1995)] mice, the mammary lymph node remains enlarged, and does not revert to the pre-lactation size (Lund, L. R., unpublished). This observation suggests that the Plg system may be important for regression of the mammary lymph node. To test this hypothesis, ecotin WT and the variant ecotin RR,

which is a potent inhibitor of uPA, were used to inhibit chymotrypsin-fold serine proteases during involution. Analysis of mammary lymph nodes from ecotin-treated mice reveals a role for the Plg system in lymphocyte egress and lymph node remodeling during involution.

Methods

Collection of lymph nodes

Mammary lymph nodes and gut-associated Peyer's patches were collected from virgin mice and from mice on the 14th day of pregnancy, 11th day of lactation and 5th day of involution. Mammary lymph nodes were collected on the 5th day of involution from mice treated with the carrier (PBS), 100 μg/day bovine serum albumin (BSA), ecotin RR or ecotin WT as previously described (Chapter Three).

To assess lymph node size, the abdominal mammary gland was collected from animals treated with ecotin and stained with Carmine dye as previously described (Chapter Three).

Substrate zymography

Blood, urine, and tissue samples from the heart, lungs, liver, kidney, spleen, thymus and gut-associated mesenteric lymph nodes were collected from a virgin mouse after perfusion with PBS, pH 7.4. Lysates were prepared from these samples and from mammary lymph nodes from involuting mice as previously described (Chapter Three). To detect uPA, tPA and sp80, casein-Plg zymography was performed as previously described (Chapter Three).

Analysis of lymphocyte populations

Lymph nodes were separated from the surrounding connective tissue and gently homogenized in PBS, pH 7.4, containing 0.3% BSA (Sigma). The cells were filtered through a 40 μM cell strainer (Falcon), washed with PBS/0.3% BSA, and counted using a cell counter. The cells were concentrated by centrifugation and approximately 10^6 cells were used per experiment after resuspension in PBS/0.3% BSA. Fluorophore-conjugated antibodies derived against the lymphocyte markers (Table 4-1) CD3, CD4, CD8α, CD8β, CD25, CD 69, CD 90, CD103, B220, and TCRαβ (Pharmingen) were used for analysis. Mammary lymph nodes from ecotin-treated mice were analyzed using antibodies against CD4, CD8α and CD103. The cells were incubated for 1 hour on ice with a combination of three antibodies per set. Each antibody was used at a dilution of 1/100. The lymphocytes were washed with PBS/0.3% BSA, resuspended in the same, and analyzed by flow cytometric three-color analysis using the FACScan (Beckton Dickinson) as per the manufacturer's instructions. During data collection, the cells were gated to eliminate dead and non-lymphocyte cells. A total of 4,000 cells was counted in each case.

Data analysis

The data were analyzed using CellQuest™ software. The forward scatter (FSC) and side scatter (SSC) profile (Figure 4-2) of each sample was analyzed to determine if the cells were gated correctly for lymphocyte populations. Data were represented on a two-parameter dot plot, and divided into quadrants based on grouped cell populations (Figure 4-3A). The fluorescence histogram was checked for each parameter to ensure accuracy of the quadrant divisions (Figure 4-3B, C). For each antibody set, the same quadrant

divisions were applied to every sample (both mammary and gut-associated lymphocytes), and the quadrant statistics were obtained (Figure 4-4). The mean of each group of data was calculated using Microsoft Excel software.

Results

Ecotin treatment leads to enlarged lymph nodes during involution

Treatment of involuting female mice with either ecotin WT or ecotin RR resulted in enlarged lymph nodes (Figure 4-5). The mammary lymph node in ecotin-treated mice was larger than that observed during lactation (data not shown). Several lines of evidence indicate that this effect is not due to an immunologic response to ecotin. First, the spleen of ecotin-treated animals was not enlarged (data not shown). Second, ecotin was administered over a period of 4 days, and naive mice normally do not mount a full-blown immunologic response until 10-14 days after exposure to the antigen. Third, the mammary lymph node is enlarged during involution in Plg-/- mice (Lund, L. R., unpublished). These data indicate that the Plg system modulates lymph node size in the mammary gland.

uPA, tPA and sp80 are present in the mammary lymph node and GALT

Since ecotin treatment and Plg-deficiency resulted in enlarged mammary lymph nodes, the expression of chymotrypsin-fold serine proteases in the mammary lymph node and GALT was assayed by casein-Plg zymography. uPA, tPA and two serine proteases that migrated at 80 kD (sp80) and 120 kD (sp120) were detected in the mammary lymph node of involuting mice (Figure 4-6A). Ecotin treatment did not affect the level of activity of

these proteases as detected by casein-Plg zymography. An activity similar to that of uPA, tPA, sp80 and sp120 was detected in mesenteric lymph nodes (GALT; Figure 4-6B). uPA and tPA were detected in the spleen and thymus, which are also lymphoid tissues.

Mammary lymph node lymphocyte subpopulations vary during lactation and involution

The lymphocyte population present in the mammary lymph node during different stages of adult mammary development was analyzed using antibodies to various lymphocyte markers and compared to the lymphocyte population present in the GALT (Peyer's patches) at the same stage. The results are summarized in Table 4-2. The predominant immune cell population present in the mammary lymph node during all stages of development was T lymphocytes that express both T-cell receptors and CD3 (TCRαβ+ CD3+). Significant numbers of B lymphocytes (B220-expressing cells) were not detected. Certain lymphocyte subpopulations appeared to vary significantly among different stages. A smaller proportion of T-lymphocytes (TCRαβ+ CD103+ and TCRαβ+ CD3+) was detected in the involuting lymph node. The percentage of T lymphocytes expressing CD103 (CD103+ CD3+ and CD103+ CD8b+), significantly increased during lactation. CD103 (α_E integrin) mediates the adhesion of lymphocytes to the gut wall, and may play a similar role in the mammary gland. The proportion of CD69-expressing T cells also increased during lactation (CD69+ B220- and CD69+ CD90-). In addition, the proportion of this subpopulation of cells was increased during involution, as compared to lactation. During involution, the percentage of CD8β-expressing T cells (CD8β+ CD8α- and CD8β+ CD103-) also increased.

Lymphocytes from Peyer's patches (GALT) were similarly analyzed at different stages of adult mammary development, and the results are summarized in Table 4-3. A majority of GALT lymphocytes expressed CD3 (CD3+ CD103-, CD3+ TCRαβ-) and CD25 (CD25+ CD8α-). Changes in the lymphocyte population were apparent in lactating and involuting mice. The proportion of CD8β-expressing cells (CD8β+ CD103- and CD8β+ CD8α-) decreased during both lactation and involution. The percentage of CD69-expressing cells (CD69+ B220- and CD69+ CD90-) decreased during involution. These changes correlated with increases in the proportion of similar lymphocytes in the mammary lymph node.

Comparision of the immune cells present in the mammary lymph node and Peyer's patches at each stage of development revealed differences in the markers expressed in these two cell populations (Table 4-4A-D). The lymphocyte subpopulations in the mammary lymph node were distinct from those detected in Peyer's patches in virgin, pregnant, lactating and involuting mice.

Ecotin treatment results in changes in the lymphocyte population

The number of immune cells present in the mammary lymph node of ecotin-treated involuting mice was increased about 5-fold compared to control mice (data not shown). The immune cell population present in the mammary lymph node of control and ecotin-treated mice was analyzed for expression of the T lymphocyte markers CD4, CD8α and CD103 (Table 4-5). Treatment with ecotin RR resulted in a decrease in the percentage of cells expressing CD4 (CD4+ CD103- and CD4+ CD8α-) and in CD8α+ CD4 - cells. Treatment with ecotin WT resulted in a decreased proportion of cells expressing CD8α

(CD8α+ CD103+ and CD8α+ CD4 -) as well as CD4+ (CD4+ CD103- and CD4+ CD8α-). These data suggest that inhibition of chymotrypsin-fold serine proteases during involution leads to an increased number of lymphocytes and changes in the subpopulations present in mammary lymph node.

Discussion

What mechanisms underlie the enlargement of the mammary lymph node observed during involution in ecotin-treated mice? One possibility is that chymotrypsin-fold serine proteases are required to remodel the mammary lymph node and thereby mediate regression. The lymph node is a highly organized lymphoid structure. The structural integrity of the lymph node is maintained by the extracellular matrix (ECM) and basement membrane (BM). Degradation of the ECM and BM by the Plg system may mediate the enlargement and regression of the lymph node. It is clear that serine proteases including uPA and tPA are expressed in mammary lymph nodes and the GALT. It remains to be determined whether these proteases are expressed by lymphocytes or by the stromal tissue associated with lymphoid structures.

Serine proteases may modulate the adhesion of lymphocytes to target tissues. Integrins play a role in adhesion of lymphocytes to endothelial and epithelial tissues (Springer, 1990). CD103 ($\alpha_E$integrin) complexes to β7 integrin, and the $\alpha_E\beta7$ integrin complex binds to E-cadherin and thereby mediates the adhesion of intestinal intraepithelial lymphocytes (IELs), a subset of T lymphocytes, to epithelial cells (Cepek et al., 1994). Extracellular proteolysis of ligands such as E-cadherin, or of adhesion

receptors such as $\alpha_E\beta7$ integrin, by serine proteases may promote lymphocyte egress during involution of the mammary gland.

In addition to adhesion, the Plg system may play a role in lymphocyte migration to non-lymphoid tissues. Lymphocytes migrate to lymphoid tissues such as the lymph node via lymphatic vessels. However, it is not known how lymphocytes migrate to tissues such as the mammary gland. Circulating lymphocytes may enter the mammary gland via the blood, and cell-surface proteolysis may be required to promote this migration. The uPA receptor, uPAR (CD87) is expressed on the surface of T lymphocytes, and may play a role in lymphocyte migration, similar to its role in mediating the migration of non-lymphoid cells during ovulation and cancer progression (Dano et al., 1985; Huarte et al., 1985).

Mammary epithelial lymphocytes are thought to derive from the GALT. Comparision of the lymphocyte subpopulation present in the mammary lymph node and Peyer's patches at different stages of mammary development indicates that mammary lymph node lymphocytes are distinct from GALT lymphocytes. However, it is interesting to note that increases in certain subpopulations in the mammary gland, notably T lymphocytes expressing CD103 (CD103+ CD3+ and CD103+ CD8b+) during lactation and CD8β-expressing T cells (CD8β+ CD8α- and CD8β+ CD103-) during involution, appear to correlate with decreases in the same subpopulations in the GALT. Further studies are necessary to determine if lymphocyte migration occurs between the GALT and the mammary lymph node during lactation and involution.

The finding that ecotin treatment results in increased number of lymphocytes, and changes in the lymphocyte subpopulations in the mammary lymph node during

involution, suggests a role for chymotrypsin-fold serine proteases in lymphocyte egress during involution. Further analysis is necessary to fully characterize the lymphocyte subpopulations present in the mammary lymph node of ecotin-treated animals. The function of serine proteases in lymphocyte migration and egress needs to be determined.

During involution of the mammary gland, the secretory epithelial tissue involved in lactation is remodeled and replaced with adipose tissue. The role played by the Plg system in adipogenesis is discussed in Chapter Five.

References

Bugge, T. H., Flick, M. J., Daugherty, C. C., and Degen, J. L. (1995). Plasminogen deficiency causes severe thrombosis but is compatible with development and reproduction. Genes Dev *9*, 794-807.

Cepek, K. L., Shaw, S. K., Parker, C. M., Russell, G. J., Morrow, J. S., Rimm, D. L., and Brenner, M. B. (1994). Adhesion between epithelial cells and T lymphocytes mediated by E-cadherin and the alpha E beta 7 integrin. Nature *372*, 190-3.

Dano, K., Andreasen, P. A., Grondahl-Hansen, J., Kristensen, P., Nielsen, L. S., and Skriver, L. (1985). Plasminogen activators, tissue degradation, and cancer. Adv Cancer Res *44*, 139-266.

Diaz-Jouanen, E., and Williams, R. C., Jr. (1974). T and B lymphocytes in human colostrum. Clin Immunol Immunopathol *3*, 248-55.

Huarte, J., Belin, D., and Vassalli, J. D. (1985). Plasminogen activator in mouse and rat oocytes: induction during meiotic maturation. Cell *43*, 551-8.

Janeway, C. A., and Travers, P. (1997). Immunobiology: the immune system in health and disease, Third Edition (New York, N. Y.: Garland).

Lamm, M. E., Weisz-Carrington, P., Roux, M. E., McWilliams, M., and Phillips-Quagliata, J. M. (1978). Development of the IgA system in the mammary gland. In Secretory Immunity and Infection, J. McGhee, J. Mestecky and J. L. Babb, eds., pp. 35-51.

Parmely, M. J., and Manning, L. S. (1983). Cellular determinants of mammary cell-mediated immunity in the rat: kinetics of lymphocyte subset accumulation in the rat mammary gland during pregnancy and lactation. Ann N Y Acad Sci *409*, 517-33.

Richie, E. R., Bass, R., Meistrich, M. L., and Dennison, D. K. (1982). Distribution of T lymphocyte subsets in human colostrum. J Immunol *129*, 1116-9.

Riordan, J. M., and Nichols, F. H. (1990). A descriptive study of lactation mastitis in long-term breastfeeding women. J Hum Lact *6*, 53-8.

Springer, T. A. (1990). Adhesion receptors of the immune system. Nature *346*, 425-34.

Sridama, V., Pacini, F., Yang, S. L., Moawad, A., Reilly, M., and DeGroot, L. J. (1982). Decreased levels of helper T cells: a possible cause of immunodeficiency in pregnancy. N Engl J Med *307*, 352-6.

Taylor, B. C., Dellinger, J. D., Cullor, J. S., and Stott, J. L. (1994). Bovine milk lymphocytes display the phenotype of memory T cells and are predominantly CD8+. Cell Immunol *156*, 245-53.

Wei, W. Z., Malone, K., Mahoney, K., and Heppner, G. (1986). Characterization of lymphocytic infiltrates in normal, preneoplastic, and neoplastic mouse mammary tissues. Cancer Res *46*, 2680-5.

Figure 4-1. Location of the abdominal mammary lymph node in mice.

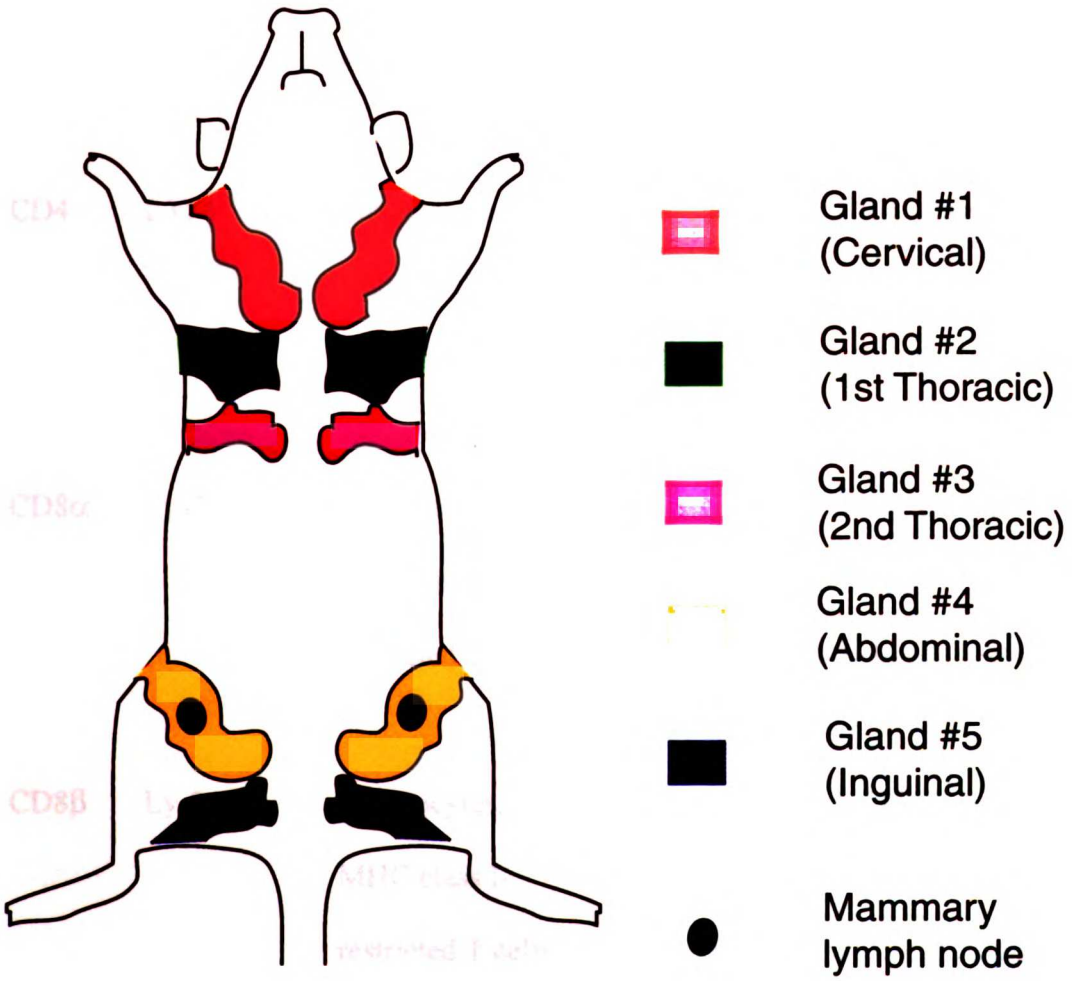

Table 4-1. Markers used to analyze mammary lymph node and Peyer's patch lymphocytes.

Name	Alternate name	Mouse expression	Function
CD3ε	T3	Thymocytes, mature T cells	Signal transduction in association with TCRαβ and TCRγδ
CD4	L3T4	Thymocytes, mature MHC class II-restricted T cells	Co-receptor for MHC class II molecules; mediates T helper/inducer cell response
CD8α	Ly-2	Thymocytes, MHC class I-restricted T cells	Co-receptor for MHC class I molecules; mediates T suppressor/cytotoxic cell response
CD8β	Ly-3	Thymocytes, MHC class I-restricted T cells	Co-receptor for MHC class I molecules; mediates T suppressor/cytotoxic cell response
CD25	IL-2 receptor α chain	Activated T and B lymphocytes	Receptor for interleukin-2

Table 4-1 (cont.)

Name	Alternate name	Mouse expression	Function
CD69	Activation inducer molecule	Activated T and B lymphocytes	Unknown, very early activation antigen
CD90	Thy-1	Thymocytes, T cells	Unknown
CD103	α_E integrin	Intestinal intraepithelial lymphocytes	Binding to gut epithelium (as complex with β_7 integrin)
B220		B lymphocytes	Marker for B cells
TCR$\alpha\beta$		Thymocytes, T lymphocytes	Recognition of antigen-MHC complexes

Figure 4-2.

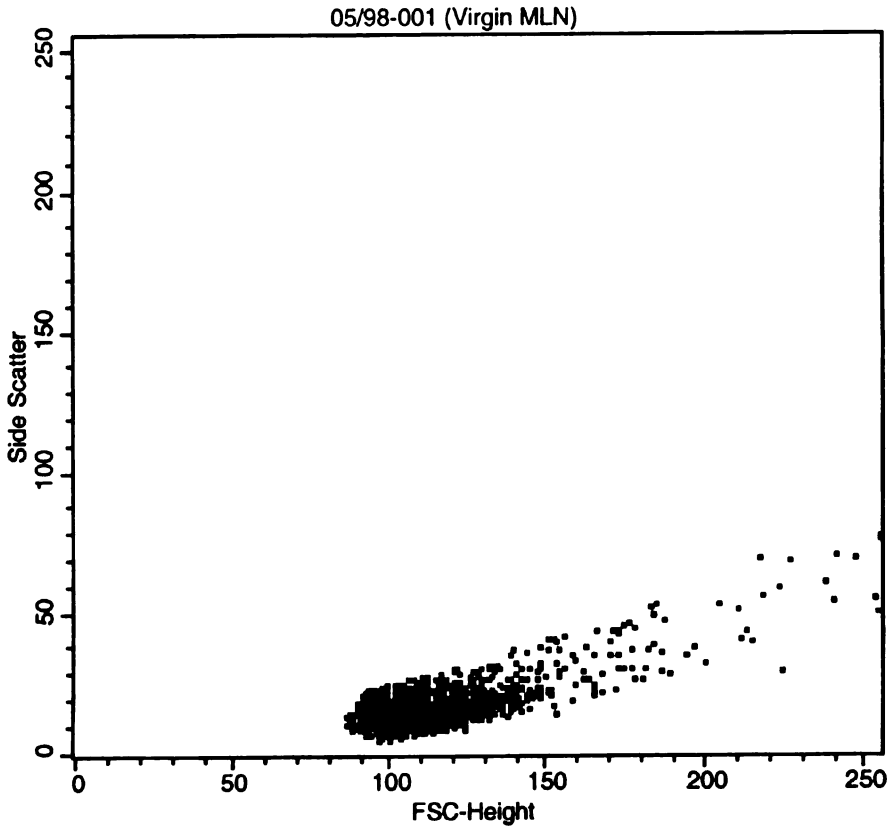
05/98-001 (Virgin MLN)
Side Scatter
FSC-Height
0
50
100
150
200
250

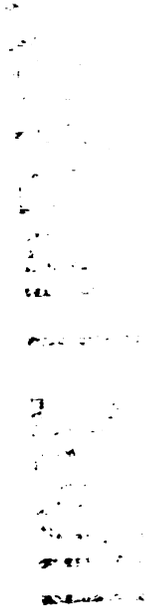

Figure 4-3A.

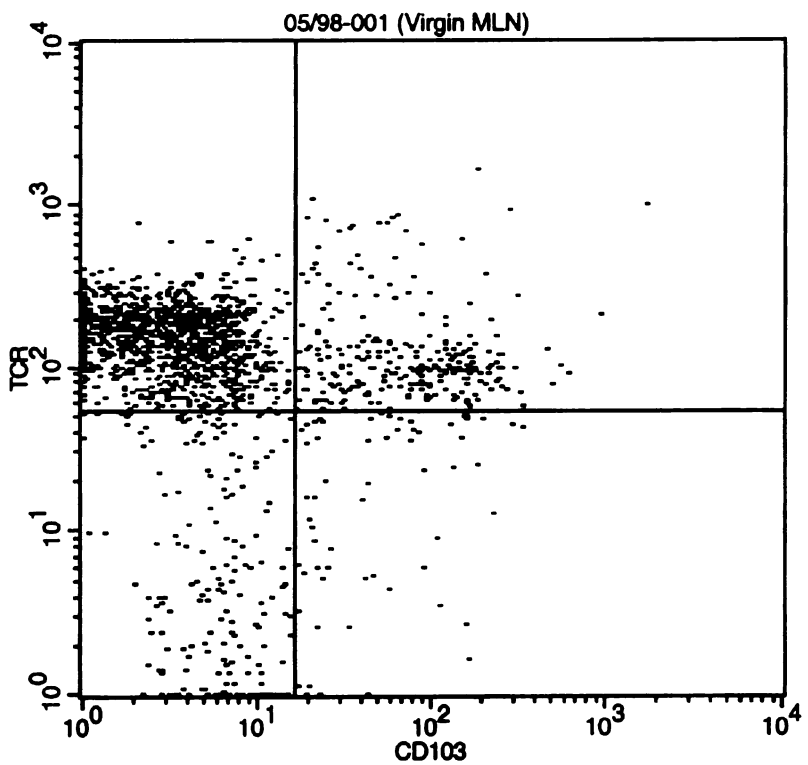

Figure 4-3B.

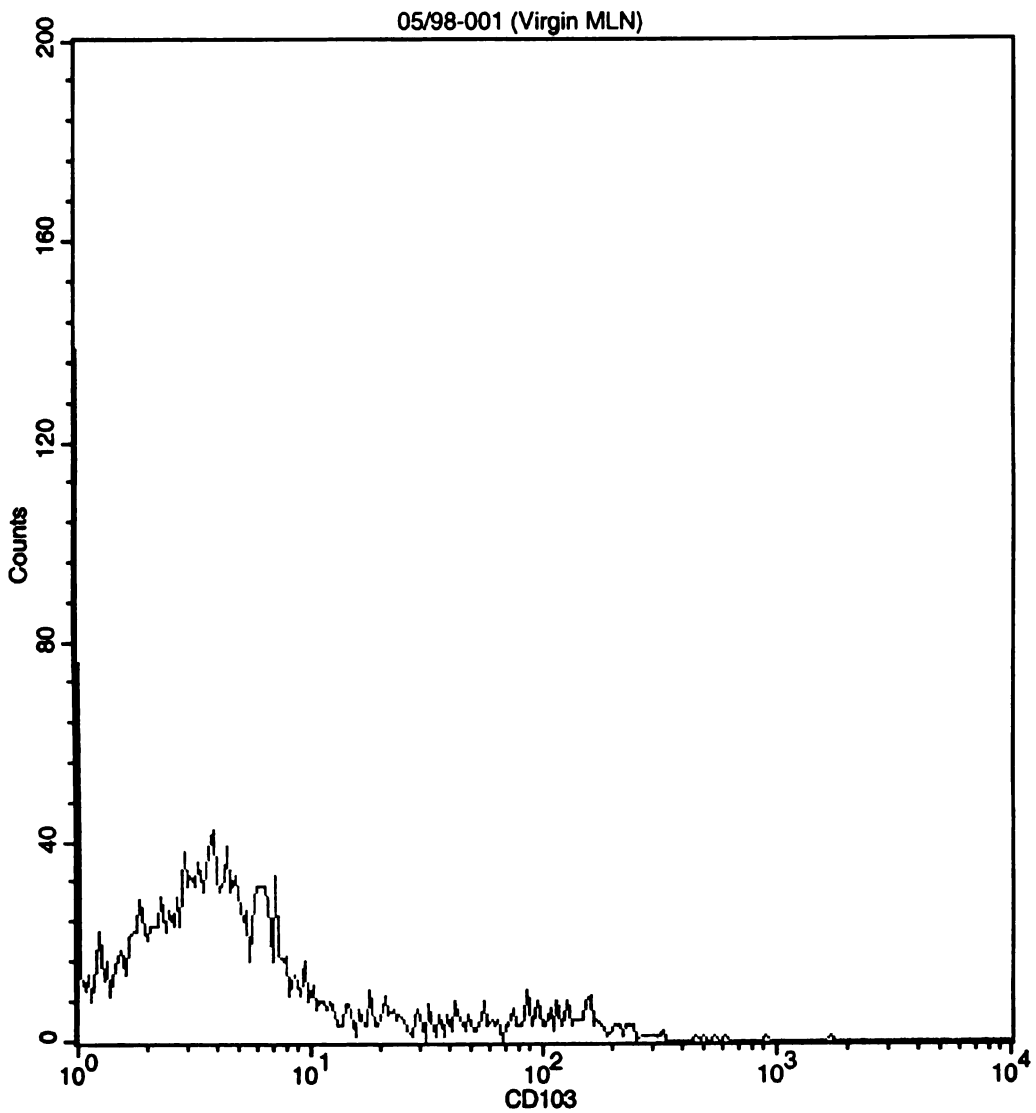
05/98-001 (Virgin MLN)
Counts
0
40
80
120
160
200
10^0
10^1
10^2
10^3
10^4
CD103

Figure 4-3C.

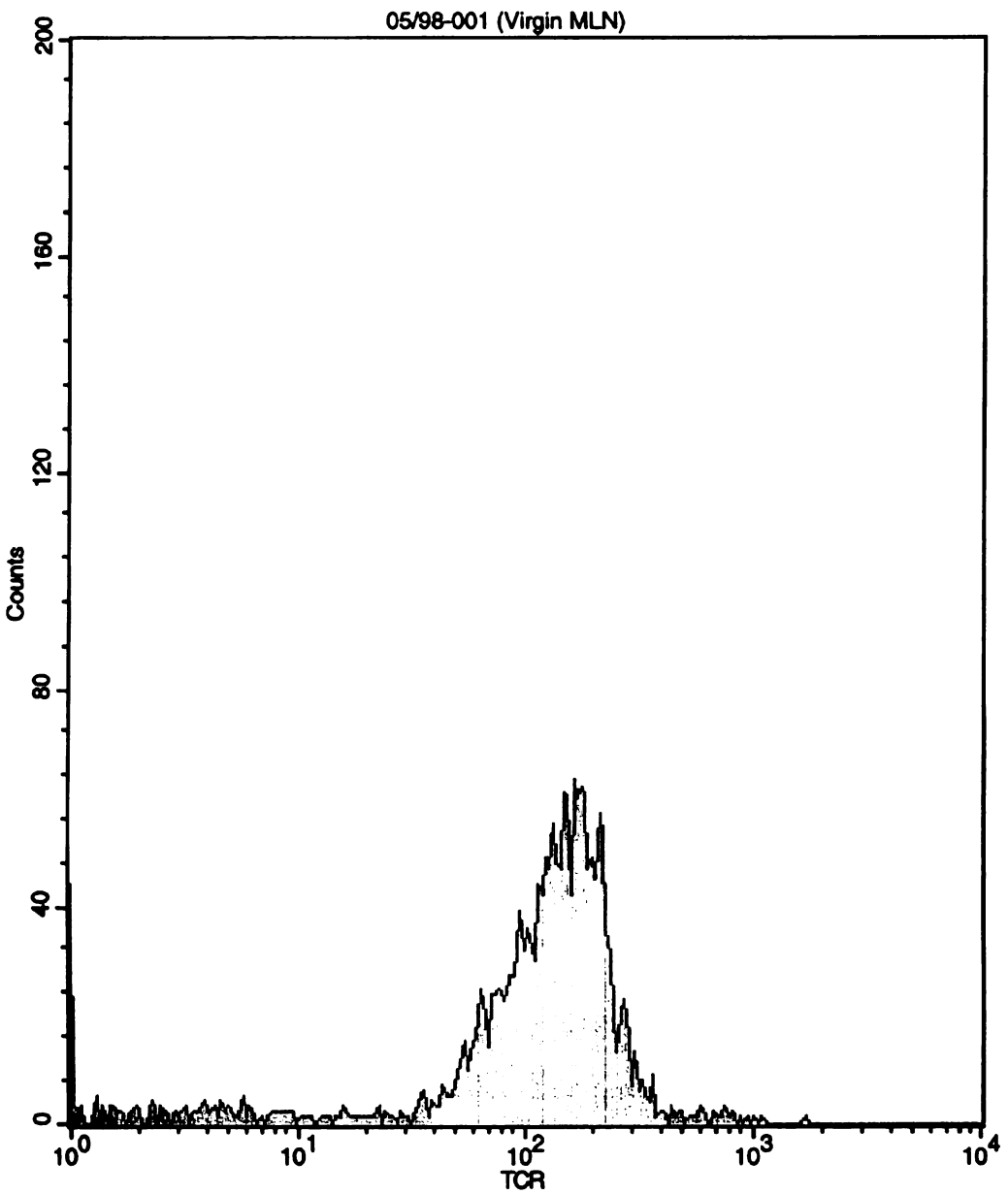
05/98-001 (Virgin MLN)
Counts
0
40
80
120
160
200
10^0
10^1
10^2
10^3
10^4
TCR

Figure 4-4.

Quadrant Statistics

File: 05/98-001 (Virgin MLN)
Log Data Units: Linear Values
Sample ID:
Patient ID:
Tube:
Panel:
Acquisition Date: 30-Apr-98
Gate: No Gate
Gated Events: 2000
Total Events: 2000
X Parameter: FL1-H CD103 (Log)
Y Parameter: FL2-H TCR (Log)
Quad Location: 16, 52

Quad	Events	% Gated	% Total	X Mean	X Geo Mean	Y Mean	Y Geo Mean
UL	1483	74.15	74.15	3.75	3.03	162.77	149.46
UR	261	13.05	13.05	105.93	71.35	167.57	121.55
LL	196	9.80	9.80	6.60	5.63	13.86	5.30
LR	60	3.00	3.00	70.80	47.60	23.58	13.58

Figure 4-2. Representative forward (FSC-Height) and side scatter profile. Lymphocytes from the mammary lymph node of a virgin mouse.

Figure 4-3. **A.** Representative two-parameter dot-plot. Lymphocytes from the mammary lymph node of a virgin mouse analyzed for TCR and CD103 expression. **B-C.** Representative fluorescence histograms. **B,** Lymphocytes from the mammary lymph node of a virgin mouse analyzed for TCR expression. **C,** Lymphocytes from the mammary lymph node of a virgin mouse analyzed for CD103 expression.

Figure 4-4. Representative quadrant statistics. Data from lymphocytes from the mammary lymph node of a virgin mouse analyzed for TCR and CD103 expression.

Table 4-2. Percentage of immune cells expressing specific lymphocyte markers in the mammary lymph node at various stages of adult mammary gland development.

	Mammary Gland Stage			
Marker	**Virgin**	**Pregnant**	**Lactating**	**Involuting**
TCRαβ+ CD103-	74.8	67.5	69.6	58.2
CD103+ TCRαβ-	0.9	0.9	0.7	0.8
TCRαβ+ CD103+	14.3	19.2	20.6	14.1
CD3+ TCRαβ-	9.8	12.0	9.2	26.3
TCRαβ+ CD3-	0.8	3.5	4.9	2.9
CD3+ TCRαβ+	88.5	83.4	85.4	69.8
CD3+ CD103-	85.7	80.4	80.1	86.4
CD103+ CD3-	0.5	0.4	0.5	0.3
CD103+ CD3+	13.0	17.8	18.3	12.1
CD8α+ CD4-	15.8	22.7	18.5	17.5
CD4+ CD8α-	13.5	15.0	14.1	16.0
CD4+ CD8α+	2.2	2.5	2.1	1.8
CD25+ CD8α-	75.2	66.4	70.0	69.9
CD8α+ CD25-	16.1	23.6	20.6	21.1
CD8α+ CD25+	7.2	7.0	6.6	4.2
CD4+ CD25-	69.9	60.1	65.2	60.9
CD25+ CD4 -	1.9	2.3	2.9	2.9
CD4+ CD25+	10.8	12.2	10.4	10.9
CD8α+ CD103-	0.6	0.3	0.3	0.8
CD103+ CD8α-	0.1	0.3	0.0	0.6
CD103+ CD8a+	18.1	25.8	22.3	21.8
CD8β+ CD8α-	13.3	15.4	12.9	29.1
CD8α+ CD8β-	12.4	13.5	8.4	13.4
CD8α+ CD8β+	7.8	14.5	15.5	11.2
CD8β+ CD103-	14.5	16.6	13.8	30.8
CD103+ CD8β-	10.6	11.6	7.4	12.6
CD103+ CD8β+	8.1	15.1	15.5	11.1
CD90+ B220-	2.7	3.3	3.1	3.4
B220+ CD90-	2.2	3.3	3.2	3.5
B220+ CD90+	0.2	0.4	0.5	0.4
CD69+ B220-	9.6	16.5	15.1	25.3
B220+ CD69-	2.6	3.6	3.6	3.5
B220+ CD69+	0.2	0.7	0.7	1.5
CD69+ CD90-	10.5	18.1	16.8	27.4
CD90+ CD69-	0.3	0.2	0.2	0.0
CD90+ CD69+	0.3	0.7	0.8	0.6

Table 4-3. Percentage of immune cells expressing specific lymphocyte markers in GALT (Peyer's patches) at various stages of adult mammary gland development.

	Mammary Gland Stage			
Marker	**Virgin**	**Pregnant**	**Lactating**	**Involuting**
TCRαβ+ CD103-	26.1	26.4	26.2	26.3
CD103+ TCRαβ-	1.2	2.4	3.1	3.2
TCRαβ+ CD103+	5.0	6.4	7.9	10.5
CD3+ TCRαβ-	60.5	59.0	47.9	50.5
TCRαβ+ CD3-	2.0	7.6	20.5	14.4
CD3+ TCRαβ+	29.3	25.4	14.0	22.9
CD3+ CD103-	90.2	85.7	69.5	74.5
CD103+ CD3-	0.3	0.8	3.4	2.9
CD103+ CD3+	4.7	5.6	4.9	8.0
CD8α+ CD4-	2.7	2.6	2.6	4.0
CD4+ CD8α-	23.3	28.0	29.4	24.4
CD4+ CD8α+	0.7	0.8	0.9	1.2
CD25+ CD8α-	77.6	79.2	76.0	72.3
CD8α+ CD25-	3.1	2.9	3.2	5.0
CD8α+ CD25+	2.4	3.9	3.5	2.9
CD4+ CD25-	67.5	66.6	63.5	61.1
CD25+ CD4 -	7.3	7.2	7.9	7.6
CD4+ CD25+	9.6	14.0	12.5	10.1
CD8α+ CD103-	1.8	1.3	1.7	4.3
CD103+ CD8α-	0.1	0.0	0.0	0.1
CD103+ CD8a+	1.4	2.5	2.5	3.7
CD8β+ CD8α-	52.8	50.3	28.5	29.4
CD8α+ CD8β-	0.6	1.2	2.2	3.9
CD8α+ CD8β+	3.1	3.2	2.4	4.9
CD8β+ CD103-	57.2	55.1	35.0	36.8
CD103+ CD8β-	0.4	1.4	1.8	2.5
CD103+ CD8β+	1.6	1.7	1.2	2.0
CD90+ B220-	4.7	7.0	7.4	9.1
B220+ CD90-	8.4	7.1	9.4	11.0
B220+ CD90+	0.7	1.0	1.4	1.8
CD69+ B220-	58.3	49.6	35.2	15.1
B220+ CD69-	9.1	7.5	10.3	14.1
B220+ CD69+	2.0	2.4	2.6	1.2
CD69+ CD90-	64.2	65.2	51.7	38.2
CD90+ CD69-	0.6	0.5	1.2	1.5
CD90+ CD69+	1.1	1.4	1.4	1.0

Table 4-4A. Comparision of the lymphocyte population present in the mammary lymph node and GALT (Peyer's patches) of a virgin mouse.

Marker	Mammary	GALT
TCRαβ+ CD103-	74.8	26.1
CD103+ TCRαβ-	0.9	1.2
TCRαβ+ CD103+	14.3	5.0
CD3+ TCRαβ-	9.8	60.5
TCRαβ+ CD3-	0.8	2.0
CD3+ TCRαβ+	88.5	29.3
CD3+ CD103-	85.7	90.2
CD103+ CD3-	0.5	0.3
CD103+ CD3+	13.0	4.7
CD8α+ CD4-	15.8	2.7
CD4+ CD8α-	13.5	23.3
CD4+ CD8α+	2.2	0.7
CD25+ CD8α-	75.2	77.6
CD8α+ CD25-	16.1	3.1
CD8α+ CD25+	7.2	2.4
CD4+ CD25-	69.9	67.5
CD25+ CD4 -	1.9	7.3
CD4+ CD25+	10.8	9.6
CD8α+ CD103-	0.6	1.8
CD103+ CD8α-	0.1	0.1
CD103+ CD8a+	18.1	1.4
CD8β+ CD8α-	13.3	52.8
CD8α+ CD8β-	12.4	0.6
CD8α+ CD8β+	7.8	3.1
CD8β+ CD103-	14.5	57.2
CD103+ CD8β-	10.6	0.4
CD103+ CD8β+	8.1	1.6
CD90+ B220-	2.7	4.7
B220+ CD90-	2.2	8.4
B220+ CD90+	0.2	0.7
CD69+ B220-	9.6	58.3
B220+ CD69-	2.6	9.1
B220+ CD69+	0.2	2.0
CD69+ CD90-	10.5	64.2
CD90+ CD69-	0.3	0.6
CD90+ CD69+	0.3	1.1

Table 4-4B. Comparision of the lymphocyte population present in the mammary lymph node and GALT (Peyer's patches) of a pregnant mouse.

Marker	Mammary	GALT
TCRαβ+ CD103-	67.5	26.4
CD103+ TCRαβ-	0.9	2.4
TCRαβ+ CD103+	19.2	6.4
CD3+ TCRαβ-	12.0	59.0
TCRαβ+ CD3-	3.5	7.6
CD3+ TCRαβ+	83.4	25.4
CD3+ CD103-	80.4	85.7
CD103+ CD3-	0.4	0.8
CD103+ CD3+	17.8	5.6
CD8α+ CD4-	22.7	2.6
CD4+ CD8α-	15.0	28.0
CD4+ CD8α+	2.5	0.8
CD25+ CD8α-	66.4	79.2
CD8α+ CD25-	23.6	2.9
CD8α+ CD25+	7.0	3.9
CD4+ CD25-	60.1	66.6
CD25+ CD4 -	2.3	7.2
CD4+ CD25+	12.2	14.0
CD8α+ CD103-	0.3	1.3
CD103+ CD8α-	0.3	0.0
CD103+ CD8a+	25.8	2.5
CD8β+ CD8α-	15.4	50.3
CD8α+ CD8β-	13.5	1.2
CD8α+ CD8β+	14.5	3.2
CD8β+ CD103-	16.6	55.1
CD103+ CD8β-	11.6	1.4
CD103+ CD8β+	15.1	1.7
CD90+ B220-	3.3	7.0
B220+ CD90-	3.3	7.1
B220+ CD90+	0.4	1.0
CD69+ B220-	16.5	49.6
B220+ CD69-	3.6	7.5
B220+ CD69+	0.7	2.4
CD69+ CD90-	18.1	65.2
CD90+ CD69-	0.2	0.5
CD90+ CD69+	0.7	1.4

Table 4-4C. Comparision of the lymphocyte population present in the mammary lymph node and GALT (Peyer's patches) of a lactating mouse.

Marker	Mammary	GALT
TCRαβ+ CD103-	69.6	26.2
CD103+ TCRαβ-	0.7	3.1
TCRαβ+ CD103+	20.6	7.9
CD3+ TCRαβ-	9.2	47.9
TCRαβ+ CD3-	4.9	20.5
CD3+ TCRαβ+	85.4	14.0
CD3+ CD103-	80.1	69.5
CD103+ CD3-	0.5	3.4
CD103+ CD3+	18.3	4.9
CD8α+ CD4-	18.5	2.6
CD4+ CD8α-	14.1	29.4
CD4+ CD8α+	2.1	0.9
CD25+ CD8α-	70.0	76.0
CD8α+ CD25-	20.6	3.2
CD8α+ CD25+	6.6	3.5
CD4+ CD25-	65.2	63.5
CD25+ CD4 -	2.9	7.9
CD4+ CD25+	10.4	12.5
CD8α+ CD103-	0.3	1.7
CD103+ CD8α-	0.0	0.0
CD103+ CD8a+	22.3	2.5
CD8β+ CD8α-	12.9	28.5
CD8α+ CD8β-	8.4	2.2
CD8α+ CD8β+	15.5	2.4
CD8β+ CD103-	13.8	35.0
CD103+ CD8β-	7.4	1.8
CD103+ CD8β+	15.5	1.2
CD90+ B220-	3.1	7.4
B220+ CD90-	3.2	9.4
B220+ CD90+	0.5	1.4
CD69+ B220-	15.1	35.2
B220+ CD69-	3.6	10.3
B220+ CD69+	0.7	2.6
CD69+ CD90-	16.8	51.7
CD90+ CD69-	0.2	1.2
CD90+ CD69+	0.8	1.4

Table 4-4D. Comparision of the lymphocyte population present in the mammary lymph node and GALT (Peyer's patches) of an involuting mouse.

Marker	Mammary	GALT
TCRαβ+ CD103-	58.2	26.3
CD103+ TCRαβ-	0.8	3.2
TCRαβ+ CD103+	14.1	10.5
CD3+ TCRαβ-	26.3	50.5
TCRαβ+ CD3-	2.9	14.4
CD3+ TCRαβ+	69.8	22.9
CD3+ CD103-	86.4	74.5
CD103+ CD3-	0.3	2.9
CD103+ CD3+	12.1	8.0
CD8α+ CD4-	17.5	4.0
CD4+ CD8α-	16.0	24.4
CD4+ CD8α+	1.8	1.2
CD25+ CD8α-	69.9	72.3
CD8α+ CD25-	21.1	5.0
CD8α+ CD25+	4.2	2.9
CD4+ CD25-	60.9	61.1
CD25+ CD4 -	2.9	7.6
CD4+ CD25+	10.9	10.1
CD8α+ CD103-	0.8	4.3
CD103+ CD8α-	0.6	0.1
CD103+ CD8a+	21.8	3.7
CD8β+ CD8α-	29.1	29.4
CD8α+ CD8β-	13.4	3.9
CD8α+ CD8β+	11.2	4.9
CD8β+ CD103-	30.8	36.8
CD103+ CD8β-	12.6	2.5
CD103+ CD8β+	11.1	2.0
CD90+ B220-	3.4	9.1
B220+ CD90-	3.5	11.0
B220+ CD90+	0.4	1.8
CD69+ B220-	25.3	15.1
B220+ CD69-	3.5	14.1
B220+ CD69+	1.5	1.2
CD69+ CD90-	27.4	38.2
CD90+ CD69-	0.0	1.5
CD90+ CD69+	0.6	1.0

Figure 4-5.

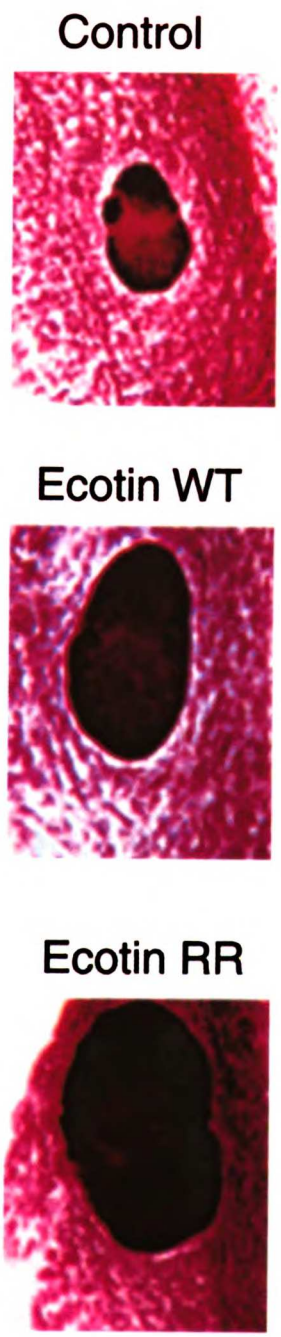

Figure 4-5. Mammary lymph nodes are enlarged in ecotin-treated mice. Carmine dye stain of whole mammary glands on day 5 of involution from control, ecotin WT-treated and ecotin RR-treated animals.

Figure 4-6.

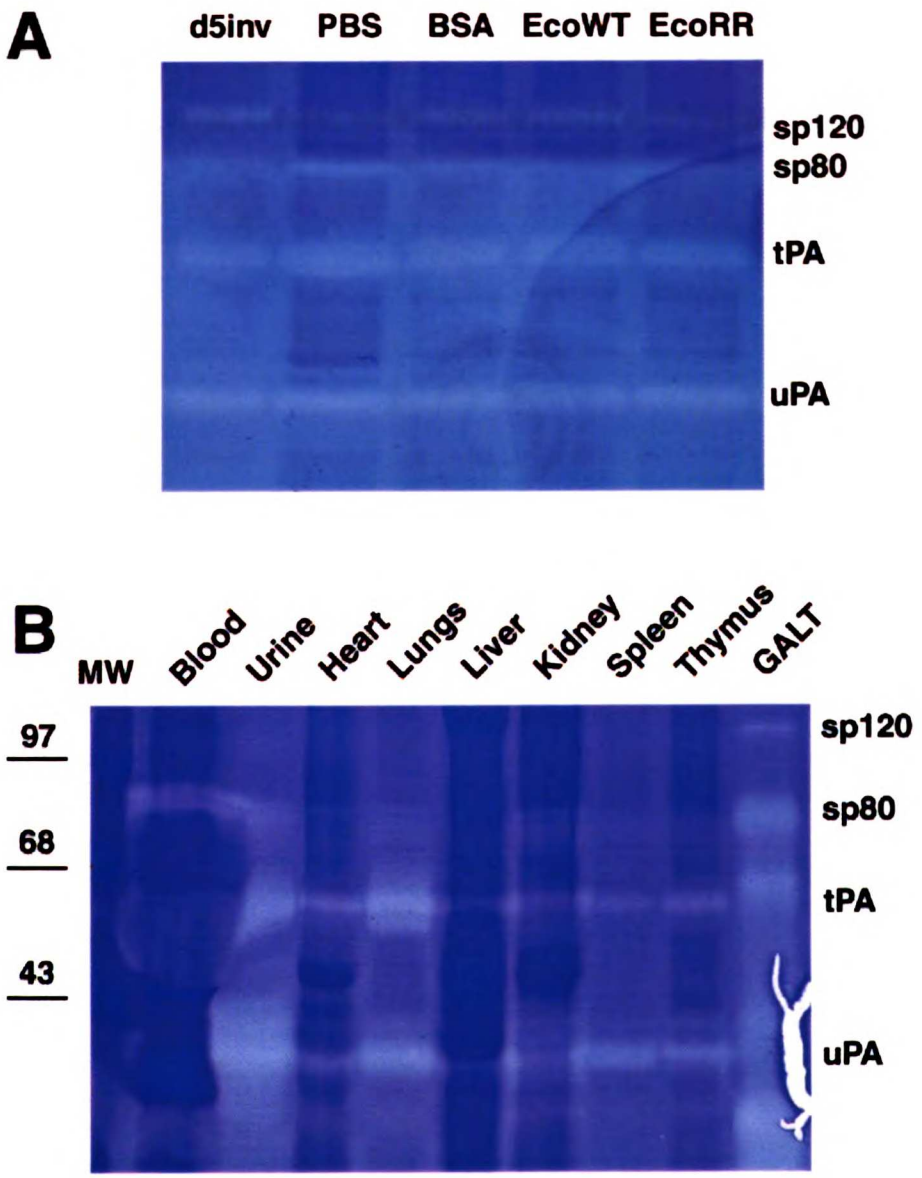
A
d5inv
PBS
BSA
EcoWT
EcoRR
sp120
sp80
tPA
uPA
B
MW
Blood
Urine
Heart
Lungs
Liver
Kidney
Spleen
Thymus
GALT
97
68
43
sp120
sp80
tPA
uPA

Figure 4-6. Casein-plasminogen zymograms. Urokinase (uPA), tissue-type plasminogen activator (tPA), and serine proteases migrating at 80 kD (sp80) and 120 kD (sp120) are detected. **A,** Mammary lymph node samples on day 5 of involution from untreated animals (d5inv), animals treated with phosphate buffered saline (PBS), bovine serum albumin (BSA) ecotin WT (EcoWT) and ecotin RR (EcoRR). **B,** Samples from blood, urine, heart, lungs, liver, kidney, spleen, thymus and Peyer's patches (GALT) of a virgin mouse.

Table 4-5. Percentage of cells expressing the lymphocyte markers CD4, CD8α, and CD103 in the mammary lymph node of ecotin-treated animals

	Treatment			
Marker	**Control**	**BSA**	**Ecotin WT**	**Ecotin RR**
CD8α+ CD103-	3.9	3.5	1.1	7.4
CD103+ CD8α-	5.7	4.3	7.0	5.5
CD8α+ CD103+	9.9	7.4	1.8	8.6
CD4+ CD103-	30.4	30.8	6.8	19.6
CD103+ CD4 -	13.5	9.7	7.2	11.9
CD4+ CD103+	1.0	0.8	0.4	0.6
CD4+ CD8α-	32.4	32.6	7.5	21.5
CD8α+ CD4 -	13.0	10.3	2.7	13.8
CD4+ CD8α+	0.0	0.0	0.0	0.0

Chapter Five

A Plasminogen Cascade Dependent on Plasma Kallikrein is Required for Adipocyte Differentiation

Abstract

We show that plasma kallikrein (PKal) mediates a plasminogen (Plg) cascade in adipocyte differentiation. The serine protease inhibitor ecotin inhibited cell shape change, adipocyte-specific gene expression, and lipid accumulation during adipogenesis in culture. Deficiency of Plg, but not urokinase (uPA) and tissue-type plasminogen activator (tPA), suppressed adipogenesis during 3T3-L1 differentiation and mammary gland involution. PKal, which is inhibited by ecotin, was required for adipose conversion, and for Plg activation and 3T3-L1 differentiation under serum-free conditions. Human plasma deficient in PKal did not support 3T3-L1 differentiation. These findings demonstrate that PKal is a physiological regulator that acts in the Plg cascade during adipogenesis. We propose that the Plg cascade fosters adipocyte differentiation by degradation of the fibronectin-rich preadipocyte stromal matrix. (Sushma Selvarajan, Leif R. Lund, Toshihiko Takeuchi, Charles S. Craik & Zena Werb; accepted for publication in *Nature Cell Biology*).

Introduction

Adipogenesis is regulated by hormones such as leptin [1,2] and transcription factors such as peroxisome proliferator-activated receptor γ (PPARγ) [3,4]. However, it is not generally appreciated that, during adipocyte differentiation, the fibronectin-rich stromal matrix of preadipocytes is converted to the basement membrane of adipocytes [5]. Thus, while we now have an understanding of some of the intracellular events that occur during adipocyte differentiation [6,7], the role of the extracellular matrix (ECM) is yet to be explored. In this study, we have tested the hypothesis that ECM-degrading proteases are required during adipogenesis. We focussed on the plasminogen (Plg) system of serine proteases because plasmin directly cleaves various ECM molecules, including fibronectin [8] and laminin [9], and releases bound cytokines such as insulin-like growth factor-I (IGF-I) [10]. Plg can be activated to plasmin by urokinase-type plasminogen activator (uPA) and by tissue-type plasminogen activator (tPA). In the present study, we utilized genetic and inhibitor-based approaches to evaluate the role of serine proteases during the adipogenic differentiation of preadipocytes in culture and the repopulation of adipocytes during involution of the murine mammary gland *in vivo*. We have identified an important role for the Plg system of serine proteases during adipocyte differentiation.

Results

Inhibition of serine proteases decreases 3T3-L1 differentiation. To determine which serine proteases in the plasminogen cascade play a role during adipocyte differentiation, we used a novel inhibitor-based approach to block their activity during 3T3-L1 differentiation. Ecotin is a macromolecular inhibitor that inhibits a broad range of

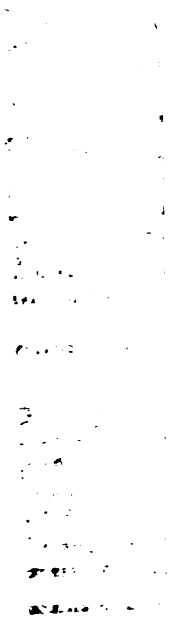

chymotrypsin-like serine proteases such as trypsin, chymotrypsin and elastase [11]. Wild-type (WT) ecotin is a poor inhibitor of uPA and plasmin; however, the variant ecotin Met84Arg/Met85Arg (RR) is a nanomolar inhibitor of uPA [12]. Addition of either ecotin WT or ecotin RR had no effect on preadipocytes, but reduced adipose conversion to less than 20% of control levels (Fig. 1a, b). Three lines of evidence indicate that the lack of lipid accumulation was due to a blockade in the differentiation pathway. First, most of the ecotin-treated cells did not undergo morphologic differentiation (rounding up). Second, CCAAT/enhancer binding protein β (C/EBP β) (Fig. 1c) and peroxisome proliferator activated receptor γ (PPARγ) (Fig. 1d), transcription factors that are required for adipogenic differentiation [3,4,13], were only weakly expressed in ecotin-treated cells. Third, levels of glycerophosphate dehydrogenase (GPDH), an enzymatic marker for differentiated adipocytes [14], were only about 20% of control in cells cultured with either ecotin (data not shown). These data support a functional role for serine proteases during the differentiation of predipocytes in culture.

To further analyze the role of plasminogen and plasminogen activators, we used the serpins α-2-antiplasmin (α2-AP, which inhibits plasmin [15,16]) and plasminogen activator inhibitor-1 (PAI-1, which inhibits uPA and tPA [17]) during 3T3-L1 differentiation. Our data support the hypothesis that plasmin is required during the differentiation of 3T3-L1 preadipocytes in culture. Treatment of cells with α2-AP during differentiation inhibited adipose conversion and lipid accumulation (Fig. 1h, i). On the other hand, uPA and tPA to not appear to be required for adipogenesis, since treatment with PAI-1 had no effect on 3T3-L1 differentiation (Fig. 1g, i).

Adipogenic differentiation of 3T3-L1 cells is Plg-dependent. We analyzed the expression of uPA and tPA in preadipocytes and differentiated adipocytes. We detected uPA and tPA in both the conditioned medium (CM) and cell lysates of 3T3-L1 preadipocytes (Fig. 2a). Two other caseinolytic serine proteases that migrated at 80 kD and 120 kD (sp80 and sp120), and were inhibited by phenylmethylsulfonyl fluoride, were present in the CM of 3T3-L1 preadipocytes and differentiated adipocytes. An activity similar to sp80 was also present in fetal bovine serum (FBS). Expression of uPA and tPA decreased with adipogenic differentiation. These data raise the question of what role Plg plays during adipogenesis. 3T3-L1 preadipocytes grew normally in 10% FBS that was depleted of Plg (Fig. 2b). However, once the cells were induced to differentiate, they showed less than 10% adipose conversion compared to cells cultured in complete FBS (Fig. 2c and d). Addition of exogenous Plg to the Plg-depleted FBS rescued differentiation (Fig. 2e). 3T3-L1 preadipocytes differentiated into adipocytes in normal human plasma, albeit to a lesser extent than in FBS. However, no adipose conversion or lipid accumulation was seen in cells that were induced to undergo differentiation in Plg-deficient human plasma. Addition of physiologic levels of exogenous human Plg restored adipose conversion to the level seen in normal human plasma (data not shown). These results demonstrate a requirement for Plg during adipocyte differentiation, when the expression of ECM proteins including fibronectin is downregulated, and suggest that plasmin may be required to remodel the stromal ECM of preadipocytes.

Serine protease inhibitors decrease adipogenesis during mammary gland involution. We next sought evidence for a role of serine proteases during adipogenesis *in vivo*. For

this analysis we exploited the mammary gland, which has an adipose stroma. Following lactation and weaning in the mouse, the mammary gland undergoes a program of remodeling during involution to replace the secretory epithelial tissue involved in lactation with adipose tissue. Adipogenesis during involution occurs in a short time frame. Infiltration of adipocytes can be detected by day 2 of involution [18]. uPA and tPA are upregulated during this process [19]. To evaluate serine protease function *in vivo* during mammary adipogenesis, we treated female CF1 mice with ecotin WT or ecotin RR from day 1 to day 4 of involution, when the mammary gland is normally repopulated with adipocytes. We observed greatly decreased density of adipose tissue on day 5 of involution in mammary glands treated with either type of ecotin (Fig. 3 a-c). These data indicate that serine proteases play an important role in adipogenesis *in vivo*. Concomitant with the decreased adipogenesis, deposition of stromal ECM, as shown by staining for collagen, increased significantly in mice treated with ecotin WT or ecotin RR (Fig. 3e and f). We observed increased deposition of the stromal proteins type I collagen (Fig. 3g-i) and fibronectin (Fig. 3j-l) in animals treated with either ecotin. Ecotin WT, which does not inhibit uPA or plasmin, was as effective as ecotin RR in blocking adipogenesis. Neither ecotin WT nor ecotin RR inhibits tPA. These data suggest that neither uPA nor tPA is required for Plg activation during adipogenesis *in vivo*.

Adipogenesis is impaired in Plg-deficient, but not uPA-deficient mice. Since Plg is required for 3T3-L1 cell adipogenesis, is it also critical *in vivo*? Plg-deficient mice [20] showed impaired adipogenesis (Fig. 4a and b) and increased collagen deposition in the mammary gland (Fig. 4e and f), similar to mice treated with ecotin WT and ecotin RR.

This genetic analysis indicates that Plg is required during involution for normal adipocyte differentiation. Interestingly, healthy adult Plg-/- mice that were the same size skeletal size (confirmed by X-rays) were leaner and lighter than wild-type controls [at 23 weeks of age, 18.8 $\pm$ 2.1 g (n =4) for Plg-/- mice vs. 22.8 $\pm$ 1.0 g (n =5) for control mice, p<0.005]. However, uPA did not appear to contribute significantly to adipocyte differentiation in the mammary gland. Mice deficient in uPA or mice deficient in both uPA and tPA [21] showed no significant alteration in adipogenesis or collagen accumulation during involution (Fig. 4c, d, g and h, and data not shown). These data indicate that neither uPA nor tPA is required for adipogenesis in the mammary gland and suggest the presence of an alternate plasminogen activator during adipogenesis.

Plasma kallikrein is present and required during adipogenesis. We sought another serine protease that is inhibited by both ecotin WT and ecotin RR and can activate Plg. Lysates of 5-day involuting mammary gland from either wild-type or Plg-/- mice, assayed by zymography on casein-Plg gels, showed a 80 kD serine protease, which was similar to the sp80 protease detected in medium conditioned by 3T3-L1 cells (Fig. 5a). sp80 was also present in normal mouse and human plasma, FBS, and in the CM of 3T3-L1 cells grown in the presence, but not absence, of FBS. These data suggest that sp80 is derived from plasma/serum, rather than from the adipogenic cells.

Of mammalian serine proteases present in databases, a compelling candidate is plasma kallikrein (PKal), which has a similar size and is inhibited by sub-nanomolar concentrations of ecotin WT [22]. The mouse sp80 and human PKal were inhibited by both ecotin WT and ecotin RR (Fig. 5b), whereas uPA was inhibited only by ecotin RR.

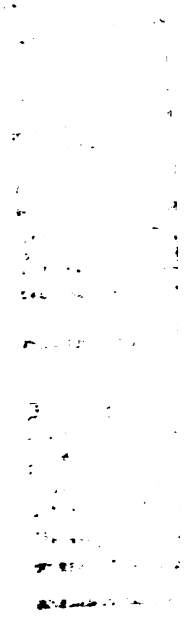

We identified sp80 as PKal by western blotting mammary lysates and mouse serum with a polyclonal anti-human prekallikrein antibody (Fig. 5c). PKal has been shown to activate both pro-uPA [23,24] and Plg [25,26]. To analyze the role of PKal during adipocyte differentiation, we took advantage of Fletcher trait, a rare form of human plasma prekallikrein deficiency [27]. Both normal and prekallikrein-deficient human plasma supported growth of 3T3-L1 preadipocytes (Fig. 5d, e). 3T3-L1 preadipocytes differentiated into adipocytes in normal human plasma, albeit to a lesser extent than in FBS (Fig. 5f, g). However, very little adipose conversion and only 14% lipid accumulation was seen in cells that were induced to undergo differentiation in prekallikrein-deficient human plasma (Fig. 5h, j). Addition of physiologic levels of exogenous human PKal restored adipose conversion to 85% of that seen in normal human plasma (Fig. 5i, j). These data indicate that PKal is required for adipogenesis.

PKal and Plg promote adipogenesis under serum-free differentiation conditions. We next sought to determine whether proteolysis by serine proteases promotes differentiation of 3T3-L1 cells. To this end, we induced the differentiation of 3T3-L1 preadipocytes in the absence of FBS. Under these conditions, the cells undergo adipose conversion to a much lesser extent than cells differentiated in the presence of FBS (Fig. 6a, b and g). The addition of exogenous Plg did not enhance the extent of adipose conversion (Fig. 6c, g). However, the addition of both Plg and PKal promoted adipose conversion to about 50% of that observed in FBS (Fig. 6a, d and g). PKal alone did not significantly increase adipose conversion (data not shown). The PKal zymogen, prekallikrein, was ineffective in promoting adipogenesis both in the presence and absence

of Plg (data not shown), suggesting that activation of prekallikrein is also required. The increase in adipose conversion observed in the presence of Plg and PKal was not significantly affected by the addition of PAI-1 (Fig. 6e, g), but was reduced in the presence of ecotin RR (Fig. 6f, g). These data indicate that although 3T3-L1 preadipocytes express both uPA and tPA (Fig. 2a), PKal is required during adipogenesis to activate Plg and promote adipose conversion.

PKal-mediated Plg cascade promotes fibronectin cleavage during adipocyte differentiation. To confirm our hypothesis that PKal activates Plg during adipocyte differentiation, we analyzed the extent of Plg activation by 3T3-L1 cells by western blot analysis of the appearance of the plasmin protease domain in the presence and absence of PKal. We first confirmed that PKal activates Plg at physiologically relevant concentrations, albeit to a lesser extent than that observed with uPA or tPA (Fig. 7a). However, PKal is present at relatively high concentrations in plasma (30-50 μg/ml) [28] compared to uPA (3-5 ng/ml) or tPA (5-10 ng/ml) [17]. We next analyzed Plg activation during adipogenesis, and found that 3T3-L1 cells that were differentiated in the absence of FBS did not effectively activate Plg, and that the addition of PKal significantly enhanced Plg activation (Fig. 7b). These data suggest that although 3T3-L1 cells express uPA and tPA (Fig. 2a), PKal is required for Plg activation during 3T3-L1 differentiation.

We next sought to determine a molecular target of the Plg cascade. Since we observed increased deposition of fibronectin in the mammary glands of ecotin-treated mice (Fig 3j-l), we tested the hypothesis that the Plg cascade mediates fibronectin cleavage during adipocyte differentiation. We assayed uPA, tPA, plasmin and PKal for

their ability to cleave fibronectin and found that only plasmin cleaves fibronectin into several fragments including a 20 kD fragment (Fig. 7c). We found that 3T3-L1 preadipocytes had cell-associated fibronectin, which was downregulated in adipocytes (Fig. 7d). When we analyzed the CM of 3T3-L1 cells for cleavage of endogenous mouse fibronectin during differentiation, we detected a 20 kD cleaved fragment in the CM of differentiated adipocytes, but not in the CM of preadipocytes or cells treated during differentiation with either ecotin WT or ecotin RR (Fig. 7e). Moreover, mammary lysates also generated fibronectin cleavage products that were suppressed by ecotin treatment (data not shown). These findings indicate that the Plg cascade may promote adipocyte differentiation by degrading the fibronectin-rich stromal ECM of preadipocytes.

PKal-mediated activation of the Plg cascade may be selective for plasmin generation in the milieu of stromal ECM. We found that PKal-mediated, but not uPA-mediated activation of Plg is enhanced in the presence of fibronectin (Fig. 7f). tPA-mediated activation of Plg was enhanced by fibrin, but not by fibronectin (data not shown). These data suggest that PKal may be an important Plg activator in fibrin-independent processes.

In support of a mechanism in which fibronectin degradation is required during adipogenesis, we found that addition of an exogenous fibronectin matrix suppressed 3T3-L1 differentiation (Fig. 7i). This suppression was overcome by the addition of cytochalasin D, which disrupts the actin cytoskeleton (Fig. 7j). Similarly, the suppressive effects of ecotin were overcome by the concomitant addition of cytochalasin D (Fig. 7k, l). These data suggest that remodeling the stromal matrix of preadipocytes may be an

important early step that promotes cell shape change and the expression of adipocyte-specific genes during differentiation.

Discussion

Our study indicates that extracellular proteolysis is a key mechanism for regulating adipocyte differentiation, and shows for the first time that PKal functions in the physiologic Plg activation cascade during adipogenesis. uPA has been considered to be the primary enzyme involved in cell-mediated Plg activation because of its high affinity for Plg and the presence of a specific receptor, uPAR. However, mice deficient in the gene for uPA, or in the genes for both uPA and tPA do not have a marked phenotype with regard to adipogenesis, suggesting the presence of other Plg activators. Other enzymes that have been implicated as Plg activators include PKal [25,26] and Factor XII [29]. PKal is a compelling candidate because of its high concentration, ubiquitous presence and ability to localize to the cell surface. It is also a potent activator of pro-uPA [30,31]. The requirement for PKal and Plg during adipogenesis indicates that PKal is a physiologic component of the Plg activation cascade. Our findings have implications for other physiologic and pathologic processes involving Plg activation *in vivo*.

It is clear that proteolysis selectively affects terminally differentiating adipocytes, not the proliferating preadipocytes, since the cleavage of cell-associated fibronectin, which is a substrate for plasmin, was regulated during adipocyte differentiation. How is the PKal/Plg system regulated during adipogenesis? During adipocyte differentiation, PKal may function as an activator of pro-uPA or as a direct activator of Plg. PKal-

mediated activation of pro-uPA can occur on the surface of platelets [30] and endothelial cells [31]. Although the expression of uPA is regulated during 3T3-L1 differentiation, uPA-deficient mice do not show an adipogenic phenotype, which leads us to favor the hypothesis that PKal directly activates Plg during adipogenesis. Our data indicate that PKal can activate Plg at physiologically relevant concentrations.

This raises the question of what the regulated process is during adipogenesis. The functions of the PKal/Plg cascade may be regulated during differentiation by endogenous cell surface receptors or inhibitors. One possibility is that cell surface binding is regulated. The uPA receptor (uPAR) may serve as an acquired receptor for PKal. uPAR binds pro-uPA at a site within uPAR domain 1 [32]. The cleaved two-chain form of high molecular weight kininogen, which is a substrate for PKal and contains a high-affinity binding site for the PKal zymogen prekallikrein [33], can also bind to uPAR through interactions within uPAR domains 2 and 3 [34]. Thus, uPAR may function to promote PKal activity at the cell surface. Another model involves plasminogen activator inhibitor type 1 (PAI-1), a serpin that inhibits both uPA and tPA [35], but not PKal (data not shown). Increased levels of PAI-1 are associated with obesity in mice and humans [36,37]. PAI-1 is expressed by mature adipocytes in culture and *in vivo* [38]. PAI-1 may also function as a regulator of adhesion to the ECM [39]. It is unclear what role PAI-1 plays in adipose tissue development. Our findings suggest that PKal, which is not inhibited by PAI-1, may function to promote adipocyte differentiation even in the presence of the high PAI-1 levels observed in obesity.

How does extracellular proteolysis of the preadipocyte microenvironment facilitate adipogenesis? Our data support the model that the Plg cascade is required for

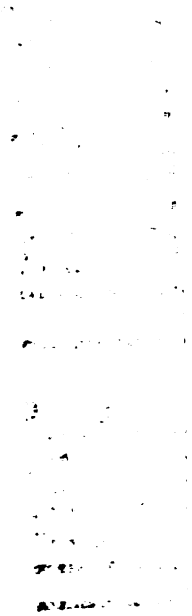

remodeling the fibronectin-rich ECM of preadipocytes. This remodeling then leads to alterations in cell-ECM adhesion and cytoskeletal attachments, and promotes the transcription of adipocyte-specific genes. Our finding that C/EBPβ and PPARγ, transcription factors crucial to adipocyte differentiation, are only weakly induced in ecotin-treated cells, suggests that serine proteases function at critical steps in adipocyte differentiation. Fibronectin is a component of the preadipocyte ECM; addition of exogenous fibronectin during differentiation of preadipocytes in culture inhibits cell shape change and prevents adipogenesis. Fibronectin is a substrate of plasmin [8] (this study). For 3T3-L1 cells, the synthesis of stromal ECM components such as fibronectin and fibrillar collagen decreases with differentiation [40,41], and cleavage of fibronectin increases with differentiation. Thus, Plg activation results in rapid removal of fibronectin from the microenvironment of committed cells.

How does fibronectin act to suppress adipogenesis? One possibility is that the cytoskeletal organization and signaling downstream of adhesion receptors for fibronectin foster a fibroblastic phenotype, whereas receptors for basement membrane proteins foster an adipogenic phenotype. In favor of this hypothesis, cytochalasin D, which disrupts adhesion and cytoskeletal structure, overcomes the suppressive effects of fibronectin and ecotin (Fig. 7j, l). A related hypothesis is that cleavage of fibronectin results in the loss of syndecan, an integral membrane heparan sulfate proteoglycan that binds to fibronectin [42]. Loss of syndecan may downregulate Wnt signaling and thereby promote adipogenesis [43,44]. These hypotheses remain to be tested.

Alternatively, the Plg system may activate and release sequestered differentiation-promoting growth factors from the stromal ECM. The bioavailability of insulin-like growth factor-I (IGF-I), a physiologically relevant regulator of adipocyte differentiation [45], is modulated by specific, high-affinity IGF-binding proteins (IGFBPs). Transgenic mice with increased IGFBP concentration show impaired adipogenesis *in vivo* [46]. Plasmin and other serine proteases can cleave IGFBPs and release active IGF [47,48]. Thus, extracellular proteolysis is an important regulatory mechanism for the function of ECM molecules, as well as for cytokines, during adipogenesis. Whether the impact of proteolysis on fibronectin or IGFBPs is rate limiting *in vivo* remains to be determined.

Plasmin acts in many fibrin-independent physiologic and pathologic processes, including mammary gland involution, neuronal cell death and cancer progression. Our study opens up further avenues of research to elucidate the physiological functions of PKal, plasmin and their substrates.

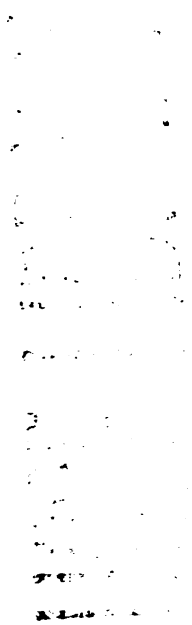

Methods

Preparation of ecotin.

Ecotins were prepared and purified as previously described [12]. The purified samples were tested and found to be free of endotoxin. Samples used for animal injections were diluted in phosphate buffered saline (PBS), pH 7.4.

3T3-L1 differentiation.

3T3-L1 cells (American Type Culture Collection) were grown to confluence in DMEM containing 4.5 g/L glucose supplemented with 10% FBS (growth medium). Differentiation was induced by culturing cells in growth medium containing the differentiation cocktail (0.22 μM insulin, 0.6 μM dexamethasone and 0.5 mM methylisobutylxanthine) as previously described [49]. Concurrently, 500 nM ecotin WT, 500 nM ecotin RR, 500 nM human PAI-1 (mutant human recombinant plasminogen activator inhibitor-1, Calbiochem) or 2 μM human α2-AP (Calbiochem) was added to the cells. Fresh growth medium was added to the cells after 2 days. Adipose conversion was analyzed six days after induction.

To assess the effects of Plg depletion, FBS was passed over a lysine-Sepharose column several times and the flow-through fraction was collected [50]. Depletion of Plg from the flow-through fraction was confirmed by western blotting using a rabbit polyclonal anti-human Plg antibody (Dako). 3T3-L1 cells were induced and maintained up to day 4 in medium containing 10% Plg-depleted FBS. For reconstitution experiments, human glu-type Plg (American Diagnostica Inc.) was added back to the medium at 50 μg/ml. To assess the effects of Plg deficiency, 3T3-L1 cells were induced

to differentiate without FBS in 5% pooled normal human plasma (George King Bio-Medical Inc.), Plg-deficient human plasma (American Diagnostica Inc.) or Plg-deficient human plasma reconstituted with 100 μg/ml human glu-type Plg (American Diagnostica Inc.) for 2 days. The cells were maintained in fresh growth medium for an additional 4 days.

To assess the effects of PKal deficiency, 3T3-L1 cells were induced to differentiate without FBS in 5% pooled normal human plasma, prekallikrein-deficient human plasma (George King Bio-Medical Inc.) or prekallikrein-deficient human plasma reconstituted with 50 μg/ml human PKal (Enzyme Research Laboratories) for 2 days. The cells were maintained in fresh growth medium for an additional 4 days.

To assess the ability of serine proteases to promote differentiation under serum-free conditions, 3T3-L1 cells were induced to differentiate as previously described but without FBS. Concurrently, human glu-type Plg was added at a concentration of 1μM, PKal at 200 nM, PAI-1 at 500 nM and ecotin RR at 500 nM. The cells were maintained under these serum-free conditions up to day 2, and then switched to serum-containing growth medium for an additional 4 days.

To assess the effects of fibronectin on 3T3-L1 differentiation, 6-well plates were coated with 50 μg/ml human fibronectin (Roche Molecular Biochemicals) at 4 ^{O}C for 12 hours. The cells were grown and differentiated as previously described. Cytochalasin D (Sigma) was added at a concentration of 0.5 μg/ml along with the differentiation cocktail. After 2 days, the cells were switched to growth medium.

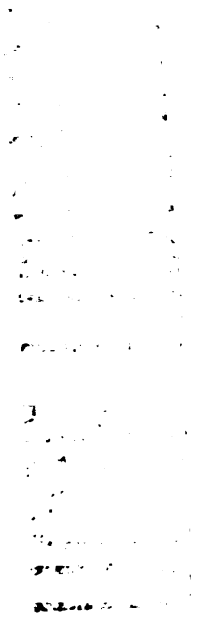

Adipocyte differentiation *in vivo*.

For ecotin treatment, female CF1 mice crossed with CD1 males were allowed to undergo a normal pregnancy. The number of pups was normalized to 8 for each experiment and they were weaned following 7-10 days of lactation (day 0 of involution). The mice were injected intraperitoneally with 100 μg of ecotin WT, ecotin RR or the carrier PBS twice a day on days 1-4 of involution and the animals were killed on day 5 of involution. Each cohort contained 4 mice/treatment and the experiments were repeated 3 times. Mammary glands from uPA-deficient C57BL/6 mice (n = 6), Plg-deficient C57BL/6 mice (n = 7), and wild-type littermate controls (n = 6 each) were collected on day 5 of involution. Plg-/- and wild-type littermates were weighed every week between 4-25 weeks of age and compared using ANOVA to calculate the p-value. Mice that were deficient in the genes for both uPA and tPA were generated as previously described [21]. Tissue samples were snap frozen in liquid nitrogen for biochemical analyses, placed in OCT and frozen for preparation of frozen sections or fixed in 4% paraformaldehyde for preparation of paraffin sections.

Oil red O staining, Masson Trichrome staining, and Immunohistochemistry.

3T3-L1 cells were stained with Oil red O as previously described [51]. The Oil red O dye was extracted into isopropanol and absorbance was measured at 510 nm. Frozen sections of mammary gland (10 μm) were fixed in 50% ethanol and stained in a 0.2% Oil red O solution, followed by counterstaining with Meyer's hematoxylin. Paraffin-embedded (CF1 mice) and frozen (uPA- and Plg-deficient mice and controls) tissue sections were stained using an Accustain™ Masson Trichrome Stain kit (Sigma). To detect fibronectin,

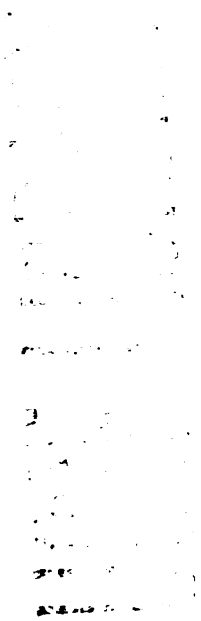

paraffin sections were stained using a rabbit polyclonal anti-rat fibronectin antibody (Calbiochem). To detect type I collagen, paraffin sections were stained using a rabbit polyclonal anti-mouse collagen type I antibody (Calbiochem).

Substrate zymography and western blotting.

Frozen mammary tissue was homogenized in RIPA buffer (50 mM Tris-Cl, pH 8.0, 150 mM NaCl, 1% NP40, 0.5% DOC, 0.1%SDS) and the supernatant was collected. CM was collected from the 3T3-L1 cells grown under normal and serum-free conditions. Cell lysates were prepared by scraping cells into RIPA buffer. 3T3-L1 nuclear lysates were prepared as previously described [52]. Mammary lysates were normalized to wet tissue weight. 3T3-L1 CM and lysates were normalized to cell number. PPARγ was detected by western blotting of nuclear lysates using a goat polyclonal antibody raised against a peptide mapping within an internal region of human PPARγ (Santa Cruz Biotechnology, Inc.). C/EBPβ was detected by western blotting of nuclear lysates using a rabbit polyclonal antibody raised against a peptide mapping at the carboxy terminus of rat C/EBPβ (Santa Cruz Biotechnology, Inc.). For substrate zymography, the samples were loaded into non-reducing SDS-PAGE gels containing 1 mg/ml casein and 10 μg/ml Plg [53]. Human tPA, high molecular weight uPA, plasmin (American Diagnostica Inc.) and PKal were used as controls. The gels were incubated overnight at 37^{O}C in the presence and absence of 500 nM ecotin WT or ecotin RR. The identity of PKal was confirmed by western blotting with a sheep polyclonal anti-human prekallikrein antibody (Enzyme Research Laboratories).

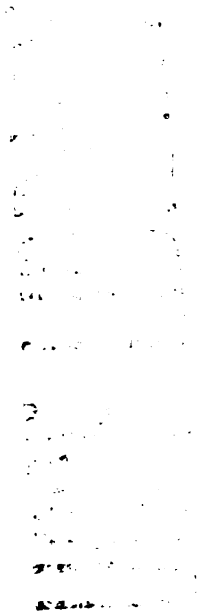

Plasminogen activation and fibronectin cleavage.

To test PKal for its ability to activate Plg, 1 μM human glu-type Plg was incubated with 10 nM human high molecular weight uPA, 40 nM tPA or 40 nM PKal at 37°C in activity buffer (50mM Tris-Cl, pH 7.5, 10 mM $CaCl_2$, 0.01% Tween-20) on a 96-well plate coated with PBS (control), 50 μg/ml human fibronectin (Roche Molecular Biochemicals), or 2 mg/ml human fibrinogen (Sigma). The fibrinogen was converted to fibrin using 500 nM human thrombin (Sigma). Aliquots were removed at 5, 10 and 15 minutes and reduced. Plg was detected by western blotting with a rabbit polyclonal anti-human Plg antibody (Dako). Reduced samples of human glu-type Plg and human plasmin were used as controls. To assay for Plg activation, 3T3-L1 cells were induced to differentiate under serum-free conditions as previously described. At the time of induction, 1 μM human glu-type Plg, 200 nM PKal and 500 nM PAI-1 were added to the medium. CM was collected 24 hours later and reduced. Plg was detected by western blotting with a rabbit polyclonal anti-human Plg antibody (Dako).

To assay for fibronectin cleavage, 500 nM human plasma fibronectin was incubated with 10 nM human tPA, high molecular weight uPA, PKal or plasmin in activity buffer for 30 minutes at 37°C. The cleavage products were reduced and electrophoresed onto a 10% SDS-PAGE gel. Fibronectin was detected by western blotting with a monoclonal mouse anti-human fibronectin antibody (Calbiochem). To detect endogenous fibronectin, CM and cell lysates were prepared from 3T3-L1 cells grown and differentiated in the presence of FBS. Cell-associated fibronectin was detected by western blotting of reduced 3T3-L1 cell lysates using a rabbit polyclonal anti-rat fibronectin antibody (Calbiochem). Cleaved mouse fibronectin present in the CM

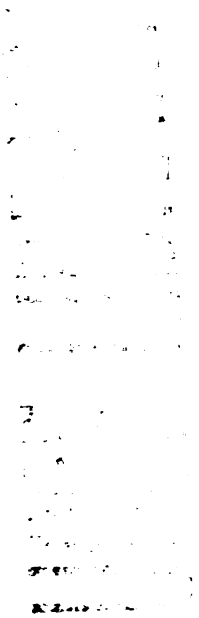

was reduced and assayed by western blotting with a rabbit anti-mouse fibronectin antibody (Gibco BRL).

References

1. Hwang, C. S., Loftus, T. M., Mandrup, S. & Lane, M. D. Adipocyte differentiation and leptin expression. *Annu Rev Cell Dev Biol* **13**, 231-259 (1997).

2. Montague, C. T. *et al.* Congenital leptin deficiency is associated with severe early-onset obesity in humans. *Nature* **387**, 903-908 (1997).

3. Lowell, B. B. PPARg: An essential regulator of adipogenesis and modulator of fat cell function. *Cell* **99**, 239-242 (1999).

4. Rosen, E. D. *et al.* PPARg is required for the differentiation of adipose tissue in vivo and in vitro. *Mol Cell* **4**, 611-517 (1999).

5. Smas, C. M. & Sul, H. S. Control of adipocyte differentiation. *Biochem J* **309**, 697-710 (1995).

6. Mandrup, S. & Lane, M. D. Regulating adipogenesis. *J Biol Chem* **272**, 5367-5370 (1997).

7. Cowherd, R. M., Lyle, R. E. & McGehee, R. E., Jr. Molecular regulation of adipocyte differentiation. *Semin Cell Dev Biol* **10**, 3-10 (1999).

8. Liotta, L. A. *et al.* Effect of plasminogen activator (urokinase), plasmin, and thrombin on glycoprotein and collagenous components of basement membrane. *Cancer Res* **41**, 4629-4636 (1981).

9. Chen, Z. L. & Strickland, S. Neuronal death in the hippocampus is promoted by plasmin-catalyzed degradation of laminin. *Cell* **91**, 917-925 (1997).

10. Booth, B. A., Boes, M. & Bar, R. S. IGFBP-3 proteolysis by plasmin, thrombin, serum: heparin binding, IGF binding, and structure of fragments. *Am J Physiol* **271**, E465-470 (1996).

11. Chung, C. H., Ives, H. E., Almeda, S. & Goldberg, A. L. Purification from Escherichia coli of a periplasmic protein that is a potent inhibitor of pancreatic proteases. *J Biol Chem* **258**, 11032-11038 (1983).

12. Wang, C. I., Yang, Q. & Craik, C. S. Isolation of a high affinity inhibitor of urokinase-type plasminogen activator by phage display of ecotin. *J Biol Chem* **270**, 12250-12256 (1995).

13. Cao, Z., Umek, R. M. & McKnight, S. L. Regulated expression of three C/EBP isoforms during adipose conversion of 3T3-L1 cells. *Genes Dev* **5**, 1538-1552 (1991).

14. Pairault, J. & Green, H. A study of the adipose conversion of suspended 3T3 cells by using glycerophosphate dehydrogenase as differentiation marker. *Proc Natl Acad Sci U S A* **76**, 5138-5142 (1979).

15. Kwaan, H. C. The plasminogen-plasmin system in malignancy. *Cancer Metastasis Rev* **11**, 291-311 (1992).

16. Lijnen, H. R. & Collen, D. *Serine proteases and their serpin inhibitors in the nervous system* (ed. Festoff, B. W.) (Plenum Press, New York, 1990).

17. Rijken, D. C. Plasminogen activators and plasminogen activator inhibitors: biochemical aspects. *Baillieres Clin Haematol* **8**, 291-312 (1995).

18. Lascelles, A. K. & Lee, C. S. in *Lactation: A Comprehensive Treatise* (ed. Larson, B. L.) 115-176 (Academic Press, New York, 1978).

19. Lund, L. R. *et al.* Two distinct phases of apoptosis in mammary gland involution: proteinase-independent and -dependent pathways. *Development* **122**, 181-193 (1996).

20. Bugge, T. H., Flick, M. J., Daugherty, C. C. & Degen, J. L. Plasminogen deficiency causes severe thrombosis but is compatible with development and reproduction. *Genes Dev* **9**, 794-807 (1995).

21. Carmeliet, P. *et al.* Physiological consequences of loss of plasminogen activator gene function in mice. *Nature* **368**, 419-424 (1994).

22. Ulmer, J. S., Lindquist, R. N., Dennis, M. S. & Lazarus, R. A. Ecotin is a potent inhibitor of the contact system proteases factor XIIa and plasma kallikrein. *FEBS Lett* **365**, 159-163 (1995).

23. Ichinose, A., Fujikawa, K. & Suyama, T. The activation of pro-urokinase by plasma kallikrein and its inactivation by thrombin. *J Biol Chem* **261**, 3486-3489 (1986).

24. Hauert, J., Nicoloso, G., Schleuning, W. D., Bachmann, F. & Schapira, M. Plasminogen activators in dextran sulfate-activated euglobulin fractions: a molecular analysis of factor XII- and prekallikrein- dependent fibrinolysis. *Blood* **73**, 994-999 (1989).

25. Colman, R. W. Activation of plasminogen by human plasma kallikrein. *Biochem Biophys Res Commun* **35**, 273-279 (1969).

26. Miles, L. A., Greengard, J. S. & Griffin, J. H. A comparison of the abilities of plasma kallikrein, beta-Factor XIIa, Factor XIa and urokinase to activate plasminogen. *Thromb Res* **29**, 407-417 (1983).

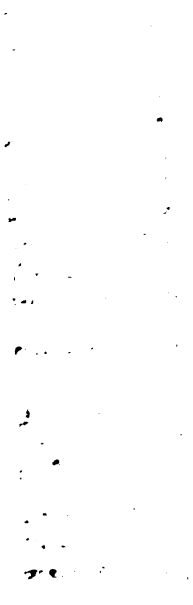

27. Saito, H. *et al.* Heterogeneity of human prekallikrein deficiency (Fletcher trait): evidence that five of 18 cases are positive for cross-reacting material. *N Engl J Med* **305**, 910-914 (1981).

28. Raspi, G. Kallikrein and kallikrein-like proteinases: purification and determination by chromatographic and electrophoretic methods. *J Chromatogr B Biomed Appl* **684**, 265-287 (1996).

29. Schousboe, I., Feddersen, K. & Rojkjaer, R. Factor XIIa is a kinetically favorable plasminogen activator. *Thromb Haemost* **82**, 1041-1046 (1999).

30. Loza, J. P., Gurewich, V., Johnstone, M. & Pannell, R. Platelet-bound prekallikrein promotes pro-urokinase-induced clot lysis: a mechanism for targeting the factor XII dependent intrinsic pathway of fibrinolysis. *Thromb Haemost* **71**, 347-352 (1994).

31. Lin, Y. *et al.* High molecular weight kininogen peptides inhibit the formation of kallikrein on endothelial cell surfaces and subsequent urokinase- dependent plasmin formation. *Blood* **90**, 690-697 (1997).

32. Behrendt, N. *et al.* The ligand-binding domain of the cell surface receptor for urokinase- type plasminogen activator. *J Biol Chem* **266**, 7842-7847 (1991).

33. Tait, J. F. & Fujikawa, K. Identification of the binding site for plasma prekallikrein in human high molecular weight kininogen. A region from residues 185 to 224 of the kininogen light chain retains full binding activity. *J Biol Chem* **261**, 15396-15401 (1986).

34. Colman, R. W. *et al.* Binding of high molecular weight kininogen to human endothelial cells is mediated via a site within domains 2 and 3 of the urokinase receptor. *J Clin Invest* **100**, 1481-1487 (1997).

35. Dano, K. *et al.* Plasminogen activators, tissue degradation, and cancer. *Adv Cancer Res* **44**, 139-266 (1985).

36. Samad, F. & Loskutoff, D. J. Tissue distribution and regulation of plasminogen activator inhibitor-1 in obese mice. *Mol Med* **2**, 568-582 (1996).

37. Juhan-Vague, I. & Alessi, M. C. PAI-1, obesity, insulin resistance and risk of cardiovascular events. *Thromb Haemost* **78**, 656-660 (1997).

38. Samad, F., Yamamoto, K. & Loskutoff, D. J. Distribution and regulation of plasminogen activator inhibitor-1 in murine adipose tissue in vivo. Induction by tumor necrosis factor-alpha and lipopolysaccharide. *J Clin Invest* **97**, 37-46 (1996).

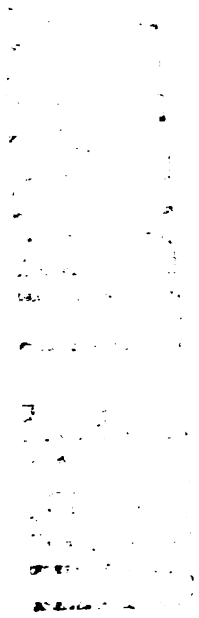

39. Loskutoff, D. J., Curriden, S. A., Hu, G. & Deng, G. Regulation of cell adhesion by PAI-1. *Apmis* **107**, 54-61 (1999).

40. Weiner, F. R., Shah, A., Smith, P. J., Rubin, C. S. & Zern, M. A. Regulation of collagen gene expression in 3T3-L1 cells. Effects of adipocyte differentiation and tumor necrosis factor alpha. *Biochemistry* **28**, 4094-4099 (1989).

41. Bortell, R., Owen, T. A., Ignotz, R., Stein, G. S. & Stein, J. L. TGF beta 1 prevents the down-regulation of type I procollagen, fibronectin, and TGF beta 1 gene expression associated with 3T3-L1 pre- adipocyte differentiation. *J Cell Biochem* **54**, 256-263 (1994).

42. Tumova, S., Woods, A. & Couchman, J. R. Heparan sulfate chains from glypican and syndecans bind the Hep II domain of fibronectin similarly despite minor structural differences. *J Biol Chem* **275**, 9410-9417 (2000).

43. Alexander, C. M. *et al.* Syndecan-1 is required for Wnt-1-induced mammary tumorigenesis in mice. *Nat Genet* **25**, 329-332 (2000).

44. Ross, S. E. *et al.* Inhibition of adipogenesis by Wnt signaling. *Science* **289**, 950-953 (2000).

45. Smith, P. J., Wise, L. S., Berkowitz, R., Wan, C. & Rubin, C. S. Insulin-like growth factor-I is an essential regulator of the differentiation of 3T3-L1 adipocytes. *J Biol Chem* **263**, 9402-9408 (1988).

46. Rajkumar, K., Modric, T. & Murphy, L. J. Impaired adipogenesis in insulin-like growth factor binding protein-1 transgenic mice. *J Endocrinol* **162**, 457-465 (1999).

47. Campbell, P. G. & Andress, D. L. Plasmin degradation of insulin-like growth factor-binding protein-5 (IGFBP-5): regulation by IGFBP-5-(201-218). *Am J Physiol* **273**, E996-1004 (1997).

48. Zheng, B., Clarke, J. B., Busby, W. H., Duan, C. & Clemmons, D. R. Insulin-like growth factor-binding protein-5 is cleaved by physiological concentrations of thrombin. *Endocrinology* **139**, 1708-1714 (1998).

49. Bernlohr, D. A., Angus, C. W., Lane, M. D., Bolanowski, M. A. & Kelly, T. J., Jr. Expression of specific mRNAs during adipose differentiation: identification of an mRNA encoding a homologue of myelin P2 protein. *Proc Natl Acad Sci U S A* **81**, 5468-5472 (1984).

50. Deutsch, D. G. & Mertz, E. T. Plasminogen: purification from human plasma by affinity chromatography. *Science* **170**, 1095-1096 (1970).

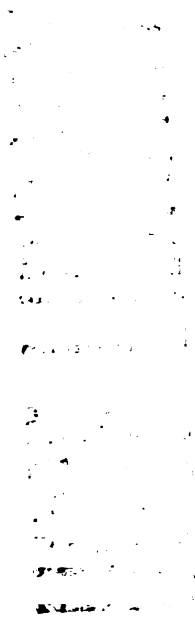

51. Ramirez-Zacarias, J. L., Castro-Munozledo, F. & Kuri-Harcuch, W. Quantitation of adipose conversion and triglycerides by staining intracytoplasmic lipids with Oil red O. *Histochemistry* **97**, 493-497 (1992).

52. Finbloom, D. S. *et al.* Growth hormone and erythropoietin differentially activate DNA-binding proteins by tyrosine phosphorylation. *Mol Cell Biol* **14**, 2113-2118 (1994).

53. Talhouk, R. S., Chin, J. R., Unemori, E. N., Werb, Z. & Bissell, M. J. Proteinases of the mammary gland: developmental regulation in vivo and vectorial secretion in culture. *Development* **112**, 439-449 (1991).

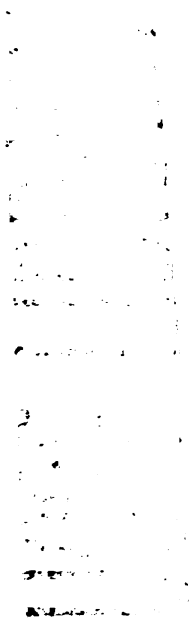

Figure 5-1.

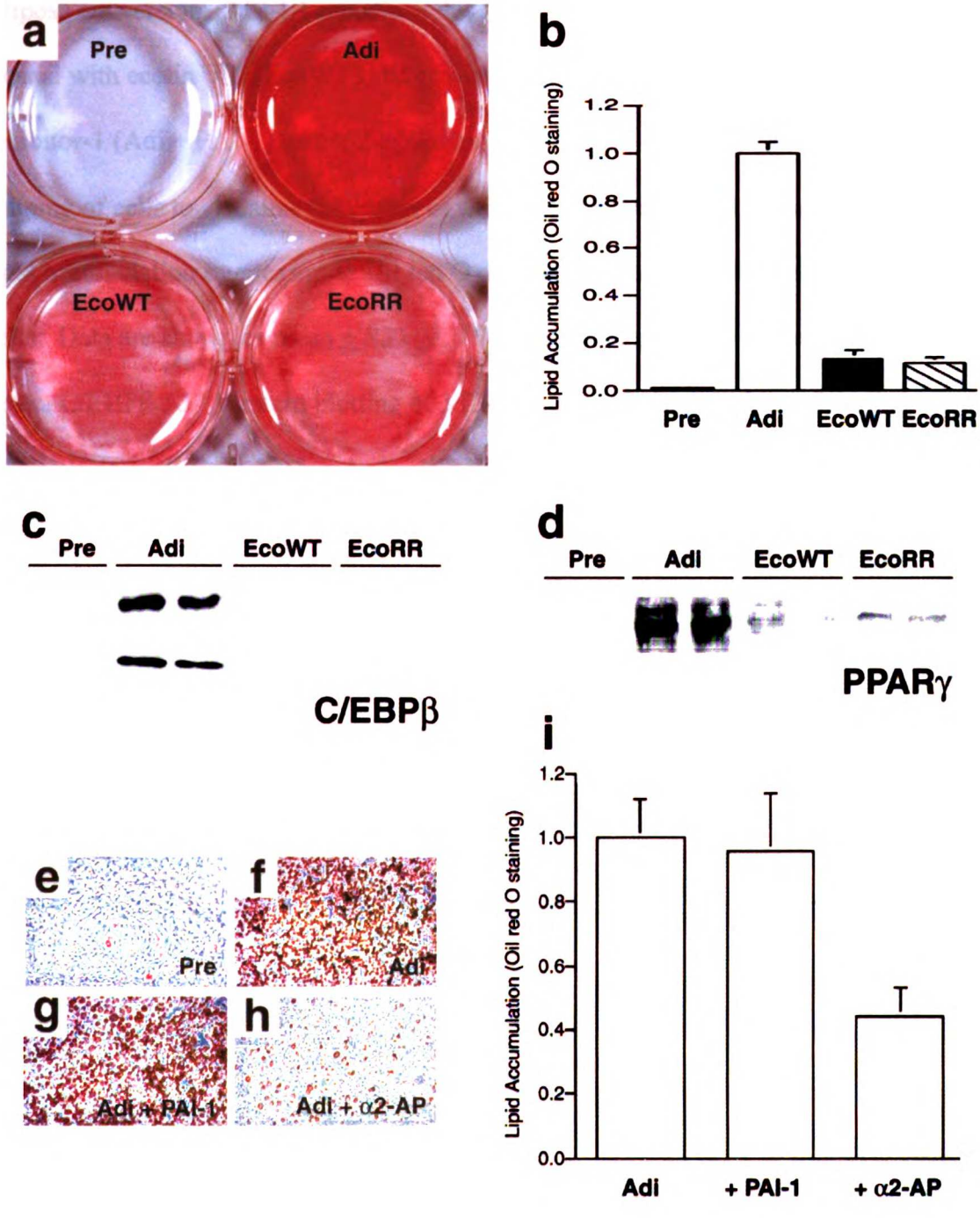
a
Pre
Adi
EcoWT
EcoRR
b
Lipid Accumulation (Oil red O staining)
1.2
1.0
0.8
0.6
0.4
0.2
0.0
Pre
Adi
EcoWT
EcoRR
c
Pre
Adi
EcoWT
EcoRR
C/EBPβ
d
Pre
Adi
EcoWT
EcoRR
PPARγ
e
Pre
f
Adi
g
Adi + PAI-1
h
Adi + α2-AP
i
Lipid Accumulation (Oil red O staining)
1.2
1.0
0.8
0.6
0.4
0.2
0.0
Adi
+ PAI-1
+ α2-AP

Figure 5-1. Inhibition of serine proteases during 3T3-L1 cell differentiation decreases adipose conversion. 3T3-L1 preadipocytes (Pre), adipocytes (Adi), differentiating cells treated with ecotin WT (EcoWT) and ecotin RR (EcoRR) (**a-d**) or plasminogen activator inhibitor-1 (Adi + PAI-1) and α-2-antiplasmin (Adi + α2-AP) (**e-i**). **a** & **e-h**, Oil red O staining of cells to visualize the extent of adipose conversion. **b** & **i**, Quantification of lipid accumulation by measuring Oil red O dye, with absorbance normalized to 1 for Adi cells. Data are shown as mean ± S.D. **c**, Western blotting of 3T3-L1 nuclear lysates to detect C/EBPβ. **d**, Western blotting of 3T3-L1 nuclear lysates to detect PPARγ.

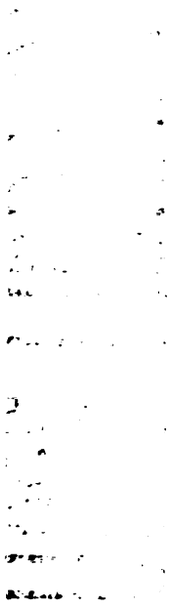

Figure 5-2.

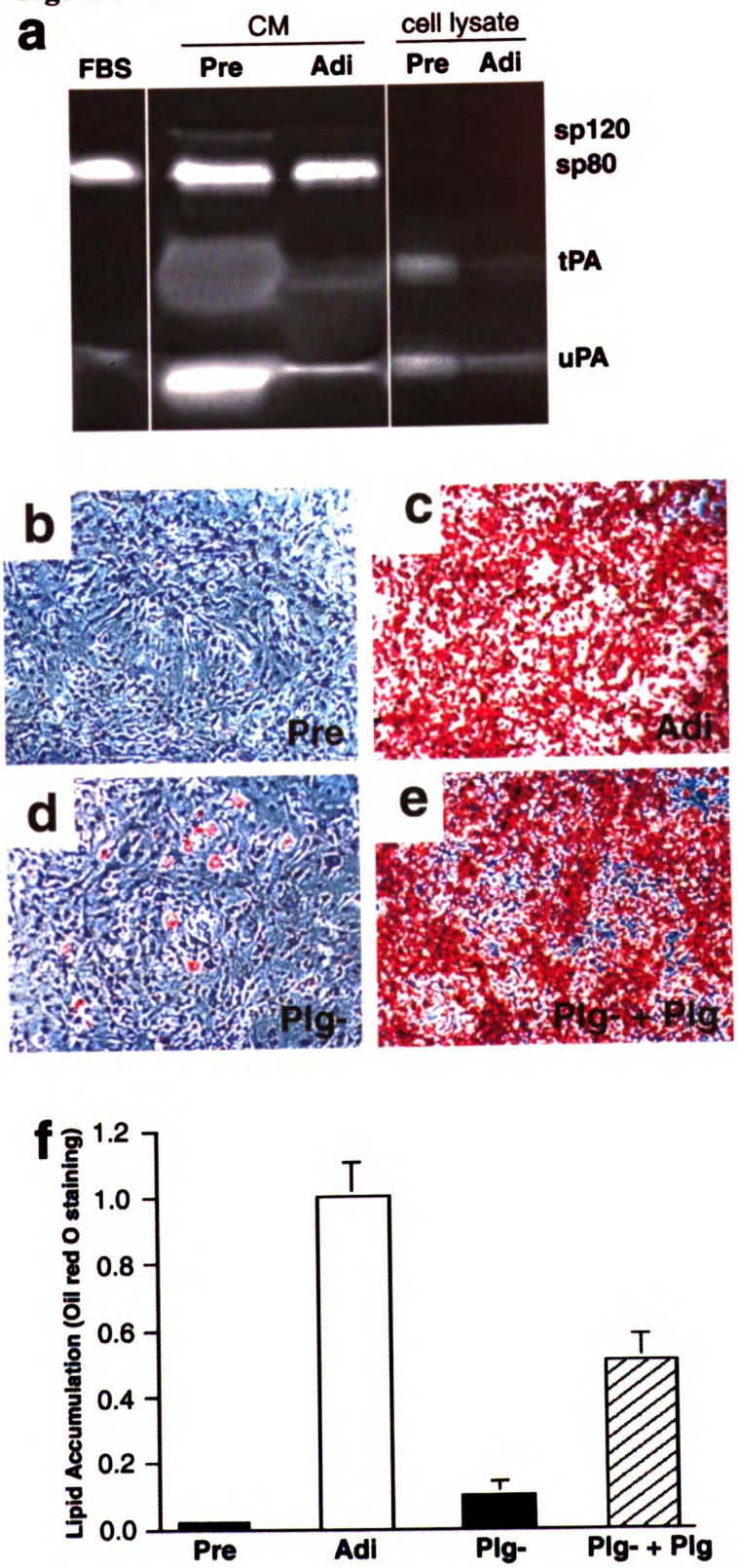
a
CM
cell lysate
FBS
Pre
Adi
Pre
Adi
sp120
sp80
tPA
uPA
b
Pre
c
Adi
d
Plg-
e
Plg- + Plg
f
Lipid Accumulation (Oil red O staining)
1.2
1.0
0.8
0.6
0.4
0.2
0.0
Pre
Adi
Plg-
Plg- + Plg

Figure 5-2. The Plg system is regulated and required during 3T3-L1 cell differentiation. **a-e**, Oil red O staining to detect adipocytes. **a**, Casein/Plg zymograms. Fetal bovine serum (FBS), conditioned medium (CM) and cell lysates from 3T3-L1 preadipocytes (Pre) and adipocytes (Adi). **b**, Preadipocytes (Pre) grown in Plg-depleted serum. **c**, Cells differentiated in normal serum (Adi). **d**, Cells differentiated in Plg-depleted serum (Plg-). **e**, Cells differentiated in Plg-depleted serum with exogenous Plg added back (Plg- + Plg). **f**, Quantification of adipose conversion by measuring Oil red O dye, with absorbance normalized to 1 for Adi cells. Data are shown as mean $\pm$ S.D.

Figure 5-3.

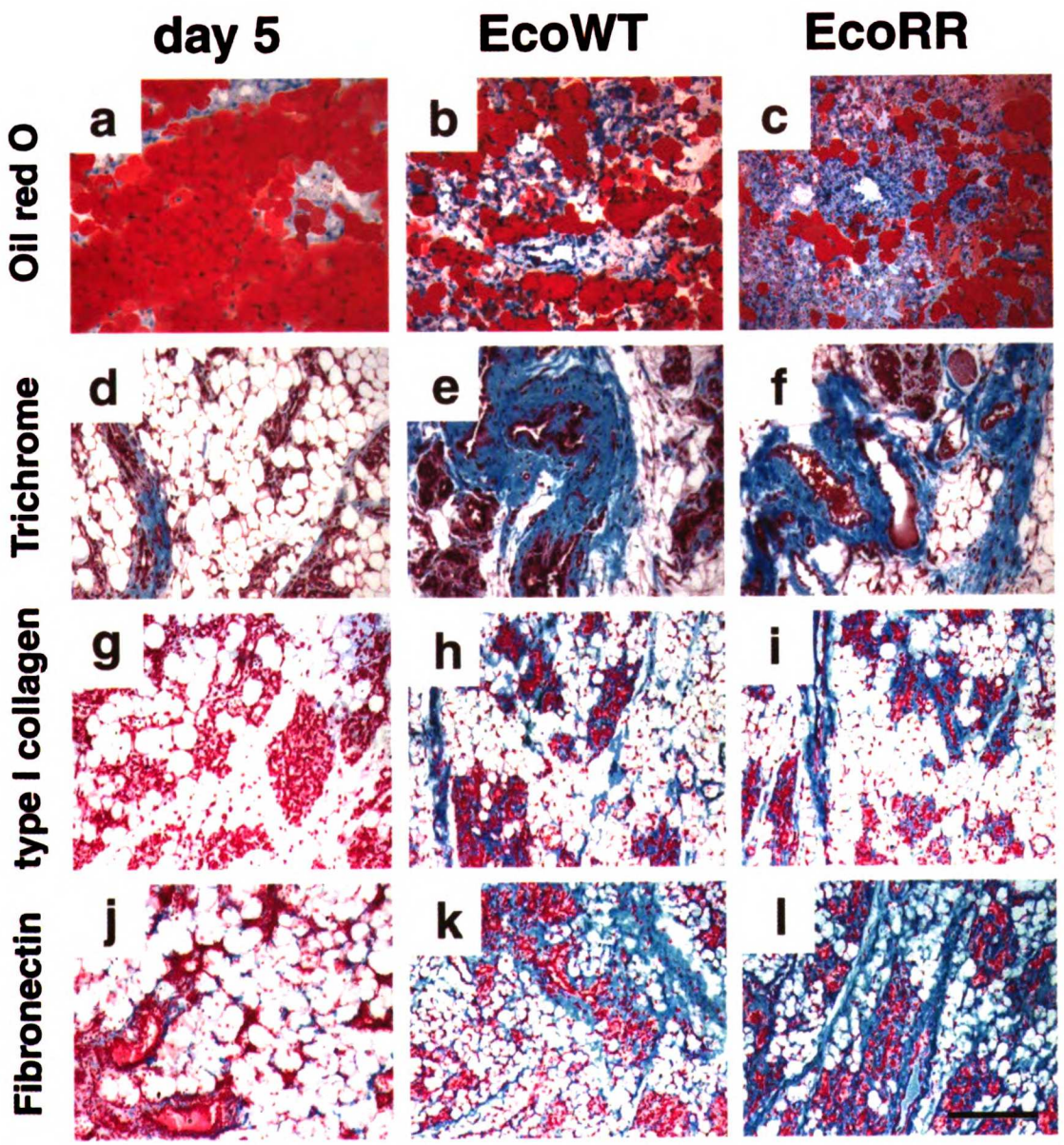
day 5
EcoWT
EcoRR
Oil red O
Trichrome
type I collagen
Fibronectin
a
b
c
d
e
f
g
h
i
j
k
l

Figure 5-3. Adipogenesis is decreased in female mice treated with ecotin during mammary gland involution. Animals were treated with carrier (cont), ecotin WT (EcoWT) or ecotin RR (EcoRR). **a-c**, Oil red O staining to detect adipocytes. **d-f**, Masson's Trichrome staining of collagen fibrils (blue). **g-i**, Immunohistochemistry to detect type I collagen (blue). **j-l**, Immunohistochemistry to detect fibronectin (blue). Bar = 100 μm.

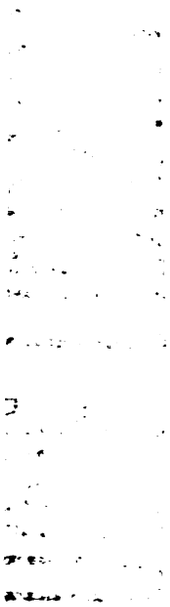

Figure 5-4.

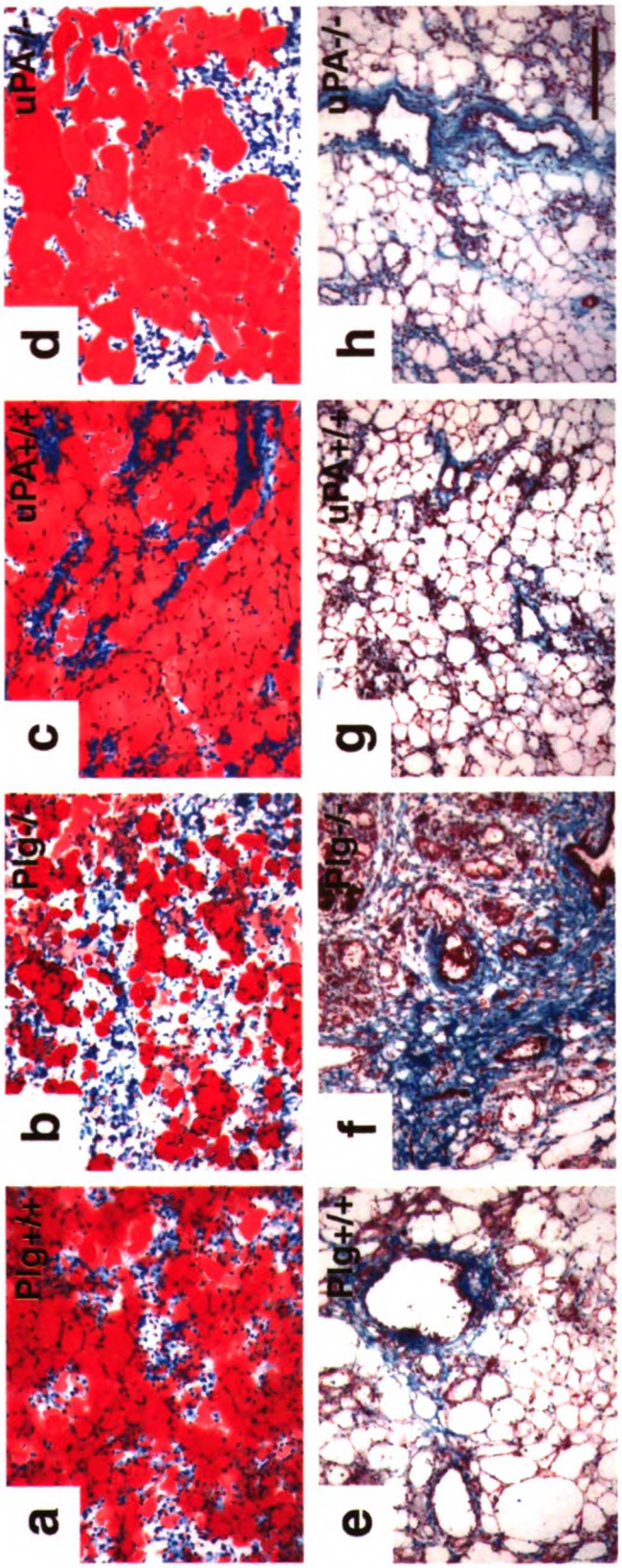

Figure 5-4. Adipocyte differentiation is impaired during involution in Plg-deficient, but not in uPA-deficient mice. **a-d**, Oil red O staining to detect adipocytes. **e-h**, Masson's Trichrome staining to detect collagen fibrils (blue). Bar = 100 μm.

Figure 5-5.

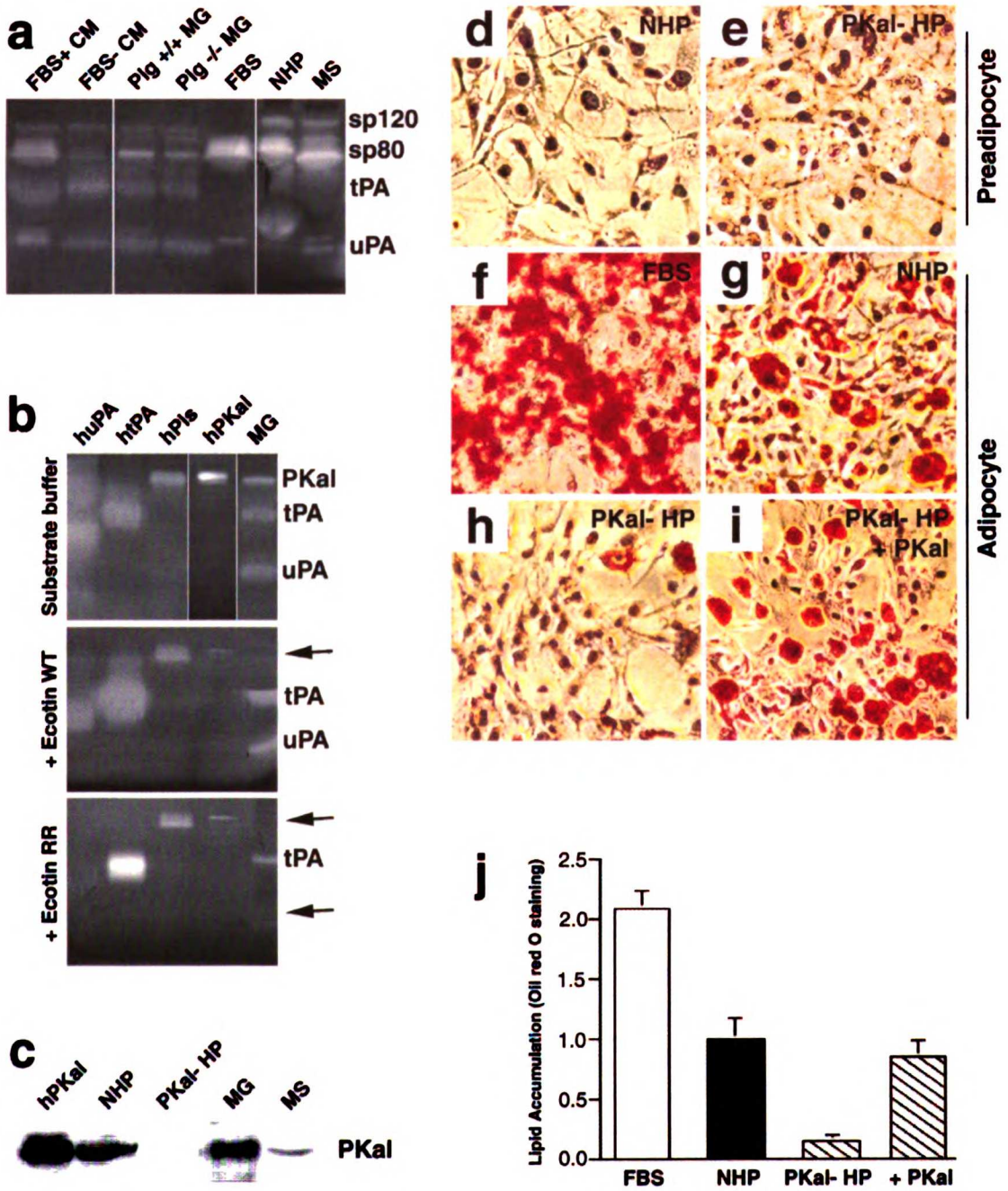
a
FBS+ CM
FBS- CM
Plg +/+ MG
Plg -/- MG
FBS
NHP
MS
sp120
sp80
tPA
uPA
b
huPA
htPA
hPIs
hPKal
MG
Substrate buffer
PKal
tPA
uPA
+ Ecotin WT
tPA
uPA
+ Ecotin RR
tPA
c
hPKal
NHP
PKal- HP
MG
MS
PKal
d
NHP
e
PKal- HP
Preadipocyte
f
FBS
g
NHP
h
PKal- HP
i
PKal- HP
+ PKal
Adipocyte
j
Lipid Accumulation (Oil red O staining)
2.5
2.0
1.5
1.0
0.5
0.0
FBS
NHP
PKal- HP
+ PKal

Figure 5-5. PKal is present during adipogenesis and is required for 3T3-L1 differentiation. **a & b**, Casein/Plg zymograms. **a**, Incubation in substrate buffer. **b**, Incubation in substrate buffer alone, or buffer containing ecotin WT or ecotin RR. Inhibited bands are indicated by arrowheads. **c**, Western blotting for PKal. Plasmin (Pls). Human enzymes are designated h. CM from preadipocytes grown in the presence (FBS+) and absence (FBS-) of FBS, mammary lysate from CF1 (MG), Plg-deficient (Plg -/-) and wild-type control (Plg+/+) mice, mouse serum (MS), normal human plasma (NHP), prekallikrein-deficient human plasma (PKal-). **d-i**, Oil red O staining to detect adipocytes. **d**, Preadipocytes grown in normal human plasma (NHP). **e**, Preadipocytes grown in prekallikrein-deficient human plasma (PKal-). **f**, Cells differentiated in FBS. **g**, Cells differentiated in normal human plasma (NHP). **h**, Cells differentiated in prekallikrein-deficient human plasma (PKal-). **i**, Cells differentiated in prekallikrein-deficient human plasma with exogenous human PKal added back (PKal- + PKal). **j**, Quantification of adipose conversion by measuring Oil red O dye, with absorbance normalized to 1 for NHP cells. Data are shown as mean $\pm$ S.D.

Figure 5-6.

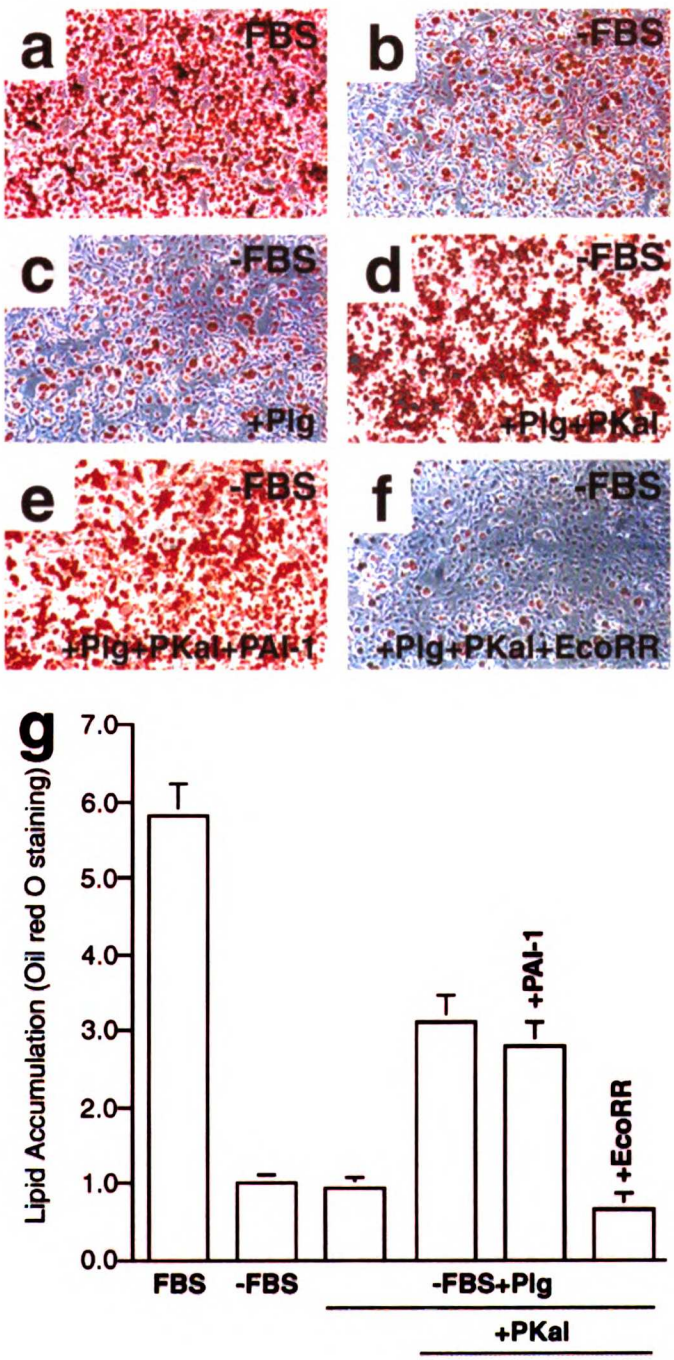
a
+FBS
b
-FBS
c
-FBS
+Plg
d
-FBS
+Plg+PKal
e
-FBS
+Plg+PKal+PAI-1
f
-FBS
+Plg+PKal+EcoRR
g
Lipid Accumulation (Oil red O staining)
7.0
6.0
5.0
4.0
3.0
2.0
1.0
0.0
+PAI-1
+EcoRR
FBS
-FBS
-FBS+Plg
+PKal

Figure 5-6. Plg and PKal promote adipose conversion in the absence of FBS. **a-f,** Oil red O staining of cells to visualize the extent of adipose conversion. **a,** Cells differentiated in the presence of FBS (FBS). **b,** cells differentiated in the absence of FBS (-FBS). **c,** cells differentiated in the absence of FBS with the addition of exogenous Plg (-FBS +Plg). **d,** cells differentiated in the absence of FBS with the addition of exogenous Plg and PKal (-FBS +Plg+PKal). **e,** cells differentiated in the absence of FBS with the addition of exogenous Plg, PKal and PAI-1 (-FBS +Plg+PKal+PAI-1). **f,** cells differentiated in the absence of FBS with the addition of exogenous Plg, PKal and ecotin RR (-FBS +Plg+PKal+EcoRR). **g,** Quantification of adipose conversion by measuring Oil red O dye, with absorbance normalized to 1 for -FBS cells. Data are shown as mean $\pm$ S.D.

Figure 5-7.

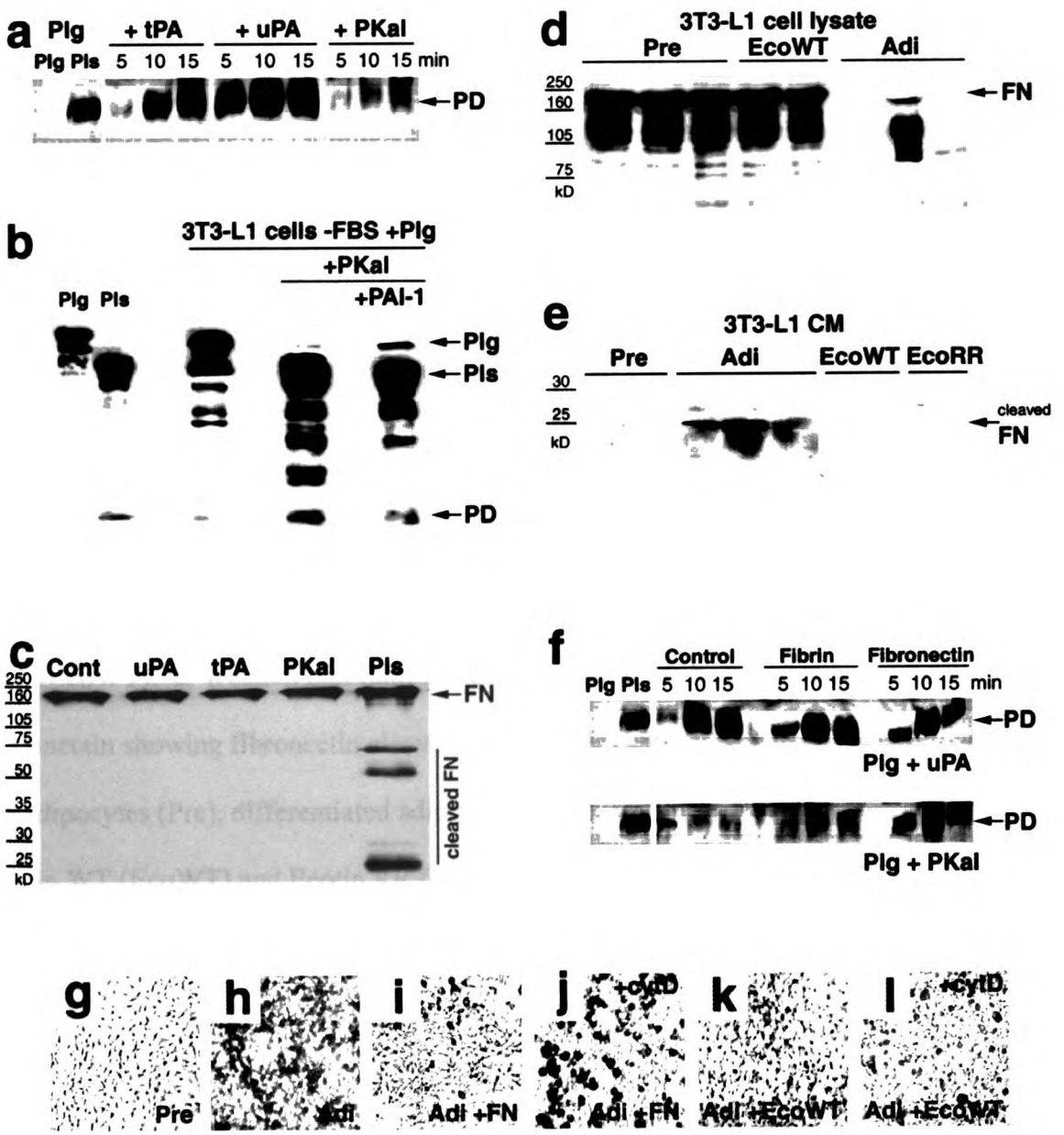
a
Plg
+ tPA
+ uPA
+ PKal
Plg Pls 5 10 15 5 10 15 5 10 15 min
PD
b
3T3-L1 cells -FBS +Plg
+PKal
+PAI-1
Plg Pls
Plg
Pls
PD
c
Cont
uPA
tPA
PKal
Pls
250
160
105
75
50
35
30
25
kD
FN
cleaved FN
d
3T3-L1 cell lysate
Pre
EcoWT
Adi
250
160
105
75
kD
FN
e
3T3-L1 CM
Pre
Adi
EcoWT
EcoRR
30
25
kD
cleaved
FN
f
Control
Fibrin
Fibronectin
Plg Pls 5 10 15 5 10 15 5 10 15 min
PD
Plg + uPA
PD
Plg + PKal
g
Pre
h
Adi
i
Adi +FN
j
+cytD
Adi +FN
k
Adi +EcoWT
l
+cytD
Adi +EcoWT

Figure 5-7. PKal-mediated Plg activation promotes fibronectin degradation during adipocyte differentiation. **a**, PKal activates Plg at physiologically relevant concentrations. Western blot showing generation of the 25 kD protease domain (PD) of plasmin at 5, 10 and 15 minutes. **b**, Plg activation in the CM of 3T3-L1 cells is enhanced in the presence of PKal. CM from 3T3-L1 cells differentiated in the absence of FBS but with exogenous plasminogen (Plg), plasma kallikrein (PKal) or plasminogen activator inhibitor (PAI-1). Western blot showing generation of plasmin (Pls) and 25 kD plasmin protease domain (PD). **c**, Western blot (anti-human fibronectin antibody) showing fibronectin (FN) cleavage products observed after incubation with serine proteases. Arrows indicate cleavage products. **d**, Western blot (anti-rat fibronectin antibody) showing that fibronectin (FN) is present in cell lysates from 3T3-L1 preadipocytes but downregulated in adipocytes. Whole cell lysates from preadipocytes (Pre), differentiated adipocytes (Adi) and cells differentiated in the presence of ecotin WT (EcoWT). **e**, Western blot (anti-mouse fibronectin antibody) of endogenous mouse fibronectin showing fibronectin cleavage during adipocyte differentiation. CM from preadipocytes (Pre), differentiated adipocytes (Adi), cells differentiated in the presence of ecotin WT (EcoWT) and Ecotin RR (EcoRR). **f**, Fibronectin enhances Plg activation by PKal but not by uPA. Western blot showing generation of the protease domain (PD) of plasmin at 5, 10 and 15 minutes in the absence (Control) and presence of fibrin (Fibrin) and fibronectin (Fibronectin). **g-l**, Cytochalasin D overcomes the suppressive effects of fibronectin and ecotin WT during adipocyte differentiation. Oil red staining to detect adipocytes. **g**, Preadipocytes (Pre). **h**, Adipocytes (Adi). **i**, 3T3-L1 cells differentiated on a fibronectin matrix (Adi +FN). **j**, 3T3-L1 cells differentiated on a fibronectin matrix

in the presence of cytochalasin D (Adi +FN +cytD). **k**, 3T3-L1 cells differentiated in the presence of ecotin WT (Adi +EcoWT). **l**, 3T3-L1 cells differentiated in the presence of ecotin WT and cytochalasin D (Adi +EcoWT +cytD).

Addendum

Methods

Inhibition assays. The concentration of active uPA, tPA, plasmin and PKal was determined using active-site titration with 4-methylumbelliferyl p-guanidinobenzoate (MUGB; (Jameson et al., 1973)). The activity of 10 nM uPA, tPA, plasmin or PKal against the chromogenic peptide substrates Spectrozyme®UK (for uPA), Spectrozyme®tPA (for tPA), Spectrozyme®PL (for plasmin) or Spectrozyme®P•Kal (for PKal) was measured in activity buffer (50mM Tris-Cl, pH 7.5, 10 mM $CaCl_2$, 0.01% Tween-20) as per the manufacturer's instructions (American Diagnostica Inc.). 10 nM of each enzyme was then incubated in assay buffer with 500 nM ecotin WT or ecotin RR, or 250 nM α2-AP or PAI-1 for 1 min at room temperature. The activity remaining after the addition of inhibitor was measured using chromogenic substrates. The data were obtained in triplicate and the results were averaged and represented as percent enzyme activity remaining, with the activity in the absence of inhibitor being 100%.

Detection of Plg and PKal. CM was collected from preadipocytes and adipocytes grown and differentiated in the presence of FBS as previously described and was reduced. Plg was detected by western blotting using a rabbit polyclonal anti-human Plg antibody (Dako). PKal was detected by casein zymography by loading samples into non-reducing SDS-PAGE gels containing 1 mg/ml casein. Human Plg and plasmin were used as controls.

Measurements of body weight. Female CF1 mice (n=4 per treatment group) were weighed prior to starting ecotin injections and after completion of ecotin treatment. The data were obtained in triplicate and analyzed using the ANOVA function of Microsoft Excel to calculate the average, standard deviation and *p*-value. Plg-/- mice (n=6) and their wild-type littermates (Plg+/+, n=6) were weighed every week between 4-25 weeks of age. The data were analyzed using the ANOVA function of Microsoft Excel to calculate the average, standard deviation and *p*-value.

Specificity of PKal. The optimal substrate specificity of PKal was determined using positional-scanning synthetic combinatorial libraries as previously described (Harris et al., 2000). The assays were performed at room temperature using 50 nM human PKal in assay buffer (50mM Tris-Cl, pH 7.5, 10 mM $CaCl_2$, 100 mM NaCl, 0.01% Tween-20).

Results

Inhibitory profile of ecotins and serpins. Ecotin WT, ecotin RR and the serpins α2-antiplasmin (α2–AP) and plasminogen activator inhibitor-1 (PAI-1) were assayed for their ability to inhibit proteases in the Plg cascade including uPA, tPA, plasmin and plasma kallikrein (Table 5-1). Ecotin WT only inhibited PKal, while ecotin RR inhibited both uPA and PKal, and to a minor extent, plasmin. PAI-1 inhibited both uPA and tPA but not PKal or plasmin, while α2-AP was specific for plasmin. These inhibitors can therefore be used to dissect the role of the different proteases in the Plg cascade. Ecotin WT can be used to target PKal, while α2-AP can be used to selectively inhibit plasmin.

PAI-1 can be used to analyze the role of both uPA and tPA, while ecotin RR can be used to study the function of uPA and PKal.

Mice deficient in the genes for both uPA and tPA do not have an adipogenic phenotype in the mammary gland. Adipogenesis was analyzed in the mammary glands of involuting uPA-/-tPA-/- double-deficient mice. No collagen deposition or decrease in adipogenesis was observed in these mice (Figure 5-8). The morphology of the mammary gland in these mice was similar to that observed in uPA-/- single-deficient mice, which also do not have a phenotype during involution of the mammary gland. However, Plg-/- mice show impaired adipogenesis during involution (Figure 5-4). These data indicate that alternate Plg activators are present and functional during involution, and provide further support for the hypothesis that PKal acts as a Plg activator during adipogenesis *in vivo*.

Neither PKal nor Plg is regulated during adipogenesis. Since PKal and Plg were required for adipocyte differentiation, were either of these proteases regulated during adipogenesis? Plg present in the CM of preadipocytes and differentiated adipocytes was assayed by western blot analysis. The level of Plg and plasmin was the same for both preadipocytes and adipocytes (Figure 5-9a). Similar levels of PKal activity were detected in the CM of preadipocytes and adipocytes analyzed using zymography (Figure 5-9b). These data indicate that neither Plg nor PKal is regulated at the level of protein quantity or activation during adipogenesis. However, the activity of these proteases may be modulated by endogenous inhibitors or cell surface receptors.

Effect of ecotins and plasminogen deficiency on body weight. To determine whether the Plg system plays a role in adipogenesis in tissues other than the mammary gland, the effect of ecotin treatment on total body weight was analyzed. Animals treated with either ecotin WT or ecotin RR during involution lost a greater amount of weight than control animals (Figure 5-10, $p<0.001$). This suggests that the Plg cascade may play a general role in adipogenesis. Adult Plg-/- mice also weighed less than their wild-type littermates (Figure 5-11; $p<0.01$ for weeks 19-21 & 25 and $p<0.005$ for weeks 22-24), indicating that Plg deficiency, similar to ecotin treatment, affects total body weight. The Plg system may therefore be a general modulator of adipogenesis in various tissues.

Specificity of PKal. To further analyze the role of PKal in the Plg cascade, the extended substrate specificity of PKal was determined using positional-scanning synthetic combinatorial libraries (Backes et al., 2000; Harris et al., 2000). PKal was found to have a marked preference for Arg at the P1 position (Figure 5-12). PKal preferred aromatic residues (Phe, Tyr, Trp) at the P2 position but was relatively non-specific at P3 and P4 (Figure 5-13). PKal exhibited a specificity profile that is similar to that of plasmin (Backes et al., 2000; Harris et al., 2000).

Specificity and activation sites of proteases in the Plg cascade. The specificity of uPA, tPA, plasmin (Harris et al., 2000) and PKal is summarized in Table 5-2. Both uPA and PKal are Plg activators, while plasmin and PKal can activate pro-uPA. Comparision of the optimal substrate sequence (Table 5-2) and activation sites of these proteases (Table 5-3) reveals that the substrate specificity of plasmin and PKal closely match the

activation sequence of pro-uPA. However, the specificities of uPA and PKal do not correlate with the Plg sequence except for the P1 position (as well as P2 for uPA). These data suggest that although positional-scanning libraries provide a rapid and convenient method to profile the substrate specificity of proteases, they do not absolutely predict the specificity of a given protease. uPA, tPA, plasmin and PKal are all multi-domain proteases and interactions with physiological substrates are likely to involve more than just the protease domain. The use of short peptide sequences as substrates *in vitro* also does not accurately reflect the cleavage of macromolecular substrates such as Plg.

Discussion

Although Plg and PKal are required for adipogenesis both *in vitro* and *in vivo*, neither protease appears to be regulated with regard to protein level or activation. However, during adipogenesis, the function of Plg and PKal may be regulated by the presence of endogenous inhibitors such as α2-AP or by cell surface receptors that determine the localization of these enzymes. In addition, the expression of a downstream substrate such as fibronectin may be regulated.

The finding that Plg-/- mice weigh less than control mice, and that animals treated with ecotin lost a greater amount during involution suggests that the Plg cascade may play a general role in regulating adipogenesis in various tissues. It would be of great interest to analyze the effect of serine protease inhibitors upon weight gain in animals fed a high fat diet.

It is clear that serine proteases in the Plg cascade play a critical role in adipocyte differentiation. Do other proteases also play a role in adipogenesis? The matrix

metalloproteases (MMPs) have been implicated in the remodeling events that occur during bone development (Vu et al., 1998) and cancer progression (Sternlicht et al., 1999). The role of stromelysin-1 (MMP-3) in adipocyte differentiation is discussed in Chapter Six.

References

Backes, B. J., Harris, J. L., Leonetti, F., Craik, C. S., and Ellman, J. A. (2000). Synthesis of positional-scanning libraries of fluorogenic peptide substrates to define the extended substrate specificity of plasmin and thrombin [see comments] [published erratum appears in Nat Biotechnol 2000 May;18(5):559]. Nat Biotechnol *18*, 187-93.

Harris, J. L., Backes, B. J., Leonetti, F., Mahrus, S., Ellman, J. A., and Craik, C. S. (2000). Rapid and general profiling of protease specificity by using combinatorial fluorogenic substrate libraries. Proc Natl Acad Sci U S A *97*, 7754-9.

Jameson, G. W., Roberts, D. V., Adams, R. W., Kyle, W. S., and Elmore, D. T. (1973). Determination of the operational molarity of solutions of bovine alpha-chymotrypsin, trypsin, thrombin and factor Xa by spectrofluorimetric titration. Biochem J *131*, 107-17.

Sternlicht, M. D., Lochter, A., Sympson, C. J., Huey, B., Rougier, J. P., Gray, J. W., Pinkel, D., Bissell, M. J., and Werb, Z. (1999). The stromal proteinase MMP3/stromelysin-1 promotes mammary carcinogenesis. Cell *98*, 137-46.

Vu, T. H., Shipley, J. M., Bergers, G., Berger, J. E., Helms, J. A., Hanahan, D., Shapiro, S. D., Senior, R. M., and Werb, Z. (1998). MMP-9/gelatinase B is a key regulator of growth plate angiogenesis and apoptosis of hypertrophic chondrocytes. Cell *93*, 411-22.

Table 5-1. Percentage of protease activity remaining after inhibition of human enzymes with ecotin WT, ecotin RR, human α2-antiplasmin (α2-AP) or recombinant human plasminogen activator inhibitor-1 (rhPAI-1).

Enzyme / Inhibitor	huPA	htPA	hPlasmin	hPKal
Ecotin WT, 500 nM	100	100	100	0
Ecotin RR, 500 nM	0	100	64	1
hα2-AP, 250 nM	100	100	0	89
rhPAI-1, 250 nM	0	6	79	96

Figure 5-8.

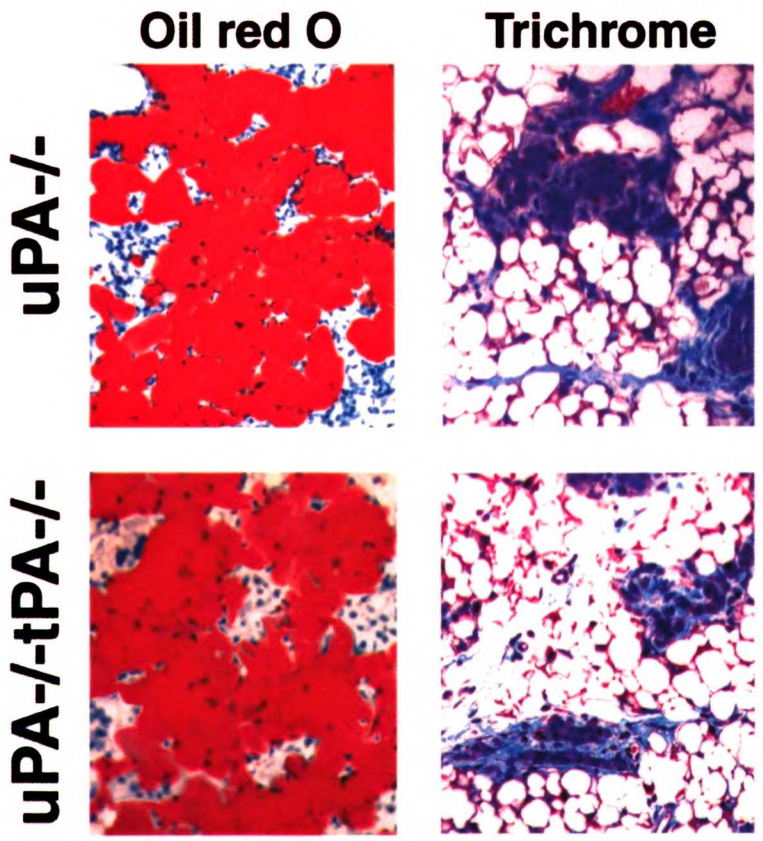

Figure 5-8. Mice doubly deficient in the genes for both uPA and tPA do not have an adipogenic phenotype. Mammary gland sections from mice deficient in the gene for uPA (uPA-/-) and both uPA and tPA (uPA-/-tPA-/-) stained with Oil red O for lipid (red) and Masson's Trichrome stain for collagen fibrils (blue).

Figure 5-9.

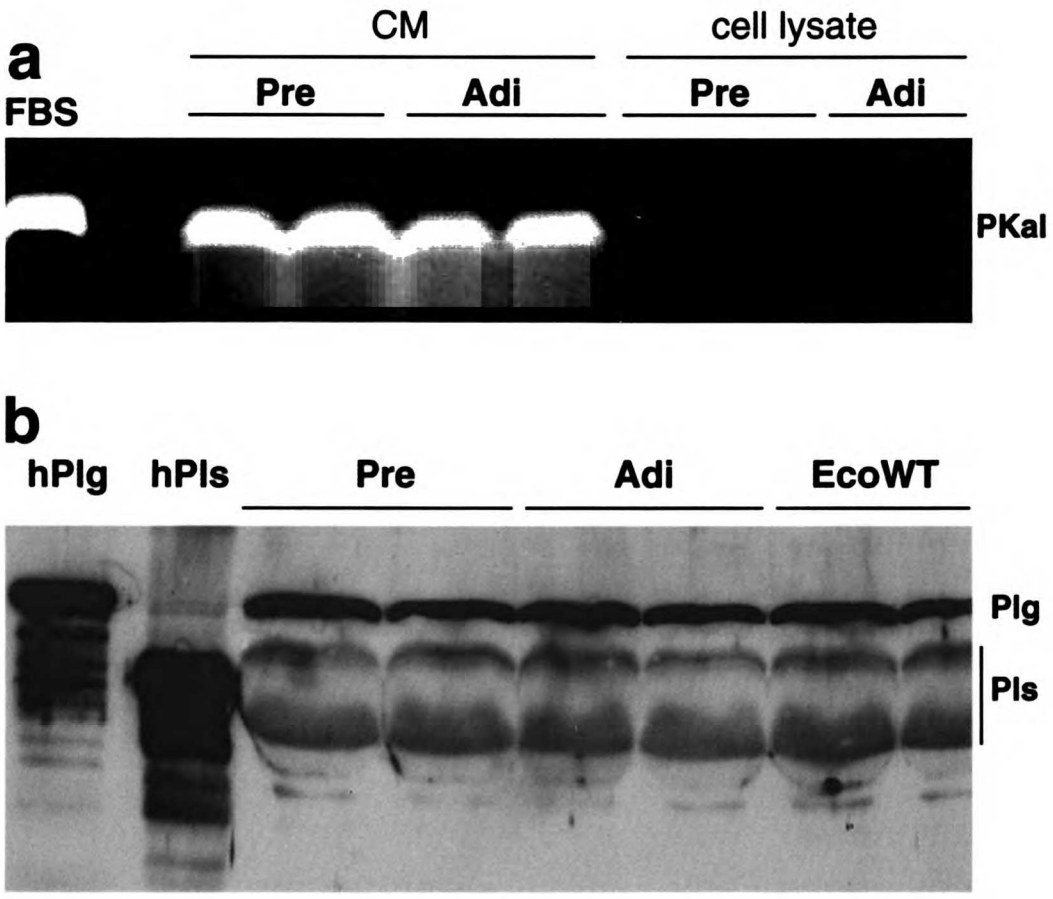
a
CM
cell lysate
FBS
Pre
Adi
Pre
Adi
PKal
b
hPlg
hPls
Pre
Adi
EcoWT
Plg
Pls

Figure 5-9. Detection of PKal and Plg in 3T3-L1 conditioned medium (CM) and cell lysates. **a**, Active plasma kallikrein (PKal) detected in fetal bovine serum (FBS) and the CM and cell lysates of preadipocytes (Pre) and adipocytes (Adi). **b**, Western blot to detect plasminogen (Plg) in the conditioned medium of preadipocytes (Pre), adipocytes (Adi) and cells treated with ecotin WT during differentiation (EcoWT). Human (h) Plg and plasmin (Pls) were used as controls.

Figure 5-10.

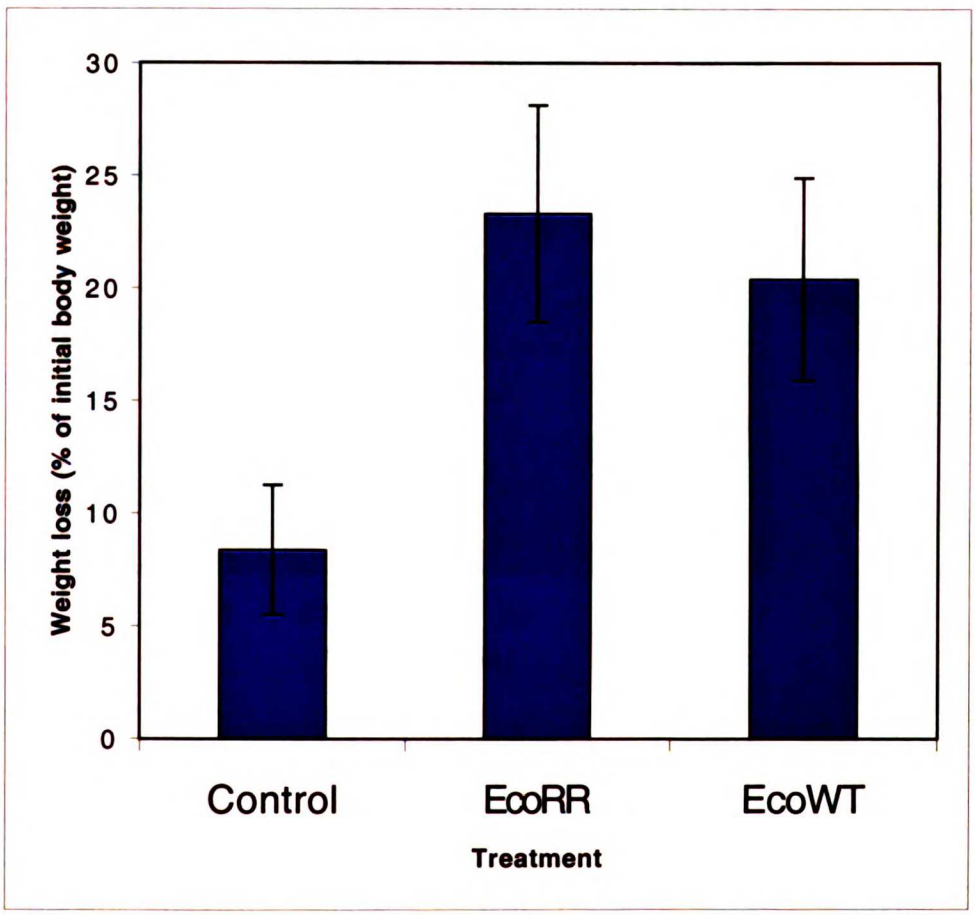
30
25
20
15
10
5
0
Weight loss (% of initial body weight)
Control
EcoRR
EcoWT
Treatment

Figure 5-11.

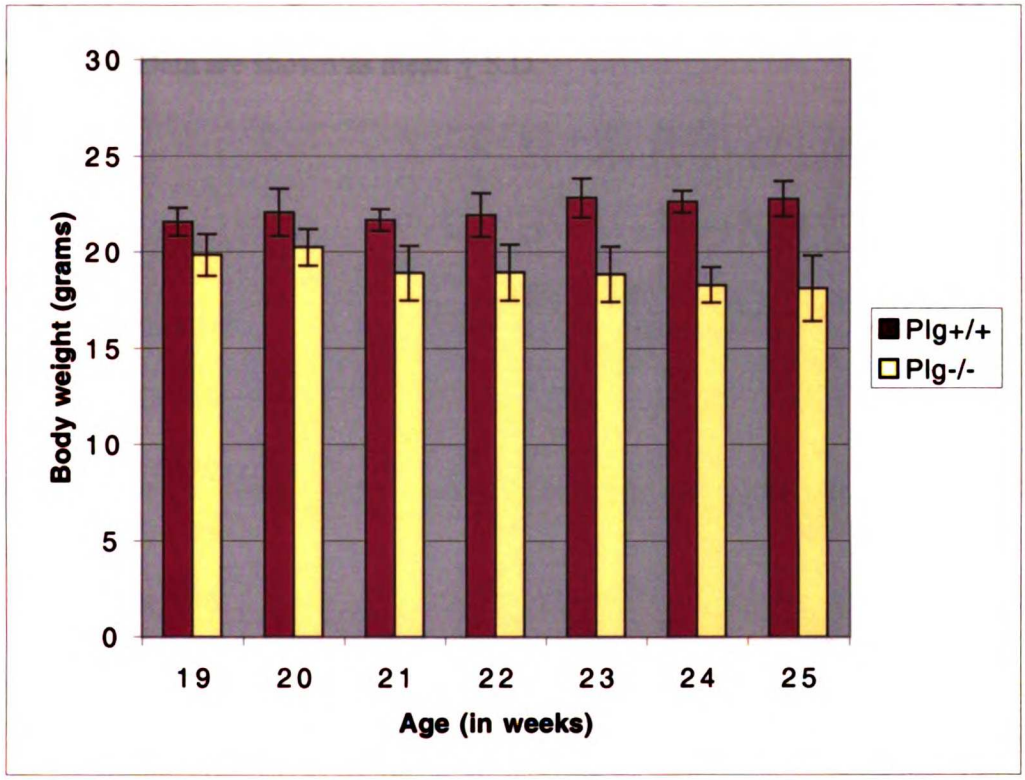
30
25
20
15
10
5
0
Body weight (grams)
19
20
21
22
23
24
25
Age (in weeks)
Plg+/+
Plg-/-

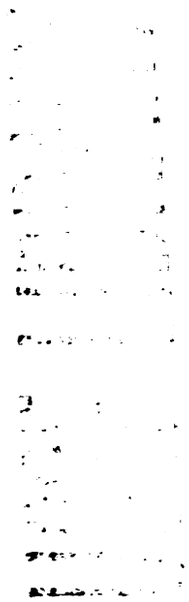

Figure 5-10. Treatment of involuting female mice with either ecotin WT or ecotin RR leads to increased weight loss. Data are shown as mean $\pm$ S.D.

Figure 5-11. Adult Plg-deficient mice (Plg-/-) weigh less than their wild-type littermates (Plg+/+). Data are shown as mean $\pm$ S.D.

Figure 5-12.

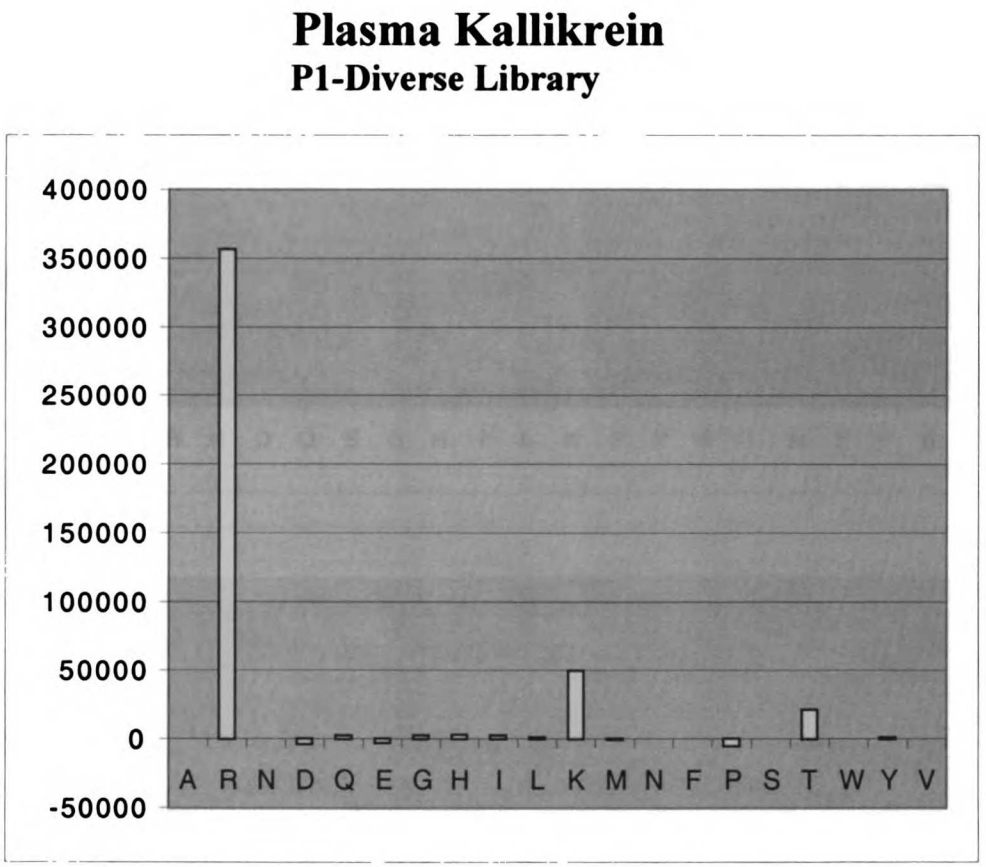
Plasma Kallikrein
P1-Diverse Library
400000
350000
300000
250000
200000
150000
100000
50000
0
-50000
A R N D Q E G H I L K M N F P S T W Y V

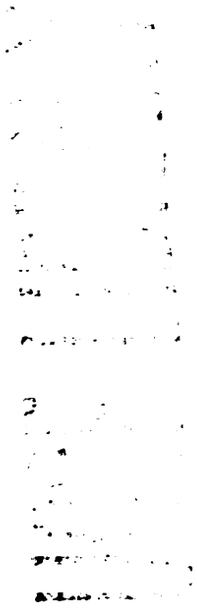

Figure 5-13.

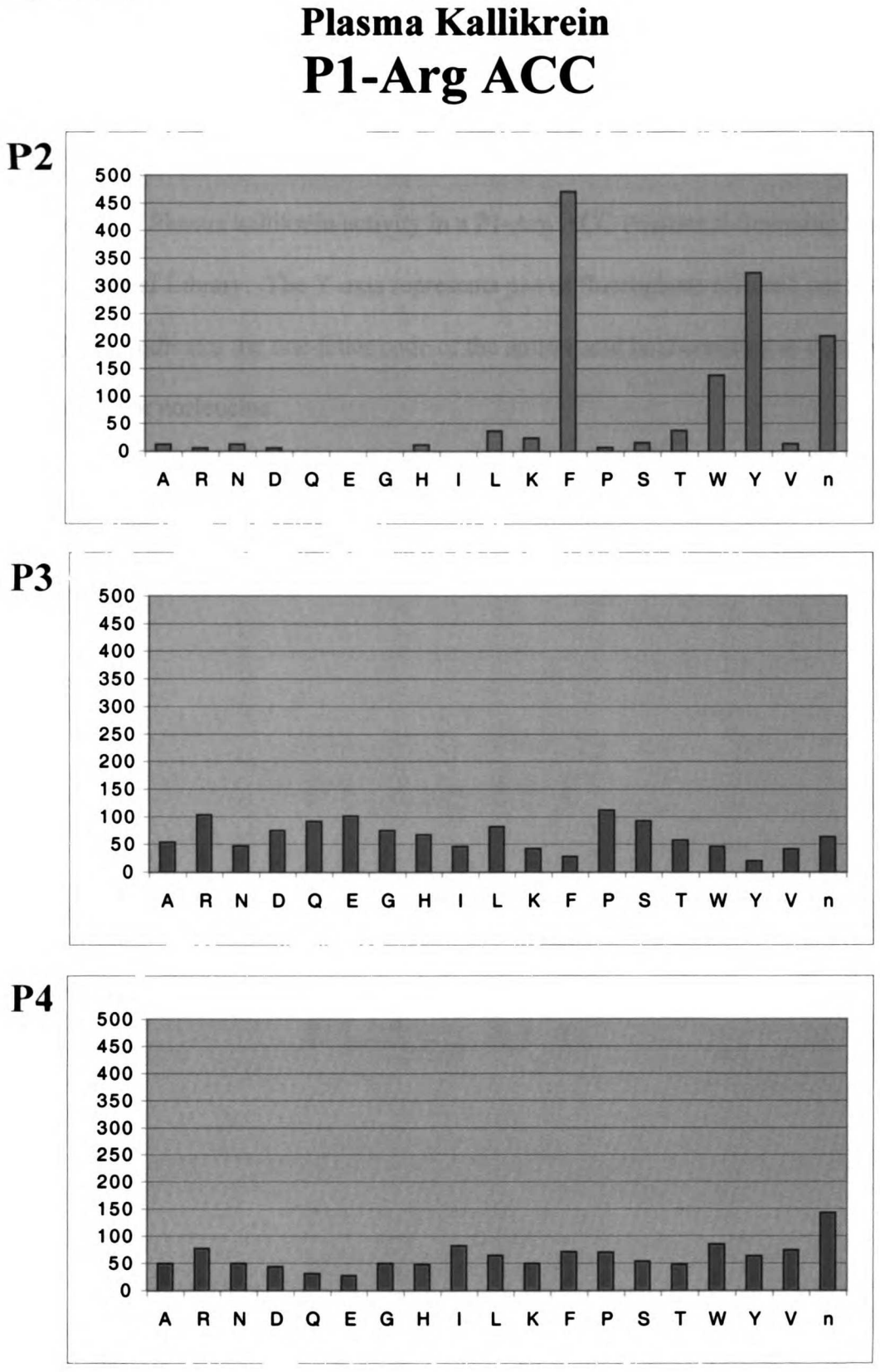
Plasma Kallikrein
P1-Arg ACC
P2
P3
P4
500
450
400
350
300
250
200
150
100
50
0
A R N D Q E G H I L K F P S T W Y V n

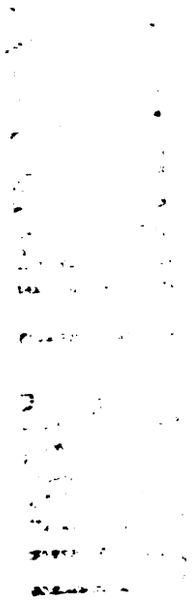

Figure 5-12. Plasma kallikrein activity in a P1-Diverse Positional-Scanning Synthetic Combinatorial Library. The Y-axis represents pM of fluorophore released per second. The X-axis indicates the one-letter code of the amino acid held constant at each position.

Figure 5-13. Plasma kallikrein activity in a P1-Arg ACC Positional-Scanning Synthetic Combinatorial Library. The Y-axis represents pM of fluorophore released per second. The X-axis indicates the one-letter code of the amino acid held constant at each position; "n" stands for norleucine.

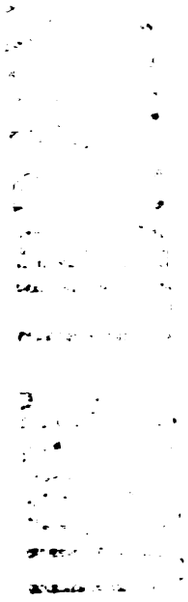

Table 5-2. Substrate specificity of proteases in the Plg cascade (adapted from Harris et. al, 2000).

	P4	P3	P2	P1
PKal	X	X	F, Y, W	R
Plasmin	K, R	X	F, Y, W	K
uPA	X	T, S	S, A	R
tPA	X	F, Y	S, G, A	R

Table 5-3. Activation sequences of proteases in the Plg cascade.

	P4	P3	P2	P1
PKal	I	N	A	R
Plg	C	P	G	R
Pro-uPA	P	R	F	K
L.M.W. uPA	A	D	G	K

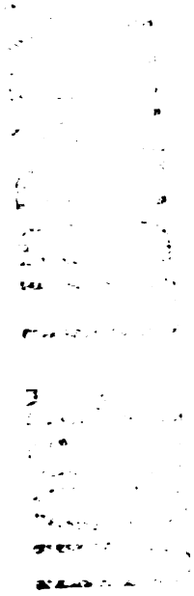

Chapter Six

Stromelysin-1 Regulates Adipogenesis during Mammary Gland Involution

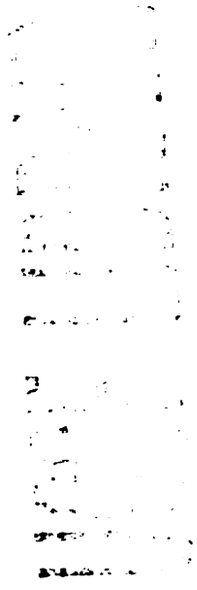

Abstract

The matrix metalloproteinase (MMP), MMP-3/stromelysin-1 (Str1) is highly expressed during mammary gland involution induced by weaning. During involution, programmed cell death of the secretory epithelium takes place concomitant with the repopulation of the mammary fat pad with adipocytes. In this study, we have used a genetic approach to determine the role of *Str1* during mammary involution. Although Str1 has been shown to induce unscheduled apoptosis when expressed ectopically during late pregnancy (Alexander et al., 1996), we found that during post-lactational involution, mammary glands from transgenic mice that overexpress the tissue inhibitor of metalloproteinases, TIMP-1 (TO) and mice carrying a targeted mutation in *Str1 (Str1-/-)* showed accelerated differentiation and hypertrophy of adipocytes, while epithelial apoptosis was unaffected. These data suggest that MMPs do not induce unscheduled epithelial cell death after weaning, but instead alter the stromal microenvironment. We next used adipogenic 3T3-L1 cells as a cell culture model to test the function of MMPs during adipocyte differentiation. Fibroblastic 3T3-L1 progenitor cells expressed very low levels of MMPs or TIMPs. TIMP-1 and TIMP3 mRNAs were upregulated in committed preadipocytes, then declined, while TIMP-2 mRNA increased throughout adipogenesis and TIMP-4 mRNA was induced in parallel with differentiated adipocyte markers. Str1, MT1-MMP, (MMP-14) collagenase-3 (MMP-13) and gelatinase A (MMP-2) mRNAs were induced in all adipogenic cells, but only differentiated adipocytes expressed activated gelatinase A. The addition of MMP inhibitors (GM 6001 and TIMP-1) dramatically accelerated the accumulation of lipid during differentiation. We conclude that MMPs, especially Str1,

determine the rate of adipocyte differentiation during involution. (Caroline M.Alexander, Sushma Selvarajan, John Mudgett and Zena Werb; submitted).

Introduction

Mammary gland involution is a two-phase process. The first phase is characterized by the onset of epithelial apoptosis, which is p53-dependent (Jerry et al., 1998), and the second phase by upregulation of proteinases, repopulation of the mammary stroma by adipocytes and completion of epithelial programmed cell death in a p53-independent manner (Li et al., 1996; Lund et al., 1996).

In cultured mammary epithelial cells, epithelial apoptosis is induced by expression of matrix metalloproteinases (MMPs), by the inhibition of integrin-mediated adhesion, or by altering cell cycle progression (Boudreau et al., 1995; Boudreau et al., 1996; Wang et al., 1994; Wiesen and Werb, 2000). When stromelysin-1 (*Str1*) is mis-expressed in the mammary gland by transgenic means, mice show precocious growth of virgin gland to a mid-pregnant equivalent (Sympson et al., 1994), stromal alteration and unscheduled apoptosis during pregnancy (Alexander et al., 1996; Boudreau et al., 1995; Thomasset et al., 1998) and tumor formation (Sternlicht et al., 1999). Therefore we hypothesize that the response of mammary epithelial cells to ectopic Str1 reflects normal roles for this enzyme.

The prototype MMP, collagenase, was isolated as a collagenolytic activity specifically induced during involution of the tadpole tail (Gross, 1966). Since the description of this activity, other MMPs have been shown to cleave structural proteins important to maintaining basement membrane integrity (Sternlicht et al., 1999; Sternlicht and Werb, 2000; Vu and Werb, 2000). Their potential for modulating the epithelial cell-substratum interaction and their reactive induction during physiological remodeling reactions is based on the finding that one such MMP, stromelysin-1 (Str1), is expressed

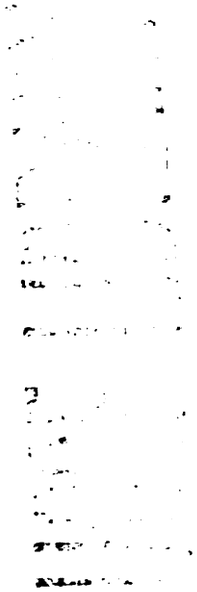

and regulated during mammary gland development and involution (Witty et al., 1995). Str1 cleaves many basement membrane proteins (Mayer et al., 1993; Werb, 1997), and can autoactivate pro-Str1 and other pro-MMPs to initiate a proteolytic cascade (Nagase, 1997). It is synthesized and secreted by a subpopulation of stromal cells in the mammary gland (Witty et al., 1995). Targets for proteinase activity are not limited to ECM molecules. Cell surface molecules such as E-cadherin can be cleaved in cultured mammary epithelial cells transfected with an inducible Str1 cDNA (Werb, 1997; Sternlicht and Werb 2000; Lochter et al., 1997). Other substrates include extracellular growth factors and cell surface molecules (Werb, 1997).

To test the importance of MMPs in involution in the present study, we have used two genetic approaches. We have investigated mammary gland involution in mice over-expressing the tissue inhibitor of matrix metalloproteinases, human TIMP-1 (TO) (Alexander et al., 1996), and in mice carrying a null mutation in *Str1 (Str1-/-)* (Mudgett et al., 1998). Both of these transgenic mice have no overt defects, are able to complete pregnancy and lactate. Analysis of mammary glands from TO mice shows that the transgene is expressed and active (Alexander et al., 1996). By combining the information from these two strains, we can identify processes that require Str1 activity (if both TO and *Str1-/-* transgenic mice share the same phenotype) and those that require TIMP-1-inhibitable MMP activity (if TO but not *Str1-/-* mice show a specific phenotype). We show here that Str1 deficiency specifically accelerates the differentiation of adipocytes during active remodeling, and that epithelial cell death is unaffected in either transgenic strain.

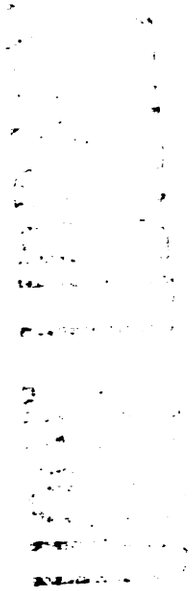

Materials and Methods

Materials

Ultraspec RNA isolation solution was from Biotecx (Houston, TX). Enhanced chemiluminescence (ECL) reagents were from Amersham. Immobilon P was from Millipore. Sources of antibodies were as follows: rabbit polyclonal anti-laminin antibody was from Collaborative Research (cat# 40023); rat monoclonal anti-entactin (nidogen-1) antibody was from Upstate Biotechnology Inc. (cat# 05-208); HRP-conjugated anti-rabbit (NA 9340) or anti-rat IgC (NA 9320) were from Amersham. Duralon-UV membrane was from Stratagene (La Jolla, CA). The source of mouse cDNA probes was as follows: stromelysin-1 (Ostrowski et al., 1988), MT-1 MMP (Sato et al., 1994), pPARγ (Tontonoz et al., 1995), TIMP-1 (Gewert et al., 1987), TIMP-2 (a 360 bp coding sequence made by RT-PCR from published sequence using oligonucleotide sequences GGTCTCGCTGGACATTGGAGGAAAG and GGGTCCTCGATGTCGAGAAACTCCTG), TIMP-3 (Leco et al., 1994) and TIMP-4 (Leco et al., 1997). 3T3-L1 cells were from the ATCC, Manassas, VA. GM6001 (3-(N-hydroxycarbamoyl-2(R)–isobutyl propionyl-L-tryptophan methylamide) was a gift of Dr. Richard Galardy, Glycomed Inc., Alameda, CA. Recombinant human TIMP-1 (rhTIMP-1) was a gift of Synergen Corp., Boulder, CO; human TIMP-1 (hTIMP-1) purified from transfected BHK cells was a gift of Dr. Joni Mott, Lawrence Berkeley National Laboratory, Berkeley, CA.

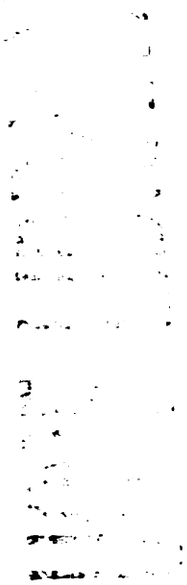

Transgenic Mice

The derivation and characteristics of transgenic mice expressing a human TIMP-1 transgene (TO mice) under the control of the β-actin promoter have been described (Alexander et al., 1996). Briefly, these mice have no gross phenotype and express approx. 50 ng/ml circulating human TIMP-1 and approx. 20 ng/ml of tissue lysate from pregnant mammary gland. Mice carrying this transgene were compared to non-transgenic siblings or CD-1 control mice (Charles River, MA). Mice carrying a targeted null mutation in the Str1 gene (*Strl-/-*) were made by homologous recombination using the AB2.1 ES cell line from 129 mice (Mudgett et al., 1998), and were compared to a control line (Str1+/+) on the 129 background. These mice were also grossly normal. To standardize lactation from mouse to mouse, litters were adjusted to 6 pups per dam, and mothers were housed individually before weaning. For time points during pregnancy, 0.5 d post coitum (p.c.) is assumed to be noon of the day of observation of the vaginal plug. Lactation is timed from the time of parturition.

Histology and Immunochemistry

For histologic evaluation, pieces of mammary gland were fixed in 4% paraformaldehyde overnight at 4°C, embedded in paraffin, sectioned and stained with hematoxylin and eosin (H&E) according to standard techniques. Epithelial colonization of involuting glands was assessed by measuring the overall density of stained epithelial tissue in an unstained background of adipocytes using Adobe Photoshop software. Similar fields (3 from each mouse) of microscopic views from test and control mice (4 each) were assayed for

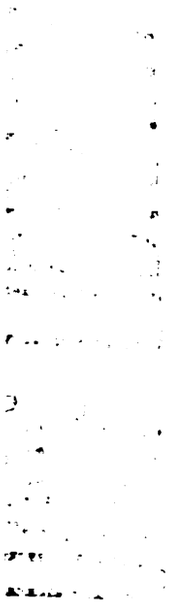

average pixel density. The number of adipocytes per field was scored manually, and the adipocyte area was deduced using NIH Image software.

For immunostaining of specific ECM molecules, 5 – 10 mm pieces of fresh mammary gland were infiltrated with 20% sucrose in 1 mM EDTA, 50 mM Tris pH 7.5 (4°C) and frozen in OCT for cryosectioning. Sections (6 – 10 μm) were cut and immediately fixed in 4% freshly prepared paraformaldehyde for 15 min, blocked in 0.1 M glycine (3 x 1 min in PBS), and then 10% sheep serum in PBS for 30 min at room temperature. Anti-entactin antibody (diluted 1: 1000 in 3% bovine serum albumin in Tris-buffered saline) was incubated on sections overnight at 4°C, washed 3x in PBS / 0.1% Tween for 5 min, and incubated with secondary antibody (HRP-conjugated anti-rat IgG, diluted 1:100 into 20% Carnation skim milk powder in PBS) for 60 min. The wash protocol was repeated and the sections were counterstained lightly with methylene blue.

Gel Electrophoresis of Mammary Gland Protein Lysates

Pieces of mammary gland tissue were homogenized in RIPA buffer (150 mM NaCl, 1% NP-40, 0.5% dexycholate, 0.1% SDS, 50 mM Tris-HCl, pH 8.0) at 0.25 mg wet weight/ml. Lysates were spun for 15 min at 4°C in a microcentrifuge, and insoluble fractions ("ECM-enriched fractions") were washed once in RIPA buffer and boiled into sample buffer containing 5% SDS as described previously (Alexander et al., 1996). Extracts equivalent to 8 mg wet weight tissue were separated on 6% SDS-PAGE gels, and either stained with Coomassie Blue or silver stain, or transferred to Immobilon P for immunoblotting of specific ECM constituents.

Assay of Apoptotic DNA Laddering

Fragments of mammary tissue (approx. 100 mg) were digested in lysis buffer (0.2 mg/ml proteinase K in 50 mM Tris, 0.1 M NaCl, 0.1 M EDTA, 1% SDS pH 8.0) overnight at 60 °C. The crude DNA preparations were extracted twice with phenol/chloroform and precipitated with propanol for 3 min at room temperature. After 1 rinse with 70% ethanol, DNA pellets were redissolved in TE with RNase A at 60 °C for 20 min and digested for 30 min at 37 °C. 10 μg of DNA was analyzed by electrophoresis on 2% agarose gels as described previously (Alexander, et al., 1996)

Northern Blotting

Total RNA was isolated by homogenization (using an Omni 2000 Polytron) of pieces (100 – 200 mg) of mammary tissue or from 3T3-L1 cultures in Ultraspec solution according to the manufacturer's instructions. 10 μg of RNA was separated by standard formaldehyde gel electrophoresis, and transferred to Duralon membrane for hybridization with specific probes.

Culture and Differentiation of 3T3-L1 Cells

3T3-L1 fibroblasts (obtained from ATCC) were routinely grown at subconfluence in 10% fetal calf serum (FCS) / DME-H21. To initiate differentiation, cells were grown to confluence in 10 cm diameter dishes or 6- or 96-well tissue culture plates. At day 0, a differentiation-inducing mix was added (DM; 0.22 mM insulin, 0.6, μM dexamethasone and 0.5 mM methylisobutylxanthine in culture medium) (Bernlohr et al., 1984) with or without MMP inhibitors (10 μM GM 6001, or 250 nM rhTIMP-1 or hTIMP-1 isolated for

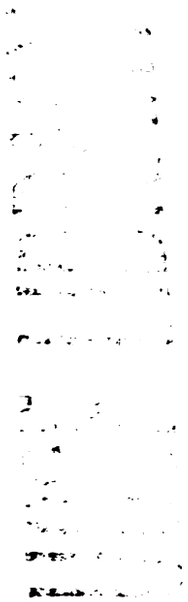

cell cultures). After 2 days, medium was replaced with fresh culture medium with or without inhibitors. To evaluate RNA expression in differentiating cultures, actively proliferating cultures (preadipocytes; pre), confluent cultures prior to DM administration (committed; com) and differentiating adipocytes after treatment with DM were scraped into Ultraspec solution, and RNA was purified according to the manufacturer's instructions. Cultures were evaluated for lipid accumulation at 4 days using an Oil Red O stain as follows: Cells were fixed in 10% formalin in PBS and stained for 2 hours with Oil Red O (Ramirez-Zacarias et al., 1992), washing well with water before and after staining. For quantification of lipid accumulation, cells were grown in 96-well plates and stained with Oil red O. The Oil Red O dye was extracted into 100 µl isopropanol and the absorbance of the solution was measured at 510 nm.

Preparation of Nuclear Extracts and Western blotting for C/EBPβ

3T3-L1 cells were treated with GM 6001 as described above and collected at 24 hours, 48 hours and 96 hours after induction of differentiation, washed with PBS, then scraped and transferred to Eppendorf tubes for preparing nuclear extracts by the method of Finbloom et al., (1994). The cells were centrifuged at 3,000 x g for 1 min and then homogenized in Buffer A (20 mM HEPES, pH 7, 10 mM KCl, 10 mM MgCl2, 20% glycerol, 0.1% NP-40, 0.5mM DTT, 0.25 mM PMSF). The resulting lysate was centrifuged at 3,000 x g for 5 min and the pellet was resuspended in Buffer A and layered onto a sucrose cushion (35% sucrose, 100mM HEPES, pH 7, 20 mM MgCl2) in an Eppendorf tube. The tube was centrifuged at 3,000 x g for 15 min and the pellet was resuspended in Buffer A supplemented with 300 mM NaCl, then centrifuged at 10,000 x g for 5 min. The

resulting supernatant (nuclear extract) was used for western blotting by standard techniques. The blots were incubated with polyclonal rabbit anti-rat C/EBP β peptide (carboxy terminus, C-19; sc-150) from Santa Cruz Biotechnology, Inc.

Results

Stromelysin-1 is Highly Upregulated During Mammary Gland Involution

Inappropriate expression of a Str1 transgene induces unscheduled apoptosis in dividing mammary epithelial cells from late pregnant gland (Boudreau et al., 1995; Alexander et al., 1996). The endogenous expression of *Str1* mRNA is regulated during mammary gland development. *Str1* expression was low in virgin glands, but it was induced during early pregnancy (3 days p.c.), continued to increase to 9 days p.c. and was not detectable after 12 days of pregnancy or during lactation (Fig. 1A).

Interestingly, the expression of endogenous Str1 is not detectable during late pregnancy, presumably protecting cells from Str1-induced cell death. Notably high ectopic *Str1* expression does not induce epithelial cell death during lactation, even though epithelial basement membranes are fragmented (Sympson et al., 1994; Alexander et al., 1996). *Str1* was highly induced during involution, when the secretory epithelium undergoes apoptosis (Talhouk et al., 1992; Lund et al., 1996; Li et al., 1994), to about 50-fold that typical of pregnant glands. This suggests that susceptibility to Str1-induced cell death depends upon the state of growth and differentiation of mammary epithelial cells.

TIMP-1 Overexpression and Stromelysin-1 Deficiency Do Not Affect Apoptosis or Loss of Mammary Epithelial Function During Mammary Gland Involution

To determine whether Str1 has a role in inducing epithelial cell apoptosis during mammary gland involution after weaning, we measured DNA laddering in tissue extracts from wild-type, TO transgenic and Str1-/- mice. In wild-type mice, ladders of DNA appeared between 1 and 3 days after weaning (Fig. 1B and C), correlating with the appearance of residual cell bodies in alveolar lumens in histological samples (data not shown; also see Lund et al., 1996). The peak of cell death was at 3 days, and cell death was significant for 8 – 10 days. After 10 days, resorption of the epithelium (> 90% of epithelial cells) was complete. DNA laddering was also evident 2 and 3 days after the removal of pups (Fig. 1C) from TO mice, indicating that the onset of epithelial involution was normal. To measure the decline of differentiated epithelial cell function that occurs during weaning, we assayed the expression of the mRNA for the milk protein, whey acidic protein (WAP). Surprisingly, both TO and Str1-/- mice showed the wild type pattern of declining expression between days 2 and 3 post-weaning (Fig. 1D). These data indicate that Str1 and other TIMP-1 inhibitible MMPs do not play a significant role in apoptosis of secretory epithelial cells. This raises the question of what the function of these MMPs is during mammary involution.

Mammary adipogenesis is accelerated in mice deficient in MMP function

We observed a striking alteration in the morphology of MMP-deficient glands during involution (Fig. 2). At first glance these glands appeared to involute more rapidly because the area occupied by epithelial ducts and alveoli decreased. However, from morphological data, we deduced that this was due to the accelerated repopulation of the gland with adipocytes. After weaning of wild-type mice allowed to lactate for 8 days,

there was a delay of about 4 days before there was significant recolonization of the mammary gland with differentiated adipocytes. In TO mice, differentiated hypertrophic adipocytes appeared in greater number than wild type as early as 2 days after weaning (Fig. 2a and b). By histomorphometry of H&E-stained paraffin sections, mammary glands of TO mice harvested 4 days after weaning contained between 40 - 50% more unilocular adipocytes (Table 1; Fig. 2c and d).

Next we altered the time course of mammary involution to determine its effect on adipocyte differentiation. When pups are removed after 2 instead of 8 days of lactation, complete alveolar development is prevented, the epithelium regresses more rapidly and cell death is complete by 4 days (Talhouk et al., 1992). Using this protocol, we found that the process of adipocyte colonization was accelerated in wild type mice, so that the relative timing of adipocyte expansion and epithelial cell regression is maintained (Fig. 2e). When TO females were weaned after 2 days lactation, the differentiation of adipocytes was also more rapid than controls (Fig. 2f).

Involuting glands from Str1-/- mice at 3 days (Fig. 2g and h) and 6 days (Fig. 2i and j) after weaning showed the same changes as the TO mice by histomorphometric analysis. The Str1-/- mice showed an increase of approximately 30% in adipocyte colonization in their mammary glands compared to controls (Table 1). These data indicate that TIMP-1-sensitive MMPs, including Str1 regulate mammary adipogenesis.

Str1 Upregulation Parallels Mammary Gland Adipogenesis, Anglogenesis and Remodeling of Stromal Matrix During Involution

Why does the absence of Str1 affect the rate of adipocyte differentiation? Previous studies give us two clues: first, *Str1* mRNA is expressed by fibroblastic cells, some of which may be preadipocytes (Lund et al., 1996). Second, Str1 protein is frequently associated with blood vessels (Talhouk et al., 1992). Detailed analysis of the timecourse of expression of *Str1* mRNA, compared to other markers of cell function showed that *Str1* was induced only after the loss of differentiated epithelial cell function, as monitored by WAP mRNA expression, and after the majority of epithelial cell death. Notably, *Str1* was induced in parallel with markers usually associated with active remodeling and morphogenesis (Fig. 3).

The repopulation of the mammary gland by differentiated adipocytes requires replacement of the interstitial ECM around the fibroblast-like preadipocytes, which is rich in fibrillar collagens and fibronectin (data not shown), by the basement membranes that surround differentiated adipocytes (Smas and Sul, 1995). Concomitantly, the vasculature of the fat pad is remodeled so that there is a dense weave of capillaries in intimate contact with adipocytes (Crandall et al., 1997). mRNA for nidogen-1/entactin, an ECM molecule that is a prominent component of adipocyte basement membranes (see Fig. 7), was induced at 3 days at the same time as *Str1* (Fig. 3A,B). We observed that the expression of PECAM-1 mRNA, a cell adhesion molecule specific to endothelial cells, was induced at 3 days, and peaked at 6 days post-weaning. Interestingly, PECAM-1 mRNA was expressed at a higher level in glands from Str1-/- mice (Table 1). These data

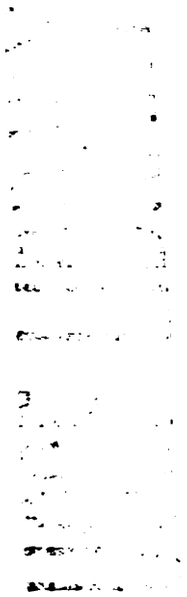

lead us to conclude that the timing of induction of Str1 mRNA is consistent with its expression during angiogenesis and remodeling by the stromal compartment.

Mammary Gland Involution is Characterized by a Biosynthetic Phase

We next verified that there was a switch in ECM at this time in involution. The activation of a biosynthetic stromal compartment was reflected in changes in the ECM of involuting glands. We observed dramatic changes in the protein profiles by SDS-PAGE analysis of ECM-enriched extracts in response to weaning. At one day after weaning, the mammary gland extracts contained collagens (identified by arrowheads in Fig 3B), entactin and laminin. These protein profiles resembled extracts from pregnant and lactating gland (Alexander et al., 1996; and data not shown). Coincident with the induction of epithelial apoptosis at two days after weaning, most basement membrane proteins, including basement membrane entactin and laminin disappeared from the ECM-enriched fraction (Fig. 3B). Immunoreative collagen type IV, entactin and laminin began to reappear after 3 days of involution (Fig. 3B), when their mRNA transcripts were upregulated (Fig. 3A, and data not shown) and were present in high amounts after 4 days.

To define better the cellular events that lead to these striking changes, we stained sections of involuting gland with antibodies to basement membrane proteins. Surprisingly, two and three days after weaning, the amount of entactin in basement membranes around epithelial alveoli appeared similar to that during lactation (Figs. 3 and 4). ECM proteins that are normally SDS-soluble become insoluble because of crosslinking by transglutaminase (Strange et al., 1992). Their antigenicity is unaffected, and the morphology of the basement membranes at the light microscopic level is

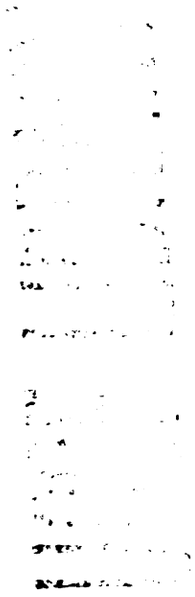

unchanged. We conclude that basement membrane proteins surrounding mammary alveoli undergo a substantial change in properties during the initiation of programmed cell death. The increase of entactin seen biochemically by SDS-PAGE analysis (Fig. 3) paralleled the increase of immunostaining observed in sections of glands 4 days after weaning (Fig. 4, 4di). During the biosynthetic phase (Fig. 4, 4di arrows) entactin protein localized not only to the regressing, insoluble epithelial basement membranes, but also to the assembling, soluble basement membranes that surround hypertrophying adipocytes.

We then sought evidence to verify that the upregulation of Str1 had functional consequences by examining the integrity of one of its in vivo substrates, entactin/nidogen-1. The co-induction of Str1 and entactin during the biosynthetic phase of involution led to a characteristic pattern of entactin fragmentation (Fig. 3C), the result of Str1 cleavage of the 150 kDa entactin molecule between the G1 and G2 domains (Alexander et al., 1996). This proteolysis was almost completely inhibited in parallel samples from TO mice (Fig. 3C). This result shows that the TIMP-1 transgene was not only highly expressed during involution, but that it was also an effective MMP inhibitor.

MMPs Regulate Adipogenesis in 3T3-L1 Cells in Culture

The results of the genetic experiments in mice described above suggest that the rate of adipocyte hypertrophy in the mammary gland is enhanced in the absence of Str1. However, *in vivo* adipogenesis could be either a direct or an indirect target of MMPs in this complex tissue. To examine whether there are direct effects of MMPs, we exploited the differentiation of 3T3-L1 cells into adipocytes in culture. The fibroblastic progenitor cells are not adipogenic in sub-confluent cultures. At confluence the cells become

committed preadipocytes. Treatment of confluent cultures with a differentiation-inducing mix (DM; dexamethasone, insulin and methylisobutylxanthine) induces the expression of proteins associated with mature adipocytes and accumulation of lipids (Bernlohr et al., 1984).

We first determined the expression of MMPs and TIMPs in 3T3-L1 cells. *Str1* expression was developmentally regulated in differentiating 3T3-L1 cells. Str1 mRNA was highly induced in confluent, committed pre-adipocytes, and expression continued in differentiating cultures (Fig. 5A). We used the expression of several transcription factors (peroxisome proliferator-activated receptor-γ (pPARγ) mRNA, a nuclear hormone receptor and C/EBPβ) expressed by differentiated adipocytes, to monitor differentiation. After 4 days of treatment with DM, pPARγ (Fig. 5A) and C/EBPβ (Fig. 6A) were highly induced, in parallel with lipid accumulation (Fig. 6B and C). Since Str1 can activate other MMPs, leading to a cascade of MMP-dependent proteolysis, we determined the expression of other MMPs. Similar to Str1, mRNA for collagenase-3 (MMP-13) was also induced with a similar time course. mRNA for the cell-surface bound MT1-MMP (MMP-14), was induced in committed cells, and expression of this enzyme increased with differentiation, while mRNA for matrilysin (MMP-7) was not detected (data not shown).

The expression of the proteolytic activity of MMPs is regulated by TIMPs. All four TIMPs were expressed in adipocytes, as they are *in vivo* in the mammary fat pad of mice during puberty (Fata et al., 1999). TIMP-1 and -3 were highly induced in committed cells, but showed little expression in differentiated adipocytes. TIMP-4 was expressed specifically by differentiated adipocytes, increasing in parallel with pPARγ.

TIMP-2 expression was characteristic of committed and differentiated cells. We conclude that differentiated cells express a higher ratio of mRNAs for MMPs compared to TIMPs than committed cells.

We found that the relative increase in MMP mRNA expression was accompanied by an induction of proteolytic activity specific to the differentiation phase of 3T3-L1 development. Gelatinase A (MMP-2) was the major MMP seen by zymography of enzymes secreted into the media of induced 3T3-L1 cells (Fig. 5B). MT1-MMP activates gelatinase A in a TIMP-2-dependent fashion (Will et al., 1996; Holmbeck et al., 1999; Caterina et al., 2000; Zhou et al., 2000; Wang et al., 2000). We observed significant activation of gelatinase A after 4 days of differentiation, and further induction and activation after 8 days. Thus, as the concentration of inhibitors declined during adipocyte differentiation, proteinases were activated.

In vivo, we found that ectopic expression of TIMP-1 expression increased the rate of adipocyte differentiation. If this effect is mediated by a direct effect on adipocytes, we would expect that the addition of an MMP inhibitor would increase the rate of adipogenesis during the differentiation of adipocytes *in vitro*. To test this hypothesis, we added three different MMP inhibitors (a synthetic hydroxamate inhibitor [GM6001; 10 μM], recombinant human TIMP-1 [250 nM], or natural human TIMP-1 purified from transfected BHK cells [250 nM]) to cultures of committed 3T3-L1 cells concomitant with the differentiation-inducing mix. An accelerated rate of differentiation with increased C/EBPβ expression was evident at day one of differentiation (Fig. 6A). All three inhibitors stimulated lipogenesis by cells 4 days after induction by more than 7-fold (Fig.

6B and C). We conclude that Str1 determines the rate of hypertrophy and lipogenesis in differentiating adipocytes, and that, in its absence, differentiation is accelerated.

Discussion

Stromelysin-1 Does Not Regulate Mammary Epithelial Cell Death During Involution Caused by Weaning

The amount of specific basement membrane proteins is cyclically regulated during the division and death of mammary epithelium typical of human breast (Ferguson et al., 1992), and basement membrane integrity is essential for mammary epithelial survival *in vivo* (Weaver and Bissell, 1999). Elvax pellets containing TIMP-1, implanted at the onset of involution, protect proximal epithelial cells from death (Talhouk et al., 1992).

Our data indicate that the major role of Str1 in mammary gland involution is to regulate the phenotypic expression of stromal cells, rather than to regulate mammary epithelial apoptosis. It is evident from earlier studies that overexpression of Str1 induces an altered stromal phenotype, with increases in collagen deposition during pregnancy (Thomasset et al, 1998). However, two lines of evidence from previous work implicated MMPs in mammary epithelial cell death during weaning. Firstly, ectopic Str1 induces unscheduled programmed cell death during late pregnancy in transgenic mice, and also induces death *in vitro* in cultured mammary epithelial cells (Boudreau et al., 1995; Sympson et al., 1994). Apoptosis of mammary epithelial cells in culture and *in vivo* can also be induced by inhibitors of β1 integrin, either by the addition of function-perturbing antibodies (Boudreau et al., 1995; Boudreau et al., 1996; Klinowska et al., 1999) or by the expression of dominant negative β1 integrin (DN β1) transgenic mice (Faraldo et al.,

1998). However, mammary epithelial cells are sensitive to apoptosis induced by Str1 (Alexander et al., 1996) and DNβ1 (Faraldo et al., 1998) only during late pregnancy. The similarities between the phenotypes induced by these two transgenes suggest they operate in the same pathway, and that Str1 cleaves a β1 integrin ligand

In fact, Str1 is not induced early enough to be the natural initiator of cell death. It appears later during the biosynthetic wave. It is not surprising, therefore, that epithelial apoptosis was unaffected in Str1-/- mice. However, the lack of effect in TO mice suggests that other TIMP-1 sensitive MMPs are not implicated either. This leaves open the possibility that an MMP that is relatively insensitive to TIMP-1 could still participate. The candidate proteinase, MT1–MMP is functionally upregulated during early mammary involution (Lund et al., 1996), and is not inhibited by TIMP-1, but is inhibited by TIMP-2 and TIMP-3 (Will et al., 1996). Unfortunately, mice with a null mutation of MT1-MMP gene die postnatally due to widespread problems associated with deficient collagen remodeling (Holmbeck et al., 1999). There are now more than 20 MMPs with little known about the expression or inhibition of MMPs cloned very recently (reviewed in Vu and Werb, 2000). Note that TIMP-1 was expressed in TO mice at a level (30 ng/ml tissue lysate of mammary gland 1 day after weaning; Alexander et al., 1996) sufficient to inhibit MMP-dependent proteolysis such as entactin fragmentation. We conclude from these data that that it is unlikely Str1 or another TIMP-1-sensitive MMP initiates cell death caused by weaning.

One hypothesis that could reconcile the inhibition of mammary epithelial cell death caused by implants of TIMP-1 (Talhouk et al., 1992) with the lack of inhibition observed in this genetic analysis of TO and Str1-/- mice is that inflammatory cytokines,

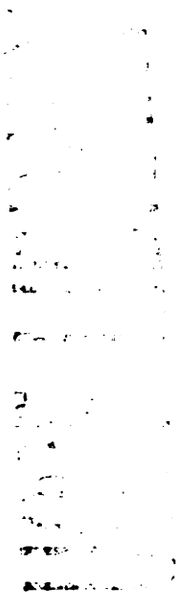

induced by surgery, are known to protect mammary epithelial cells from cell death (Lund et al., 1996). Another explanation could be that the TIMP-1 concentration was likely much higher in the affected zone proximal (100-200 μm) to the implanted pellets containing 10 μg of TIMP-1 (as high as 1 - 5 mM). At these levels, MTI-MMP and other metalloproteinases might be inhibited. By contrast, plasma and tissue levels of TIMP-1 in the transgenic TO-1 mice are in the range of 0.1 - 2 nM (Alexander et al., 1996). For full efficacy, TIMP-1 was added to 3T3-L1 cell cultures at 250 nM and the peptide hydroxamate GM 6001 inhibitor at 10 μM, well below the concentrations of TIMP near the implants. At higher concentrations, TIMP-1 inhibits gelatinase A and unrelated metalloproteinases such as ADAM-TS metalloproteinase aggrecanase-1 (Arner et al., 1999), and may affect ADAMs, which are responsible for cleavage and shedding of many cell surface proteins that regulate cell function and death (Amour et al., 1998).

Mice with null mutations for other MMPs have been tested for defects of involutive processes: uterine involution is normal in mice with a null mutation in matrilysin/MMP-7, possibly due to compensatory expression of other MMPs (Rudolph-Owen et al., 1997). On the other hand, apoptosis of chondrocytes during the ossification of growth plates in juvenile bone is inhibited by the absence of gelatinase-B/MMP-9 (Vu et al., 1998). This effect is not mediated by cleavage of ECM components but instead by reduced bioavailability of the growth factor, VEGF (Gerber et al., 1999). If MMPs do not mediate epithelial cell apoptosis during mammary gland involution, are proteinases required at all? From studies with plasminogen-deficient mice, it is now clear that the plasminogen cascade plays a significant role in development of lactational competence

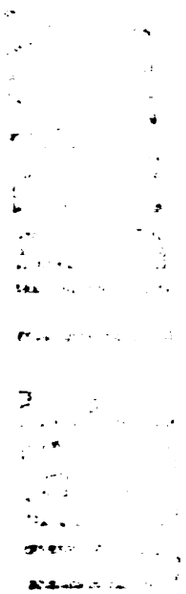

during pregnancy and in mammary epithelial cell apoptosis during involution (Lund et al., 2000).

Stromelysin-1 Expression Occurs During a Biosynthetic Wave That Remodels the Mammary Gland During Involution

Using light microscopy and immunohistochemistry, we found no substantial change in the amount, distribution or appearance of specific components of the epithelial basement membranes during early involution. However, biochemically, the properties of these basement membrane proteins is dramatically affected between 1 and 2 days after weaning. Most become detergent-insoluble and disappear from protein profiles of gland extracts. Soluble ECM components are almost completely absent during the onset of apoptosis. Using high-resolution techniques, some investigators have reported the apparent thickening of basement membranes during this phase (Strange et al., 1992; Warburton et al., 1982).

The induction of the enzyme tissue transglutaminase (tTG) may explain these alterations of basement membrane morphology and biochemistry. This enzyme is associated with the onset of apoptosis in a number of cell types (Melino and Piacentini, 1998), and is induced in early involuting mammary gland (Guenette et al., 1994; Strange et al., 1992). By cross-linking many extracellular proteins, including basement membrane proteins such as laminin, collagen IV and entactin, this enzyme is capable of inducing the biochemical alterations we observed in the ECM fractions at the onset of apoptosis. Whether tTG, and tTG-induced ECM alteration is an inducer of cell death, or whether tTG is induced in response to the initiation of cell death to limit cell debris and

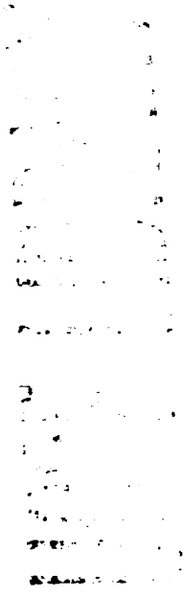

control the inflammatory response, is not yet clear. The stimulus for mammary involution clearly involves withdrawal of lactogenic hormones, and may include local stimuli such as milk edema (Lascelles and Lee, 1978; Tenniswood et al., 1992).

The histological data, together with the transcriptional activation of gene products typically associated with biosynthesis, describe an anabolic process that follows, and is closely coordinated with, the catabolic loss of epithelial cell function (see Fig. 7). Taking advantage of the ability to manipulate the absolute timing of epithelial involution by altering the number of pups suckled and the length of lactation, we observed that the biosynthetic phase begins when WAP expression is reduced to less than 10% of lactating levels and the number of live differentiated epithelial cells is reduced by 50%. During late pregnancy and immediately following parturition, the number of differentiated adipocytes in the fat pad (depending upon the mouse strain) is reduced to almost zero and the majority of the gland becomes epithelial (Elias et al., 1972). Differentiated adipocytes collapse, but persist as thin, elongated undifferentiated cells during lactation (Ailhaud et al., 1992; Neville et al., 1998), which resemble the mammary fibroblasts surrounding the ductal network in the resting gland (Cunha and Hom, 1996). During involution, adipocytes recolonize the inter-alveolar spaces, differentiate and accumulate lipid until a fat pad of approximately virgin size is reconstituted. Clearly adipocytes and epithelial cells interact to maintain a relative balance of these two cell types in the gland. Although several growth and transcription factors affect apoptosis or survival in mammary glands (Furth, 1999), the specific factors involved in local reciprocal control of adipocyte differentiation and epithelial involution are not yet understood.

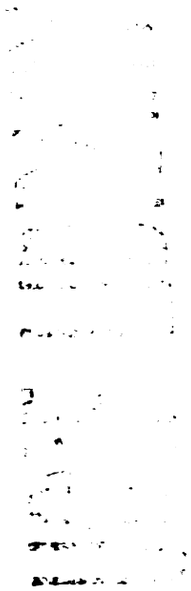

Stromelysin-1 Accelerates Adipocyte Differentiation Both in a Culture Model and *in vivo* During Fat Pad Expansion

Str1-/- and TO mice showed unusual patterns of adipocyte colonization in involuting glands. Although the activation of the biosynthetic phase is not changed in these mice, the differentiation and hypertrophy of adipocytes is enhanced by 50%. Since Str1 mRNA is highly induced during fat cell differentiation, and fat cell differentiation is accelerated in glands with a null mutation, we hypothesize that Str1 normally inhibits adipocyte lipogenesis.

In support of this notion, the addition of MMP inhibitors to a culture model of differentiating adipocytes (3T3-L1 cells) accelerated lipogenesis 7-fold. 3T3-L1 cells were originally isolated as a lipogenic substrain of 3T3 fibroblasts (Green and Meuth, 1974), and have been validated as a model of adipogenesis (Cornelius et al., 1994). Confluent precursor cells express markers specific to preadipocytes. After stimulation with inducers of cAMP accumulation, cells accumulate triglycerides, express many markers of terminal differentiation and resemble multilocular adipocytes. Our data analyzing expression of an array of MMPs and their inhibitors suggest that high expression of stromelysin-1, collagenase-3 (MMP-13) and MT-1 (MMP-14) and of the inhibitors TIMP-1, -2 and -3 parallel the commitment of undifferentiated 3T3-L1 fibroblast precursors to the adipocyte lineage. This co-induction of enzymes and inhibitors generates a low proteolytic index (proteinases / inhibitors), associated with the appearance of secreted latent gelatinase A (MMP-2). Other groups have shown that the amount of MMP-2 increases and TIMP-1 decreases during adipocyte differentiation (Brown et al., 1997; Johnson et al., 1994). An increase in the proteolytic index

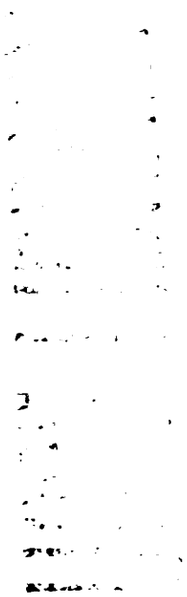

accompanies the transition from pre-adipocyte to terminally differentiated fat cells in culture. Specifically, the expression of mRNA for all 3 enzymes continues at high level, whereas that for TIMP-1 and –3 decreases. Concomitant with these changes, active MMP-2 appears in the medium. The expression of TIMP-2 mRNA is unaffected by differentiation. This inhibitor has a dual regulatory function for MMP-2, catalyzing the formation of a ternary activating complex for MT1 MMP at the cell surface, and inhibiting soluble enzyme activity (Gomez et al., 1997). TIMP-3 is an ECM-bound inhibitor that has a highly distinct inhibitor profile, inhibiting TACE and other membrane-bound disintegrin metalloproteinases (Amour et al., 1998). Interestingly, we found that TIMP-4, (Gomez et al., 1997) is induced in parallel with classic markers of terminal differentiation (Ailhaud et al., 1992), such as pPARγ. TIMP-4 may be the endogenous mediator that promotes terminal differentiation in adipocytes and may be a useful, novel adipocyte marker. By adding MMP inhibitors to maintain a low proteolytic index experimentally during the onset of differentiation in these cultures, lipogenesis is accelerated, mimicking the result observed *in vivo* in the transgenic mice.

There are several plausible mechanisms by which inhibition of MMPs could accelerate adipogenesis. The bioavailability of positive differentiation factors, such as IGF-1/IGF binding protein (Rajkumar et al., 1999) and negative differentiation factors, such as Wnts (Cunha and Hom, 1996; Ross et al., 2000) may be regulated by MMP action. Alternatively, MMPs may regulate the assembly of basement membrane *per se*. We favor the latter mechanism, because adipocyte differentiation is characterized by the dramatic upregulation of synthesis of basement membrane proteins (Aratani and Kitagawa, 1988). Accumulation of basement membrane distinguishes the preadipocyte

from its mesenchymal precursor, and may initiate terminal differentiation by stabilizing the adipocyte cell surface and generating specific intracellular signals. Assembly of ECM is likely to be rate limiting for the differentiation of these cells, therefore by co-expressing Str1 during differentiation, adipocytes may limit their own development. Indeed, Str1 cleaves entactin/nidogen-1 *in vivo* (Alexander et al. 1996), and entactin fragments inhibit the rate of basement membrane assembly (Pujuguet et al., 2000). Using primary rat adipocytes, Brown et al. (1997) found that the accumulation of ECM by differentiating clusters of cells was facilitated by the zinc chelator, 1,10-phenanthroline. In the present study we observed that, under conditions inhibiting MMP function, entactin fragmentation ceases and adipocyte differentiation increases.

If MMPs are important in adipogenesis then Str1-/- and TO mice could show increased adipogenesis in other tissues. MMPs may be rate limiting for differentiation only under situations where adipogenesis is very rapid as it is during mammary involution. Fat pads of Str1-/- mice on a 129 background were normal. However, the Str-/- mice backcrossed onto an FVB/N background become obese with increasing age, reaching weights of up to 60 g (unpublished observations). By feeding high fat diets to mice with decreased MMP levels, we may be able to observe an increased rate of fat acquisition. It may be relevant that humans with an allele that decreases *Str1* promoter function to 25-50% show accelerated progression of their atherosclerotic lesions (Ye et al., 1996).

In conclusion, we have revealed a novel physiological role for MMPs as negative regulators of adipocyte metabolism and differentiation. The mechanisms by which epithelial death and basement membrane remodeling are regulated still remain elusive.

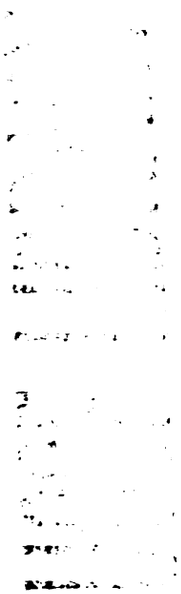

Acknowledgments

We are grateful to Dr. Rabih Talhouk for performing the Str1 Northern blot. We thank Dr. Lisa Coussens for bringing to our attention the obesity in FVB/N-Str1-/- mice. This work was supported by grants from the National Cancer Institute (CA 57621 and CA 72006 to ZW) and an Arthritis Foundation Investigator award (CMA).

References

Ailhaud, G., P. Grimaldi, and R. Negrel. 1992. Cellular and molecular aspects of adipose tissue development. *Ann. Rev. Nutr.* 12:207-233.

Alexander, C.M., E.W. Howard, M.J. Bissell, and Z. Werb. 1996. Rescue of mammary epithelial cell apoptosis and entactin degradation by a TIMP-1 transgene. J. Cell Biol. 135:1669-1677.

Amour, A., P.M. Slocombe, a. Webster, M. Butler, C.G. Knight, B.J. Smith, P.E. Stephens, C. Shelley, M. Hutton, V. Knauper, A.J. Docherty, and G. Murphy. 1998. TNF-a converting enzyme (TACE) is inhibited by TIMP-3. *FEBS Lett.* 435:39-44.

Aratani, Y., and Y. Kitagawa. 1988. Enhanced synthesis and secretion of type IV collagen and entactin during adipose conversion of 3T3-L1 cells and production of unorthodox laminin complex. *J. Biol. Chem.* 263:16163-16169.

Arner, E.C., M.A. Pratta, J.M. Trzaskos, C.P. Decicco, and M.D. Tortorella. 1999. Generation and characterization of aggrecanase. A soluble cartilage-derived aggrecan-degrading activity. *J. Biol. Chem.* 274:6594-6601.

Bernlohr, D.A., C.W. Angus, M.D. Lane, M.A. Bolanowski, and T.J. Kelly. 1984. Expression of specific mRNAs during adipocyte differentiation: Identification of an mRNA encoding a homologue of myelin P2 protein. *Proc.Natl.Acad.Sci.* 81:5468-5472.

Boudreau, N., C.J. Sympson, Z. Werb, and M.J. Bissell. 1995. Suppression of ICE and apoptosis in mammary epithelial cells by extracellular matrix. *Science*. 267:891-893.

Boudreau, N., Z. Werb, and M.J. Bissell. 1996. Suppression of apoptosis by basement membrane requires three-dimensional tissue organization and withdrawal from the cell cycle. *Proc. Natl. Acad. Sci.* 93:3509-3513.

Brown, L.M., H.L. Fox, S.A. Hazen, K.F. LaNoue, S.R. Rannels, and C.J. Lynch. 1997. Role of the matrixin MMP-2 in multicellular organization of adipocytes cultured in basement membrane components. *Am. J. Pathol.* 272:C937-C949.

Caterina, J.J., S. Yamada, N.C. Caterina, G. Longenecker, K. Holmback, J. Shi, A.E. Yermovsky, J.A. Engler and H. Birkedal-Hansen. 2000. Inactivating mutation of the mouse tissue inhibitor of metalloproteinases-2(Timp-2) gene alters ProMMP-2 activation. J. Biol. Chem. 275:26416-26422.

Cornelius, P., O.A. MacDougald, and M.D. Lane. 1994. Regulation of adipocyte development. *Ann. Rev. Nutr.* 14:99-129.

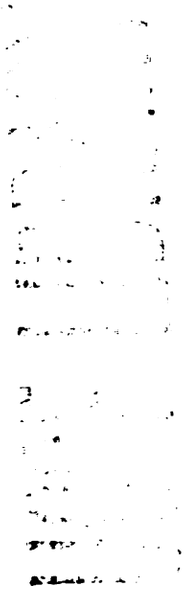

Crandall, D.L., G.J. Hausmann, and J.G. Kral. 1997. A review of the microcirculation of adipose tissue: anatomic, metabolic and angiogenic perspectives. *Microcirculation.* 4:211-232.

Cunha, G.R., and Hom, Y.K.1996. Role of mesenchymal-epithelial interactions in mammary gland development. *J. Mammary Gland Biol. Neoplasia.* 1:21-35.

Elias, J.J., D.R. Pitelka, and R.C. Armstrong. 1972. Changes in fat cell morphology during lactation in the mouse. *Anat. Rec.* 177:533-548.

Faraldo, M.M., M.-A. Deugnier, M. Lukashev, J.P. Thiery, and M.A. Glukhova. 1998. Perturbation of b1-integrin function alters the development of murine mammary gland. *EMBO J.* 17:2139-2147.

Fata, J.E., K.J. Leco, R.A. Moorehead, D.C. Martin and R. Khokha. 1999. Timp-1 is important for epithelial proliferation and branching morphogenesis during mouse mammary development. *Dev. Biol.* 211:238-254.

Ferguson, J.E., A.M. Schor, A. Howell, and M.W.J. Ferguson. 1992. Changes in the extracellular matrix of the normal human breast during the menstrual cycle. *Cell Tissue Res.* 268:167-177.

Finbloom D.S., E.F. Petricoin 3rd, R.H. Hackett, M. David, G. M. Feldman. K. Igarashi, E. Fibach, M.J. Weber, M.O. Thorner, C.M. Silva, et al. 1994 . Growth hormone and erythropoietin differentially activate DNA-binding proteins by tyrosine phosphorylation. Mol. Cell Biol. 14:2113-2118)

Furth, P.A. 1999. Mammary gland involution and apoptosis of mammary epithelial cells. *J. Mam. Gland Biol. Neo.* 4:123-127.

Gerber, H.-P., T.H. Vu, A.M. Ryan, J. Kowalski, Z. Werb, and N. Ferrara. 1999. VEGF couples hypertrophic cartilage remodeling, ossification and angiogenesis during endochondral bone formation. *Nature Med.* 5:623-628.

Gewert, D.R., B. Coulombe, M. Castelino, D. Skup, and B.R.G. Williams. 1987. Characterization and expression of a murine gene homologous to human EPA/TIMP: A virus-induced gene in the mouse. *EMBO J.* 6:651-657.

Gomez, D.E., D.F. Alonso, H. Yoshiji, and U.P. Thorgeirsson. 1997. TIMPs: structure, regulation and biological functions. *Eur. J. Cell Biol.* 74:111-122.

Green, H., and M. Meuth. 1974. An established pre-adipocyte cell line and its differentiation in culture. *Cell.* 3.

Gross, J. 1966. How tadpoles lose their tails. *J. Invest. Derm.* 47:274 - 277.

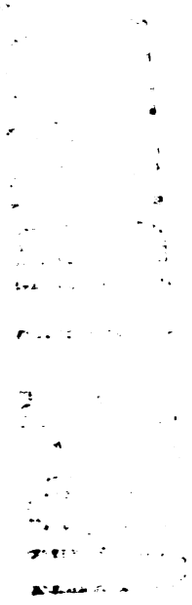

Guenette, R.S., H.B. Corbeil, J. Leger, K. Wong, V. Mezl, M. Mooibroek, and M. Tenniswood. 1994. Induction of gene expression during involution of the lactating mammary gland of the rat. *J. Mol. Endocrin.* 12:47-60.

Holmbeck, K., P. Bianco, J. Caterina, S. Yamada, M. Kromer, S.A. Kuznetsov, M. mankani, P.G. Robey, A.R. Poole, I. Pidoux, J.M. Ward, and H. Birkedal-Hansen. 1999. MT1-MMP-deficient mice develop dwarfism, osteopenia, arthritis, connective tissue disease due to inadequate collagen turnover. *Cell.* 99:81-92.

Jerry, D.J., C. Kuperwasser, S.R. Downing, J. Pinkus, C. He, E. Dickinson, S. Marconi, and S.P. Naber. 1998. Delayed involution of the mammary epithelium in BALB/c-p53 null mice. *Oncogene.* 17:2305-2312.

Johnson, M.D., H.R. Kim, L. Chesler, G. Tsao-Wu, N. Bouck, and P.J. Polverini. 1994. Inhibition of angiogenesis by tissue inhibitor of metalloproteinase. *J. Cell Physiol.* 160:194-202.

Klinowska, T.C., J.V. Soriano, G.M. Edwards, J.M. Oliver, A.J. Valentijn, R. Montesano, and C.H. Streuli. 1999. Laminin and b1 integrins are crucial for normal mammary gland development in the mouse. *Develop. Biol. (Orl).* 215:13-32.

Lascelles, A.K., and C.S. Lee. 1978. Involution of the mammary gland.

Leco, K.J., S.S. Apte, G.T. Taniguchi, S.P. Hawkes, R. Khokha, G.A. Schultz, and D.A. Edwards. 1997. Murine tissue inhibitor of metalloproteinase-4 (TIMP-4): cDNA isolation and expression in adult mouse tissues. *FEBS Lett.* 401:213-217.

Leco, K.J., R. Khokha, N. Pavloff, S.P. Hawkes, and D.R. Edwards. 1994. Tissue inhibitor of metalloproteinases-3 (TIMP-3) is an extracellular matrix-associated protein with a distinctive pattern of expression in mouse cells and tissues. *J. Biol. Chem.* 269:9352-9360.

Li, F., R. Strange, R.R. Friis, V. Djonov, H.-J. Altermatt, S. Saurer, H. Niemann, and A.-C. Andres. 1994. Expression of stromelysin-1 and TIMP-1 in the involuting mammary gland and in early invasive tumors of the mouse. *Int. J. Cancer.* 59:560-568.

Li, M., J. Hu, K. Heermeier, L. Hennighausen, and P.A. Furth. 1996. Apoptosis and remodeling of mammary gland tissue during involution proceeds through p53-independent pathways. *Cell Growth Diffn.* 7:13-20.

Lochter, A., S. Galosy, J. Muschler, N. Freedman, Z. Werb, and M.J. Bissell. 1997. Matrix metalloproteinase stromelysin-1 triggers a cascade of molecular alterations that leads to stable epithelial-to mesenchymal conversion and a premalignant phenotype in mammary epithelial cells. *J. Cell Biol.* 1139:1861-1872.

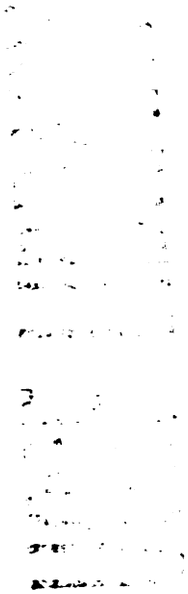

Lund, L.R., J. Romer, N. Thomasset, H. Solber, C. Pyke, M.J. Bissell, K. Dano, and Z. Werb. 1996. Two distinct phases of apoptosis in mammary gland involution: proteinase-independent and -dependent pathways. *Development.* 122:181-193.

Lund, L.R., S.F. Bjørn, M.D. Sternlicht, B.S. Nielsen, H. Solberg, P. Autzen, R. Østerby, I.J. Christensen, T.H. Bugge', R.W. Stephens, K. Dano and Z. Werb. 2000. Lactational development and involution of the mammary gland requires plasminogen. *Development.* In press.

Mayer, U., K. Mann, R. Timpl, and G. Murphy. 1993. Sites of nidogen cleavage by proteases involved in tissue homeostasis and remodelling. *Eur J Biochem.* 217:877-884.
Melino, G., and M. Piacentini. 1998. Tissue transglutaminase in cell death: a downstream or a multifunctional upstream effector? *FEBS Letts.* 430:59-63.

Mudgett, J.S., N.I. Hutchinson, N.A. Chartrain, A.J. Forsyth, J. McDonnell, I.I. Singer, E.K. Bayned, J. Flanagan, D. Kawka, C.F. Shen, K. Stevens, H. Chen, M. Trumbauer, and D.M. Visco. 1998. Susceptibility of stromelysin-1-deficient mice to collagen-induced arthritis and cartilage destruction. *Arthritis and Rheumatism.* 41:110-121.

Nagase, H. 1997. Activation of matrix metalloproteinases. *Biol. Chem.* 378:151-160.
Neville, M.C., D. Medina, J. Monks, and R.C. Hovey. 1998. The mammary fat pad. *J. Mamm.Gland Biol. Neo.* 3:109-115.

Ostrowski, L.E., J. Finch, P. Krieg, L. Matrisian, G. Patskan, J.F. O'Connell, J. Phillips, T.J. Slaga, R. Breathnach, and G.T. Bowden. 1988. Expression pattern of a gene for a secreted metalloproteinase during late stages of tumor progression. Mol. Carcin. 1:13-19.

Pujuguet, P., M. Simian,J. Liaw, R. Timpl, Z. Werb and M.J. Bissell. 2000. Nidogen-1 regulates laminin-1-dependent mammary-specific gene expression. *J. Cell Sci.* 113:849-858.

Rajkumar, K., T. Modric, and L.J. Murphy. 1999. Impaired adipogenesis in insulin-like growth factor binding protein-1 transgenic mice. *J. Endocrinol.* 162:457-465.
Ramirez-Zacarias, J.L., F. Castro-Munozledo, and W. Kuri-Harcuch. 1992. Quantitation of adipose conversion and triglycerides by staining intracytoplasmic lipids with Oil Red O. *Histochemistry.* 97:493-497.

Ross, S.E., N. Hemati, K.A. Longo, C.N. Bennett, P.C. Lucas, R.L. Erickson, and O.A. MacDougald . 2000. Inhibition of adipogenesis by Wnt signaling. *Science.* 289:950-953.

Rudolph-Owen, L.A., D.L. Hulboy, C.L. Wilson, J. Mudgett, and L.M. Matrisian. 1997. Coordinate expression of matrix metalloproteinase family members in the uterus of normal, matrilysin-deficient, and stromelysin-1-deficient mice. *Endocrinology.* 138:4902-4911.

Sato, H., T. Takino, Y. Okada, J. Cao, A. Shinagawa, E. Yamamoto, and M. Seiki. 1994. A matrix metalloproteinase expressed on the surface of invasive tumour cells. *Nature*. 370:61-65.

Smas, C.M., and H.S. Sul. 1995. Control of adipocyte differentiation. *Biochem. J.* 309:697-710.

Sternlicht, M.D., A. Lochter, C.J. Sympson, B. Huey, J.-P. Rougier, J.W. Gray, D. Pinkel, M.J. Bissell, and Z. Werb. 1999. The stromal proteinase MMP3/Stromelysin-1 promotes mammary carcinogenesis. *Cell*. 98:137-146.

Strange, R., F. Li, S. Saurer, A. Burkhardt, and R.R. Friis. 1992. Apoptotic cell death and tissue remodelling during mouse mammary gland involution. *Development*. 115:49-58.

Sympson, C.J., R.S. Talhouk, C.M. Alexander, J.R. Chin, S.M. Clift, M.J. Bissell, and Z. Werb. 1994. Targeted expression of stromelysin-1 in mammary gland provides evidence for a role of proteinases in branching morphogenesis and the requirement for an intact basement membrane for tissue-specific gene expression. *J. Cell Biol.* 125:681-693.

Talhouk, R.S., M.J. Bissell, and Z. Werb. 1992. Coordinated expression of extracellular matrix-degrading proteinases and their inhibitors regulates mammary epithelial function during involution. *J. Cell Biol.* 118:1271-1282.

Tenniswood, M.P., R.S. Guenette, J. Lakins, M. Mooibroek, P. Wong, and J.-E. Welsh. 1992. Active cell death in hormone-dependent tissues. *Canc. Metast. Rev.* 11:197-220.

Thomasset, N., A. Lochter, C.J. Sympson, L.R. Lund, D.R. Williams, O. Behrendtsen, Z. Werb, and M.J. Bissell. 1998. Expression of autoactivated stromelysin-1 in mammary glands of transgenic mice leads to a reactive stroma during early development. *Am. J. Path.* 153:457-467.

Tontonoz, P., E. Hu, and B.M. Spiegelman. 1995. Regulation of adipocyte gene expression and differentiation by peroxisome proliferator activated receptor gamma. *Curr. Opin. Gen. Dev.* 5:571-576.

Vu, T.H. and Z. Werb. 2000. Matrix metalloproteinases: effectors of development and normal physiology. *Genes Dev.* 14: 2123-2133.

Vu, T.H., J.M. Shipley, G. Bergers, J.E. Berger, J.A. Helms, D. Hanahan, S.D. Shapiro, R.M. Senior, and Z. Werb. 1998. MMP-9 / Gelatinase B is a key regulator of growth plate angiogenesis and apoptosis of hyperptrophic chondrocytes. *Cell*. 93:411-422.

Wang, T.C., R.D. Cardiff, L. Zukerberg, E. Lees, A. Arnold, and E.V. Schmidt. 1994. Mammary hyperplasia and carcinoma in MMTV-cyclin D1 transgenic mice. *Nature*. 369:669-671.

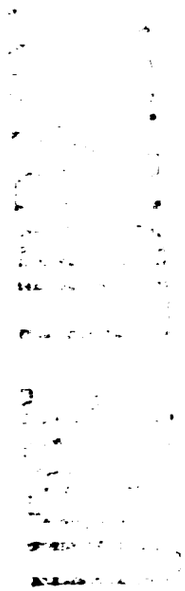

Wang, Z., R. Juttermann and P.D. Soloway. 2000. TIMP-2 is required for efficient activation of proMMP-2 in vivo. *J. Biol. Chem.* 275:26411-26415.

Warburton, M.J., D. Mitchell, E.J. Ormerod, and P. Rudland. 1982. Distribution of myoepithelial cells and basement membrane proteins in the resting, pregnant, lactating and involuting rat mammary gland. *J. Histochem. Cytochem.* 30:667-676.

Weaver, V.M., and Bissell, M.J. 1999. Functional culture models to study mechanisms governing apoptosis innormal and malignant mammary epithelial cells. *J Mammary Gland Biol Neoplasia* 4:193- 201

Werb, Z. 1997. ECM and cell surface proteolysis: regulating cellular ecology. *Cell.* 91:439-442. Wiesen, J.F., and Z. Werb. 2000. Proteinases, cell cycle regulation and apoptosis during development and involution of the mammary gland. *Mol. Reprod. Dev.* 56:534-540.

Will, H., S.J. Atkinson, G.S. Butler, B. Smith, and G. Murphy. 1996. The soluble catalytic domain of membrane type 1 matrix metalloproteinase cleaves the propeptide of progelatinase A and initiates autoproteolytic activation. Regulation by TIMP-2 and TIMP-3. *J. Biol. Chem.* 271:17119-17123.

Witty, J.P., J.H. Wright, and L.M. Matrisian. 1995. Matrix metalloproteinases are expressed during ductal and alveolar mammary morphogenesis, and misregulation of stromelysin-1 in transgenic mice induces unscheduled alveolar development. *Mol. Biol. Cell.* 6:1287-1303.

Ye, S., P. Eriksson, A. Hamsten, M. Kurkinen, S.E. Humphries, and A.M. Henney. 1996. Progression of coronary artherosclerosis is associated with a common genetic variant of the human stromelysin-1 promoter which results in reduced gene expression. *J. Biol. Chem.* 271:13055-13060.

Zhou, Z., S.S. Apte, R. Soininen, R. Cao, G.Y. Baaklini, R.W. Rauser, J. Wang, Y. Cao and K. Tryggvason. 2000. Impaired endochondral ossification and angiogenesis in mice deficient in membrane-type matrix metalloproteinase I. 2000. *Proc. Natl. Acad. Sci. USA.* 97:4052-4057.

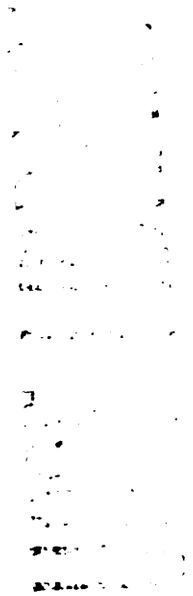

Figure 6-1.

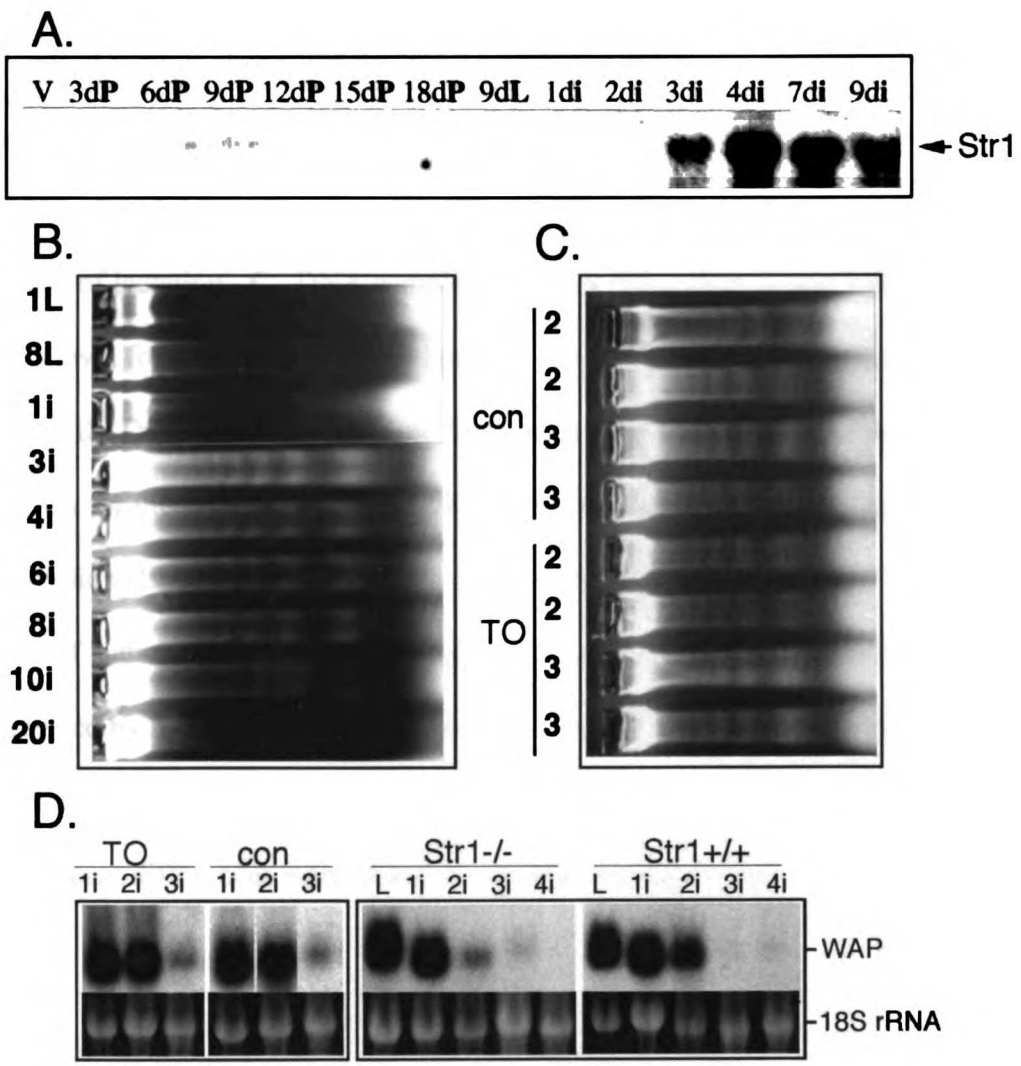
A.
V 3dP 6dP 9dP 12dP 15dP 18dP 9dL 1di 2di 3di 4di 7di 9di
Str1
B.
1L
8L
1i
3i
4i
6i
8i
10i
20i
C.
con
2
2
3
3
TO
2
2
3
3
D.
TO
1i 2i 3i
con
1i 2i 3i
Str1-/-
L 1i 2i 3i 4i
Str1+/+
L 1i 2i 3i 4i
WAP
18S rRNA

Figure 6-1. Apoptosis and epithelial function during gland involution in transgenic mice. **A.** Total RNA was extracted from mammary glands at various timepoints, separated by agarose gel electrophoresis (10 μg / track), transferred to membranes and probed with a Str1 cDNA. V, virgin; dP, days pregnant; dL, days lactating; di, days after weaning of pups. **B.** To measure the onset of programmed cell death, DNA was extracted from glands at various stages and analyzed by agarose gel electrophoresis for evidence of laddering. Epithelial cells began to die between 1 and 3 days after weaning of pups. 1L and 8L, 1 and 8 days lactation; 1i – 20i: 1 – 20 days involution after removal of pups after 8 days of lactation. **C.** DNA samples from key timepoints, 2 and 3 days after weaning, are shown for 2 of each of TO and control mice. The onset of apoptosis is normal in TO mice. **D.** Differentiated epithelial function was assayed by measuring the expression of mRNA for the milk protein WAP. RNA was extracted from glands at various stages of involution (L, lactating; 1i – 4i, 1 – 4 days of involution after removal of pups after 8 days of lactation) from TO and control mice, and from Str1-/- and Str1+/+ mice, and was analyzed by hybridizing Northern blots with a WAP cDNA probe. Ethidium bromide-stained gel tracks prior to membrane transfer are shown for comparison (18S rRNA). No significant differences were observed in either transgenic line.

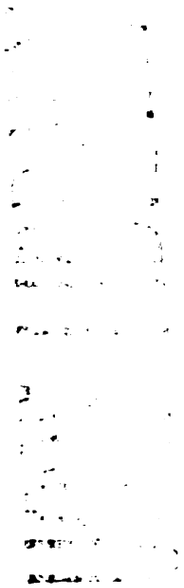

Figure 6-2.

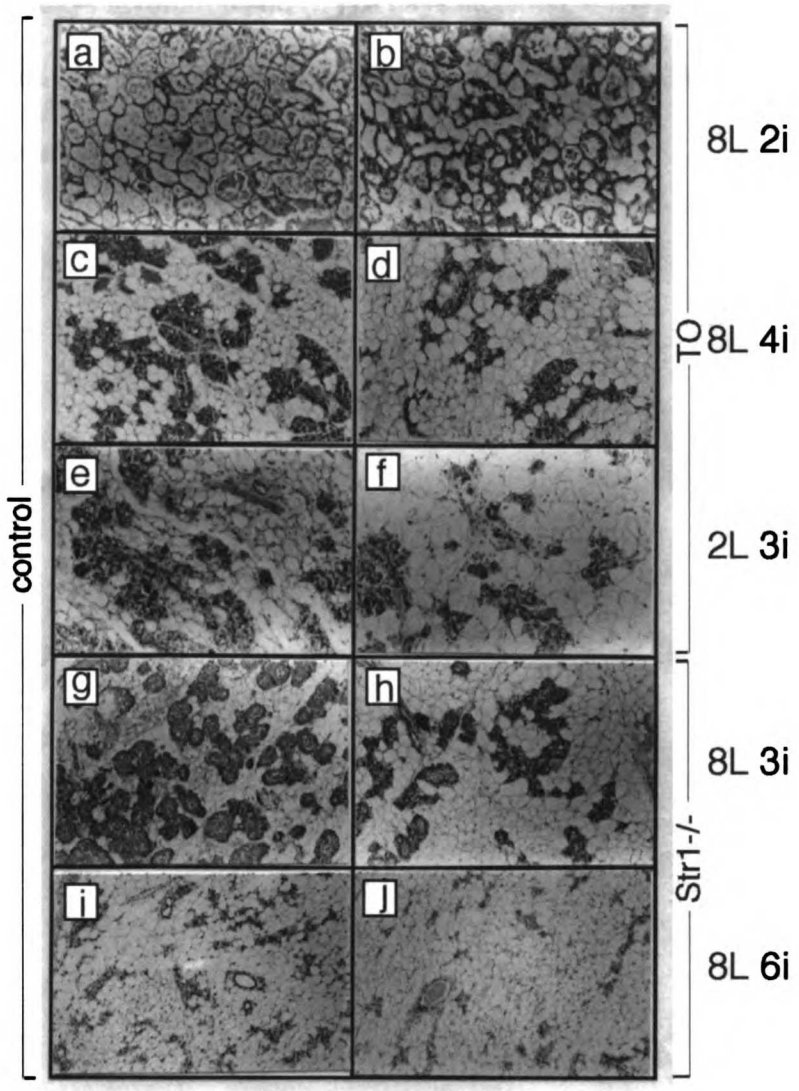

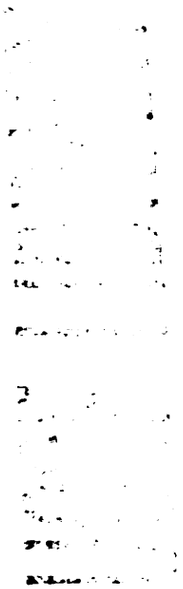

Figure 6-2. Inhibition of MMP activity affects the dynamics of the remodeling involuting mammary gland. H&E stained sections of wildtype (**a, c, e**), TO (**b, d, f**), Str+/+ (**g, i**) and Str1-/- (**h, j**) mammary glands at (**a, b**) 8 days lactation, 2 days involution; (**c, d**) 8 days lactation, 4 days involution; (**e, f**) 2 days lactation, 3 days involution; (**g, h**) 8 days lactation, 3 days involution and (**i, j**) 8 days lactation, 6 days involution. Glands deficient in MMP activity show increased numbers of hypertrophic adipocytes during mammary gland involution.

Figure 6-3.

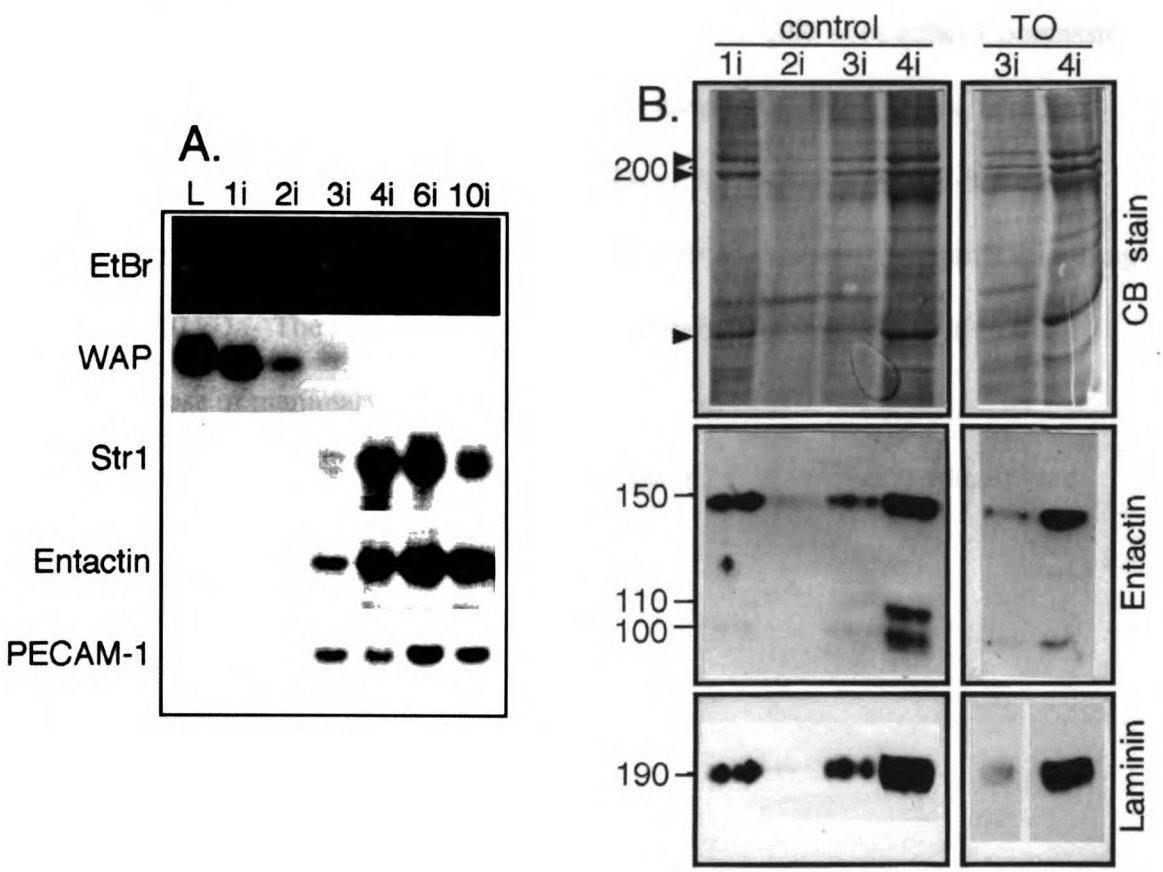
A.
L 1i 2i 3i 4i 6i 10i
EtBr
WAP
Str1
Entactin
PECAM-1
B.
control
TO
1i 2i 3i 4i
3i 4i
200
150
110
100
190
CB stain
Entactin
Laminin

Figure 6-3. Upregulation of Str1 mRNA expression during stromal remodeling of involuting mammary gland. **A.** mRNA was extracted from mammary glands at various timepoints (L, lactating, 1i – 10i, 1 – 10 days of involution after weaning pups), Northern blots were prepared and probed with cDNAs encoding the milk protein WAP (WAP), Str1, the basement membrane protein entactin and the endothelial cell surface adhesion molecule PECAM-1. **B.** ECM-enriched extracts of glands from control and TO mice 1-4 days after weaning (1i – 4i) were analyzed by SDS-PAGE; gels were either Coomassie Blue-stained (CB) or transferred to membranes for incubation with antisera to either entactin or laminin. Molecular weights of proteins are indicated at the left-hand side. Entactin migrates at 150 kDa, with specific MMP-derived cleavage fragments migrating at 100 and 110 kDa. The ECM-enriched fraction changes dramatically during the involutive phase of mammary gland remodeling (2 - 4 days after weaning). The collagens (arrowheads) and basement membrane proteins (entactin and laminin) are substantially reduced.

Figure 6-4.

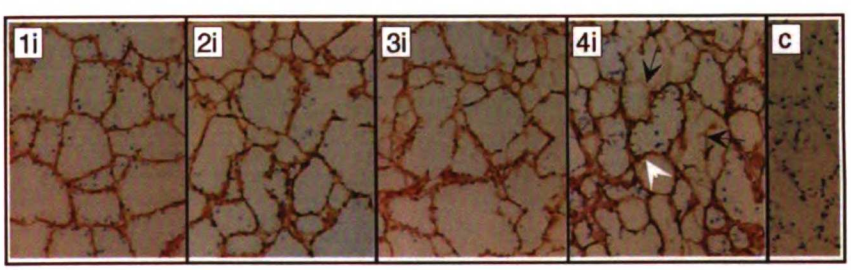

Figure 6-4. Immunostaining of entactin shows that epithelial basement membranes are retained during involution. Fixed cryosections from normal glands 1 – 4 days after weaning were stained for entactin. During gland involution (1i – 4i), basement membranes around epithelial alveoli stained positively for entactin (brown HRP-linked product; arrowheads). 4 days after weaning (4di) entactin also appears around hypertrophying adipocytes (arrows). Immunostaining experiments using a sub-saturating, diluted primary antibody (1:2000), aimed at ensuring that this assay was quantitative for glands 2 – 3 days after weaning, did not show the dramatic loss of entactin observed biochemically (Figure 6-3). Control sections (incubated with rat antiserum in place of primary antibody) are blank except for methylene blue-stained nuclei (c).

Figure 6-5.

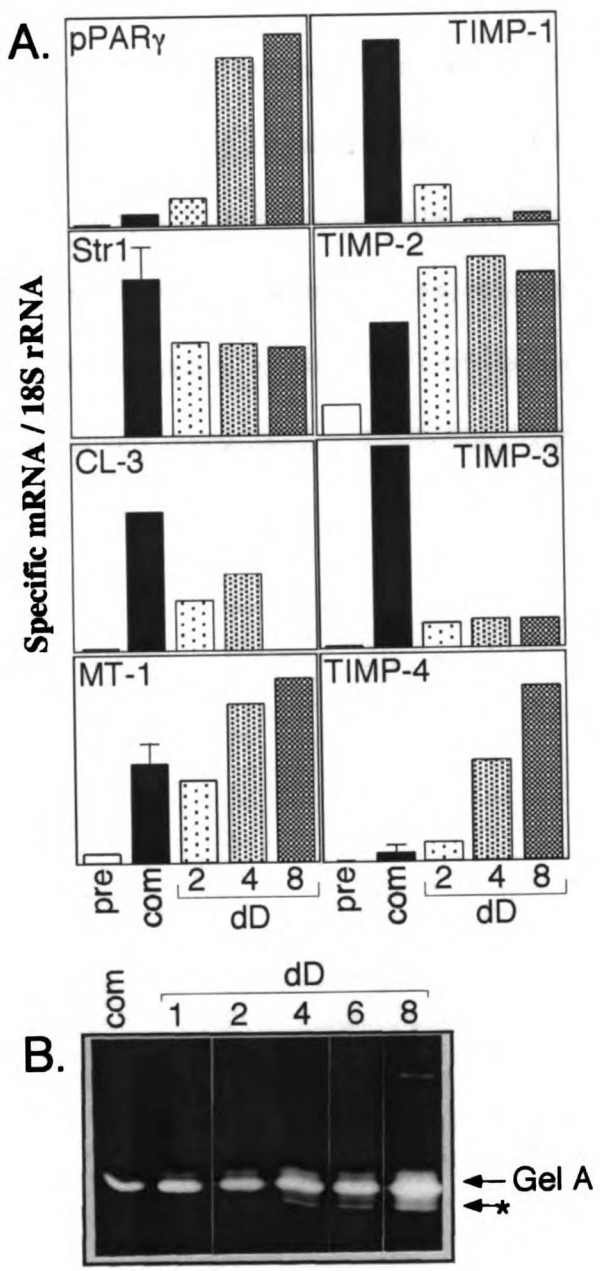
A.
pPARγ
TIMP-1
Str1
TIMP-2
CL-3
TIMP-3
MT-1
TIMP-4
Specific mRNA / 18S rRNA
pre
com
2
4
8
dD
B.
com
dD
1
2
4
6
8
Gel A
*

Figure 6-5. Expression of MMPs and TIMPs during adipocyte differentiation. **A.** RNA was extracted from cultures of 3T3-L1 cells at various stages of differentiation. pre, subconfluent fibroblastic precursor; com, confluent, committed stage at day 0 of differentiation; 2 - 8 dD, 2 – 8 days differentiation after administration of DM. RNA was separated by agarose gel electrophoresis and transferred to membranes for analysis of expression of specific MMP and inhibitor mRNAs. Autoradiograms were scanned and the relative expression of specific mRNAs as a ratio of EtBr-stained 18S rRNA was quantified. **B.** Enzymes secreted by adipocytes into supernatant media were analyzed by gelatin zymography. Gelatinase A, identified by comparison with mouse enzyme standards, was progressively upregulated and activated (*) as 3T3-L1 cells differentiated.

Figure 6-6.

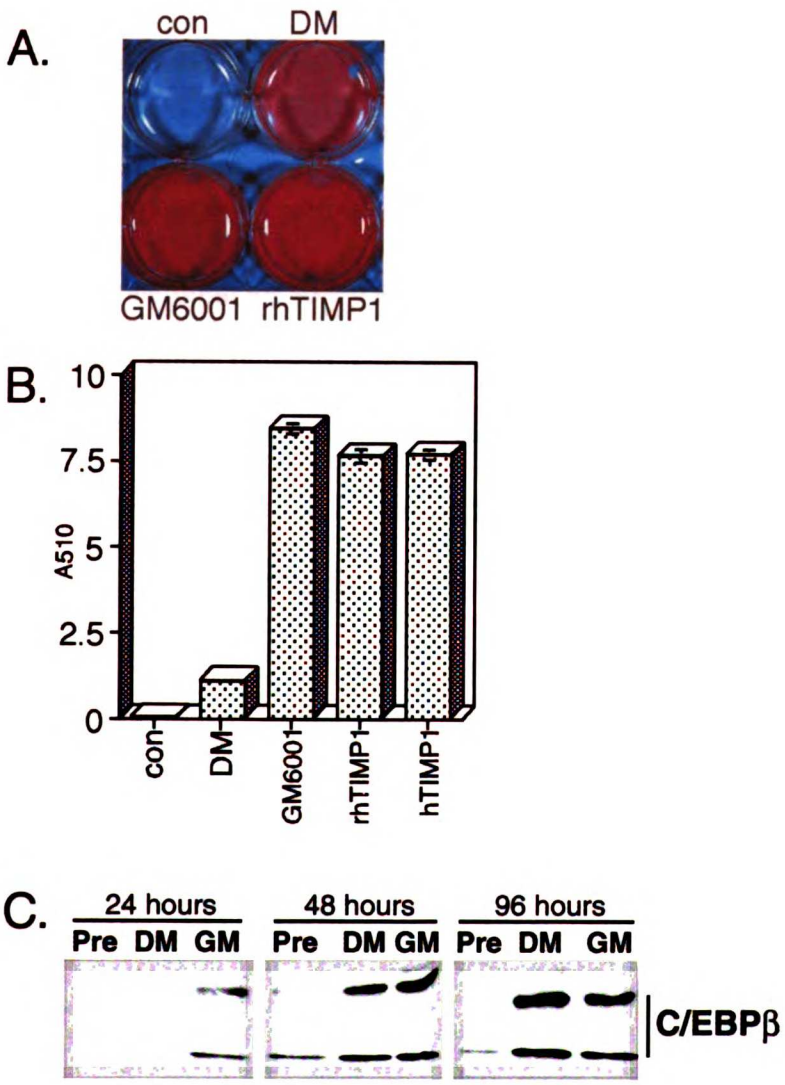
A.
con
DM
GM6001
rhTIMP1
B.
10
7.5
5
2.5
0
A510
con
DM
GM6001
rhTIMP1
hTIMP1
C.
24 hours
48 hours
96 hours
Pre DM GM
Pre DM GM
Pre DM GM
C/EBPβ

Figure 6-6. Inhibition of MMP activity accelerates lipogenesis in 3T3-L1 cultures. Confluent cultures of 3T3-L1 cells were induced to differentiate by adding DM, either in the presence or absence of the hydroxamate inhibitor GM6001, recombinant human TIMP-1 (rhTIMP1) or purified human TIMP-1 (hTIMP1). **A.** Western blot of 3T3-L1 nuclear lysates to detect C/EPBβ at 24 hours, 48 hours and 96 hours after the induction of differentiation. Preadipocytes (Pre), cells induced to differentiate in DM alone (DM) or in the presence of GM6001 (GM). **B.** After 4 days the accumulation of lipid was assessed by Oil Red O staining of tissue culture dishes containing 3T3-L1 cells. **C.** To quantify Oil Red O staining, the dye was extracted in propanol and the absorbance at 510 nm was measured. Control cultures (con) were not treated with DM. Results shown are the average of six determinations and the bars indicate standard deviations. Cells treated with DM alone were normalized to 1 to reveal the fold-induction of lipogenesis in the presence of MMP inhibitors. p values were determined using the student t-test.

Figure 6-7.

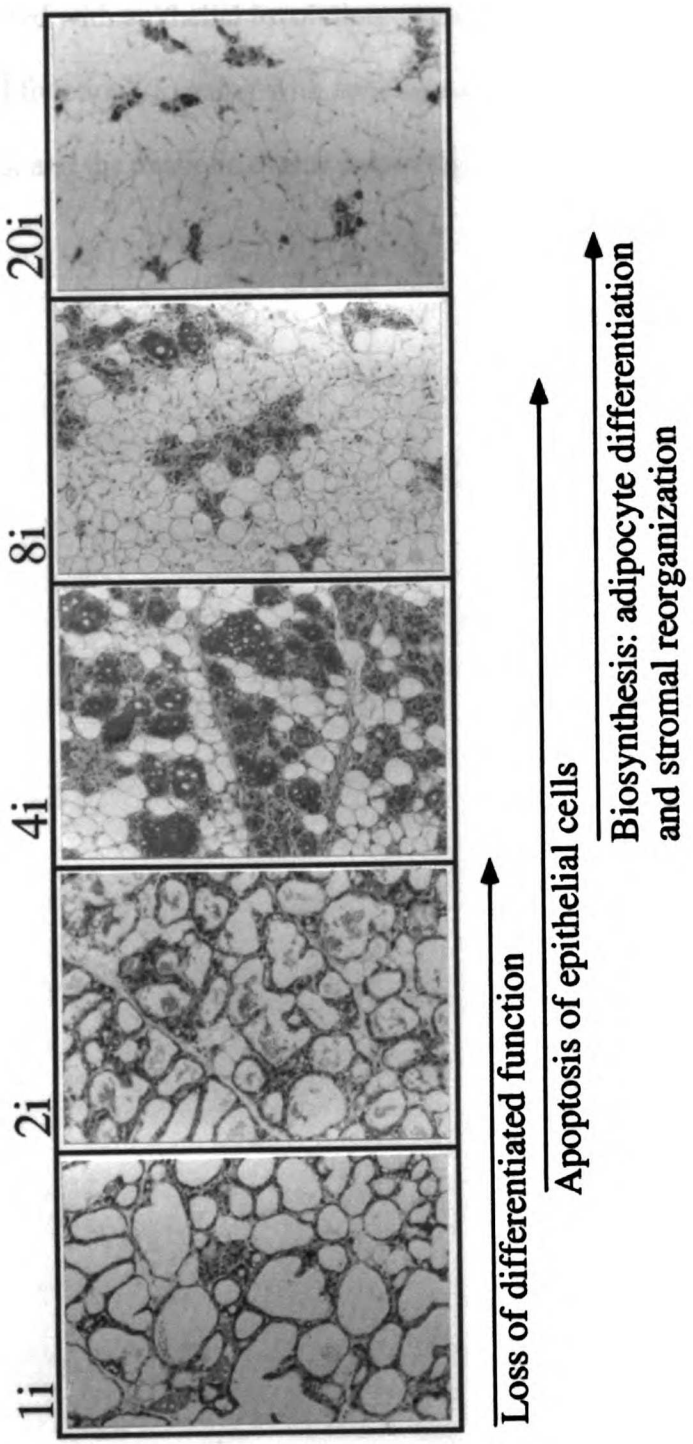
1i
2i
4i
8i
20i
Loss of differentiated function
Apoptosis of epithelial cells
Biosynthesis: adipocyte differentiation
and stromal reorganization

Figure 6-7. Mammary involution is divided into two interactive phases for epithelial and stromal remodeling. This scheme summarizes the relative timecourse of the catabolic events associated with epithelial involution, namely the loss of milk protein synthesis (differentiated function), together with apoptosis and regression of the majority of the epithelial cells, and the anabolic events responsible for re-expanding the fat pad.

Table 6. Altered Adipogenesis and PECAM Expression in Involuting Mammary Glands of Str1-/- and TO Mice.

Mouse Strain	Alveolor Density (pixels)	Nomalized PECAM-1 mRNA Altered mRNA	Adipocytes Number/ Field	Adipocytes Area/Field (x100)
Str+/+	9890±604	0.65±0.06	650±39	72
Str-/-	6824±550	0.95±0.04	842±55	91
Ratio Str-/- / Str+/+ (x100)	69±8	150±4	129±7	126±2.2
Control (normal TIMP)	15980±785	n.d.	310±21	56±4
TO	10120±802	n.d.	420±29	79±7
Ratio TO/Control (x100)	63±8	n.d.	145±7	141±8

Addendum

Methods

Str-1 mice. Adult male FVB/N Str-1+/+ (n=2) and Str-1-/- (n=3) mice were weighed. Their epididymal fat pads were collected, weighed and photographed, and the average weight per group was calculated.

Gelatin zymography. CM was collected from 3T3-L1 preadipocytes and adipocytes (8 days after the induction of differentiation) grown under serum-free conditions for 24 hours. Cell lysates were prepared by scraping cells into RIPA buffer (50 mM Tris-Cl, pH 8.0, 150 mM NaCl, 1% NP40, 0.5% DOC, 0.1%SDS). The samples were loaded into non-reducing SDS-PAGE gels containing 5 mg/ml gelatin. Active human gelatinase A and B (Calbiochem) were used as controls. The gels were incubated overnight at 37^{O}C in substrate buffer (50 mM Tris-Cl, pH 8.0, 5 mM $CaCl_2$, 0.02% NaN_3).

Results

Str-1-deficient mice are heavier and have larger fat pads. The total body weight of Str-1+/+ and Str-1-/- mice (on the FVB/N background) was compared and Str-1-deficient mice were found to be significantly heavier than their wild-type counterparts (Figure 6-8). In addition, the epididymal fat pads of Str-1-/- mice were larger and weighed more than those from Str-1+/+ mice (Figure 6-9A and B). These data provide further support for the hypothesis that Str-1 regulates adipogenesis.

Gelatinase A and B are regulated during 3T3-L1 differentiation. To determine whether MMPs other than Str-1 play a role in adipocyte differentiation, the conditioned medium (CM) and cell lysates of 3T3-L1 preadipocytes and adipocytes were analyzed for expression of gelatinases. 3T3-L1 preadipocytes expressed both gelatinase A (MMP-2) and gelatinase B (MMP-9). Both the pro- and active forms of gelatinase A were detected in the CM of preadipocytes and adipocytes (Figure 6-10), and the active form was detected in cell lysates as well. The expression of both these MMPs is significantly downregulated in adipocytes, and gelatinase B was not detected in CM from adipocytes. These observations indicate that the expression of gelatinase A and B is regulated during adipogenesis. Further studies are necessary to determine whether these proteases play a role in adipocyte differentiation.

Discussion

The Plg cascade of serine proteases (Chapter Five) is pro-adipogenic; inhibition of serine proteases decreases adipogenesis both *in vitro* and *in vivo*. Plg-deficient mice show decreased adipogenesis in the mammary gland. However, MMPs appear to exert an anti-adipogenic effect. Inhibition of MMPs leads to accelerated adipogenesis in culture, and Str-1 deficient and TIMP overexpressor mice show greater proportion of adipose tissue in the mammary gland. How is the function of these two classes of proteases, which exert opposing influences during adipocyte differentiation, regulated *in vivo*? It would be of great interest to understand if there is any cross-talk between MMPs and the Plg cascade, and what the critical substrates are for each protease during adipogenesis.

Figure 6-8.

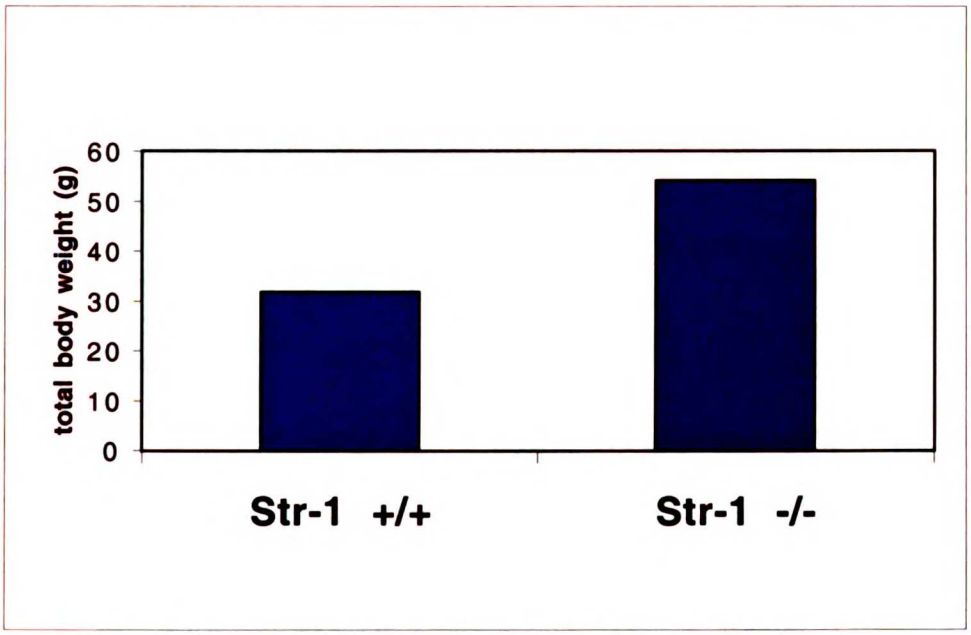

Figure 6-9.

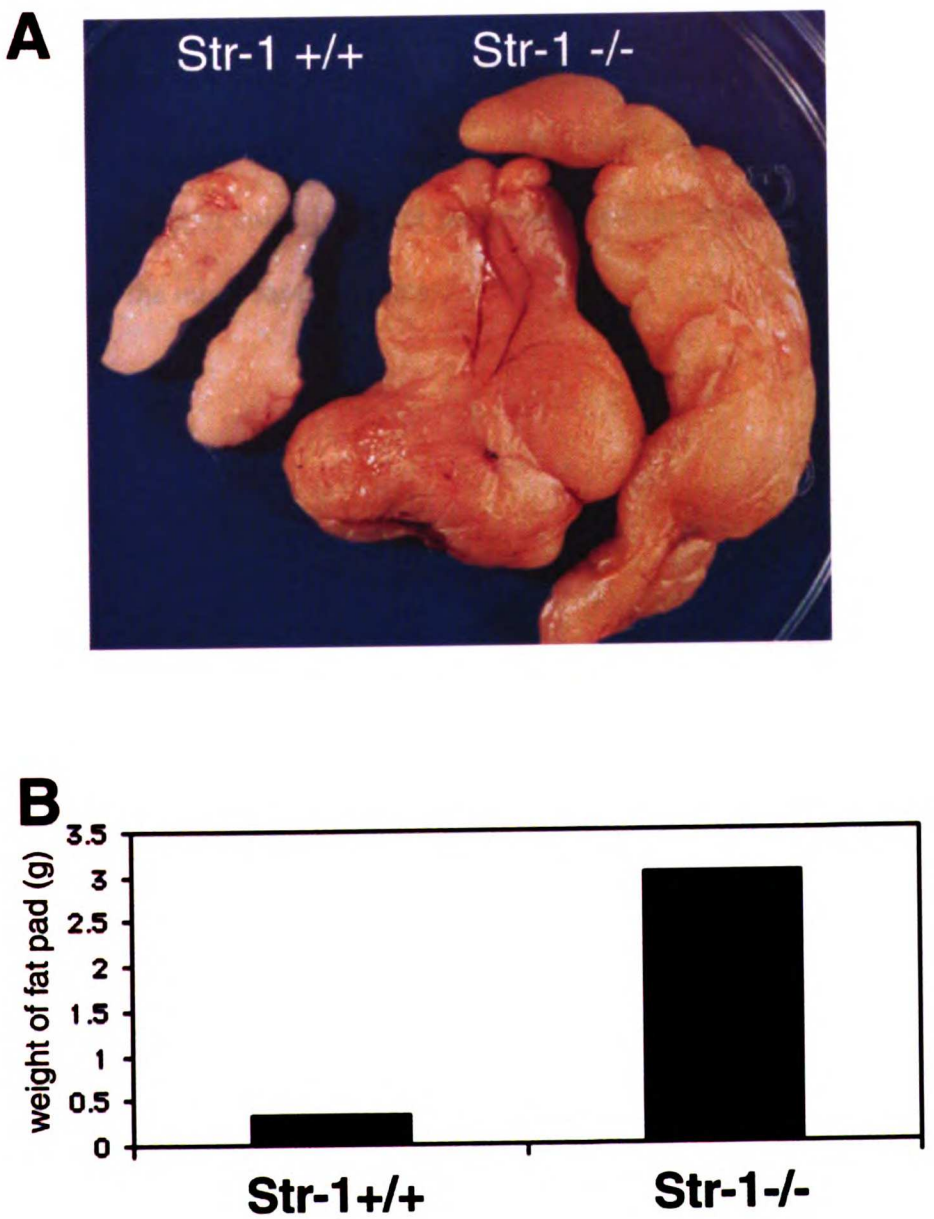

Figure 6-8. Str-1-deficient mice are significantly heavier than their wild-type counterparts. Total body weight of Str-1+/+ and Str-1-/- mice. Data are represented as the mean for each group.

Figure 6-9. Epididymal fat pads from Str-1-deficient mice are larger and weigh more than fat pads from wild-type controls. **A,** Epididymal fat pads from Str-1+/+ and Str-1-/- mice. **B,** Weight of epididymal fat pads from Str-1+/+ and Str-1-/- mice. Data are represented as the mean for each group.

Figure 6-10.

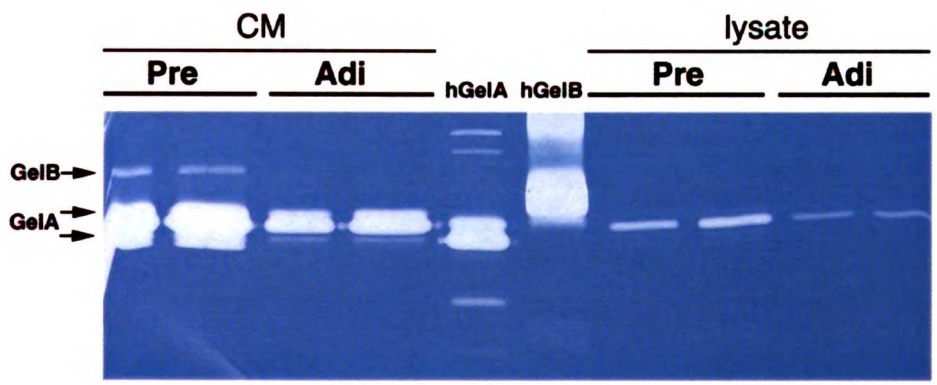

Figure 6-10. Gelatinase expression is regulated during 3T3-L1 differentiation. Gelatin zymogram. Gelatinase A (GelA) and gelatinase B (GelB) detected in the conditioned medium (CM) and cell lysates (lysate) of 3T3-L1 preadipocytes (Pre) and adipocytes (Adi). Human enzymes were used as controls (h).

Chapter Seven

Conclusions and Future Directions

Summary of major findings

Focalized proteolysis of the extracellular matrix (ECM) is an important regulator of various physiological and pathological processes. Involution of the mouse mammary gland is a model system to study the role of proteolytic enzymes, including the plasminogen system, in ECM remodeling. The plasminogen (Plg) system, which consists of urokinase (uPA), tissue-type Plg activator (tPA) and plasmin(ogen), was found to play an important role in the epithelial remodeling, lymph node regression and adipogenesis that occur during involution.

Inhibition of target proteases is an effective approach to study the function of serine proteases both *in vivo* and *in vitro*. Ecotin is a bidentate inhibitor of serine proteases that have a chymotrypsin fold, and can be altered by site-directed mutagenesis to increase its affinity and specificity. Ecotin was used to isolate uPA and plasma kallikrein (PKal) from whole tissue lysates derived from involuting mouse mammary glands. It was found that haptoglobin, which contains a chain that is a serine protease homologue without catalytic activity, also bound to ecotin. Binding to haptoglobin did not prevent proteolytic inhibition of uPA.

The variant ecotin Met84Arg/Met85Arg (ecotin RR), which is a potent inhibitor of uPA, delayed epithelial remodeling during involution. The Plg system was required for the degradation of extracellular matrix (ECM) molecules including entactin and laminin and regulated the activation of gelatinases A and B, and the bioavailability of transforming growth factor-β.

uPA and tPA expression was detected in the mammary lymph node during involution, and treatment of involuting mice with ecotin resulted in enlarged lymph

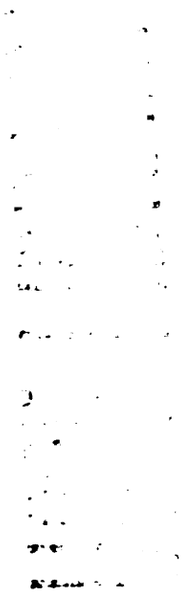

nodes, increased numbers of lymphocytes, and changes in the lymphocyte subpopulations present in the mammary lymph node. Although mammary epithelial lymphocytes are thought to derive from the gut (GALT), mammary lymph node lymphocytes were found to be distinct from GALT lymphocytes. The lymphocyte subpopulations in the mammary lymph node varied depending on the functional state of the mammary gland.

Plasma kallikrein (PKal) was found to mediate a plasminogen (Plg) cascade that is required for adipocyte differentiation both in culture and during involution of the mammary gland. Ecotin inhibited cell shape change, adipocyte-specific gene expression, and lipid accumulation during adipogenesis in culture. Deficiency of Plg, but not uPA and tPA, suppressed adipogenesis during 3T3-L1 differentiation and mammary gland involution. PKal, which is inhibited by ecotin, was required for adipose conversion, and for Plg activation and 3T3-L1 differentiation under serum-free conditions. Human plasma deficient in PKal did not support 3T3-L1 differentiation. The PKal-mediated Plg cascade appeared to foster adipogenesis by degradation of the fibronectin-rich stromal matrix of preadipocytes.

The matrix metalloprotease (MMP), MMP-3/stromelysin-1 (Str1), is highly expressed during mammary gland involution. Tissue inhibitor of metalloproteases-1 (TIMP-1) overexpressor mice (TO), and mice carrying a targeted mutation in *Str1 (Str1-/-)* showed accelerated differentiation and hypertrophy of adipocytes. The addition of MMP inhibitors (GM 6001 and TIMP-1) dramatically accelerated the accumulation of lipid during differentiation in culture.

Future directions

This research demonstrates a role for the Plg system in epithelial and stromal remodeling during involution of the mammary gland. It shows for the first time that Plg and PKal mediate adipocyte differentiation *in vivo* and in culture, and that the Plg system is required for lymph node regression during involution. These findings open up several new areas of research.

The macromolecular inhibitor ecotin is a novel tool that can be modified for use in various applications to probe the function of chymotrypsin-fold serine proteases. The finding that ecotin binds to haptoglobin suggests the intriguing possibility that haptoglobin may serve as a carrier for ecotin *in vivo*. Ecotin has a long half-life *in vivo* (about 12 hours), and it would interesting to compare the relative affinity of ecotin for haptoglobin and target proteases to test this hypothesis.

The results obtained with ecotin RR suggest that uPA plays an important role in epithelial remodeling during involution, and that uPA-mediated Plg activation is required for gelatinase B activation *in vivo*. Mice deficient in the gene for uPA (uPA-/-) have been generated, and it would be of interest to analyze their phenotype during involution, and to determine the levels of active gelatinase B in these mice. The relationship between the Plg system and TGF-β function needs to be studied further to determine whether the Plg cascade directly cleaves TGF-β or modulates the function of TGF-binding proteins.

The finding that inhibition of the Plg system affects the lymphocyte population in the mammary lymph node leads to several questions. Does the Plg system merely serve to remodel the lymph node during involution and thereby promote lymphocyte egress?

Or is it the case that serine proteases are actively involved in the migration of lymphocytes to and from the mammary lymph node, and perhaps the mammary gland itself? The Plg system may modulate lymphocyte adhesion and migration by cleavage of adhesion ligands or receptors. While uPA, tPA and PKal are clearly present in the mammary lymph node, it needs to be determined whether these proteases (and/or their receptors or inhibitors) are expressed by lymphocytes.

Further studies are also necessary to determine the role of the mammary lymph node lymphocytes. The hypothesis that lymphocytes migrate between the GALT and mammary lymph node during lactation and involution needs to be studied. The mechanisms underlying this migration are not known, and it would be of interest to determine if serine proteases play a general role in lymphocyte adhesion and migration in the immune system.

This research provides compelling evidence for a role for a PKal-mediated Plg cascade in adipogenesis. Figure 7, a modified version of Figure 1-1, shows that feedback loops exist for the activation of Factor XII and uPA (urokinase), and that PKal can directly activate both uPA and Plg. However, our data indicate that uPA (and tPA) is not required for Plg activation during adipogenesis. PKal may be an important Plg activator in fibrin-independent systems such as adipogenesis, and its role needs to further investigated. Furthermore, active uPA was detected in Plg-/- mice, suggesting that plasmin is not the major physiological activator of uPA, and that PKal may serve as a uPA activator *in vivo*. The mechanisms by which Plg and PKal are regulated during adipogenesis also need to be further investigated. Active PKal is detected in the environment of both preadipocytes and adipocytes. Does the activation of PKal require

Factor XII and/or HMW kininogen? Since the activation of PKal and Plg do not appear to be regulated, is the activation of an upstream protease such as Factor XII regulated? Do PKal and Factor XII activate each other in a reciprocal fashion? Does the regulation of any of the proteases in this cascade involve endogenous inhibitors or cell surface receptors?

Congenital prekallikrein deficiency (Fletcher trait) in humans has not been described as resulting in any clinical symptoms other than a delayed partial thromboplastin time detected in laboratory clotting tests. However, this condition is relatively rare, and shows variable penetrance. No data is available with regard to weight gain or adipogenesis in individuals with this trait. In light of the findings described in this research, it would be of interest to generate mice deficient in the gene for PKal to elucidate the role of this protease in adipogenesis and Plg activation.

The Plg cascade is required for adipogenesis both *in vivo* and *in vitro*. How does extracellular proteolysis of the preadipocyte microenvironment facilitate adipogenesis? One possibility suggested by this research is that the Plg cascade fosters adipocyte differentiation by degradation of the fibronectin-rich preadipocyte stromal matrix. Other possibilities include the regulation of differentiation-promoting cytokines such as insulin-like growth factor-1, or modulation of intracellular signaling by integrin receptors. These hypotheses remain to be tested. Adipose tissue is highly vascularized, and uPA has been hypothesized to play a role in angiogenesis. It would therefore be of interest to study the role of the Plg system in angiogenesis in the mammary gland.

In contrast to the role played by the Plg system, matrix metalloproteases (MMPs) were found to be anti-adipogenic, and inhibition of MMPs increased adipogenesis both *in*

vitro and *in vivo*. How is the function of these two classes of proteases, which exert opposing influences during adipocyte differentiation, regulated *in vivo*? It would be of great interest to understand if there is any cross-talk between MMPs and the Plg cascade, and what the critical substrates are for each protease during adipogenesis.

This research demonstrates a central role for the Plg system in tissue remodeling and adipogeneis, and shows for the first time that PKal is a physiological regulator of the Plg cascade. These findings have implications for other physiologic and pathologic processes involving Plg activation *in vivo,* and open up new avenues of research to elucidate the physiological functions of PKal, plasmin and their substrates.

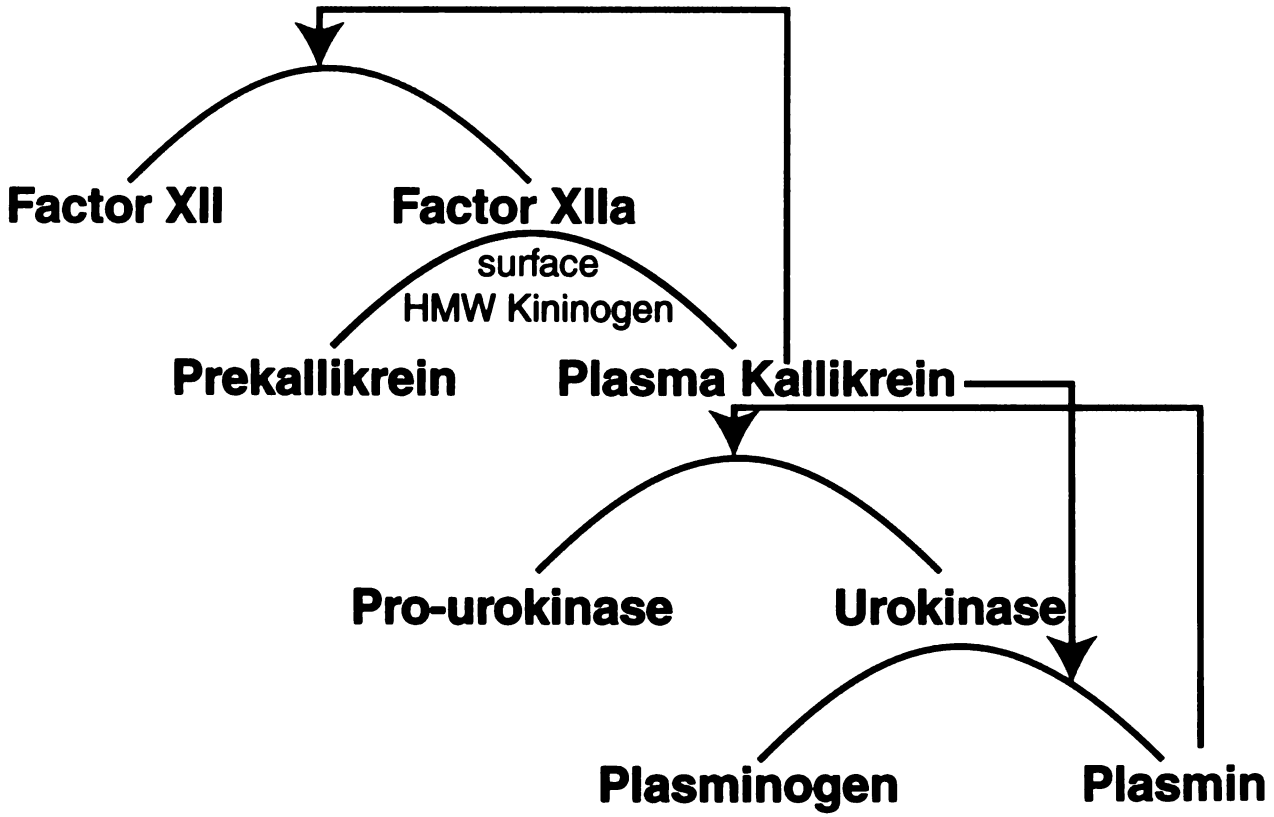

Figure 7. Plasma kallikrein-mediated plasminogen cascade. Plasma kallikrein reciprocally activates Factor XII, and directly activates both pro-urokinase and plasminogen. Plasmin activates pro-urokinase in a feedback loop.

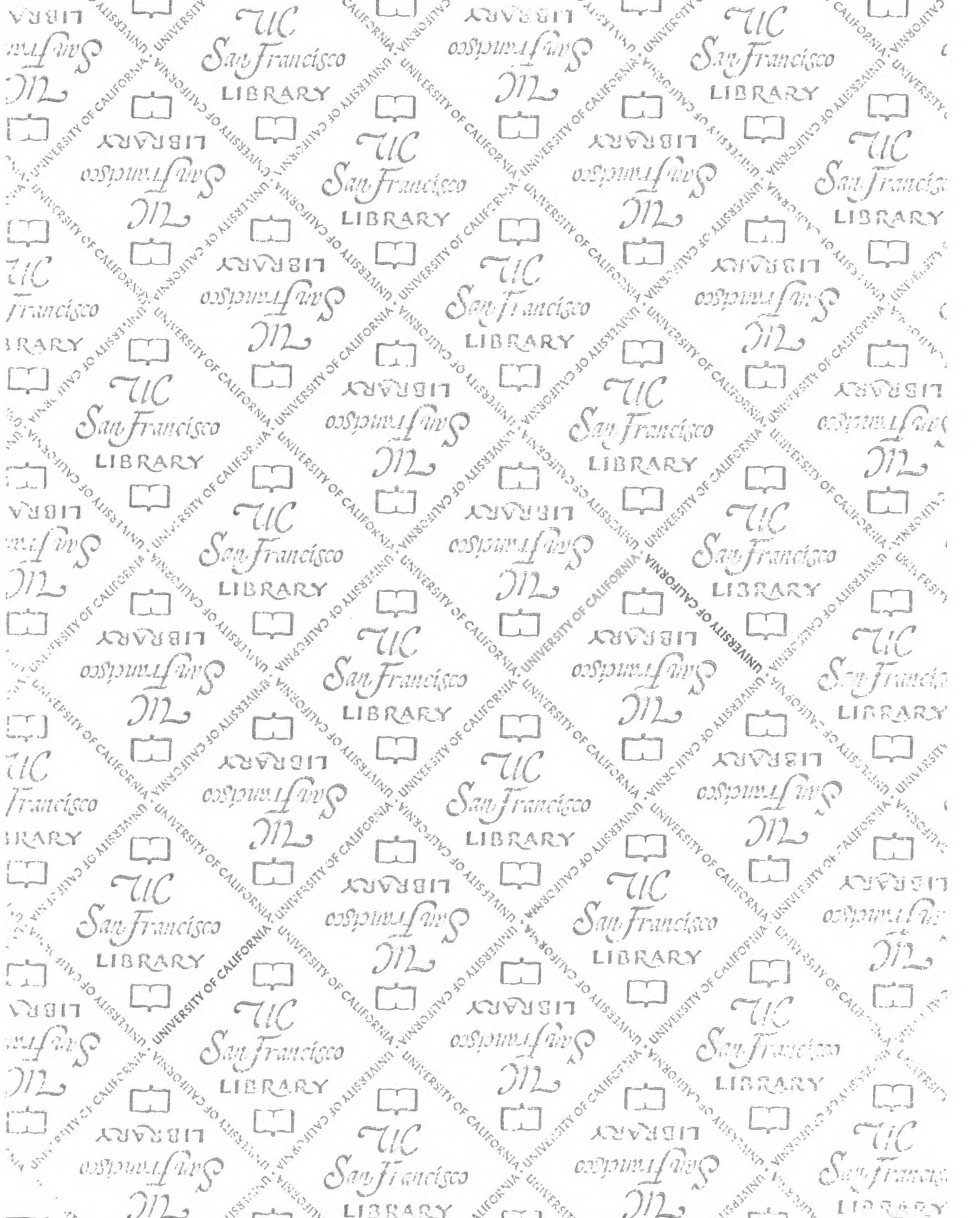
UC
San Francisco
LIBRARY
UNIVERSITY OF CALIFORNIA